

Regulation of senescence in *Arabidopsis thaliana* and barley

Gloria Comadira

Submitted in accordance with the requirements for the degree of
Doctor of Philosophy

The University of Leeds
Faculty of Biological Sciences

August 2015

The candidate confirms that the work submitted is his/her own, except where work which has formed part of jointly-authored publications has been included. The contribution of the candidate and the other authors to this work has been explicitly indicated below. The candidate confirms that appropriate credit has been given within the thesis where reference has been made to the work of others.

Quain MD, Makgopa ME, Marquez-Garcia B, Comadira G, Fernandez-Garcia N, Olmos E, Schnaubelt D, Kunert KJ, Foyer CH (2014) Ectopic phytocystatin expression leads to enhanced drought stress tolerance in soybean (*Glycine max*) and *Arabidopsis thaliana* through effects on strigolactone pathways and can also result in improved seed traits. *Plant Biotechnol J* **12**: 903-913

Part of the experimental work described in Chapter 3 of the thesis and included in the publication is directly attributable to the candidate.

This copy has been supplied on the understanding that it is copyright material and that no quotation from the thesis may be published without proper acknowledgement.

Acknowledgements

I would like to thank to my supervisor Christine Foyer for her support and guidance during these years. Many thanks to Rob Hancock for his supervision during my time at the James Hutton Institute and constant help in the WHIRLY project. Thanks to Karl Kunert for so many discussions and ideas about OCI.

Many thanks to all the members of my lab team in Leeds. I should not forget the ones who already left, specially Belen, Eugene and Marian, thanks for your help and nice times at work.

I would like to thank all the colleagues from the James Hutton Institute. Many thanks to Jennifer Stephens' group for their patience and assistance in cloning and transgenic barley lines production, they were really nice and helpful. Many thanks to Jenny Morris, who processed the microarray slides, and to Pete Hedley, who has been a great help in the analysis of the microarray data. Thanks to Johannes Rauscher for performing the metabolomics experiments with me and for so many experiences during my first period in Dundee. Thanks to Susan Verrall for the statistical analyses. Special thanks to all the people I met at the James Hutton Institute during my stay, particularly to those who became my closest friends.

I am very grateful to the European Union for funding my PhD studentship in the framework of Croplife. Through the Croplife network I had the opportunity to attend different training courses and conferences and, most importantly, to make a lovely group of friends.

Finally, thanks a lot to my friends Kasia, Merce, Ambra, Rocio and Yoselin for being part of my PhD adventure and for their unconditional support, without them it would not had been the same. Thanks to all my family and friends.

Abstract

Senescence is the last stage of leaf development. During leaf senescence essential nutrients are remobilised to the growing parts of the plant. This highly regulated process involves the expression of senescence-associated genes and a decrease in photosynthesis accompanied by chloroplast protein degradation. The following studies were performed in order to characterise the functions of the papain-like cysteine proteases and the WHIRLY1 protein in the regulation of senescence. Transgenic Arabidopsis lines expressing the rice cystatin, oryzacystatin-I (OCI) in either the chloroplasts or cytosol were characterized. These lines had a slow growth phenotype relative to the wild type. Furthermore, ectopic OCI expression in Arabidopsis increased leaf numbers and enhanced shoot and root branching at flowering. Transgenic barley lines with decreased levels of WHIRLY1 transcripts were grown under optimal and low nitrogen stress conditions. Under optimal conditions, the WHIRLY1 transgenic lines had similar CO₂ assimilation rates to those of the wild type but they had significantly more chlorophyll and less sucrose. Moreover, these lines produced fewer tillers and seeds than the wild type. The WHIRLY1 transgenic plants grew better than the wild type under nitrogen deficiency, maintaining higher photosynthetic capacity and chlorophyll content. The WHIRLY1 protein influenced the expression of specific subsets of transcripts encoding chloroplast proteins including thylakoid NADH and cytochrome b6/f complexes. Additionally, the transcript profile revealed new target proteins for WHIRLY1, supporting the involvement of this protein in chloroplast signalling and stress responses. Finally, this study allowed the successful production of barley plants expressing SAG21 and wheat plants expressing the OCI gene in the cytosol, which have the potential to improve stress tolerance and increase seed yield.

Table of Contents

Acknowledgements	iii
Abstract	iv
Table of Contents	v
List of Abbreviations	xi
List of Tables	xii
List of Figures	xiv
Chapter 1. Introduction	2
1.1 Senescence	2
1.2 Protein degradation during leaf senescence	4
1.2.1 Rubisco degradation	5
1.3 Cysteine proteases and cystatins.....	9
1.4 Proteases, cystatins and stress.....	11
1.5 OCI.....	13
1.6 The effect of nitrogen deficiency on leaf protein turnover and photosynthesis	15
1.7 The WHIRLY1 protein	16
1.7.1 The WHIRLY1 protein in barley.....	23
1.8 Hypothesis and project objectives	26
Chapter 2. Materials and Methods	29
2.1 Plant material and growth conditions.....	29
2.1.1 Barley	29
2.1.1.1 Barley plants grown under nitrogen deficiency.....	30
2.1.1.2 Barley plants grown under drought stress	30
2.1.2 Arabidopsis	31
2.1.2.1 Soil	31
2.1.2.2 PANG2 medium preparation and plate growth	31
2.2 Root morphology measurements	32
2.3 Shoot and root biomass determination	32
2.4 Soil and leaf water content	33
2.5 Experimental design used for transcriptomic and metabolomic profiles.....	33
2.6 Microarray processing and analysis	34
2.6.1 60 K barley array	36
2.7 Quantitative Real-Time RT-PCR (qRT-PCR)	36

2.8 Metabolite analysis.....	38
2.8.1 Determination of ascorbic acid, glutathione and pyridine nucleotides	38
2.8.1.1 Ascorbate and glutathione extraction	38
2.8.1.1.1 Ascorbate assay	38
2.8.1.1.2 Glutathione assay	39
2.8.1.2 NAD, NADH, NADP and NADPH assays	40
2.8.2 Carbon and nitrogen content measurements	41
2.8.3 Total protein quantification	41
2.8.4 Leaf pigment analysis.....	42
2.8.5 Targeted metabolomics.....	43
2.8.5.1 Extraction of polar and non-polar fractions.....	43
2.8.5.2 Derivatization of polar fraction.....	44
2.8.5.3 Derivatization of non-polar fraction.....	44
2.8.5.4 Sample analysis	45
2.9 Volatiles assay	46
2.10 Physiological measurements.....	48
2.10.1 Photosynthetic gas exchange	48
2.10.1.1 Light response curves	48
2.10.1.2 CO ₂ response curves	48
2.11 Production of transgenic barley and wheat plants expressing the <i>SAG21</i> and <i>OCI</i> genes.....	50
2.11.1 Production of <i>SAG21</i> -YFP expression clone and transformed plants verification	50
2.11.1.1 Competent cells transformation and selection of positive clones.....	52
2.11.1.2 Create <i>SAG21</i> -YFP expression clones using the LR recombination reaction	53
2.11.1.3 AGL1 competent cells production	54
2.11.1.4 Agrobacterium-mediated barley transformation	55
2.11.2 Cloning of <i>OCI</i> gene into pDONR and pENTR-type vectors	56
Chapter 3. Characterization of Arabidopsis transgenic lines with ectopic <i>OCI</i> expression	59
3.1 Introduction	59
3.2 Results	60
3.2.1 Phenotype of Arabidopsis plants with ectopic expression of <i>OCI</i>	61

3.2.1.1 Phenotype of Arabidopsis lines expressing OCI in the chloroplast.....	61
3.2.1.2 Phenotype of Arabidopsis lines expressing OCI in the cytosol.....	62
3.2.2 Shoot biomass, chlorophyll and protein contents in OCI Arabidopsis plants at 3 different time points.....	63
3.2.2.1 Shoot biomass, chlorophyll and protein contents in Arabidopsis lines expressing OCI in the chloroplast.....	63
3.2.2.2 Shoot biomass, chlorophyll and protein contents in Arabidopsis lines expressing OCI in the cytosol.....	66
3.2.3 Percentage of flowering in OCI Arabidopsis plants	68
3.2.4 Root morphology of the OCI Arabidopsis seedlings.....	70
3.2.4.1 Root morphology of the Arabidopsis lines with ectopic expression of OCI in the chloroplast.....	70
3.2.4.2 Root morphology of the Arabidopsis lines with ectopic expression of OCI in the cytosol	70
3.2.5 Number of leaves and leaf area of the Arabidopsis lines expressing OCI in the cytosol	73
3.3 Discussion.....	74
3.3.1 Arabidopsis plants expressing OCI in the cytosol	74
3.3.2 Arabidopsis plants expressing OCI in the chloroplast	75
3.3.3 Ectopic expression of OCI in Arabidopsis plants.....	75
3.3.4 Experimental plan for the ATG-OCI Arabidopsis plants	76
Chapter 4. Production of transgenic barley and wheat plants expressing the SAG21 and OCI genes	77
4.1 Introduction	77
4.2 Results	78
4.2.1 Gateway cloning overview.....	78
4.2.1.1 Create an entry clone.....	79
4.2.1.2 Create an expression clone.....	80
4.2.2 Production of barley transgenic plants expressing SAG21-YFP	81
4.2.2.1 Create a SAG21-YFP entry clone	81
4.2.2.1.1 Obtain <i>attB</i> _SAG21-YFP PCR products	81
4.2.2.2 Create a SAG21-YFP expression clone	82
4.2.2.3 <i>Agrobacterium</i> transformation with SAG21-YFP expression clone	84
4.2.2.4 Barley plants transformation.....	84

4.2.2.5 State of the work with the SAG21-YFP transgenic barley plants	87
4.2.3 Cloning of OCI gene into pDONR and pENTR-type vectors	88
4.2.3.1 pENTR1A-OCI construction	88
4.2.3.1.1 OCI amplification with <i>Bam</i> HI and <i>Xho</i> I restriction sites	88
4.2.3.1.2 OCI and pENTR1A plasmid digestions and ligation	90
4.2.3.2 pDONR-OCI construction	92
4.2.3.2.1 Obtain <i>att</i> B_OCI PCR products	92
4.2.3.2.2 Create OCI entry clones using the BP recombination reaction	93
4.2.3.3 Positive OCI clone selection	94
4.3 Discussion: future uses of the transformed barley and wheat plants	95
4.3.1 Analysis of the barley transgenic plants expressing SAG21-YFP	95
4.3.2 Analysis of the wheat transgenic plants expressing OCI	96
Chapter 5. Characterization of WHIRLY1 RNAi barley lines under optimal and stress conditions	97
5.1 Introduction	97
5.2.1 Shoot phenotypes of plants grown in soil	99
5.2.1.1 Volatile emission from leaves	103
5.2.2 Shoot phenotypes of plants grown in vermiculite with complete nutrient solution	107
5.2.3 The effect of nitrogen limitation on the growth and physiology of wild type barley	121
5.2.4 The effect of nitrogen limitation on the growth and physiology of W1-7 seedlings	127
5.2.5 The effect of drought on the growth and physiology of wild type and W1-7 seedlings	136
5.3 Discussion	140
5.3.1 The phenotype of the WHIRLY1-deficient lines is similar to the wild type in the absence of stress	140
5.3.2 The WHIRLY1-deficient lines are more resistant to nitrogen deficiency than the wild type	141
5.3.3 The WHIRLY1-deficient lines show lower drought sensitivity in terms of leaf water content than the wild type	142

Chapter 6. Transcript profile of the WHIRLY1 transgenic leaves under optimal and nitrogen deficient conditions	143
6.1 Introduction	143
6.2 Results	145
6.2.1 An overview of the number of transcripts changed in expression between WT and W1-7 under the two nitrogen conditions	145
6.2.2 Transcript changes in the W1-7 line relative to the wild type under nitrogen replete conditions	146
6.2.3 Transcript changes in the W1-7 relative to the wild type in response to nitrogen deficiency	150
6.2.4 Transcript changes in the W1-7 relative to the wild type in both nitrogen conditions	155
6.2.5 Transcript changes in the wild type barley seedlings in response to nitrogen deficiency.....	158
6.2.5.1 Most of the signalling transcripts changed in expression under nitrogen deficiency were receptor kinases.....	161
6.2.5.2 Many transcription factors were changed in expression under nitrogen deficiency.....	162
6.2.5.3 The majority of the up regulated transcripts in the protein group had functions in protein degradation.....	163
6.2.6 Microarray validation and sample variation	165
6.3 Discussion.....	167
6.3.1 Transcripts whose abundance was changed in the W1-7 line relative to wild type under optimal growth conditions.....	168
6.3.2 Transcripts whose abundance was changed in the W1-7 line relative to wild type under nitrogen deficiency conditions.....	169
6.3.3 Transcripts whose abundance was changed in the W1-7 line relative to wild type under both growth conditions ...	170
6.3.4 Transcripts that are changed in wild type barley in response to nitrogen deficiency.....	171
Chapter 7. Metabolic profile of the WHIRLY1 transgenic leaves under optimal and nitrogen deficient conditions	173
7.1 Introduction	173
7.2 Results	175
7.2.1 Metabolites that are changed in wild type barley in response to nitrogen deficiency.....	175
7.2.1.1 Amino acids.....	175

7.2.1.2 Sugars and carboxylic acids.....	177
7.2.3 Metabolite changes in the W1-7 relative to the wild type in response to nitrogen deficiency.....	181
7.2.4 Sample variation	183
7.3 Discussion.....	184
Chapter 8. General discussion.....	187
8.1 OCI and Rubisco degradation during senescence	187
8.2 WHIRLY1 in barley.....	191
8.2.1 Effect of WHIRLY1 on photosynthesis under optimal nitrogen	193
8.2.2 Effect of WHIRLY1 on photosynthesis under low nitrogen	193
8.2.3 The WHIRLY1 protein has important functions within the chloroplasts.....	194
8.2.4 Other potential roles of WHIRLY1 in barley.....	195
Bibliography	199
Appendix.....	222
Appendix I. Chloroplast localization of the 35S::PRK-YFP plasmid in transiently transformed tobacco leaves.	222
Appendix II. Barley transcripts homologous to plastid encoded genes in Arabidopsis that exhibit significant differences in abundance in WT and W1-7 seedlings	223
Appendix III. Transcripts significantly altered in abundance in response to N deficiency in wild type barley leaves.	226
Appendix IV. A comparison of the WHIRLY1 transcript abundance in the wild type and W1-7 leaves under N replete and N deficient conditions.....	232

List of Abbreviations

ABA	abscisic acid
CaMV	cauliflower mosaic virus
CP	cysteine protease
GC-MS	gas chromatography – mass spectrometry
GSH	reduced glutathione
GSSG	glutathione disulphide
JA	jasmonic acid
LB	Luria-Bertani
MS	Murashige and Skoog
NADPH	nicotinamide adenine dinucleotide phosphate
NPR-1	NON-EXPRESSOR OF PR PROTEINS
OCI	Oryzacystatin I
PCR	polymerase chain reaction
PR	pathogenesis-related
qRTPCR	quantitative reverse transcription PCR
ROS	reactive oxygen species
Rubisco	Ribulose-1,5-bisphosphate carboxylase/oxygenase
SA	salicylic acid
SAG	senescence associate gene
W1-7	WHIRLY1 RNAi line 7
WT	wild-type
YFP	yellow fluorescent protein

List of Tables

Table 1.1 Summary of functions of the WHIRLY1 protein.	17
Table 2.1 Primers used for qRT-PCR in barley.	37
Table 2.2 <i>attB</i> PCR primers for SAG21.	50
Table 2.3 Components for each 50 µl reaction.	51
Table 2.4 PCR thermal cycling conditions.	51
Table 2.5 BP recombination reaction.	52
Table 2.6 LR recombination reaction.	54
Table 2.7 PCR components for SAG21 and control lines screening.	56
Table 2.8 Primer sequences for OCI gene amplification.	57
Table 2.9 PCR thermal cycling conditions.	57
Table 2.10 pENTR1A and OCI digestions.	58
Table 2.11 <i>attB</i> PCR primers for OCI.	58
Table 5.1 Seed yield in W1-7 and wild type barley plants.	103
Table 6.1 Transcripts with significantly different abundance in the W1-7 and wild type leaves under N replete conditions.	148
Table 6.2 Transcripts with significantly different abundance in the W1-7 and wild type leaves under N deficient conditions.	152
Table 6.3 Barley transcripts homologous to plastid encoded genes in Arabidopsis that exhibit significant differences in abundance in WT and W1-7 seedlings.	155
Table 6.4 Transcripts with significantly different abundance in W1- 7 and wild type barley leaves under differing nitrogen availability.	156
Table 6.5 Classification of the signalling related transcripts changed in expression in the wild type barley seedlings grown under nitrogen deficiency relative to the nitrogen replete conditions.	161
Table 6.6 Classification of the RNA related transcripts changed in expression in the wild type barley seedlings grown under nitrogen deficiency relative to the nitrogen replete conditions.	163
Table 6.7 Classification of the protein related transcripts changed in expression in the wild type barley seedlings grown under nitrogen deficiency relative to the nitrogen replete conditions.	164
Table 7.1 Influence of N availability on amino acid content in barley leaves.	176

Table 7.2 Influence of N availability on content of metabolites associated with sugar and carboxylic acid metabolism in barley leaves.....	177
Table 7.3 Influence of N availability on phytol content in barley leaves.....	179

List of Figures

Figure 1.1 Shoot phenotype of the 10 week-old SAG21 antisense (AS) and overexpressing (OEX) Arabidopsis lines.	3
Figure 1.2 The ultrastructure of Rubisco Containig Bodies (RCB) in wheat.....	7
Figure 1.3 Chloroplast proteins degradation pathways during leaf senescence.....	8
Figure 1.4 A proposed model of CV-mediated chloroplast degradation.....	9
Figure 1.5 Cysteine protease inhibition by phytocystatin.	10
Figure 1.6 Effect of cysteine protease and cystatin expression in stress and senescence.....	11
Figure 1.7 OCI over expressing tobacco lines (OCE) and wild type tobacco plants after 8 (A) and 14 weeks (B).	14
Figure 1.8 The effects of ectopic OCI expression on senescence in soybean.....	14
Figure 1.9 WHIRLY1 and NPR1 are required for SA-responsive gene expression in Arabidopsis.	19
Figure 1.10 Comparison of the phenotypes of maize plants deficient in the WHIRLY1 protein to the wild type maize.....	21
Figure 1.11 Whirly proteins and microhomology-mediated U-turn-like inversions.	22
Figure 1.12 Morphology and distribution of chloroplast nucleoids in leaves of the wild type (WT) and the transgenic RNAi-W1-7 plants (W1-7).....	23
Figure 1.13 Hypothetical model of HvS40 regulation by WHIRLY1.....	24
Figure 1.14 Hypothetical model of the role of WHIRLY1 in perception and transduction of redox signals from chloroplast to nucleus.....	26
Figure 1.15 WHIRLY1, OCI and SAG21 localization in the cell.....	28
Figure 2.1 Barley seedlings growing on vermiculite under controlled conditions.....	30
Figure 2.2 Arabidopsis seedlings growing on PANG2 plate (A) and soil (B).	32
Figure 2.3 Experimental design used for time course transcriptomic and metabolomic analyses of the W1-7 line and wild type barley seedlings grown under N replete and N deficient conditions.	33
Figure 2.4 Sample preparation and array processing scheme.	35
Figure 2.5 Pyridine nucleotides determination.....	41

Figure 2.6 Volatile collection in W1-7 and wild type barley seedlings.....	47
Figure 2.7 Photosynthetic gas exchange measurement in a W1-7 barley seedling using CIRAS2.	49
Figure 3.1 A comparison of the rosette diameter at 18 days (A), rosette phenotypes at 30 days (B); and shoot phenotypes at 10 weeks in the three independent transgenic lines with ectopic expression of OCI targeted to the chloroplast (PC2, PC7 and PC9) to the wild type (WT).....	61
Figure 3.2 A comparison of the rosette diameter at 17 days (A), rosette phenotypes at 30 days (B); and shoot phenotypes at 10 weeks in the three independent transgenic lines with ectopic expression of OCI in the cytosol (Cys1, Cys3 and Cys4) to the wild type (WT).	62
Figure 3.3 A comparison of shoot biomass at 25 days (A), and total chlorophyll (B) and leaf soluble protein contents (C) in three independent transgenic lines with ectopic expression of OCI targeted to the chloroplast (PC2, light grey; PC7, dark grey; and PC9, black) to the wild type (WT, white).....	65
Figure 3.4 A comparison of shoot biomass (A), total chlorophyll (B) and leaf soluble protein contents (C) in the three independent transgenic lines expressing OCI in the cytosol (Cys1, light grey; Cys3, dark grey; and Cys4, black) to the wild type (WT, white).....	67
Figure 3.5 A comparison of the percentage of flowering plants in the three independent transgenic lines with ectopic expression of OCI in the chloroplast (PC2, green; PC7, red and PC9, grey; A) and the three independent transgenic lines with ectopic expression of OCI in the cytosol (Cys1, green; Cys3, grey; and Cys4, red; B) to the wild type (WT, black).	69
Figure 3.6 A comparison of primary root length (B), number of lateral roots (C) and lateral root density (D) in 11-day old plants of the transgenic lines with chloroplast targeted OCI (PC2, PC7 and PC9) to the wild type (WT).....	71
Figure 3.7 A comparison of primary root length (B), number of lateral roots (C) and lateral root density (D) in 11-day old plants of the transgenic lines expressing OCI in the cytosol (Cys1, Cys3 and Cys4) to the wild type (WT).	72
Figure 3.8 A comparison of the number of leaves (A) and leaf area (B) in the in 63-day old plants of the cytosol OCI transgenic lines (Cys1, Cys3 and Cys4) to the wild type (WT).....	73
Figure 4.1 Gateway recombination steps.....	79
Figure 4.2 pDONR207 vector used to generate entry vector.	80
Figure 4.3 SAG21-YFP gene amplification with <i>attB</i> PCR primers.	81
Figure 4.4 Map of the pDONR207 vector containing the SAG21-YFP gene.....	82

Figure 4.5 pBRACT-type vector used to generate expression vector	83
Figure 4.6 Map of the sequence which is located between left border (LB) and right border (RB) in the expression clone pBRACT214_SAG21-YFP.....	83
Figure 4.7 Barley transformation process	85
Figure 4.8 Method to obtain homozygous plants with a single insert.	86
Figure 4.9 PCR results of the SAG21-YFP barley lines.....	87
Figure 4.10 Experimental design of the OCI cloning into pENTR1A vector using <i>Bam</i> HI and <i>Xho</i> I restriction enzymes.....	89
Figure 4.11 OCI PCR product containing <i>Bam</i> HI and <i>Xho</i> I sites.....	90
Figure 4.12 <i>Bam</i> HI + <i>Xho</i> I digests of mini-preps.....	91
Figure 4.13 OCI PCR product containing <i>att</i> B sites.....	92
Figure 4.14 Map of pDONR201 vector with restriction sites.....	93
Figure 4.15 Digestions of the two OCI constructs produced.	94
Figure 5.1 A comparison of shoot phenotypes of 14-day old seedlings of the transgenic W1-1 and W1-7 lines to the wild type (WT) and a transgenic control line (C W1-7) lacking the transgene.....	100
Figure 5.2 A comparison of leaf numbers (A, C) and shoot biomass (B, D; expressed on a fresh weight basis) in 14-day old seedlings of the transgenic W1-1 and W1-7 lines to the wild type (WT) and a transgenic control line (C W1-7) lacking the transgene.....	101
Figure 5.3 A comparison of leaf soluble protein (A, C) and chlorophyll (B, D) contents and shoot biomass in 14-day old seedlings of the transgenic W1-1 and W1-7 lines to the wild type (WT) and a transgenic control line (C W1-7) lacking the transgene.....	102
Figure 5.4 A comparison of the volatile compounds emitted by wild type barley and W1-7 seedlings.....	104
Figure 5.5 Identification of volatile compound emitted by wild type barley and W1-7 seedlings.	105
Figure 5.6 Identification of volatile compound emitted by wild type barley and W1-7 seedlings.	106
Figure 5.7 Identification of volatile compound emitted by wild type barley and W1-7 seedlings.	107
Figure 5.8 A comparison of shoot phenotypes of 14-day old seedlings of the transgenic W1-1 and W1-7 lines to the wild type (WT) and a transgenic control line (C W1-7) lacking the transgene.....	109

Figure 5.9 A comparison of leaf number (A, C) and shoot biomass (B, D; expressed on a fresh weight basis) in 14-day old seedlings of the transgenic W1-1 and W1-7 lines to the wild type (WT) and a transgenic control line (C W1-7) lacking the transgene.....	110
Figure 5.10 A comparison of leaf soluble protein (A, C) and chlorophyll (B, D) contents and shoot biomass in 14-day old seedlings of the transgenic W1-1 and W1-7 lines to the wild type (WT) and a transgenic control line (C W1-7) lacking the transgene.....	111
Figure 5.11 A comparison of shoot phenotypes (A), shoot and root biomass (B), shoot/ root ratio (C), chlorophyll (D), carotenoid (E) and leaf soluble protein contents (F) of 14-day old seedlings of the transgenic W1-1, W1-7 and W1-9 lines to the wild type (WT) grown on vermiculite.....	112
Figure 5.12 A comparison of CO ₂ assimilation (A), stomata conductance (B) and transpiration in 14-day old seedlings of the transgenic W1-7 line (white squares) to the wild type (WT, black diamonds).....	113
Figure 5.13 A comparison of CO ₂ assimilation (A), stomata conductance (B), transpiration and internal CO ₂ concentration (Ci, D) in 23-day old seedlings of the transgenic W1-1, W1-7 and W1-9 lines to the wild type (WT).	114
Figure 5.14 A comparison of CO ₂ assimilation (A) and stomatal conductance (B) responses to different CO ₂ concentrations in 14-day old seedlings of the transgenic W1-7 line to the wild type (WT).....	116
Figure 5.15 A comparison of the total nitrogen and total carbon contents in leaves (A), and roots (B), and the C/N ratios (C) of leaves and roots in 24-day old seedlings of the transgenic W1-7 line to the wild type (WT).	117
Figure 5.16 A comparison of leaf ascorbate (A), glutathione (B), NAD and NADH (C) and NADP and NADPH (D) in leaves of the 14-day old seedlings of the transgenic W1-7 line to the wild type (WT).....	118
Figure 5.17 A comparison of shoot phenotypes of wild type barley and lines deficient in the WHIRLY1 protein (W1-1, W1-7 and W1-9) at 18 (A), 27 (B), 81 (C) and 130 days (D) after sowing.	119
Figure 5.18 A comparison of number of tillers (A), leaf total protein (B), and chlorophyll contents (C) of seedlings of the transgenic W1-1, W1-7 and W1-9 lines to the wild type (WT).	120
Figure 5.19 A comparison of the phenotypes (A), leaf chlorophyll contents (B), photosynthesis (C) and leaf protein contents (D) in 14 day old seedlings that had been grown for 7 days in the absence of nitrogen and grown with solutions containing either 5 mM KNO ₃ (N-replete, black lines) or 0.1 mM KNO ₃ (N-deficient, grey lines).....	122

Figure 5.20 A comparison of the phenotypes (A), shoot biomass expressed as fresh weight (B), shoot/root ratios (C) and root biomass expressed as fresh weight (D) of 23-day old seedlings that had been grown for 7 days in the absence of nitrogen and grown with solutions containing either 5 mM KNO_3 (N-replete) or 0.1 mM KNO_3 (N-deficient).	123
Figure 5.21 A comparison of the total nitrogen and total carbon contents in leaves (A), and roots (B), and the C/N ratios (C) of leaves and roots of 24-day old seedlings grown with either 5 mM (N-replete) or 0.1 mM (N-deficient) KNO_3 for 17 days.	124
Figure 5.22 A comparison of leaf ascorbate (A), glutathione (B), NAD and NADH (C) and NADP and NADPH (D) in 14 day-old seedlings grown with either 5 mM (N-replete) or 0.1 mM (N-deficient) KNO_3 for 7 days.	126
Figure 5.23 A comparison of the effects of nitrogen limitation in the phenotype (A), shoot biomass (B), root biomass (C) and shoot/ root ratio (D) in 23-day old seedlings of the transgenic W1-1, W1-7 and W1-9 lines to the wild type (WT).	129
Figure 5.24 A comparison of the effects of nitrogen limitation in CO_2 assimilation (A), stomata conductance (B), transpiration (C) and internal CO_2 concentration (C_i , D) in 23-day old seedlings of the transgenic W1-1, W1-7 and W1-9 lines to the wild type (WT).	130
Figure 5.25 A comparison of the effects of nitrogen limitation in leaf pigment (A) and total protein content (B) in 16-day old seedlings of the transgenic W1-1, W1-7 and W1-9 lines to the wild type (WT).	131
Figure 5.26 A comparison of the effects of nitrogen limitation in total carbon (A) and total nitrogen contents, and in C/N ratios (C) of 24-day old seedlings of the transgenic W1-1, W1-7 and W1-9 lines to the wild type (WT).	132
Figure 5.27 A comparison of the effects of nitrogen limitation on leaf ascorbate (A), glutathione (B), NAD and NADH (C) and NADP and NADPH (D) in 14 day-old seedlings that been grown with either 5 mM (N-replete) or 0.1 mM (N-deficient) KNO_3 for 7 days.	133
Figure 5.28 A comparison of the effects of nitrogen limitation on light response curves of 7-day old and 14-day old seedlings of the transgenic W1-7 line to the wild type (WT).	134
Figure 5.29 A comparison of the effects of nitrogen limitation in CO_2 assimilation and stomata conductance at 400 μmol of light intensity of 7-day old and 14-day old seedlings of the transgenic W1-7 line to the wild type (WT).	135
Figure 5.30 A comparison of shoot phenotypes of 18-day old seedlings of the transgenic W1-7 line to the wild type (WT) grown under control conditions (A) and subjected to 10 days of drought stress (B).	136

Figure 5.31 A comparison of soil (A) and leaf (B) water content of 7-day old to 14-day old seedlings of the transgenic W1-7 line to the wild type (WT) under drought stress.	138
Figure 5.32 A comparison of the effects of 7 days of drought stress in CO ₂ assimilation (A), stomata conductance (B), and transpiration rates (C) of 14-day old seedlings of the transgenic W1-7 line to the wild type (WT).	139
Figure 6.1 Transcript profile comparison of 14 day old wild type barley and the WHIRLY1 deficient barley line 7 (W1-7) grown for 7 days under either nitrogen replete (N replete) or nitrogen deficient (N deficient) conditions.	145
Figure 6.2 Transcript profile of the 14 day-old W1-7 leaves relative to the wild type grown in N replete conditions.	147
Figure 6.3 Transcript profile of the 14 day-old W1-7 leaves relative to the wild type grown in N deficiency.	151
Figure 6.4 Functional classification of the total number of transcripts exhibiting significantly different abundance under N replete or N deficient conditions.	159
Figure 6.5 Number of transcripts that were up regulated (A) or down regulated (B) in the wild type barley leaves grown under nitrogen deficiency relative to the nitrogen replete conditions classified into functional categories.	160
Figure 6.6 Validation of microarray data by qRT-PCR.	166
Figure 6.7 Principal components analysis (PCA) of the transcript profile of the W1-7 line and wild type seedlings subjected to 7 days of nitrogen deprivation.	167
Figure 7.1 Glycine to serine (A), glutamine to glutamate (B) and asparagine to aspartate (C) ratios in wild type barley leaves in N limited and N replete conditions.	175
Figure 7.2 A comparison of the leaf metabolite profiles of 17 day old wild type seedlings and WHIRLY-1 deficient barley line W1-7, shown as schematic of key metabolic pathways.	180
Figure 7.3 Sucrose and octadecanol relative concentrations in N replete conditions in the wild type and W1-7 leaves.	181
Figure 7.4 Glucose (A), fructose (B), malic acid (C) and pentadecanoic acid (D) relative concentrations in N deficient conditions in the wild type and W1-7 leaves.	182
Figure 7.5 Principal components analysis (PCA) of the metabolic profiles of the W1-7 (WH) and wild type (WT) leaves under optimal nitrogen (WT h, WH h) and after 7 days of nitrogen deprivation (WT I, WH I).	183
Figure 8.1 A comparison of the rosette phenotypes at 30 days of the three independent transgenic lines with ectopic expression of OCI in the cytosol (A) and OCI targeted to the chloroplast (B) to the wild type (WT).	189

Figure 8.2 Scheme of potential pathways of chloroplast protein degradation during leaf senescence with OCI located to cytosol and chloroplast..... 191

Chapter 1. Introduction

1.1 Senescence

Senescence is the final stage of leaf development. It is largely a reversible process that becomes irreversible only in the final stages, when programmed cell death is initiated (Roberts et al., 2012). During senescence, nutrients accumulated in the leaves are remobilised and redirected to other organs such as younger leaves or developing seeds. In particular, the ribulose-1,5-bisphosphate carboxylase oxygenase (Rubisco) protein contains a huge amount of nitrogen which has to be remobilized to support seed growth and development (Chiba et al., 2003; Feller et al., 2008; Masclaux-Daubresse et al., 2010). For this reason, Rubisco degradation has been extensively studied although the precise mechanisms remain uncertain (Ishida et al., 2008; Prins et al., 2008).

The orchestration of leaf senescence requires the activation of complex transcriptional regulatory networks in which the expression of some genes such as the ones related to photosynthesis is down-regulated, while that of others such as senescence-associated genes (SAGs) is up-regulated (Lin and Wu, 2004; Breeze et al., 2011; Guo, 2013). For example, SAG12, which encodes a cysteine protease, is only expressed in senescent leaves (Lohman et al., 1994; Otegui et al., 2005). The abundance of SAG12 transcripts is therefore often used as a molecular marker for the developmental senescence program. Like SAG12, the expression of a large number of other proteases is modified during senescence. The expression of SAGs in leaves is required to coordinate the dismantling of the photosynthetic apparatus and remobilization of cellular components. While a large number of the SAGs encoding proteases are activated during senescence (Roberts et al., 2012), the functions of other SAGs such as SAG21 are largely unknown. SAG21/AtLEA5 (At4g02380) belongs to an anomalous late embryogenesis abundant (LEA) protein group (type 3 group)

in *Arabidopsis thaliana*. Members of this group are exclusively targeted to either plastids or mitochondria. *SAG21/AtLEA5* is expressed in leaves in the dark but not in the light except when plants are exposed to stress (Mowla et al., 2006). Although the functions of *SAG21* in leaf senescence are unknown, overexpression of *SAG21/AtLEA5* in *Arabidopsis thaliana* increases shoot growth under optimal and oxidative stress conditions (Figure 1. 1) (Salleh et al., 2012).

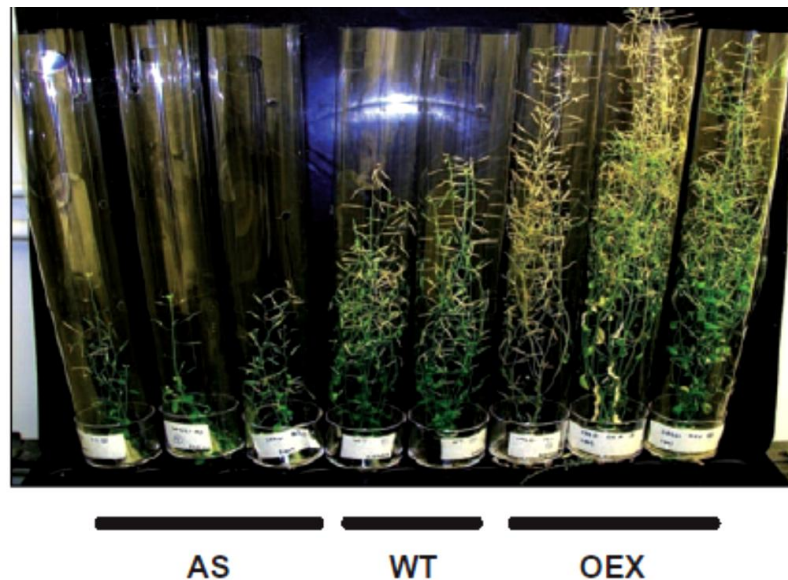


Figure 1.1 Shoot phenotype of the 10 week-old *SAG21* antisense (AS) and overexpressing (OEX) *Arabidopsis* lines. Figure from Salleh et al. (2012).

While it is widely accepted that the onset and duration of leaf senescence has a major agronomic influence on seed yield and quality, particularly in crop plants, the relationship between photosynthesis and grain yield is complex (Thomas and Howarth, 2000; Gregersen et al., 2013). For example, no significant relationships were found between photosynthetic parameters and grain yield in elite UK wheat varieties (Driever et al., 2014). The absence of a marked effect on grain yield of extending the period of photosynthesis by delaying leaf

senescence, particularly in plants grown under optimal conditions, can be explained by limitations in the capacity of the sink tissues, particularly the seeds. Seed growth is widely considered to be limited by the capacity of the sink tissues to grow (Reynolds et al., 2005; Serrago and Miralles, 2014). Nevertheless, relatively minor reductions in photosynthetic capacity can adversely affect grain yield (Beed et al., 2007; Sandaña et al., 2009). Moreover, several studies have demonstrated a link between the duration of flag leaf photosynthesis and grain yields (Kichey et al., 2007; Gaju et al., 2014). Additionally, adverse environmental conditions which impair photosynthesis and growth cause premature termination of grain growth and filling causing severe yield loss (Makino, 2011). It has been speculated therefore that extending the lifespan of the leaf canopy by delaying senescence will extend the grain filling period and increase grain yield (Hawkesford et al., 2013). In many crop species, delaying stress-induced leaf senescence and extending green canopy duration in plants experiencing stress has an impact on yield (Thomas and Ougham, 2014). A relationship between seed yield and a prolonged period of flag leaf photosynthesis was only observed under drought and heat stress in wheat and maize (Lopes and Reynolds, 2012). Crucially, a correlation was found between the period of flag leaf photosynthesis and increased yield in plants grown under conditions of nitrogen deficiency but not under optimal nitrogen (Derkx et al., 2012; Gaju et al., 2014). The stability and longevity of the photosynthetic processes in optimal and stress conditions are determined by regulated protein turnover and degradation.

1.2 Protein degradation during leaf senescence

Proteases are crucial enzymes in senescence due to their role in nutrient recycling, especially nitrogen (Hortensteiner and Feller, 2002). Proteases cleave peptide bonds between two amino acid residues. There are two types of proteases, endopeptidases, which cleave peptide bonds within the polypeptide chain, and exopeptidases, which cleave peptide bonds at the termini of polypeptide chains. Endopeptidases are classified into aspartic, cysteine, serine, threonine and glutamic proteases, based on the amino acid residue at

the active site involved directly in peptide bond hydrolysis, and into metalloproteases that require a divalent metal ion as part of the active site.

Serine and cysteine proteases are the most abundant proteases found in senescent leaves (Bhalerao et al., 2003; Martinez et al., 2012; Roberts et al., 2012). Relatively little is known about the mechanisms involved in chloroplast protein degradation but this process may be initiated in the organelle by the action of local proteases. In the case of thylakoid membrane proteins such as those in photosystem II, degradation is mediated by serine and metalloproteases such as FtsH-, Clp-, and Lon-like ATP-dependent proteases and DegP ATP-independent proteases (Olinares et al., 2011). The pathways of stromal protein degradation are much less well characterised. However, the leaves of CND41 mutants show delayed senescence with stable levels of Rubisco indicating that the chloroplast CND41 aspartic protease is involved in Rubisco degradation (Kato et al., 2004; Kato et al., 2005). Nevertheless, there is little consensus of opinion concerning how Rubisco protein degradation is mediated or regulated (Feller et al., 2008).

1.2.1 Rubisco degradation

There is still no well-defined pathway for Rubisco degradation with characterized proteolytic events. For example, several processes may be involved such as an initial interaction with reactive oxygen species that leads to cleavage of the polypeptide chain and thereafter, chloroplast or vacuolar enzymes may act on this stromal protein (Feller et al., 2008). Alternatively, as discussed in detail below, Rubisco protein degradation may involve the formation of one or more types of vesicles that remove the enzyme from the chloroplast. Once outside the chloroplast, proteolysis can occur by the action of C1A cysteine protease and other vacuolar proteases (Thoenen et al., 2007; Ishida et al., 2008; van Doorn et al., 2011). In addition, cysteine proteases have been implicated in the process of Rubisco degradation (Prins et al., 2008). Regardless of the mechanism involved, chloroplast proteins are thought to be

degraded during chloroplast-to-vacuole transit (Prins et al., 2008; Carrion et al., 2013).

The Rubisco protein has been detected inside different types of vesicles in the cytosol of senescent leaves. Firstly, Rubisco has been observed in Rubisco Containing Bodies (RCB) which are considered to be formed from stromules (stroma-filled tubes) that are continuously produced from the chloroplast, even in young leaves (Figure 1.2). Such vesicles are probably a type of autophagosome, which are delivered to the vacuole (Ishida et al., 2008; Prins et al., 2008). Secondly, Rubisco and other stromal and thylakoid proteins are increasingly found in Senescence Associated Vesicles (SAVs) as the senescence process progresses (Figure 1.3). The origin of these vesicles is uncertain but it is likely that they come from the endoplasmic reticulum (Otegui et al., 2005; Martinez et al., 2008; Carrion et al., 2013). Thirdly, Rubisco has been detected in chloroplast vesiculation-containing vesicles (CVVs) (Figure 1.4). The chloroplast vesiculation process is induced under stress by a novel plastid protein, which is called CV (Wang and Blumwald, 2014). To date, CVVs have only been identified in stress-induced senescence but they appear to be involved in the degradation of all types of chloroplast proteins. Cysteine proteases are considered to present in RCB and SAV. However, proteolytic activity has been only proven in SAVs, which contain the senescence-associated protease SAG12 (Otegui et al., 2005; Carrion et al., 2013).

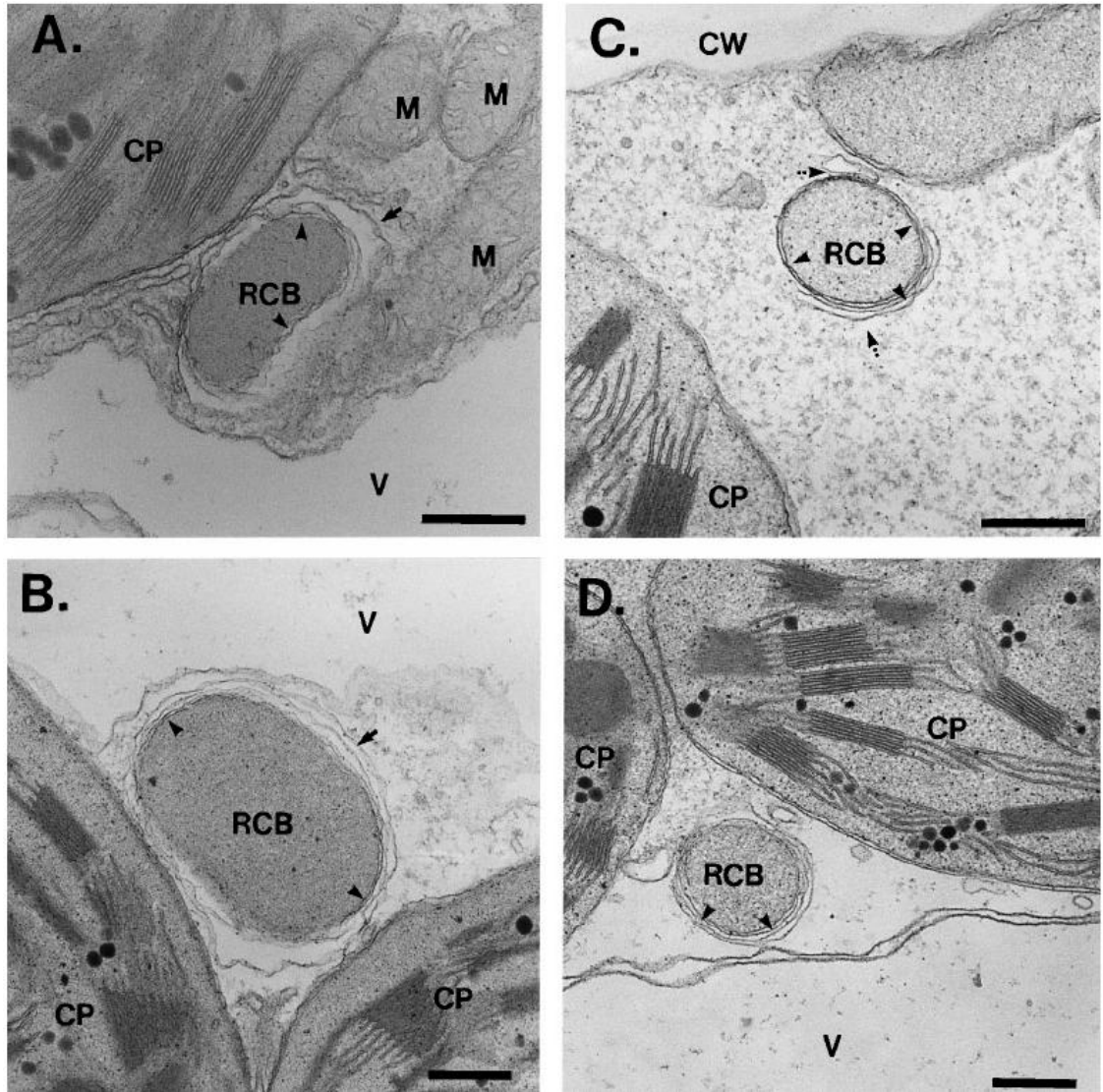


Figure 1.2 The ultrastructure of Rubisco Containig Bodies (RCB) in wheat. 21-day-old primary leaves (A), the fourth leaves 6 days after the full expansion (B), and the fourth leaves of dark-treated plants (C, D). Double membranes of RCB are indicated by arrowheads. Bars = 0.5 μm . CP, chloroplast; CW, cell wall; M, mitochondria; V, vacuole. Figure from Chiba et al. (2003).

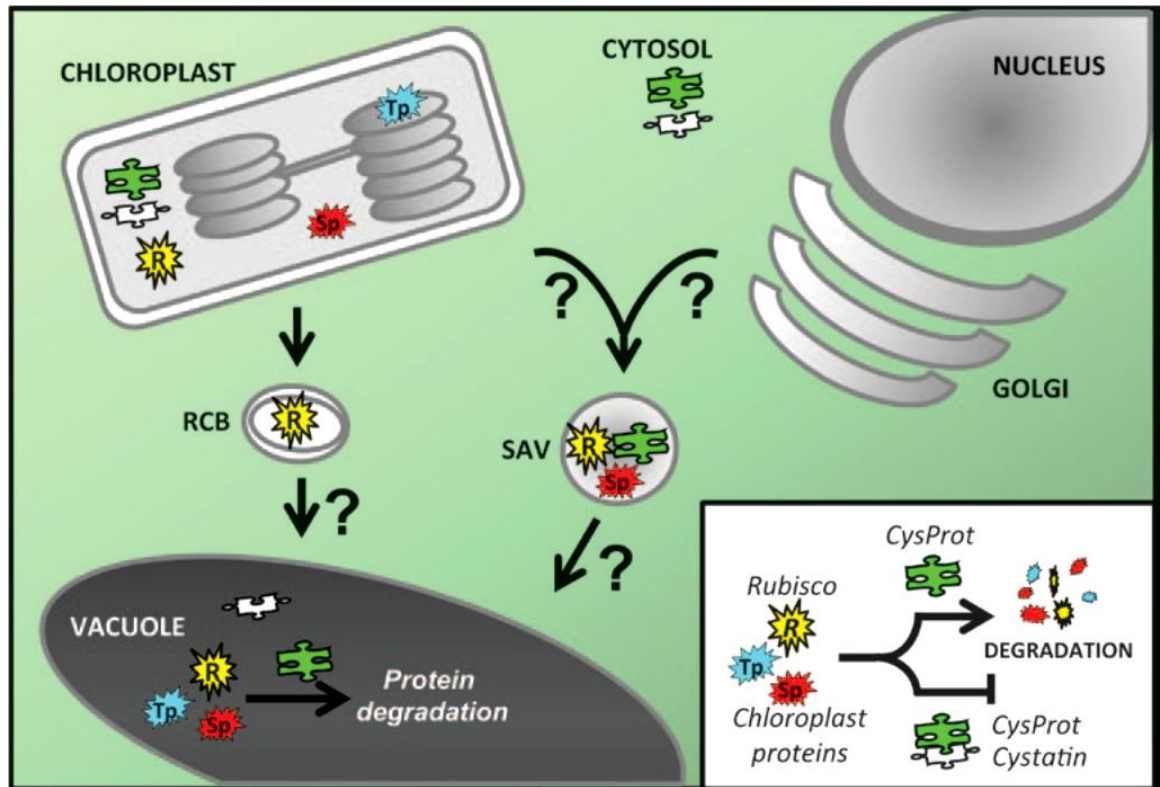


Figure 1.3 Chloroplast proteins degradation pathways during leaf senescence. Right box: scheme of cysteine protease-cystatin interaction regulating the protein degradation process. Cys-Prot, cysteine protease (green); cystatin (white); R, Rubisco (yellow); RCB, Rubisco-containing body; SAV, senescence-associated vacuole; Sp, stromal protein (red); Tp, thylakoid protein (blue). Figure from Diaz-Mendoza et al. (2014).

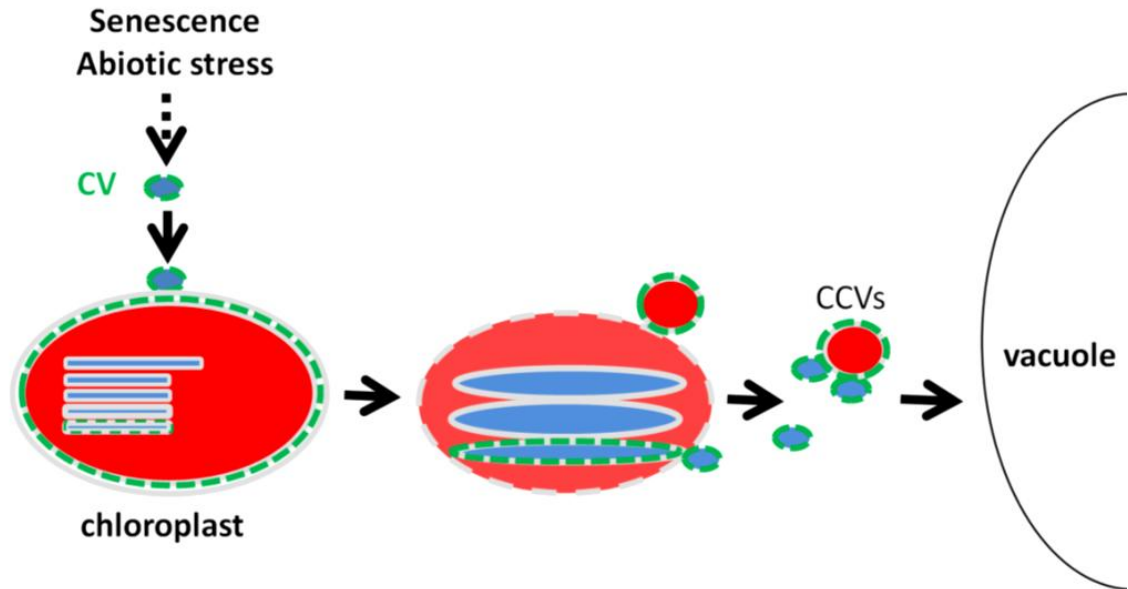


Figure 1.4 A proposed model of CV-mediated chloroplast degradation. The CV protein is activated by senescence and abiotic stress. CV induces vesicle formation in the chloroplast. The CV-containing vesicles (CCVs) are formed from the disrupted chloroplast membrane. CCVs carry stromal (red) and thylakoid (blue) proteins to the vacuole for degradation. Figure from Wang and Blumwald (2014).

1.3 Cysteine proteases and cystatins

Cysteine proteases are involved in diverse processes from growth and development to senescence and programmed cell death (Corr-Menguy et al., 2002; Belenghi et al., 2003; Kiyosaki et al., 2007; Weeda et al., 2009). Many cysteine proteases such as the vacuolar processing enzymes and SAG12 are expressed predominantly in senescent tissues. While such enzymes are considered to function principally in remobilization of nutrients, they may also have other roles. For example, in *Arabidopsis*, the senescence-regulated

potato cysteine protease SPCP2 is important in the control of development and it confers resistance to salt and drought stress (Chen et al., 2010).

Proteases inhibitors regulate protease activities, thus controlling intracellular protein degradation for the maintenance of protein homeostasis (Figure 1.5). In particular, cystatins inhibit cysteine protease activity by binding to the active site of their protease targets in an irreversible manner. They contain a Gln–Xaa–Val–Xaa–Gly motif in the centre of the polypeptide chain (where Xaa is any amino acid), a Pro–Trp (or Leu–Trp) dipeptide motif in the C-terminal region and a conserved Gly residue in the N-terminal (Benchabane et al., 2010). Essentially, the functions of plant cystatins include protein turnover regulation in developing seeds and inhibition of digestive cysteine proteases of herbivore arthropods, parasitic nematodes and microbial pathogens (Abe et al., 1987; Kondo et al., 1990; Arai et al., 2002).

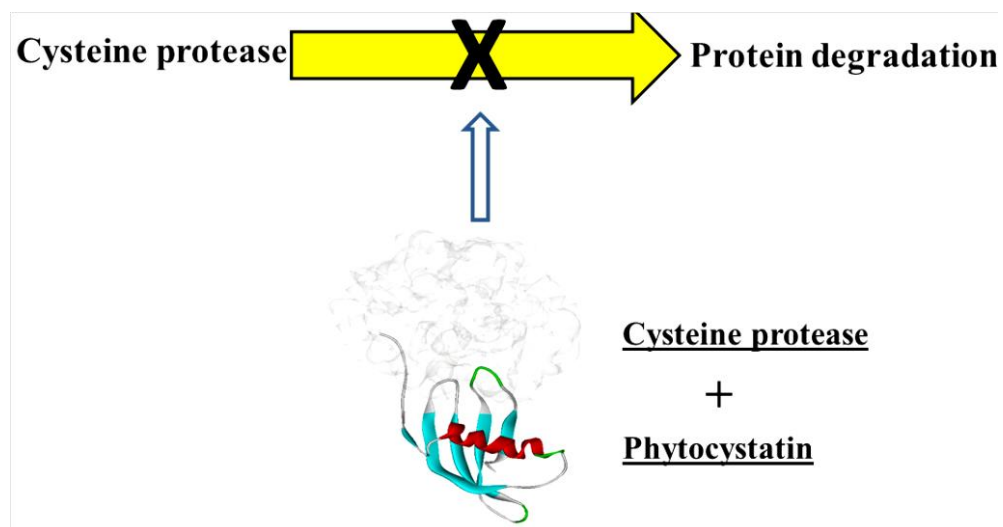


Figure 1.5 Cysteine protease inhibition by phytocystatin. After the formation of the cysteine protease-phytocystatin complex the cysteine protease activity on protein degradation is inhibited. Figure from Kunert et al. (2015).

1.4 Proteases, cystatins and stress

One of the current challenges in plant breeding is to achieve plant varieties with enhanced stress tolerance, which are able to resist the constant environmental changes (Araus et al., 2008; Witcombe et al., 2008). In the particular case of drought stress, most of the modified plants are more resistant due to alterations in their morphology or development, since smaller or dwarf phenotypes require lower amounts of water to survive in comparison with larger varieties (Lawlor, 2013). Nevertheless, the plant response to drought involves other factors such as nutrient and cell osmolyte contents.

The levels of expression and activity of certain proteases and proteases inhibitors are involved in the plant response to abiotic stress (Figure 1.6).

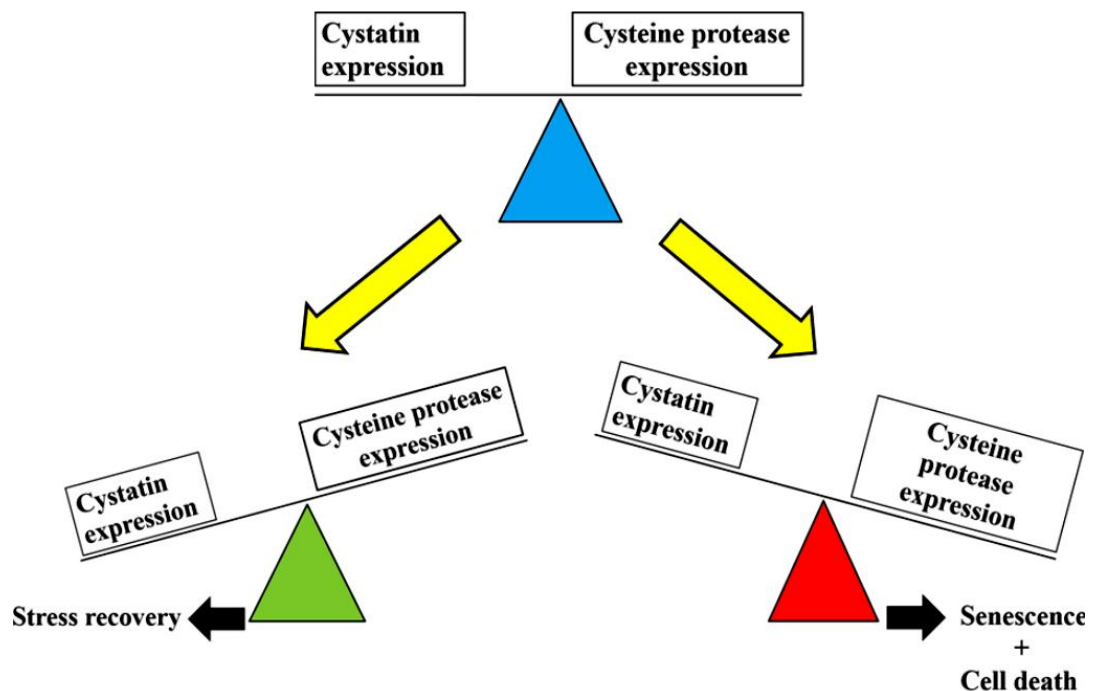


Figure 1.6 Effect of cysteine protease and cystatin expression in stress and senescence. Figure from Kunert et al. (2015).

Abiotic stress has an influence on the activity of proteases and their inhibitors at different levels i.e. gene expression, translation of transcripts to proteins, posttranslational modification leading to their activation, and by direct action on the molecule itself (Kunert et al., 2015). Regulation of protease activity by modification of their protease inhibitor systems has been effectively used in pest control (Christou et al., 2006; Kiggundu et al., 2010). At the same time, overexpressing genes encoding proteases have been reported to impart enhanced tolerance to stress, for instance, the increased expression of an aspartic protease gene, *ASPG1*, confers drought tolerance in *Arabidopsis* (Yao et al., 2012). Similarly, plants with constitutive expression of a gene coding for a putative papain-like cysteine protease have been shown to be more tolerant to salt and drought stress (Chen et al., 2010). Additionally, *Arabidopsis* plants overexpressing a barley gene coding for methionine aminopeptidase were more resistant to freezing (Jeong et al., 2011).

The expression of other genes encoding phytolectins is regulated by diverse abiotic stresses in different species. For example, phytolectin genes are expressed in *Arabidopsis thaliana* plants exposed to high salt, drought or heat stress (Zhang et al., 2008; Je et al., 2014). Interestingly, *AtCYS3*, which is induced by drought and cold, contains a conserved DRE element in its promoter sequence which has been identified in plant responses to drought, high salt and cold (Seki et al., 2001; Shinozaki et al., 2003; Yamaguchi-Shinozaki and Shinozaki, 2005). Moreover, high temperatures or wounding increase the expression of two other phytolectin encoding genes, *AtCYS1* and *AtCYS2* (Hwang et al., 2010).

The large increase in protease activity observed during abiotic stress is similar to that occurring in senescence. Examples of that are either drought stress (Cruz de Carvalho et al., 2001; Simova-Stoilova et al., 2009) or waterlogging (Stieger and Feller, 1994). Nonetheless, the type of proteases induced in developmental senescence differs to those expressed under drought conditions (Khanna-Chopra et al., 1999). In addition, constitutive expression of certain cystatins also increases resistance to biotic stress. For example, the wheat cystatin TaMDC1 prevents *in vitro* mycelium growth of the snow-mold fungus

(Christova et al., 2006), and the expression of a second wheat cystatin, WCM, destroys the fungus *Tellitia indica* when it is expressed in bacteria (Purwar et al., 2012). Likewise, the rice cystatin OCI has been shown to confer resistance to different types of stress detailed below.

1.5 OCI

Among all the plant cystatins, Oryzacystatin-I (OCI) is the best characterized to date (Abe et al., 1987). The cysteine proteases that are the substrates for OCI are involved in the degradation and mobilization of proteins during plant development. Constitutive expression of OCI in tobacco and soybean has shown that OCI protects photosynthesis against developmental and stress-induced senescence (Van der Vyver et al., 2003; Prins et al., 2008; Quain et al., 2014). Ectopic OCI expression delays the degradation of chloroplast proteins such as Rubisco (Prins et al., 2008). Besides, OCI expression protects plants against abiotic stresses such as chilling (Van der Vyver et al., 2003), biotic stresses such as insect herbivory (Zhao et al., 1996; Delledonne et al., 2001; Christou et al., 2006; Kiggundu et al., 2010) and virus infection (Gutiérrez-Campos et al., 2001). The ectopic expression of OCI in tobacco and soybean led to changes in plant developmental and senescence programmes (Figures 1.7 and 1.8). OCI overexpressing tobacco (OCE) plants present a slow growth phenotype; however, they are taller and with higher biomass accumulated when the vegetative growth stops (Figure 1.7) (Prins et al., 2008). Similarly, constitutive OCI expression caused slower development in soybean plants. The shoots of the soybean transgenic lines also have more branching and higher chlorophyll content (Figure 1.8) (Quain et al., 2014), plus their seeds accumulate higher amounts of soluble protein. Furthermore, OCI expressing soybean plants are more tolerant to drought, maintaining greater photosynthetic rates under such conditions. The drought resistance capacity has been also observed in *Arabidopsis* plants with ectopic OCI expression (Quain et al., 2014).

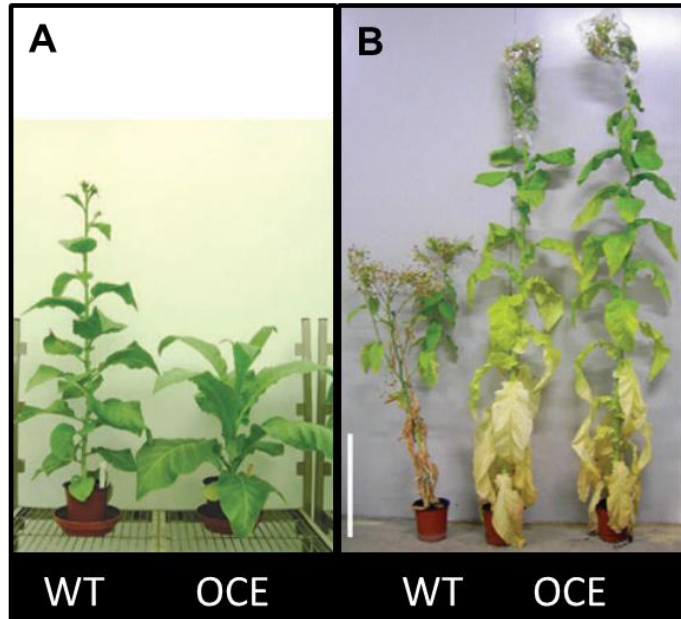


Figure 1.7 OCI over expressing tobacco lines (OCE) and wild type tobacco plants after 8 (A) and 14 weeks (B). Figure from Prins et al. (2008).

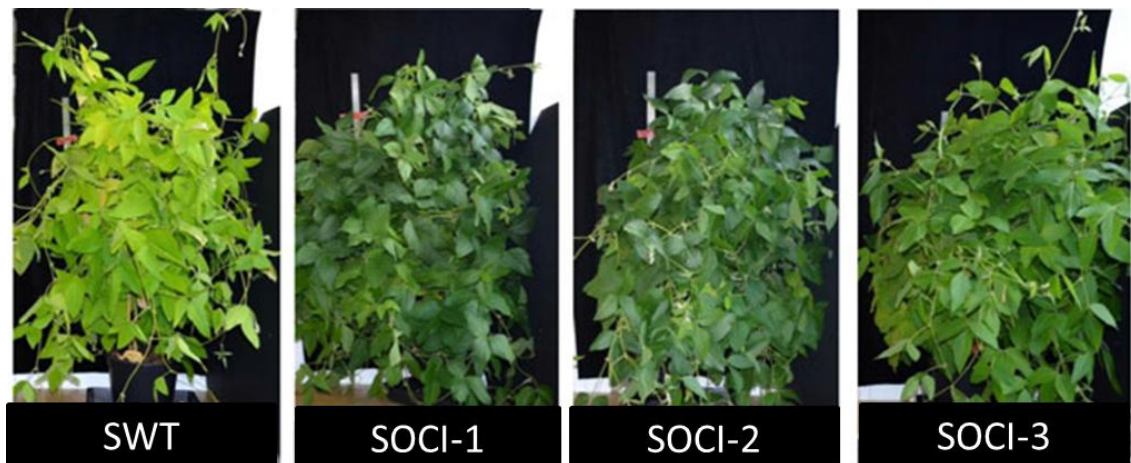


Figure 1.8 The effects of ectopic OCI expression on senescence in soybean. A comparison of shoot phenotype of three independent soybean lines with constitutive OCI expression (SOC1-1, SOC1-2, SOC1-3) and wild type soybean (SWT) at 18 weeks. Figure from Quain et al. (2014).

1.6 The effect of nitrogen deficiency on leaf protein turnover and photosynthesis

Nitrogen is the most important mineral nutrient required for plant growth (Marschner et al., 1996). Nitrogen deficiency triggers premature senescence and rapid degradation and turnover of leaf proteins. The loss of chlorophyll, the main component of the photosynthetic apparatus, is one of the first symptoms of senescence. Consequently, photosynthesis and TCA cycle activity are reduced, as strategy to save energy and nutrients (Lian et al., 2006). In contrast to photosynthetic genes, the expression of transcripts encoding Ndh subunits is increased during senescence (Lascano et al., 2003; Guera et al., 2005; Zapata et al., 2005). Ndh complex is homologous to the mitochondrial NADH dehydrogenase (Burrows et al., 1998; Casano et al., 2000; Casano et al., 2004). This complex binds photosystem I and together function in cyclic and chlororespiratory electron transport (Peng et al., 2009). In parallel, chloroplasts are dismantled and free fatty acids are released as a result of the thylakoid membrane dissolution (Harris and Arnott, 1973; Hortensteiner, 2006). Toxic metabolites such as fatty acids, or other catabolic products, are accumulated in plastoglobules which become abundant during nitrogen limitation (Kaup et al., 2002; Ischebeck et al., 2006; Vidi et al., 2006; Gaude et al., 2007; Besagni and Kessler, 2013). A massive turnover of proteins is needed to re-localize nutrients to the growing parts of the plant (Martínez et al., 2012). Chloroplast proteins, principally Rubisco, which contains a high content of nitrogen are degraded by proteases (Masclaux-Daubresse et al., 2008; Masclaux-Daubresse et al., 2010; Breeze et al., 2011; Roberts et al., 2012). Plant growth is in general limited by nitrogen deficiency. However, leaf protein and amino acid levels can be maintained as part of the adaptive response to such stress conditions (Tschoep et al., 2009). Recent evidence has shown that the single-stranded DNA-binding protein WHIRLY1 functions as an upstream suppressor of WRKY53 during leaf senescence in Arabidopsis (Miao et al., 2013). Moreover, WHIRLY1 was found to bind to the promoter of the barley *HvS40* gene, which is a marker for leaf senescence that is expressed during developmental and stress-induced senescence (Krupinska et al., 2014). However, little is known about the precise regulation and functions of WHIRLY1.

1.7 The WHIRLY1 protein

The whirly proteins share the DNA-binding KGKAAL domain which allow them to bind single stranded DNA (ssDNA) (Desveaux et al., 2000). In general, ssDNA binding proteins are responsible for binding and stabilising ssDNA until it is utilized by DNA polymerase or other proteins involved in DNA recombination and repair. The whirly protein family comprises two or three members depending on the plant species. For example, in Arabidopsis there are three whirly proteins, WHIRLY1 (ATWHY1) targeted to nucleus and chloroplast, and WHIRLY2 (ATWHY2) and WHIRLY3 (ATWHY3) located in mitochondria and chloroplast, respectively (Krause et al., 2005). In barley there are two whirly proteins, WHIRLY1 in the nucleus and chloroplasts, and WHIRLY2 in the mitochondria (Melonek et al., 2010).

At first, WHIRLY1 was believed to be exclusively restricted to the nucleus (Desveaux et al., 2000; Desveaux et al., 2004). Its presence in the chloroplasts was later confirmed by *in vitro* import assays into isolated chloroplasts, and immunological identification finally revealed that the WHIRLY1 protein localizes in the two compartments of the same cell (Krause et al., 2005; Grabowski et al., 2008). The WHIRLY1 protein has the same molecular weight in chloroplasts and the nucleus; it is synthesized on 80S ribosomes and then targeted to chloroplasts where it is processed by cleavage of an N-terminal plastid transit peptide (Grabowski et al., 2008). Immunological studies on tobacco transformed plants suggest that WHIRLY1 moves from chloroplast to nucleus (Isemer et al., 2012). The WHIRLY1 protein associates in tetramers and then in 24-oligomers, the latter structure is thought to bind to the thylakoid membrane (Desveaux et al., 2002; Cappadocia et al., 2010; Cappadocia et al., 2012).

Interestingly, the dual localization make these proteins ideal candidates for nucleus-to-plastid signalling. Besides, their roles vary depending on the plant species to which they belong; they were first identified in potato involved in pathogen defence (Despres et al., 1995) and thereafter different functions have been characterized.

The diverse roles of WHIRLY1 are detailed next and summarized in Table 1.1.

Table 1.1 Summary of functions of the WHIRLY1 protein.

Protein	Function	References
StWhy1	Pathogen response	Despres et al. (1995)
	ssDNA binding	Desveaux et al. (2000)
	Transcriptional activator	Desveaux et al. (2002)
AtWhy1	SA-mediated pathogen response	Desveaux et al. (2004)
	Regulator of telomere homeostasis	Yoo et al. (2007)
	Plastid genome stability	Marechal et al. (2009)
	Negative regulator of <i>AtKP1</i>	Xiong et al. (2009)
	Organelle genome repair	Cappadocia et al. (2010)
	ABA sensitive in seed germination	Isemer et al. (2012)
	WRKY53 repressor, delays senescence	Miao et al. (2013)
	Plastid DNA stability with polIB	Lepage et al. (2013)
	U-turn-like rearrangements suppression	Zampini et al. (2015)
ZmWhy1	Plastid biogenesis; ribosomal RNA metabolism and RNA splicing	Prikryl et al. (2008)
HvWhy1	Plastid nucleoids compact	Krupinska et al. (2014)
	HvS40 promoter binding	Krupinska et al. (2014)
	Redox sensor	Foyer et al. (2014)

At, *Arabidopsis thaliana*; *Hv*, *Hordeum vulgare*; *St*, *Solanum tuberosum*; *Zm*, *Zea mays*.

Pathogenesis-related (*PR*) genes are induced or repressed in response to pathogen attack (van Loon et al., 1994). In potato, the *PR-10a* binding factors 1 and 2 (PBF-1 and PBF-2) activate the *PR-10a* gene by binding the elicitor response element (ERE) of the promoter (Matton et al., 1993; Despres et al., 1995). Phosphorylation regulates PBF-1 and PBF-2 activity, which in the case of PBF-2 is determined by a homolog of the mammalian protein kinase C (Subramaniam et al., 1997). PBF-2 is a ssDNA binding protein composed of p24 subunits, which was called "whirly" because its quaternary structure has a whirligig appearance (Desveaux et al., 2000; Desveaux et al., 2002). In Arabidopsis, *WHIRLY1* participates in Salicylic Acid (SA) response in a NON-EXPRESSION OF PATHOGENESIS-RELATED PROTEINS (*NPR1*) independent manner (Desveaux et al., 2004). *AtWHIRLY1* and *NPR1* genes work simultaneously but in separate pathways in SA-responsive gene expression. Under SA treatment, both *AtWHIRLY1* and *NPR1* are activated. *AtWHIRLY1* binds to PB element and *NPR1* blocks *SNI1* gene inhibition and activates TGA transcription factors, as a consequence of the two actions the SA-responsive gene is expressed (Figure 1.9).

Additionally, *WHIRLY1* functions regulating other Arabidopsis genes such as the kinesin protein 1 (*AtKP1*). *AtKP1* belongs to a family involved in different cargo transport along microtubules, more specifically it interacts with the mitochondrial outer membrane regulating respiration during seed germination at low temperature (Yang et al., 2011; Li et al., 2012). Interestingly, over expression of *ATWHY1* and *ATWHY3* decreases *AtKP1* gene expression, having a stronger effect when SA is present (Xiong et al., 2009). In this line, studies with different *atwhy1 wrky53* mutants suggest that *WHIRLY1* represses the transcription factor *WRKY53* activity and subsequently delays senescence (Miao et al., 2013).

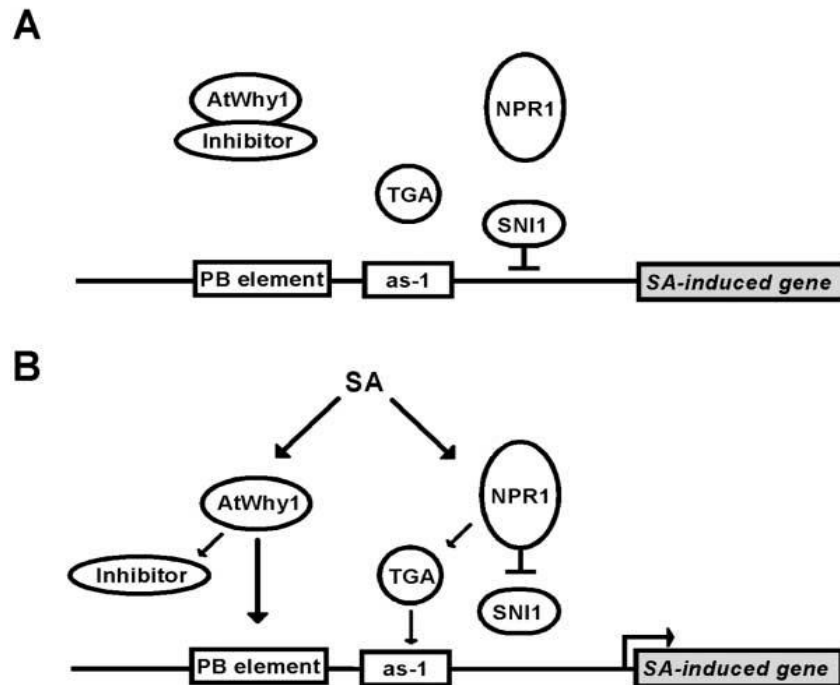


Figure 1.9 WHIRLY1 and NPR1 are required for SA-responsive gene expression in Arabidopsis. In natural conditions *ATWHY1* is inhibited and *SNI1* is repressing the expression of the SA-induced gene (A). Under SA, *ATWHY1* is released from the inhibitor and induces the PB element. *NPR1* activates *TGA* transcription factors which acts on *as-1* like elements and, simultaneously, it represses the *SNI1* gene inhibition (B). Figure from Desveaux et al. (2004).

The Arabidopsis WHIRLY1 protein has been also implicated in ABA signalling. The inhibition of seed germination by SA is thought to depend on ABA biosynthesis (Shakirova et al., 2003; Rajjou et al., 2006). *AtWhy1* mutants are less responsive to abscisic acid (ABA), such response greatly increases in lines over expressing the plastid *WHIRLY1*, suggesting that this form enhances ABA sensitivity during germination (Isemer et al., 2012).

In addition to the described roles as a transcriptional regulator, WHIRLY1 also maintains telomere homeostasis by regulation of telomerase activity, as demonstrated by studies of telomere length in Arabidopsis lines with altered levels of the *ATWHY1* expression (Yoo et al., 2007). Furthermore, the plastid DNA of Arabidopsis double knockout mutants *atwhy1 why3* showed errors in their sequence such as short direct repeats, indicating that WHIRLY1 and WHIRLY3 contribute to plastid genome stability preventing the illegitimate recombination (Marechal et al., 2009). Moreover, the Arabidopsis whirly proteins bind to ssDNA preventing microhomology-mediated break-induced replication (MMBIR), this type of DNA repair pathway causes errors in the plastid and mitochondrial DNA sequences (Cappadocia et al., 2010). The phenotype of the double knockout mutants *atwhy1 why3* is similar to the wild type (Marechal et al., 2009; Cappadocia et al., 2010). In contrast, a *atwhy1 why3 pollb-1* mutant that is also PollB defective, one of the two type-I chloroplast DNA polymerases, exhibited a more extreme yellow-variegated phenotype (Lepage et al., 2013). The *atwhy1 why3 pollb-1* mutants had a higher level of illegitimate recombination between repeated sequences and greater plastid genome instability than the wild type (Lepage et al., 2013). Moreover, these mutants showed lower photosynthetic electron transport efficiencies than the wild type leaves and they had a higher accumulation of reactive oxygen species (ROS) (Lepage et al., 2013). The higher level of oxidation observed in the *atwhy1 why3 pollb-1* triple mutants links these proteins to chloroplast to nucleus signalling and enhanced adaptation to oxidative stress (Lepage et al., 2013). These results suggest a potential interaction between chloroplast DNA polymerases and WHIRLY1.

The most extreme phenotype was observed in *WHIRLY1* knockout maize (Figure 1.10). In these plants, *WHIRLY1* is associated to plastid DNA and plastid RNA, plus it co-immunoprecipitates with CRS1, a protein involved in the splicing of a specific set of chloroplast introns. *Zmwhy1* mutants showed defects in ribosome synthesis which led to incorrect plastid biogenesis, suggesting an implication of WHIRLY1 in chloroplast RNA metabolism (Prikryl et al., 2008).

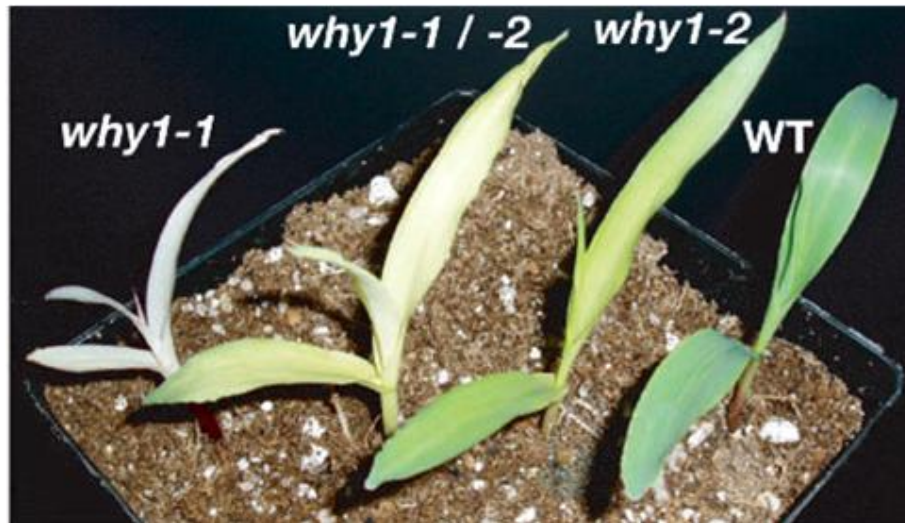


Figure 1.10 Comparison of the phenotypes of maize plants deficient in the WHIRLY1 protein to the wild type maize. Figure from Prikryl et al. (2008).

The use of next generation sequencing clarifies more specific roles of the *Arabidopsis* *WHIRLY1* and *WHIRLY3* genes in DNA repair mechanisms. Different combination of mutants indicate that the plastid whirlyies interact with RecA1 and PolIB preventing U-turn like rearrangements (Zampini et al., 2015). Such rearrangements are wrong strand fusions which finally result in organelle genome instability (Figure 1.11).

Moreover, sequencing of *atwhy1 why3*, *atpolIB* and *atrecA* independent mutants indicate that the WHIRLY proteins exclusively protect against microhomology-mediated recombination and not from other types of error prone mechanisms like non-homologous end joining (NHEJ) (Zampini et al., 2015).

Taken together, the different studies on plants with altered levels of *WHIRLY1* point to important roles of this protein in chloroplasts and DNA repair, hence a possible interaction with the plastid DNA polymerase should be considered. Moreover, WHIRLY1 seems to regulate the expression of certain genes related with pathogen defence (*PR* genes) and senescence (*WRKY53*).

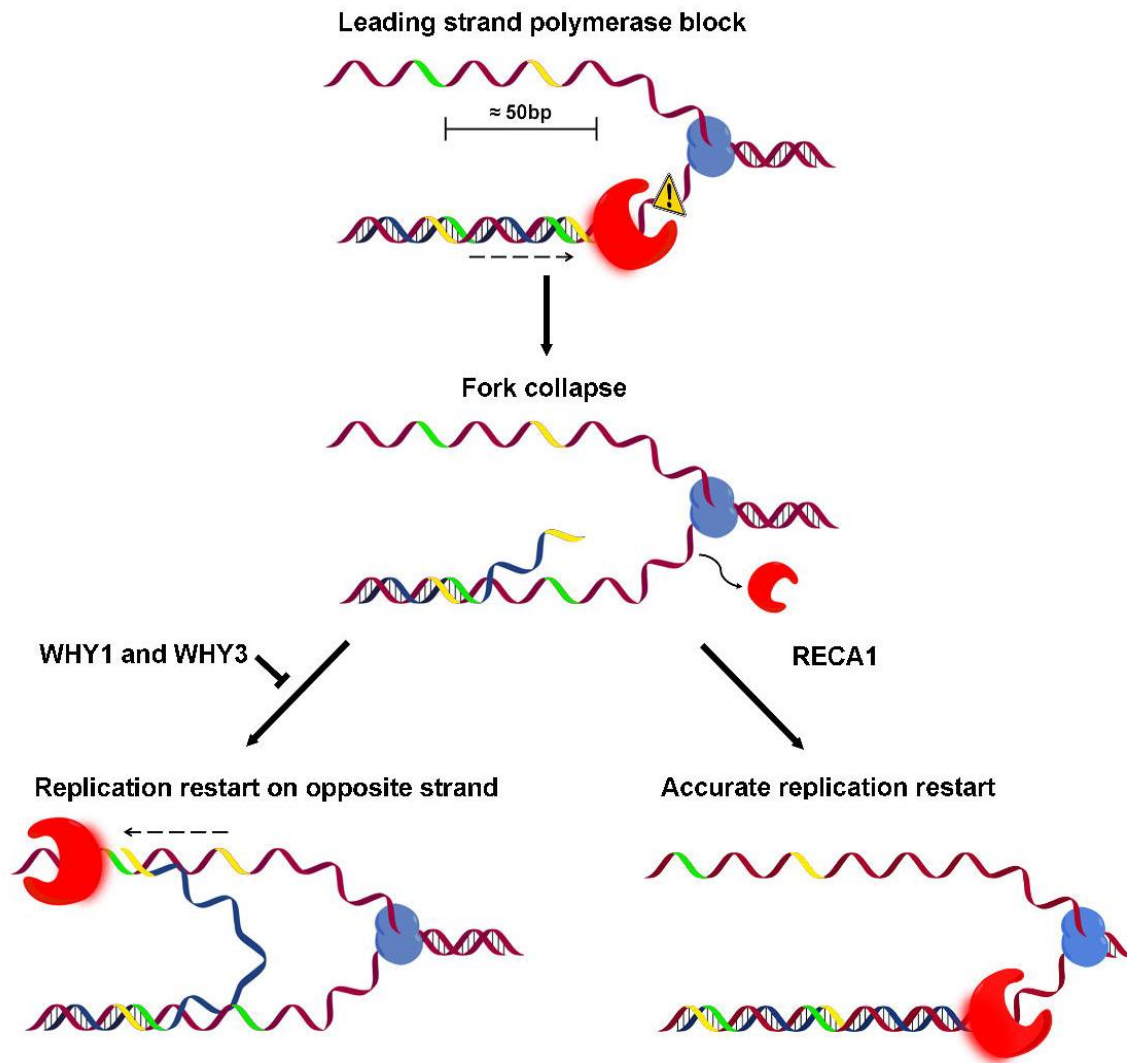


Figure 1.11 Whirly proteins and microhomology-mediated U-turn-like inversions. The red shape represents the DNA polymerase and the blue shape represents the DNA helicase. Yellow and green strands represent inverted microhomologies. Failures in polymerase activity can be corrected by RecA. However, without whirly and RecA proteins, inverted microhomologies result in the polymerase annealing to the opposite strand, therefore the replication cannot be continued correctly. Figure from Zampini et al. (2015).

1.7.1 The WHIRLY1 protein in barley

Chloroplasts contain up to 200 copies of the plastid DNA that is associated with non-histone proteins and RNA, which are arranged into nucleoids located to the inner envelope membrane (Sakai et al., 2004; Powikrowska et al., 2014). It has been shown that WHIRLY1 associates with plastid nucleoids in barley and maize (Melonek et al., 2010; Majeran et al., 2012). Recent analysis on WHIRLY1 deficient barley lines demonstrated that the absence of this protein largely increase the ptDNA levels and those of the transcript encoding the organelle DNA polymerase (Krupinska et al., 2014). Moreover, nucleic acid staining revealed that WHIRLY1 regulates the organization of plastid nucleoids, which were more compact when WHIRLY1 was over expressed in plastids and less compact in the transgenic knock down line 7 with very low levels of the *WHIRLY1* transcript (W1-7; Figure 1.12).

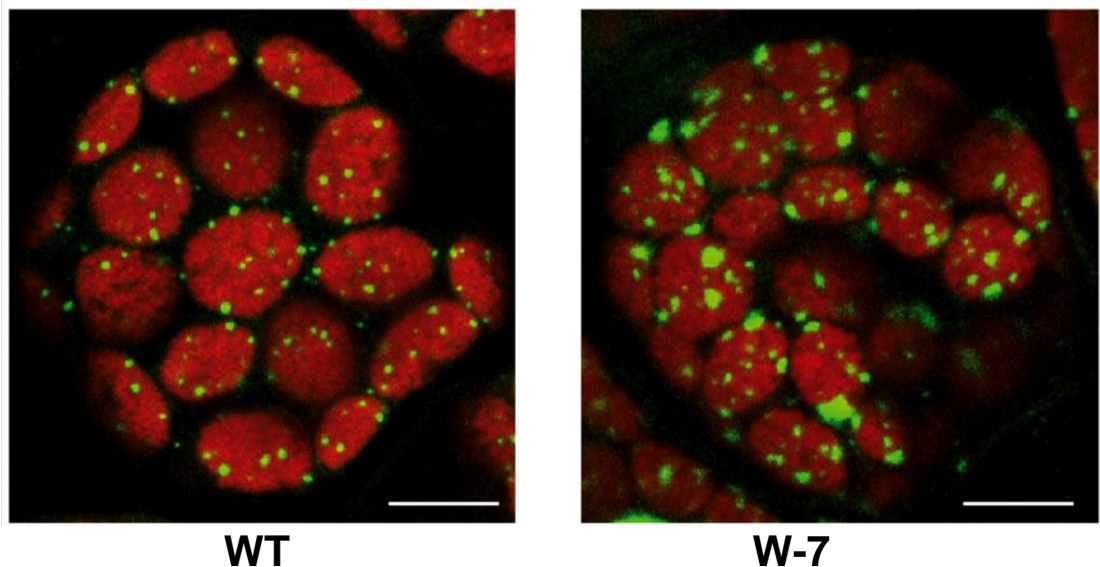


Figure 1.12 Morphology and distribution of chloroplast nucleoids in leaves of the wild type (WT) and the transgenic RNAi-W1-7 plants (W1-7). (Scale bar = 5 μ m). DNA stained in green (YO-PRO[®]-1). Figure from Krupinska et al. (2014).

Differently from other species, the barley lines with a knock down in *WHIRLY1* have similar phenotype to the wild type. Recent studies indicate that *WHIRLY1* binds to one of the two ERE motifs of the *HvS40* gene before senescence. Accordingly, *WHIRLY1* would release this motif becoming available for other transcription factors which would activate *S40* for the onset of senescence. A new potential role for *WHIRLY1* arises following this hypothesis, where it would regulate senescence through the control of *S40* expression (Figure 1.13) (Krupinska et al., 2014).

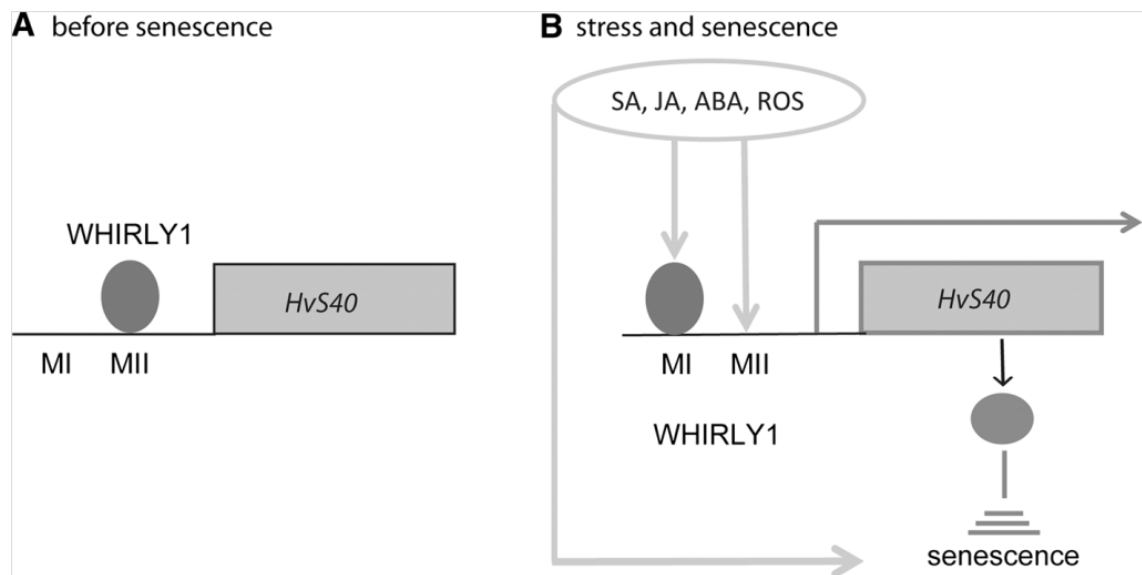


Figure 1.13 Hypothetical model of *HvS40* regulation by *WHIRLY1*. Before senescence, *WHIRLY1* is bound to the second elicitor response-like motif (MII) in the promoter of the *HvS40* gene (A). During senescence and stress, *WHIRLY1* moves to the first elicitor response-like motif (MI), and MII become available to other transcription factors controlled by hormones and ROS which induce *HvS40* expression (B) Krupinska et al. (2014).

The specific localization of WHIRLY1 suggests a role in chloroplast signalling and response mechanisms by regulation of gene expression (Foyer et al., 2014). It has been hypothesized that the WHIRLY1 protein acts as a sensor of the redox signals coming from changes in the photosynthetic electron transport chain, which are then translated to the nucleus (Figure 1.14). For that, the WHIRLY1 oligomer is released from the thylakoid membrane and subsequently the monomeric proteins are transferred into the nucleus. The exact mechanisms are presently unknown; however, it is possible that WHIRLY1 monomerization and relocation mechanisms are similar to those of the NONEXPRESSOR OF PATHOGENESIS-RELATED GENES 1 (NPR1). Such proteins are found in the cytosol and they move to the nucleus on the basis of the cell redox state; thioredoxin-dependent reduction of S–S bridges, protein nitrosylation and phosphorylation by kinases are likely to be involved in this process. It has been proposed that both, WHIRLY1 and NPR1, are implicated in cell redox response (Foyer et al., 2014).

A large number of studies are consistent with the link between chloroplast redox signals and nuclear gene expression as an acclimation response (Leister et al., 2011; Estavillo et al., 2012; Leister, 2012; Xiao et al., 2012; Foyer et al., 2014). However, the proteins and mechanisms involved in the transmission of signals from one compartment to another is not completely described. Due to its localization, WHIRLY1 could be considered as one of the proteins implicated in retrograde signalling (Foyer et al., 2014).

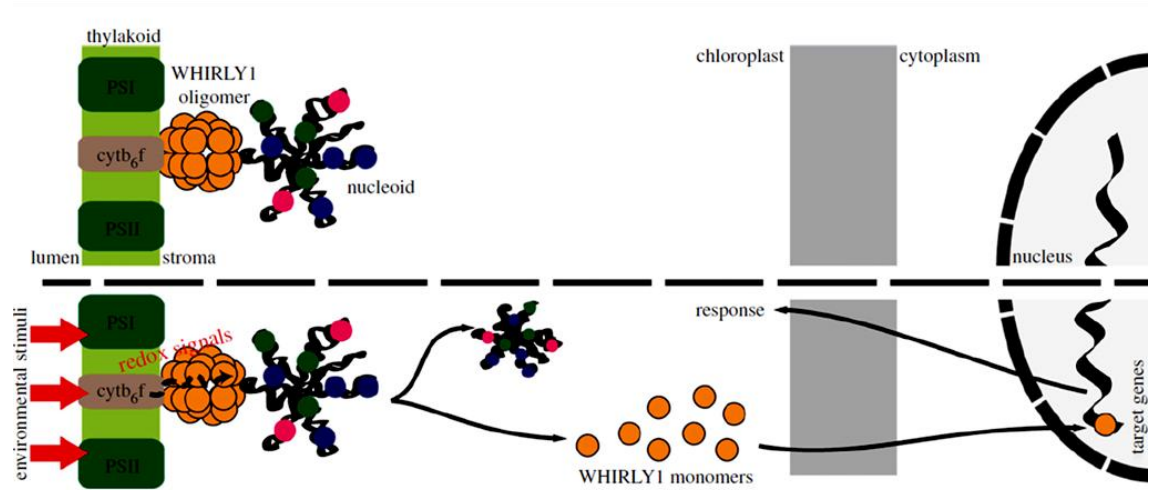


Figure 1.14 Hypothetical model of the role of WHIRLY1 in perception and transduction of redox signals from chloroplast to nucleus. In standard conditions, WHIRLY1 is anchoring the plastid nucleoid to the thylakoid membrane. Under stress, the redox signals from the photosynthetic apparatus release monomers of WHIRLY1 which are translocated to nucleus where they regulate gene expression. Figure from Foyer et al. (2014).

1.8 Hypothesis and project objectives

The hypothesis on which the following study is based is that it is possible to increase plant productivity through the control of lifespan and senescence. Moreover, leaf senescence and hence lifespan is influenced the WHIRLY1, OCI and SAG21 proteins. Since the precise functions of these proteins in regulating leaf protein turnover and senescence are poorly understood, the aim of the study was to characterise the functions of these three proteins in leaves in relation to photosynthesis and Rubisco protein turnover, carbon/nitrogen interactions, cellular redox state and protease activities during natural and stress-induced senescence. These studies were conducted in a model plant species (*Arabidopsis*) and on a major crop species (barley), which is an excellent grain crop model for research and crop development in Europe.

The specific objectives of this thesis study were as follows:

1. To characterise transgenic barley plants that are deficient in the WHIRLY1 protein in terms of plant physiology (photosynthesis, pigment and protein content, C and N contents, shoot and root biomass) and using transcriptomic and metabolomic approaches during natural and low N stress-induced senescence. These studies aim to provide novel insights into the role of the WHIRLY1 protein in regulating leaf metabolism and senescence.
2. To produce and characterise transgenic Arabidopsis and barley plants constitutively expressing different types of proteinase inhibitor in the cytosol and chloroplasts. The effects of these inhibitors on chloroplast protein turnover and leaf senescence were studied under optimal and stress conditions. The aim of these studies was to identify whether the ectopic expression of proteinase inhibitors can alter plant development and delay senescence.
3. To produce and characterise transgenic barley plants constitutively expressing the *SAG21/LEA5* protein. The effects of constitutive expression of the *SAG21/LEA5* protein on chloroplast protein turnover and leaf senescence was studied under optimal and stress conditions. These studies aimed to provide new information on how mitochondrial proteins influence plant development and delay senescence as well as the induction of autophagy.
4. To determine the precise functions of the WHIRLY1, OCI and SAG21 proteins in barley in natural and low N stress-induced senescence in relation to the regulation of photosynthesis, cellular redox state, protein turnover and the induction of autophagy genes, and to use this information to plan new strategies for plant improvement by manipulation of senescence.

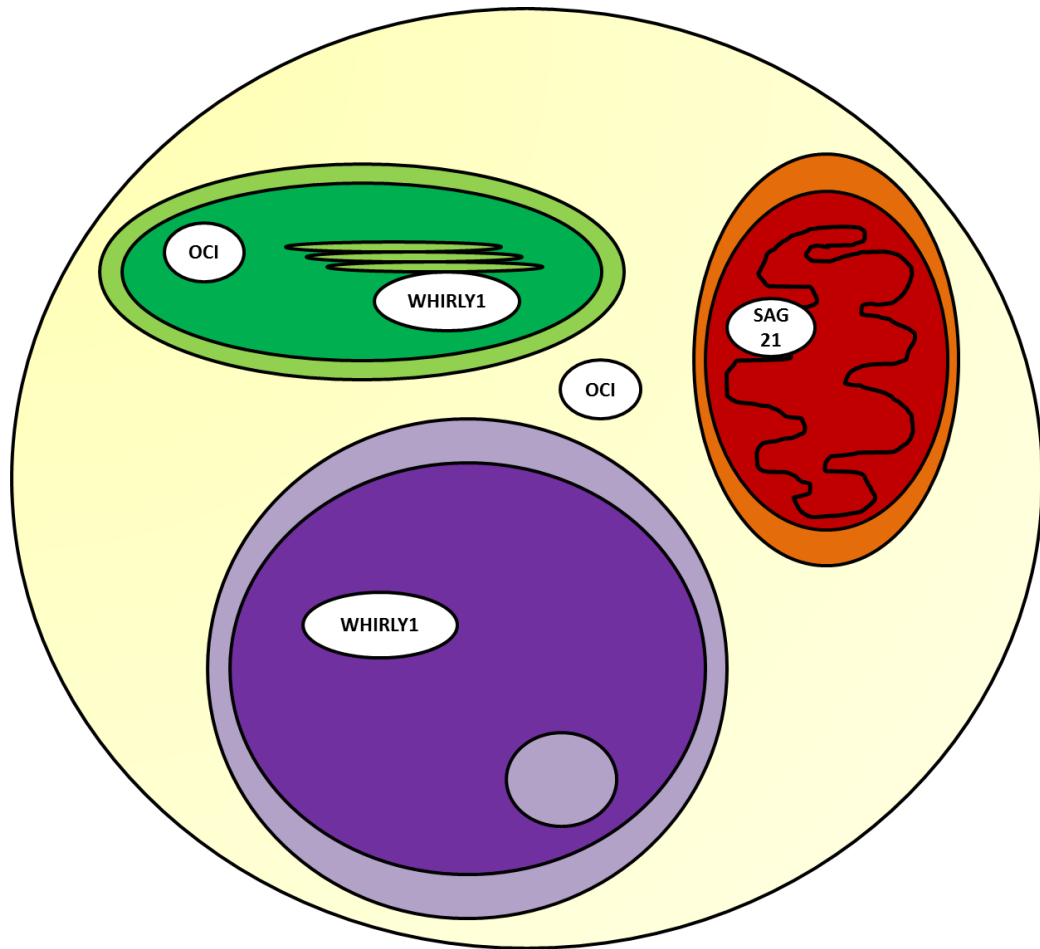


Figure 1.15 WHIRLY1, OCI and SAG21 localization in the cell.

The OCI protein is found largely in the cytosol, but also a small fraction in the chloroplasts and in the vacuole (Prins et al., 2008). The SAG21 protein is located in the mitochondria (Salleh et al., 2012). The WHIRLY1 protein is located in the plastids and the nucleus of the same cell (Grabowski et al., 2008).

Chapter 2. Materials and Methods

2.1 Plant material and growth conditions

2.1.1 Barley

Seeds of three independent transgenic barley (*Hordeum vulgare* L. cv. Golden Promise) lines with RNAi knockdown of the *WHIRLY1* gene (W1-1, W1-7 and W1-9) and wild type controls were provided by Dr Karin Krupinska (University of Kiel). Seeds (1 per pot) were germinated and grown in vermiculite in controlled environment chambers with a 16h light/ 8h dark photoperiod (irradiance $450 \mu\text{mol m}^{-2}\text{s}^{-1}$), 21°C/16°C day/night temperature regime and 60% relative humidity. The trays were provided with water every 2 days so that the bottom of each tray always contained liquid. In addition, 1L of nutrient solution was added per tray. The nutrient solution consisted of 0.2 mM KH_2PO_4 , 0.2 mM K_2SO_4 , 0.3 mM $\text{MgSO}_4 \cdot 7\text{H}_2\text{O}$, 0.1 mM NaCl, 0.1 μM MnCl_2 , 0.8 μM $\text{Na}_2\text{MoO}_4 \cdot 2\text{H}_2\text{O}$, 0.7 μM ZnCl_2 , 0.8 μM $\text{CuSO}_4 \cdot 5\text{H}_2\text{O}$, 2 μM H_2BO_3 , 50 μM Fe(III)-ethylenediaminetetraacetic acid (EDTA)-Na (modified from Anders et al., 2011). The plants were also provided with nitrogen (5 mM KNO_3) in the nutrient solution every 7 days. Wild type barley and *WHIRLY1* deficient lines were also germinated and grown on soil under the controlled conditions described above. Plants were harvested between 14-27 days after planting.

2.1.1.1 Barley plants grown under nitrogen deficiency

For the low nitrogen stress the WHIRLY1 knock down lines (W1-1, W1-7 and W1-9) and wild type barley seedlings were grown on vermiculite and nutrient solution was regularly added as described in 2.1.1. Once per week 2 litres of 0.1 mM KNO₃ were added to the tray.

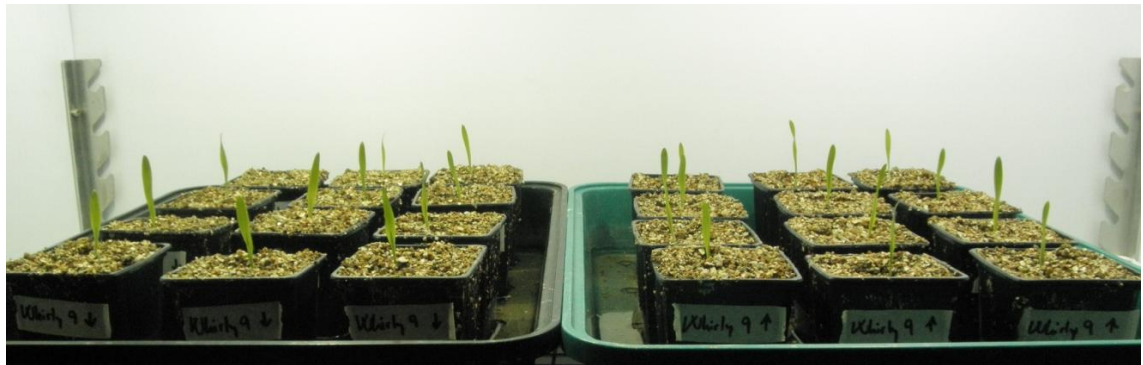


Figure 2.1 Barley seedlings growing on vermiculite under controlled conditions.

2.1.1.2 Barley plants grown under drought stress

Seeds of the wild type barley and WHIRLY1 transgenic line 7 (W1-7) were germinated on a mix of soil and perlite in controlled environment chambers with a 16h light/8h dark photoperiod (irradiance 300 $\mu\text{mol m}^{-2}\text{s}^{-1}$), 21°C/16°C day/night temperature regime and 60% relative humidity. After germination all plants were watered for a further 4 days, and then separated into 2 trays. One set of plants were watered regularly as described in 2.1.1 and those subjected to drought stress were completely deprived of water.

2.1.2 Arabidopsis

The OCI expressing Arabidopsis plants used were previously produced by Dr. Eugene Makgopa. pTF101.1_Cys-I was transformed into the plants by the floral dip method using the *A.tumefaciens* strain GV3101 (Clough and Bent, 1998). The plasmid contained the OCI cystatin encoding gene controlled by a double 35S promoter of the CaMV, ampicillin resistance gene and a CaMV terminator. In the following studies the T3 generation of these transformed plants was used.

2.1.2.1 Soil

Seeds of wild type Arabidopsis and the OCI transgenic lines were grown in 5 cm² pots containing soil in controlled environment chambers at 20-25°C and an irradiance of 400 μmol m⁻²s⁻¹ with a photoperiod of 8/16 hour light/dark cycle until the points of measurement or harvest.

2.1.2.2 PANG2 medium preparation and plate growth

For PANG2 medium a solution containing the following components was prepared: 1000 μl 1 M KNO₃, 500 mg MES, 400 μl 1 M FeS, 400 μl microstock (750 mg/l KI; 3000 mg/l H₃BO₃; 2000 mg/l ZnSO₄.7H₂O; 25 mg/l CuSO₄; 250 mg/l Na₂MoO₄.2H₂O; 25 mg/l CaCl₂.6H₂O) 150 μl 1 M CaCl₂, 100 μl 1 M NaH₂PO₄ and 20 μl 1 M MgSO₄, all of which was dissolved in H₂O and made up to 1 l. Then 5 g sucrose were added to the solution. The pH was adjusted to 5.7 with 0.2 M KOH and after that 10 g of agarose were added. The medium was autoclaved for 20 min at 121°C. PANG2 medium was poured into 12 cm² agar plates in a flow hood. The top 2 cm of medium was removed using a razor blade and seeds were placed at 1 cm intervals along the top of the medium. Following 48 hours stratification at 4°C in the dark, plates were positioned upright in a controlled environment at 20°C an irradiance of 400 μmol m⁻²s⁻¹ with a photoperiod of 8/16h light/dark cycle for seed germination.

2.2 Root morphology measurements

Seedlings of *Arabidopsis* with ectopic OCI expression and controls were grown for 11 days post germination. The plates were then photographed and analysed using the software Image J[®]. Primary root length and lateral root number were recorded and lateral root density calculated as the number of visible lateral roots per millimetre of primary root length for each root analysed.

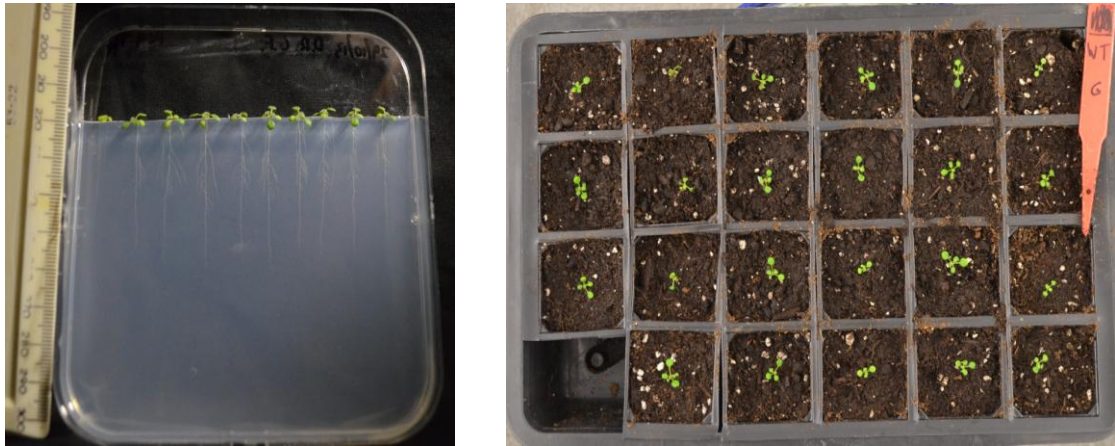


Figure 2.2 *Arabidopsis* seedlings growing on PANG2 plate (A) and soil (B).

2.3 Shoot and root biomass determination

Whole *Arabidopsis* or barley plants were harvested and separated into shoots and roots. These were weighed immediately and then dried in an oven at 80°C for 2 days after which the tissues were weighed again.

2.4 Soil and leaf water content

Soil and leaf water content was measured in WHIRLY1 transgenic line 7 (W1-7) and wild type barley seedlings during the drought experiment. Soil and leaf samples were collected and weighed every 2 days. They were dried in an oven at 80°C for 2 days after which the tissues were weighed again.

2.5 Experimental design used for transcriptomic and metabolomic profiles

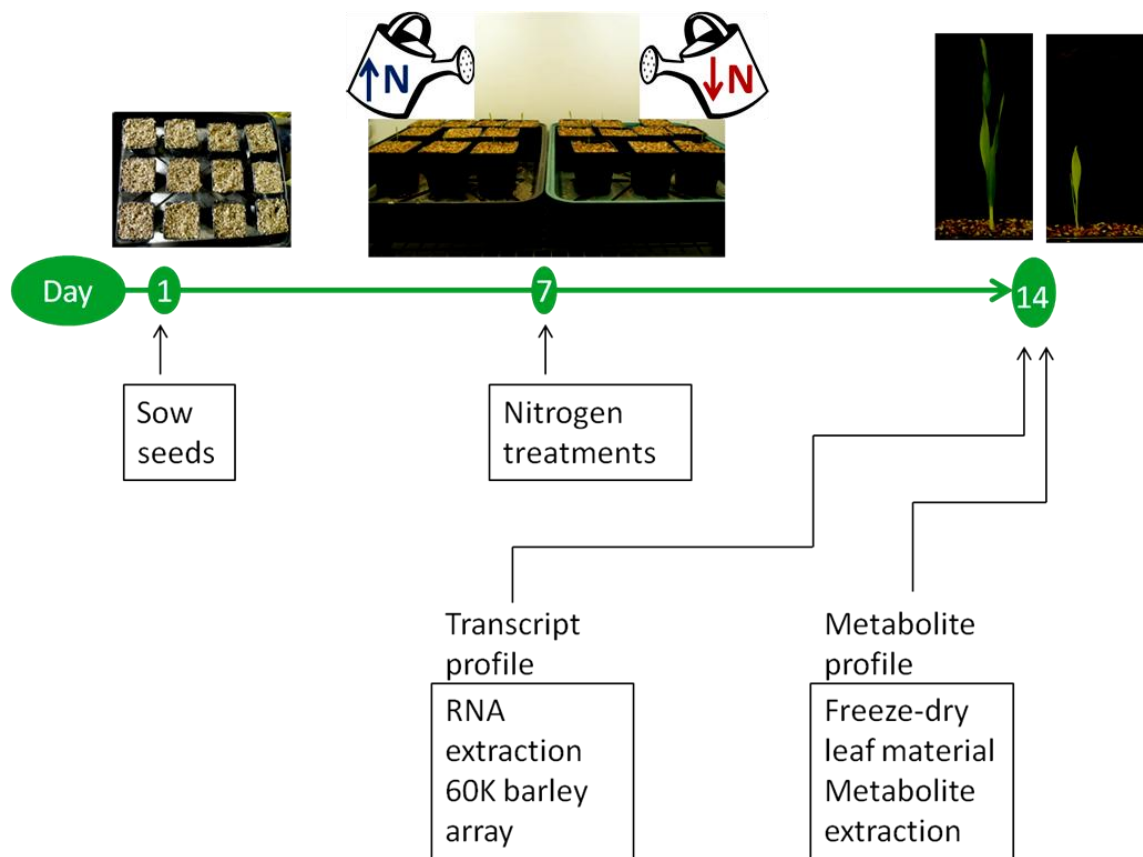


Figure 2.3 Experimental design used for time course transcriptomic and metabolomic analyses of the W1-7 line and wild type barley seedlings grown under N replete and N deficient conditions.

Seven days after sowing, seedlings of the W1-7 line and wild type barley were subjected to nitrogen replete (5 mM KNO₃) or nitrogen deficient (0.1 mM KNO₃) treatments in independent trays. The seedlings were grown for a further seven days, then leaves were harvested for analysis. RNA was extracted from first leaves for the microarray analysis. Second leaves were freeze-dried for metabolite analysis.

2.6 Microarray processing and analysis

The experimental procedures related to the microarray processing were performed by Jenny Morris at the James Hutton Institute, Dundee. Data extraction, quality control analysis and initial statistical analysis were carried out by Pete Hedley at the James Hutton Institute, Dundee.

Barley plants were germinated on vermiculite for one week, then grown with nitrogen repletion or nitrogen deficiency for a further 7 days. Microarray processing was performed on leaf RNA extracts from 4 biological replicates per genotype (WT and W1-7) and per treatment (N replete or N deficiency), using a custom-designed barley Agilent microarray (A21 MEXP-2357; www.ebi.ac.uk/arrayexpress). Microarray processing was performed according to the 'One-Color Microarray-Based Gene Expression Analysis' protocol (v. 6.5; Agilent Technologies). The procedure steps are illustrated in Figure 2.4. In short, cDNA was transcribed into cRNA which was amplified and purified to be finally labelled with Cy3. The mix was then hybridized to the array slides overnight. Next day the hybridized slides were washed twice and then dried. Agilent G2505B scanner was used to scan the hybridized slides at a resolution of 5 µm at 532 nm.

Data were extracted using Feature Extraction (FE) software (v. 10.7.3.1; Agilent Technologies) with default settings, and subsequently analysed using GeneSpring GX (v. 7.3; Agilent Technologies) software. Data were normalised

using default Agilent FE one-colour settings in GeneSpring and filtered to remove inconsistent probe data flagged as absent in more than one replicate per sample. Probes were identified as significantly changing between genotype & nitrogen treatment using 2-way Analysis Of VAriance (ANOVA) with a pvalue of <0.05 with Bonferroni multiple-testing correction. Raw data can be accessed via the array express website (www.ebi.ac.uk/arrayexpress) using accession number EMTAB-2242.

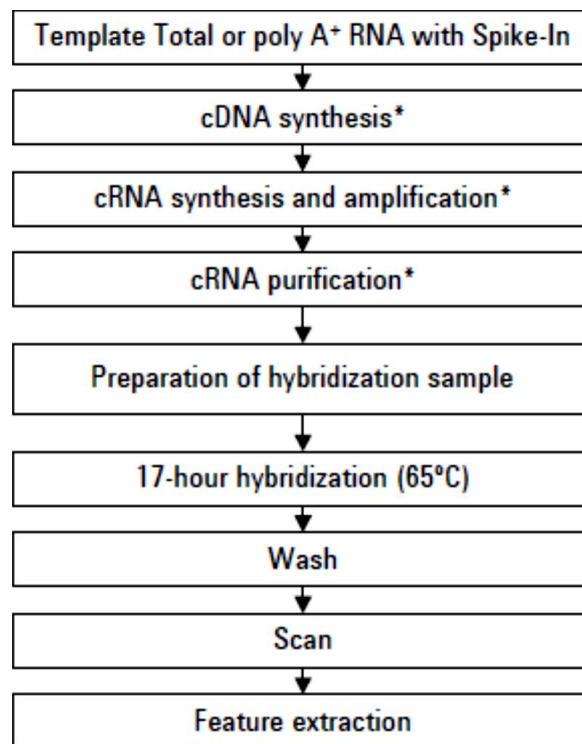


Figure 2.4 Sample preparation and array processing scheme.

2.6.1 60 K barley array

The microarray contains c. 61,000 60-mer probes derived from predicted barley transcripts and full-length cDNAs (IBGSC, 2012). These probes were selected from a total of ~80,000 predicted genes by prioritising them according to their annotation (see section S7.1.4 and Figure S18 in supplementary material file of IBGSC, 2012). The high-confidence gene set was used in its entirety (n = 26,159). This set of predicted genes is based on being supported by homology to at least one closely related species (*Brachypodium distachyon*, *Sorghum bicolor*, *Oryza sativa* and *Arabidopsis thaliana*). Next, 14,481 genes were added that had been annotated as “remote homologs”, based on a lack of homology to monocot proteins. Then, another 7,999 genes from the “Triticeae-specific” category were added, which is defined as having significant BLASTN hits to the wheat fl-cDNA library but no significant BLASTX hit to angiosperm reference protein sequences. The remainder of sequences on the chip (n = 12,848) derive from genes that had no homology to any of the databases used and are assumed to be specific to barley. This resulted in a total of 61,487 genes represented on the chip by a single probe sequence each.

2.7 Quantitative Real-Time RT-PCR (qRT-PCR)

For the microarray validation, 8 genes were selected based on their different expression between the genotypes. qRT-PCR was performed using Roche FastStart Mix and the Universal Probe Library (UPL) system (Campbell et al., 2010). The cDNA equivalent of 10 to 20 ng of total RNA was used in a 25 µl PCR reaction on a StepOne Plus machine (Applied Biosystems). The reaction mixture comprised of 5 µl cDNA, 12.5 µl FastStart Mix (+Rox) (Roche), 6.75 µl H₂O, 0.25 µl of each forward (F) and reverse (R) primer (20 µM) and 0.25 µl of each probe (10 µM). Reactions were performed on 96 well plates in three technical replicates. The same master mix recipe without cDNA was used as negative control. Real-time cycler conditions were as follows: incubation at

95°C for 10 min; 40 cycles of amplification consisting of 95°C for 15 s, 60°C for 1 min; and 72°C for 30 s.

To normalize the qRT-PCR data for barley, the *At3g18780 (Actin-2)* gene was used. Primers were designed using the Universal Probe Library System (Roche) so that the target amplicon size is 60-65 nucleotides.

Table 2.1 Primers used for qRT-PCR in barley.

Description	Accession	Probe	Primer sequence
Cysteine proteinase	AK364080	20	F 5'-gctgattcggtcagtggtg-3' R 5'-cggtgcttatagcgtagcgt-3'
Heat shock transcription factor	MLOC 74270	29	F 5'-cagcttcgctgtcttcagc-3' R 5'-tgcttgaagtacttggggaga-3'
Amino acid permease	AK369769	80	F 5'-gtcgaggtcgtcctgtcg-3' R 5'-cacgatggagacgaaggtg-3'
Alternative oxidase	AK365405	160	F 5'-tctcagtcacagctgttacg-3' R 5'-atccaaattaacgggacgaa-3'
Poly [ADP-ribose] polymerase	MLOC 5569	25	F 5'-gcagtgaaaagattggtggaa-3' R 5'-ttcatgtattgcgtcagttttg-3'
Glutaredoxin family protein	MLOC 55037	97	F 5'-cttcatcacgcggccat-3' R 5'-gcgcgctacacataacata-3'
NAD(P)H-quinone oxidoreductase chain 4	MLOC 24854	142	F 5'-tcgagataaacaagacgcatc-3' R 5'-ccatggattattggtgcta-3'
Ammonium transporter	AK252569	149	F 5'-cttcatggcgtctacgc-3' R 5'-atgtttaggccagacgac-3'

2.8 Metabolite analysis

2.8.1 Determination of ascorbic acid, glutathione and pyridine nucleotides

Ascorbate, glutathione and pyridine nucleotides were measured in W1-7 and wild type barley leaves following the protocol described by Queval and Noctor (2007). All the steps were performed on ice (with the exception of the sample treatments which are indicated) and all the reactions were carried out in triplicate. The buffers and reagents used in the assays were freshly prepared.

2.8.1.1 Ascorbate and glutathione extraction

100 mg of frozen barley leaves were ground in liquid nitrogen. Samples for ascorbate and glutathione were extracted in 1 ml 0.2 M HCl, and then centrifuged 10 min at 14000 rpm and 4°C. 50 µl NaH₂PO₄ 0.2 M pH 5.6 were added to 0.5 ml supernatant, then sufficient NaOH 0.2 M was added to obtain pH 3-4.

2.8.1.1.1 Ascorbate assay

Ascorbate oxidase (AO) converts reduced ascorbate to oxidized ascorbate. Reduced ascorbate is measured in non-treated samples. Then the two ascorbate forms are measured together as “total ascorbate” after a complete reduction of the ascorbate present in the extracted samples by incubation with dithiothreitol (DTT).

For total ascorbate 100 µl sample was incubated with 140 µl 0.2 M NaH₂PO₄ (pH 7) and 10 µl 25 mM DTT for 30 min at room temperature. Total and reduced ascorbate were measured mixing 40 µl treated or non-treated sample,

100 μl 0.2 M NaH_2PO_4 (pH 5.6) and 55 μl water per well. To oxidize the samples, 0.2 U of AO were added to each well. The absorbance of each reaction mixture was measured at A_{265} before and after enzyme addition. The ascorbate contents were calculated deducting the values obtained after the addition of ascorbate oxidase from the ones recorded before the enzyme addition.

2.8.1.1.2 Glutathione assay

This method is based on the GR-dependent reduction of 5,5'-dithiobis (2-nitrobenzoic acid) (DTNB, Ellman's reagent), monitored at 412 nm. Without pretreatment of extracts, total glutathione is measured, which consists of both the reduced (GSH) and oxidised (GSSG) forms. GSSG content is measured by treating the extracted samples with 2-vinylpyridine (2VPD).

For total glutathione 0.2 nmol, 0.4 nmol and 1 nmol standards were prepared from an initial 10 mM GSH stock. Each reaction mixture consisted of: 20 μl sample or standard, 100 μl 0.2 M NaH_2PO_4 EDTA (pH 7), 50 μl water, 10 μl 10 mM NADPH and 10 μl 12 mM DNTB (prepared in 0.2 M NaH_2PO_4 , pH 7.5). Reaction was started by adding 0.2 U of glutathione reductase (GR) per well. For oxidized glutathione 0.02 nmol, 0.04 nmol and 0.08 nmol standards prepared from stock solution of 10 mM GSSG. Samples and standards were treated with 3 μl 2VPD for 30 min at RT. Samples and standards were then centrifuged for 10 min at 4°C twice (140 μl of the supernatant from the first centrifugation were transferred to another tube which was again centrifuged, from here 20 μl of supernatant were added to the plate). Following that, treated samples were measured using the same reaction mixture as the non-treated samples for total glutathione. Finally the rate of change of absorbance was read at A_{412} and glutathione content in samples estimated by reference to standard curves.

2.8.1.2 NAD, NADH, NADP and NADPH assays

To measure pyridine nucleotides 1 ml 0.2 M HCl (NAD and NADP) or 1 ml 0.2 M NaOH (NADH and NADPH) was added to the frozen ground sample in the mortar, and then centrifuged 10 min at 14000 rpm and 4°C. Samples were heated at 90°C for 1 min. Then 50 µl NaH₂PO₄ 0.2 M pH 5.6 were added to the samples. For NAD and NADP NaOH 0.2 M was slowly added until pH was 5-7 (approximately 400 µl). For NADH and NADPH HCl 0.2 N was slowly added until pH was 7-9 (approximately 300 µl). The standard curves were prepared diluting 10 mM stock of NAD, NADH, NADP and NADPH to concentrations of 2 µM, 1 µM and 0.5 µM. For NAD and NADH measurement, 20µl of either sample or standard was added to wells containing 100µl 0.1 M HEPES EDTA (pH 7.5), 25 µl water, 20 µl 1.2 mM DCPIP, 10 µl 20 mM PMS, 10 µl 2.5 M ADH (prepared in 0.1 M HEPES EDTA, pH 7.5) and finally 15 µl absolute ethanol to start the reaction. For NADP and NADPH measurement, reactions were carried out in triplicate and 20 µl of either sample or standard were added to wells containing 100 µl 0.1 M HEPES EDTA (pH 7.5), 30 µl water, 20 µl 1.2 mM DCPIP, 10 µl 20 mM PMS, 10 µl 10 mM G6P and 10 µl 0.2 M G6PDH to start the reaction. The reactions were read at 600 nm for 5 min (12 cycles of 25 s with plate shaking between each).

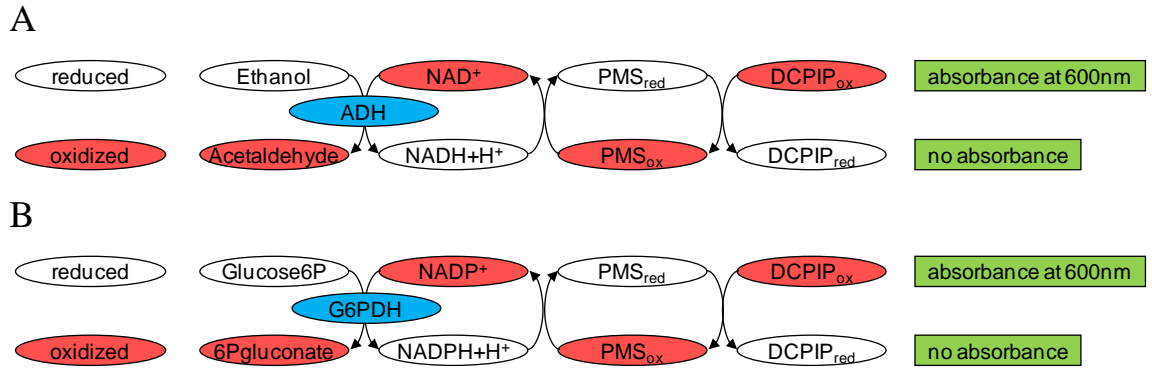


Figure 2.5 Pyridine nucleotides determination. The method is based on the reduction of dichlorophenol indolphenol (DCPIP) by phenazine metho sulphate (PMS) in the presence of alcohol dyhydrogenase (ADH) and ethanol (NAD/NADH, A) or glucose-6-phosphate and Glucose-6-phosphate dehydrogenase (NADP/NADPH, B). The reduction of DCPIP can be visualized during the assay, as it changes from blue colour to a colourless DCPIPH being measured by a decrease in absorbance at 600 nm (Ke et al., 1995).

2.8.2 Carbon and nitrogen content measurements

The carbon and nitrogen contents were determined on the dried leaf and root material from 5 biological replicates per genotype (W1-1, W1-7, W1-9 and wild type barley) and per treatment (N replete or N deficient), using a LECO Trumac combustion analyser (Yara UK Limited Company, York, UK).

2.8.3 Total protein quantification

Total protein content was determined following the method of Bradford (1976). Individual leaves were harvested and weighed. 100 mg of each sample were placed in labelled foil wraps. Metabolism was then immediately stopped by placing the foils in liquid N followed by storage at -80°C until analysis. Prior to analysis samples were placed in pre-cooled mortars and ground in liquid N₂. 1 ml of ice-cold extraction buffer (50 mM Tris-HCl, pH 7.5) was added to each

sample. Then, samples were centrifuged at 12000 g for 10 min and the supernatant was collected. A calibration curve was made using BSA (1 mg/ml) as standard and sequential dilutions to have 0.5, 0.25, 0.125, 0.06325 mg/ml. For the assay in the plate reader, 5 µl of sample or standard and 250 µl of Bradford reagent were added to each well. The blank was made using 5 µl of the buffer used and 250 µl of reagent. Samples, blanks and standards were added in triplicates. The plate was kept at room temperature for 5 min and the absorbance read at 595 nm. The final concentration was calculated as mg protein/g FW.

2.8.4 Leaf pigment analysis

Individual leaves were harvested and weighed. 100 mg of each sample were placed in labelled foil wraps. Metabolism was then immediately stopped by placing the foils in liquid N followed by storage at -80°C until analysis. Prior to analysis samples were placed in pre-cooled mortars and ground in liquid N₂. 1 ml of ice-cold 95% ethanol was added to each sample. The samples were then centrifuged at 4°C for 10 min and the supernatants were collected for analysis. Samples were added to the plate in triplicates. The absorbance at 470 nm, 649 nm and 664 nm was recorded in the plate reader or spectrophotometer using a standard 95% ethanol solution as a blank. To calculate the pigment concentrations the following equations were used (Lichtenthaler, 1987):

$$\text{Chlorophyll } a = 13.36A_{664} - 5.19A_{649}$$

$$\text{Chlorophyll } b = 27.43A_{649} - 8.12A_{664}$$

$$\text{Total chlorophyll } (a+b) = 5.24A_{664} + 22.24A_{649}$$

$$\text{Carotene} = (1000A_{470} - 2.13Ca - 97.64Cb)/209$$

The amount of pigment per g FW was then calculated as µg protein/g FW.

2.8.5 Targeted metabolomics

Second leaves of 14 day old W1-7 and wild type barley seedlings grown under nitrogen replete and nitrogen deficiency were weight and freeze-dried for 48 h. The samples were lyophilised in a Gamma 1-16 LSC freeze drier (Martin Christ Gefriertrocknungsanlagen GmbH, Germany) at a pressure of 0.7 mbar using a shelf temperature of 25°C and a condenser temperature of -50°C. For extraction and derivatization of polar and non-polar metabolites, the freeze-dried samples were subjected to sequential extraction with methanol, chloroform and water in the presence of internal standards of ribitol and nonadecanoic acid methyl ester. Polar and non-polar compounds were transferred to separate vials following phase separation of the extraction medium. An aliquot of the polar extract was dried and derivatized with methoxylamine hydrochloride (to form methyloximes of sugars) and then N-methyl, N-trimethylsilyl trifluoroacetamide [MSTFA; to form trimethylsilyl (TMS) derivatives of hydroxyl and carboxyl groups]. The non-polar extract was dried, transesterified with methanolic sulphuric acid and treated with MSTFA. Retention standards were added to aliquots of the derivatized polar and non-polar samples and they were measured by GC-MS. The protocol used for the extraction and analysis are described in detail below.

2.8.5.1 Extraction of polar and non-polar fractions

Freeze-dried barley leaves were weighed out into a culture tube (150 x 16 mm). Weight was recorded, and extraction volumes were adjusted according to sample weight. For 100 mg sample weight the following extraction procedure was used. 3 ml methanol was added to each sample and tubes were capped and transferred to a rotary shaker and shaken at 1500 revolutions min⁻¹ at 30°C for 30 min. 100 µl each of polar (ribitol 2 g L⁻¹ in water) and non-polar (nonadecanoic acid methyl ester 0.2 g L⁻¹ in methanol) internal standards were added along with 0.75 ml water and samples were shaken as previously described for a further 30 min. 6 ml chloroform was added and samples were shaken for a further 30 min at 2500 revolutions min⁻¹ at 30°C. Finally an

additional 1.5 ml water was added and the samples were vigorously shaken by hand prior to separation of the polar and non-polar phases by centrifugation at 1000 g for 10 min. Polar (upper layer) and non-polar (lower layer) fractions were separated using a pasteur pipette into different amber vials (8 ml) and stored at -20°C until derivatization which was undertaken within a maximum of 2 days.

2.8.5.2 Derivatization of polar fraction

Tubes containing the polar extracts were removed from freezer and allowed to warm up to room temperature. 250 µl of the polar fraction were pipetted into culture tubes (100 x 16 mm) and. For nitrogen deficient samples 1 ml was pipetted as the weight was lower. Next, tubes were transferred to a centrifugal evaporator until dry. In order to oximate samples, a solution of 20 mg methoxylamine hydrochloride (98%) was made up in 1 ml of anhydrous pyridine. 80 µl of methoxylamine hydrochloride solution were added to the dried polar fractions and they were incubated at 50°C for 4 h. During the incubation period, 50 µl of a retention standard mixture comprising linear alkanes of chain lengths C11, C13, C16, C20, C24, C30, C34 and C38 dissolved in isohexane were added to amber autosampler vials (300 µl fixed glass inserts with PTFE coated snap caps) and the isohexane was allowed to evaporate in the vials at room temperature. Following oximation, 80 µl of N-methyl, N-trimethylsilyl trifluoroacetamide (MSTFA) were added to samples using a 100 µl glass syringe, and incubation continued for a further 30 min at 37°C. Finally, 40 µl of the derivatized polar fractions and 40 µl of dry pyridine were added to the amber autosampler vials containing the dried retention time standards. The polar fractions were then ready for analysis by GC-MS.

2.8.5.3 Derivatization of non-polar fraction

Non-polar fraction was dried in a centrifugal evaporator for 30 min without heating. Then 1 ml chloroform and 2 ml 1% methanolic sulphuric acid were

added (1 ml concentrated sulphuric acid in 100 ml methanol, freshly made up). The tubes were heated for 16 h at 50°C to release free fatty acids. Tubes were removed from the heating block and cooled to room temperature. 5 ml of 5% (w/v) aqueous sodium chloride and 3 ml chloroform were added to each tube, they were shaken vigorously and polar and non-polar layers allowed to settle. Then the top aqueous layer was removed and discarded. 3 ml of 2% (w/v) aqueous potassium hydrogen carbonate was added to the lower solvent layer and the sample was again vigorously shaken. Following settling, the top aqueous layer was again removed and the lower chloroform:methanol layer was pipetted through freshly prepared columns of anhydrous sodium sulphate (3 cm columns prepared in cotton wool plugged pasteur pipettes, and prewashed with 4 ml chloroform) to remove any residual water. Column flow through was collected in culture tube (100 x 16 mm) and the columns were washed with an additional 2 ml chloroform that was collected with the fractions. Then the fractions were dried down in the centrifugal evaporator for 60 min. Following that, 50 µl chloroform, 10 µl anhydrous pyridine and 40 µl MSTFA were added and heated at 37°C for 30 min in an incubator. Finally, 40 µl of the derivatized non-polar fraction were added to 40 µl of anhydrous pyridine in autosampler vials that had previously been prepared with retention time standards as described in 2.8.5.2 The non-polar fraction was then ready for analysis by GC-MS.

2.8.5.4 Sample analysis

Samples were analysed on a DSQ II Single Quadrupole GC-MS system (Thermo). 1 µl of the sample was injected with a split ratio of 40:1 into a programmable temperature vaporising injector under the following conditions: injection temperature of 132°C for 1 min, transfer rate 14.5°C/s, transfer temperature 320°C for 1 min, clean rate 14.5°C/s and clean temperature 400°C for 2 min. Analytes were chromatographed on a DB5-MSTM column (15 m x 0.25 mm x 0.25 µm; J&W, Folsom, USA) using helium at 1.5 ml/min in constant flow mode as mobile phase. The temperature gradient was 100°C for 2.1 min, then 25°C/min to 320°C, and isothermal for 3.5 min. The interface temperature was 250°C. Mass data were acquired at 70 eV electron impact ionization

conditions over a 35 – 900 a.m.u mass range at 6 scans per sec with a source temperature 200°C and a solvent delay of 1.3 min. Acquisition rates were set to give approximately ten data points across a chromatographic peak. Xcalibur™ v1.4 and Xcalibur™ v2.0.7 software packages were used to acquire and analyze the data, respectively. A processing method developed at James Hutton Institute was used to assign identities to the peaks. It uses the retention times and masses of known standards and the Genesis algorithm (part of the Xcalibur™ package) for peak integration. The expected retention time for each peak was adjusted using the retention times of the retention standards. The integrated area of the annotated peaks was normalized against the integrated area of the respective internal standards, ribitol and nonadecanoic acid for the polar and non-polar fractions, respectively. The peak area ratios were normalized on a dry weight basis.

2.9 Volatiles assay

Volatile emission was measured in W1-7 and wild type barley seedlings at 16 and 18 days after sowing. Volatiles were collected by exposing a CAR/PDMS-coated 85 mm SPME fibre within an enclosed chamber close to the leaf lamina for 2 h. Volatiles were analysed using a Thermo Finnigan Trace gas chromatograph coupled to a Finnigan Tempus PLUS TOF mass spectrometer (Thermo Scientific, UK). Volatiles were desorbed in the injection port (280°C) for 3 min and resolved on a DB1701 GC column (30 m x 0.25 mm x 0.25 mm; J&W Scientific, Folsom, CA, USA) using helium as carrier gas at 1 ml min⁻¹ in constant flow mode. The GC temperature was held isothermally at 45°C for 2 min, ramped to 180°C at 5°C min⁻¹ and then to 220°C at 20°C min⁻¹. Detection was achieved in the electron impact mode at 70eV. Data were acquired and analysed using the Xcalibur software package v. 1.4. Compounds were identified using a combination of mass spectra and retention indices.

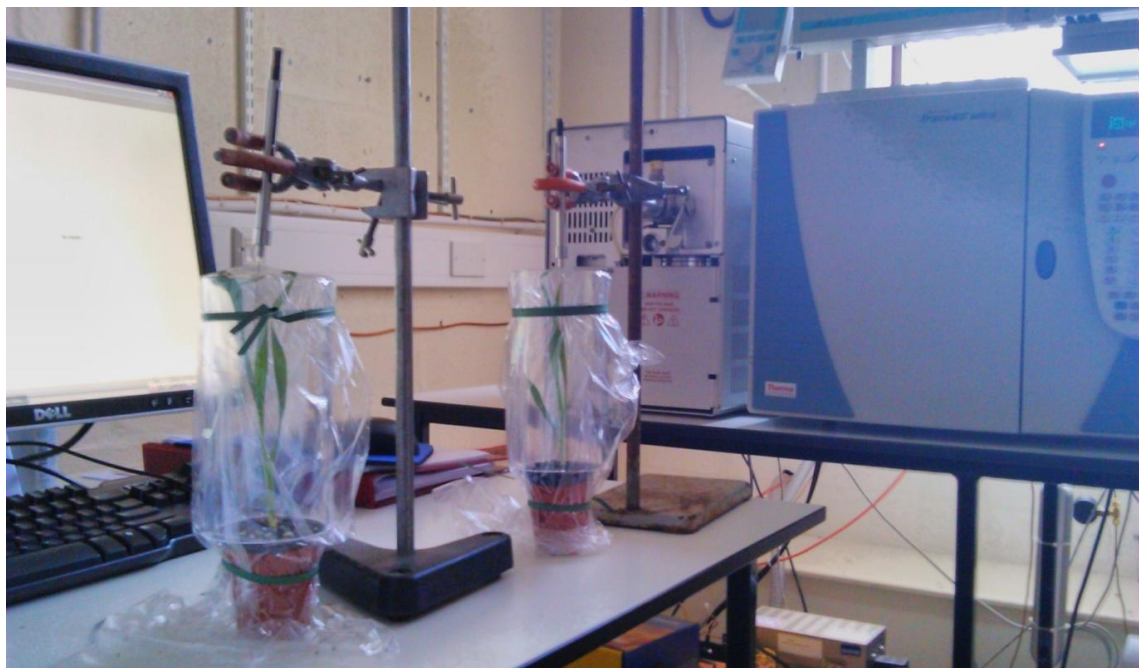


Figure 2.6 Volatile collection in W1-7 and wild type barley seedlings. SPME fibre exposed to barley leaves volatile emission in the enclosed chamber.

2.10 Physiological measurements

2.10.1 Photosynthetic gas exchange

Photosynthesis, transpiration, stomatal conductance and C_i were measured using infra red gas analysis (IRGA) using a two different portable systems (LI-6400XT and CIRAS2). The light intensity used was $300 \mu\text{mol m}^{-2} \text{s}^{-1}$ and CO_2 level was $400 \mu\text{mol mol}^{-1}$. One leaf of each plant was inserted in the machine and left in for 10 min prior to data recording.

2.10.1.1 Light response curves

Light response curves were measured in 7 and 14 old day W1-7 and wild type barley seedlings, which is coincident with the start and the final of the nitrogen treatments. The LICOR apparatus was programmed to take photosynthetic values at different light intensities: 0, 20, 50, 100, 200, 400, 800 and $1600 \mu\text{mol m}^{-2} \text{s}^{-1}$. CO_2 level was kept constant at $400 \mu\text{mol mol}^{-1}$. Each plant was clipped for about 2 h to complete all the measurements. Final data was calculated on an average of 3 technical replicates at the same time points taken from 3 recurring experiments.

2.10.1.2 CO_2 response curves

CO_2 response curves were measured in 14 old day W1-7 and wild type barley seedlings. The LICOR apparatus was programmed to take photosynthetic values at different CO_2 concentrations: 0, 200, 400, 600, 800 and $1000 \mu\text{mol mol}^{-1}$. The light intensity was kept at $300 \mu\text{mol m}^{-2} \text{s}^{-1}$. Each plant was clipped for about 20 min to complete all the measurements. Final data was calculated on an average of 3 biological replicates.



Figure 2.7 Photosynthetic gas exchange measurement in a W1-7 barley seedling using CIRAS2.

2.11 Production of transgenic barley and wheat plants expressing the *SAG21* and *OCI* genes

SAG21 and *OCI* were cloned into various constructs to be expressed in barley and wheat plants, respectively. The components and conditions used for the vectors production are shown in the next sections. Further steps and results are discussed in the chapter 4.

2.11.1 Production of *SAG21*-YFP expression clone and transformed plants verification

attB PCR primers were designed as described in the Gateway manual (Table 2.2). The manufacturer's instructions for the *Pfu* DNA polymerase were followed to obtain PCR products (#EP0501, Fermentas; Table 2.3). The components of the PCR are shown in Table 2.3, 20 ng of DNA were used in each case. The annealing temperature used was 50°C (Table 2.4).

Table 2.2 *attB* PCR primers for *SAG21*.

Primer	Sequence
Forward <i>SAG21</i>	<i>attB</i> - 5- GGGGACAAGTTTGTACAAAAAAGCAGGCTTAATGGCTCGT TCTATCTCT -3
Reverse <i>SAG21</i>	<i>attB</i> - 5- GGGGACCACTTTGTACAAGAAAGCTGGGTATACAACTCA AGAAGGAC -3

Four guanine (G) residues at the 5' end followed by the 25 bp *attB1* site (italics) and the *SAG21* sequence (bold).

Table 2.3 Components for each 50 μ l reaction.

Component	Volume/ concentration
<i>Pfu</i> DNA Polymerase	1.25-2.5 u
10X <i>Pfu</i> Buffer with MgSO ₄ *	5 μ l
dNTP Mix, 2 mM each	5 μ l (0.2 mM of each)
Forward primer	0.1-1.0 μ M
Reverse primer	0.1-1.0 μ M
Template DNA	50 pg - 1 μ g
Water, nuclease-free	make up to 50 μ l

Table 2.4 PCR thermal cycling conditions.

Step	Temperature, °C	Time	Number of cycles
Initial denaturation	95	1-3 min	1
Denaturation	95	30 s	
Annealing	50	30 s	25-35
Extension	72	2 min/kb	
Final extension	72	5-15 min	1

For the BP recombination reaction the components outlined in Table 2.5 were mixed in 1.5 ml microcentrifuge tubes at room temperature. The BP Clonase™ enzyme mix was removed from -80°C and thawed on ice (~2 min). The BP Clonase™ enzyme mix was vortexed briefly twice (2 s each time). To each sample, 4 μ l of BP Clonase™ enzyme mix were added and well mixed by vortexing briefly twice (2 s each time). Reactions were incubated at 25°C O/N.

To stop the reaction, samples were incubated for 10 min at 37°C with 2 µl of the Proteinase K solution.

Table 2.5 BP recombination reaction.

Components	Sample	Positive control
attB-PCR product	1-10 µl	-
pDONR vector (150 ng/ µl)	2 µl	2 µl
pEXP7-tet positive control (50 ng/ µl)	-	2 µl
5X BP Clonase™ Reaction Buffer	4 µl	4 µl
TE Buffer, pH 8.0	To 16 µl	8 µl

2.11.1.1 Competent cells transformation and selection of positive clones

Competent dh5α bacteria were transformed with the SAG21-YFP entry clones using heat-shock method. For each transformation, 50 µl of competent cells were aliquoted into a sterile 1.5 ml microcentrifuge tube. 1 µl of the BP recombination reaction was added into the tube containing 50 µl competent cells and gently mixed. The samples were incubated on ice for 30 min. The cells were placed for 45 s at 42°C without shaking then immediately transferred to ice for 2 min. 300 µl of room temperature LB medium was added to each tube and they were shaken (200 rpm) at 37°C for 1 h. 200 µl of the transformed bacteria were spread onto plates containing 10 µg/ml gentamicin. They were incubated overnight at 37°C.

PCR was performed for each colony with pDONR207 primers and Taq polymerase enzyme. After inoculating the well containing the PCR mix with each colony, the tip was placed in 5 ml LB medium containing 10 µg/ml

gentamicin and grown O/N. After checking the sequences by DNA sequencing, the overnight culture from the positive clones was miniprepmed to provide plasmid DNA for next step.

Once the SAG21-YFP attB-PCR products were verified and purified they were ready to be recombined into the donor vector to create the entry clone. For the BP recombination reaction the components outlined in Table 2.5 were mixed in 1.5 ml microcentrifuge tubes at room temperature. The BP Clonase™ enzyme mix was removed from -80°C and thawed on ice (~2 min). The BP Clonase™ enzyme mix was vortexed briefly twice (2 s each time). To each sample, 4 µl of BP Clonase™ enzyme mix were added and well mixed by vortexing briefly twice (2 s each time). Reactions were incubated at 25°C O/N. To stop the reaction, samples were incubated for 10 min at 37°C with 2 µl of the Proteinase K solution.

2.11.1.2 Create SAG21-YFP expression clones using the LR recombination reaction

Using an LR recombination reaction, the SAG21-YFP insert was placed into an expression vector which to be used for plant transformation. For barley transformation pBRACT214 vector was chosen (Figure 4.5). It contains an ubiquitin promoter for high-level constitutive expression of the gene in monocotyledonous plants. It has a kanamycin resistance gene (*npt1*) for bacteria selection and hygromycin resistance gene for transformed plants selection.

For the LR recombination reaction the following components were added to 1.5 ml microcentrifuge tubes at room temperature and mixed (Table 2.6). The LR Clonase™ enzyme mix removed from -80°C and thaw on ice (~ 2 min). The LR Clonase™ enzyme mix was vortexed briefly twice (2 s each time). To each sample, 4 µl of LR Clonase™ enzyme mix was added and well mixed by vortexing briefly twice (2 seconds each time). Reactions were incubated at 25°C

O/N. To stop the reaction, samples were incubated for 10 min at 37°C with 2 µl of the Proteinase K solution.

Table 2.6 LR recombination reaction.

Components	Sample	Negative control	Positive control
Entry clone (100-300 ng/ reaction)	1-10 µl	-	-
Destination vector (300 ng/ reaction)	2 µl	2 µl	2 µl
pENTR™ gus (50 ng/ µl)	-	-	2 µl
5X LR Clonase™ Reaction Buffer	4 µl	4 µl	4 µl
TE Buffer, pH 8.0	To 16 µl	10 µl	8 µl

2.11.1.3 AGL1 competent cells production

A single colony of *Agrobacterium* (strain AGL1) was inoculated from a fresh agar plate into a 2-litre flask containing 200 ml YEB (1g yeast extract, 5 g peptone, 5 g beef extract, 5 g sucrose, 0.5 g MgSO₄; dissolved in a litre of distilled water, pH 7.0). The culture was incubated at 28° 250 rpm for 3 days. After that, the flask was opened under the hood and shaken to give the culture fresh air. It was closed and grown for another 4 h at 28° 250 rpm. Then it was chilled in iced water for 30 min and cells were harvested in a prechilled rotor at 4000 rpm for 10 min. Cells were washed in 200 ml of ice cold 10% glycerol (1:1). Cells were harvested in a prechilled rotor at 6000 rpm for 10 min. Cells were washed in 100 ml of ice cold 10% glycerol (1:0.5). Cells were harvested in a prechilled rotor at 6000 rpm for 10 min. Pelleted cells were resuspended in 4 ml of ice cold 10% glycerol (1:0.02). The cells were aliquoted into 2 ml eppendorf tubes and spun at 6000 rpm. Cells were resuspended in 2 ml (final

volume) of ice cold 10% glycerol (1:0.01). They were divided into 40 µl aliquots in prechilled 0.5 ml eppendorf tubes and stored at -80°C.

2.11.1.4 Agrobacterium-mediated barley transformation

Agrobacterium-mediated transformation of barley was done with the help of Dr. Jennifer Stephens at The James Hutton Institute, Dundee.

Agrobacterium Electroporation protocol

An aliquot of AGL1 competent cells, plasmid DNA for the SAG21-YFP destination vector and a 2 mm cuvette were incubated on ice till cold. 1 µl of plasmid DNA was transferred into the 50 µl aliquot of competent cells and all transferred to the 2 mm cuvette. The cuvette was pulsed in an electroporator. Biorad Gene Pulser II was used with these conditions:

- 1-2 mm gap cuvettes,
- 2.5 KV (can use 1.8 KV)
- Capacitance 25 mF
- Resistance 200 Ω.

1 ml SOC medium was added to the cuvette and the solution transferred to a 2 ml Eppendorf and grown for 2 h in a shaker at 28°C, 250 rpm. 50 µl and 200 µl aliquots were plated onto LB media containing 50 mg/ml kanamycin and incubated at 28°C O/N. From the overnight cultures 1 ml stocks were frozen at -80°C for transformation while the remainder was used to extract plasmid DNA using a Qiagen kit. This plasmid DNA was retransformed into dH5a as previously to confirm positive clones by sequencing.

Sequencing of *Agrobacterium* minipreps is not recommended as they contain many contaminants. Positive LR reactions containing pBRACT214_SAG21-YFP transformed in *Agrobacterium* were confirmed by sequencing.

The SAG21 transgenic plants were selected by PCR using hygromycin primers and $T_m = 64^\circ\text{C}$ following the indications described in the Table 2.7.

Table 2.7 PCR components for SAG21 and control lines screening.

Components	1 reaction	40 reactions
5x Green gotaq buffer	5 μl	200 μl
dNTPs 10 mM	0.5 μl	20 μl
Primer Forward 10 μM	1 μl	40 μl
Primer Reverse 10 μM	1 μl	40 μl
Go Taq DNA Pol	0.25 μl	10 μl
SDW	16.25 μl	650 μl
DNA per reaction	1.0 μl	1.0 μl
Total	25 μl	1000 μl

2.11.2 Cloning of OCI gene into pDONR and pENTR-type vectors

Cut and paste cloning was performed in order to insert the OCI gene into the pENTR1 vector. Primers containing *Bam*HI and *Xho*I restriction sites were then designed (Table 2.8), OCI plasmid was diluted 1:30 and 1 μl of it was used in 50 μl PCR reaction using Phusion II polymerase, 2 reactions were performed in a final volume of 50 μl using PCR conditions shown in Table 2.9.

Table 2.8 Primer sequences for OCI gene amplification.

Primer	Sequence
Forward <i>Bam</i> HI_OCI	5' -GAAAGGAT CC <u>CCACC</u> ATGTCGAGCGACGGAGGGCC- 3'
Reverse <i>Xho</i> I_ OCI	5'-GAAACT CGAG TTAGGCATTTGCACTGGCATC- 3'

*Bam*HI and *Xho*I restriction sites sequences in bold. Kozak sequence (CCACC) underlined in the forward primer, it facilitates the initiation of the translation process.

Table 2.9 PCR thermal cycling conditions.

Step	Temperature, °C	Time	Number of cycles
Initial denaturation	98	1 min	1
Denaturation	98	20 s	
Annealing	62	20 s	35
Extension	72	30 s	
Final extension	72	5 min	1

The amplified OCI insert was purified and digested together with the pENTR1A plasmid at 37°C for 30 min (Table 2.10).

Table 2.10 pENTR1A and OCI digestions.

Component	Volume
pENTR1A/ OCI insert	20 µl
<i>Bam</i> HI	1 µl
<i>Xho</i> I	1 µl
Fast AP	1 µl
SDW	5 µl

For the OCI Gateway cloning, the primers designed are shown in the Table 2.11.

Table 2.11 *attB* PCR primers for OCI.

Primer	Sequence
Forward	<i>attB</i> 5'- GGGGACAAGTTTGTACAAAAAAGCAGGCT <u>CCACCATG</u>
OCI	TCGAGCGACGGAGGGCC - 3'
Reverse	<i>attB</i> 5'- GGGGACCACTTTGTACAAGAAAGCTGGGTTT AGGCAT
OCI	TTGCACTGGCATC - 3'

Four guanine (G) residues at the 5' end followed by the 25 bp *attB*1 site (bold), the Kozak sequence (CCACC, underlined) and the OCI sequence.

Chapter 3. Characterization of Arabidopsis transgenic lines with ectopic OCI expression

3.1 Introduction

The characterization of the OCI expressing Arabidopsis plants was undertaken as part of the research within the EU CropLife program. The objective of this project is to study the interactions between proteases and protease inhibitors in the control of leaf protein turnover.

Cysteine proteases have been shown to be upregulated during senescence (Bhalerao et al., 2003; Guo et al., 2004), some of them being newly synthesized in that moment to take part in the protein breakdown process. Apart from the vacuole and cytosol, they have been observed in senescence-associated vacuoles (SAVs). SAVs are small and acidic vacuoles with proteolytic activity, they are thought to conduct chloroplast proteins to the central vacuole for degradation only during senescence (Otegui et al., 2005; Carrion et al., 2013; Diaz-Mendoza et al., 2014). Although so far only aspartic proteases have been suggested to participate in Rubisco degradation in the chloroplast (Kato et al., 2004), other proteases such as cysteine proteases might participate as well. Rubisco degradation can happen inside and outside of the chloroplast (Irving and Robinson, 2006), it may be possible that the first steps occur in the chloroplast resulting in a fragmented Rubisco which would then be transported outside ending in the vacuole. However, the enzymes and mechanisms involved in the process are not fully described yet.

Cystatins inhibit cysteine protease activity, thus they are implicated in the regulation of chloroplast protein turnover. The rice cystatin Oryzacystatin I (OCI) is the best characterised plant cystatin. OCI tobacco over expressing plants

showed a delayed senescence phenotype; they grow slower with delayed flowering and their vegetative phase is longer leading to bigger plants (Van der Vyver et al., 2003). The relation of OCI and senescence makes this protein an ideal candidate to study this process with special focus on protein turnover. The OCI protein is mostly found in the cytosol and a small portion in the vacuole and chloroplasts (Prins et al., 2008). Expressing OCI in different cell compartments would allow a better knowledge of the interactions between cysteine proteases and cystatins. Arabidopsis plants with an ectopic expression of OCI in the cytosol or targeted to the chloroplast were previously produced in our lab by Dr. Eugene Makgopa. Wild type *Arabidopsis* (ecotype Col-0) plants were transformed with *Agrobacterium tumefaciens* strain GV3101 carrying the plasmid pTF101.1-Cys-I. The expression cassette contains a cauliflower mosaic virus 35S promoter (CaMV P35S), the OCI gene and a CaMV terminator. The chloroplast targeted expression cassette carried a phosphoribulokinase (PRK, Appendix I) signal gene before the OCI gene. The presence and the expression of the OCI transgene was verified in all the transformed Arabidopsis lines using PCR and qRT-PCR. This data can be found in Dr. Eugene Makgopa's thesis (Chapter 5).

The aim of the following studies was to characterise the transformed Arabidopsis lines with ectopic OCI expression either in the cytosol (Cys1, Cys3 and Cys4) or targeted to the chloroplasts (PC2, PC7 and PC9). Part of the results presented in this chapter have been already published in Quain et al. (2014).

3.2 Results

The growth and development of the Arabidopsis lines with ectopic OCI expression either in the cytosol or targeted to the chloroplasts were analyzed in order to study the interactions of this cystatin and their target proteases during protein degradation.

3.2.1 Phenotype of Arabidopsis plants with ectopic expression of OCI

3.2.1.1 Phenotype of Arabidopsis lines expressing OCI in the chloroplast

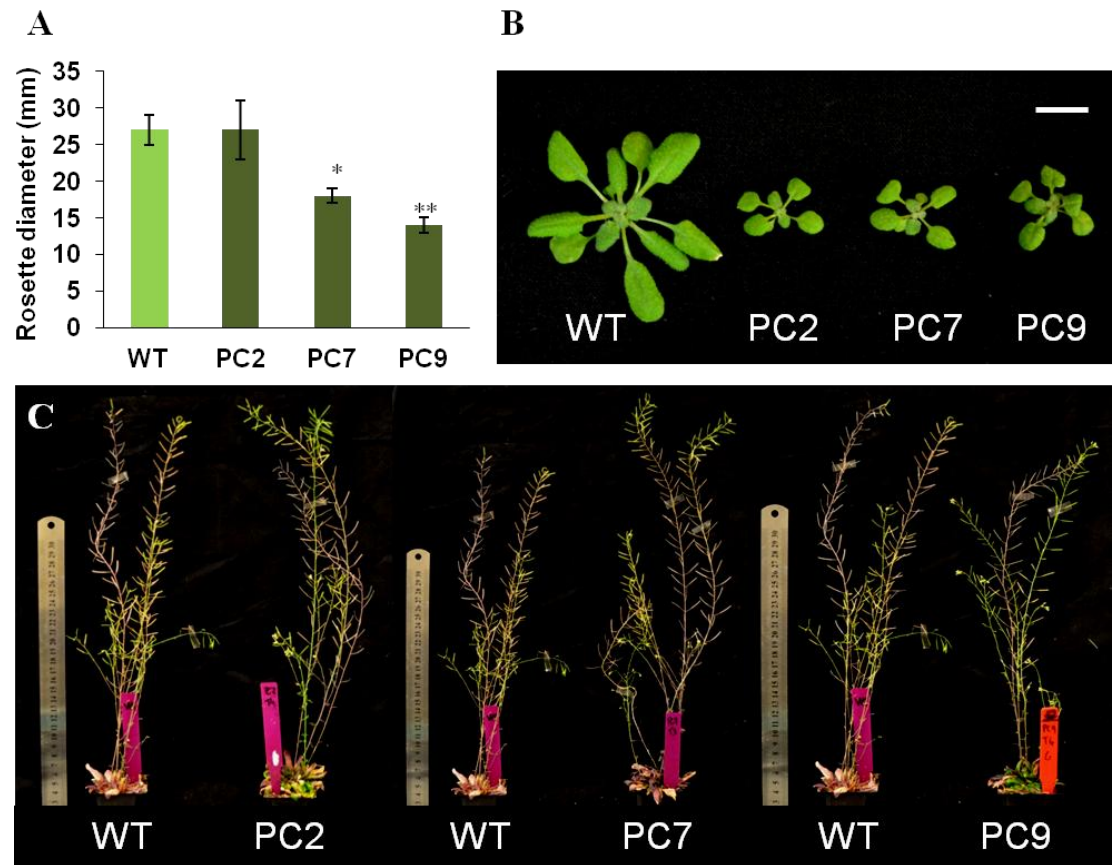


Figure 3.1 A comparison of the rosette diameter at 18 days (A), rosette phenotypes at 30 days (B); and shoot phenotypes at 10 weeks in the three independent transgenic lines with ectopic expression of OCI targeted to the chloroplast (PC2, PC7 and PC9) to the wild type (WT). Rosette diameter expressed as mean \pm SE ($n = 16$) * $p < 0.05$. ** $p < 0.01$. (Scale bar = 1 cm).

3.2.1.2 Phenotype of Arabidopsis lines expressing OCI in the cytosol

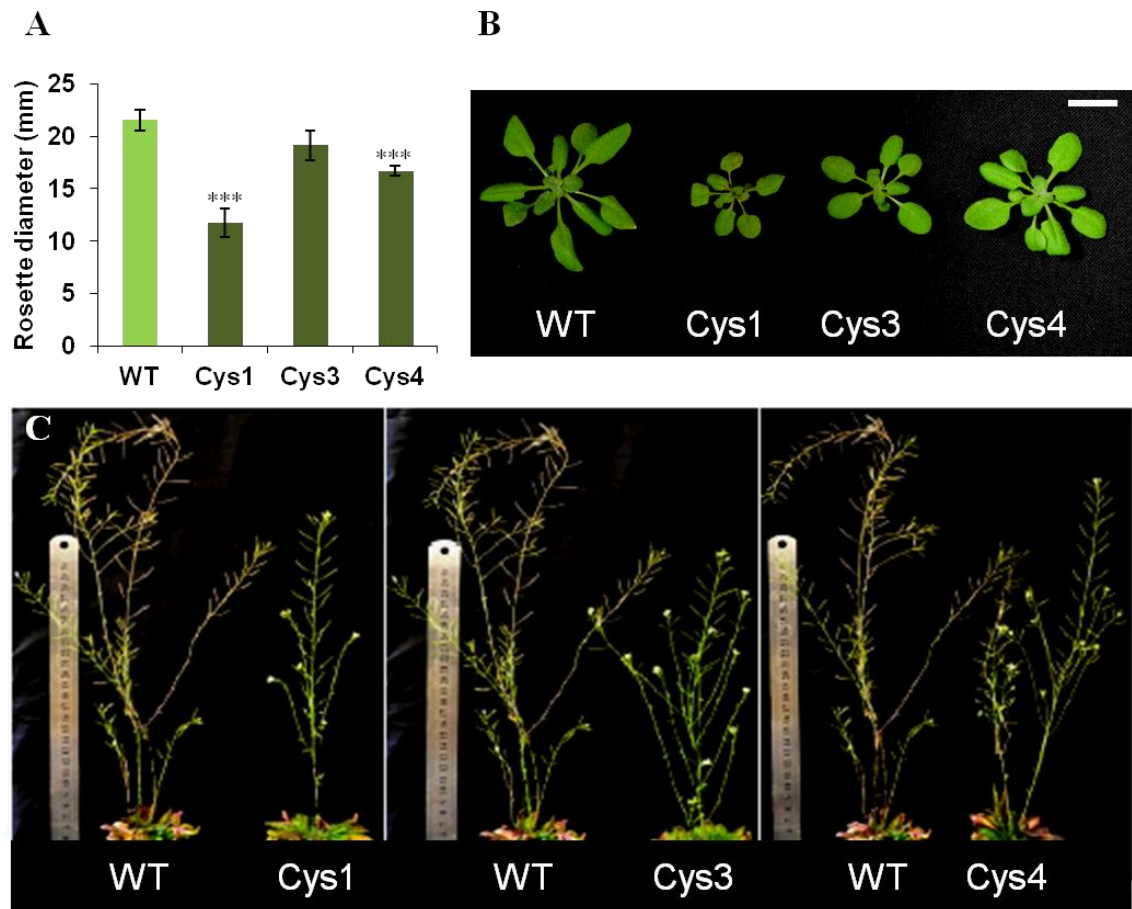


Figure 3.2 A comparison of the rosette diameter at 17 days (A), rosette phenotypes at 30 days (B); and shoot phenotypes at 10 weeks in the three independent transgenic lines with ectopic expression of OCI in the cytosol (Cys1, Cys3 and Cys4) to the wild type (WT). Rosette diameter expressed as mean \pm SE (n = 10) ***p<0.001. (Scale bar = 1 cm).

The rosette diameter of two of the transgenic lines with ectopic expression of OCI in the chloroplast, PC7 and PC9, was significantly smaller than the wild type (Figure 3.1 A). Similarly, one month old transgenic plants presented smaller rosettes than the control (Figure 3.1 B). In contrast, after three months no visible differences were observed between the transgenic lines and the wild type (Figure 3.1 C).

The rosette diameter of the plants with ectopic expression of OCI in the cytosol, Cys1 and Cys4, was significantly smaller than the wild type (Figure 3.2 A). 30 day old transgenic plants were smaller than the wild type, specifically the rosette of the line Cys1 had a size of about the half of that of the wild type (Figure 3.2 B). In the final stages these differences between the three transgenic lines and the wild type were still appreciated, in general the OCI transgenic plants were shorter in comparison with the controls (Figure 3.2 C).

3.2.2 Shoot biomass, chlorophyll and protein contents in OCI Arabidopsis plants at 3 different time points

3.2.2.1 Shoot biomass, chlorophyll and protein contents in Arabidopsis lines expressing OCI in the chloroplast

Shoot biomass was analyzed at 25 days in plants of transgenic Arabidopsis lines with ectopic expression of OCI in the chloroplast and the wild type (Figure 3.3 A). At this age, PC2 line had similar shoot biomass than the wild type plants. In contrast, PC7 and PC9 lines had significantly lower shoot biomass than the wild type (Figure 3.3 A).

The chlorophyll and total protein content of transgenic lines with ectopic expression of OCI targeted to the chloroplast and the wild type was analyzed at three different time points. At 25 days, PC2 line had significantly lower chlorophyll content than the wild type, while the other two lines presented similar contents (Figure 3.3 B). At 39 and 53 days, no significant differences were observed between the wild type and the three transgenic lines with OCI targeted to the chloroplast (Figure 3.3 B).

The protein content of PC2 and PC7 was similar to that of the wild type at 25 days; however, PC9 leaves had significantly higher protein content (Figure 3.3 C). At 39 days there were no significant differences in the protein content between PC7 and PC9 compared to the wild type, but PC2 had significantly more protein (Figure 3.3 C). At 53 days the leaves of the PC7 had higher protein content than those of the wild type. In contrast, the other two lines presented similar protein content than the wild type (Figure 3.3 C).

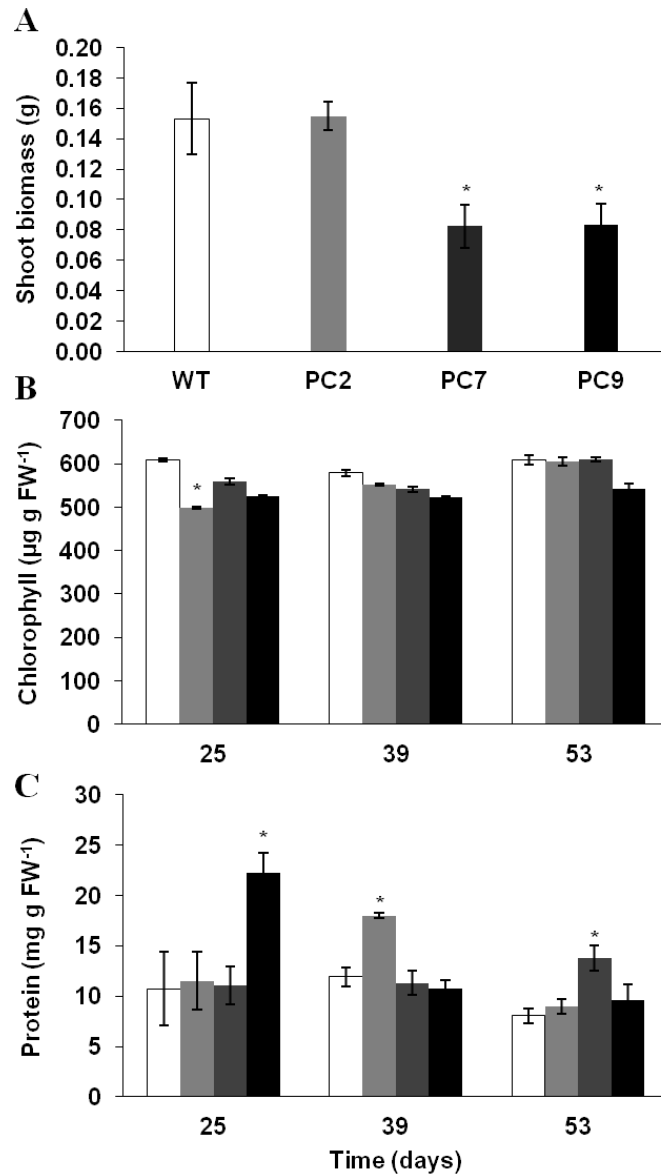


Figure 3.3 A comparison of shoot biomass at 25 days (A), and total chlorophyll (B) and leaf soluble protein contents (C) in three independent transgenic lines with ectopic expression of OCI targeted to the chloroplast (PC2, light grey; PC7, dark grey; and PC9, black) to the wild type (WT, white). Data are the mean values \pm SE ($n = 3$). Significant differences between WT and the transgenic lines were calculated with T-test, $*p < 0.05$.

3.2.2.2 Shoot biomass, chlorophyll and protein contents in Arabidopsis lines expressing OCI in the cytosol

Shoot biomass, total chlorophyll and protein content were analyzed at different time points in plants of transgenic Arabidopsis lines with ectopic expression of OCI in the cytosol and the wild type (Figure 3.4). At 25 days, the shoot biomass of the wild type plants and transgenic lines was similar (Figure 3.4 A). In later stages of development, 39 and 53 days, transgenic lines Cys1 and Cys3 had significantly lower shoot biomass than the wild type plants (Figure 3.4 A).

The chlorophyll content of the transgenic cytosolic OCI lines was higher at 25 days, this difference was significant for lines Cys3 and Cys4 (Figure 3.4 B). At this point, the chlorophyll content of the wild type plants was approximately $500 \mu\text{g g FW}^{-1}$, Cys4 line had significantly higher chlorophyll content than the wild type while the other two lines did not differ (Figure 3.4 B). Transgenic OCI lines Cys3 and Cys4 had also a significantly higher amount of chlorophyll in their leaves than the wild type after 39 and 53 days (Figure 3.4 B).

The protein content of the transgenic lines was similar to that of the wild type at 25 days, all of them showed values around 10 mg g FW^{-1} (Figure 3.4 C). At 39 days there was also no significant difference in the protein content between OCI plants and the control. Although protein content decreased after this time point in both transgenic and wild-type leaves, at 53 days the transgenic line Cys1 had still significantly more protein than the wild type (Figure 3.4 C).

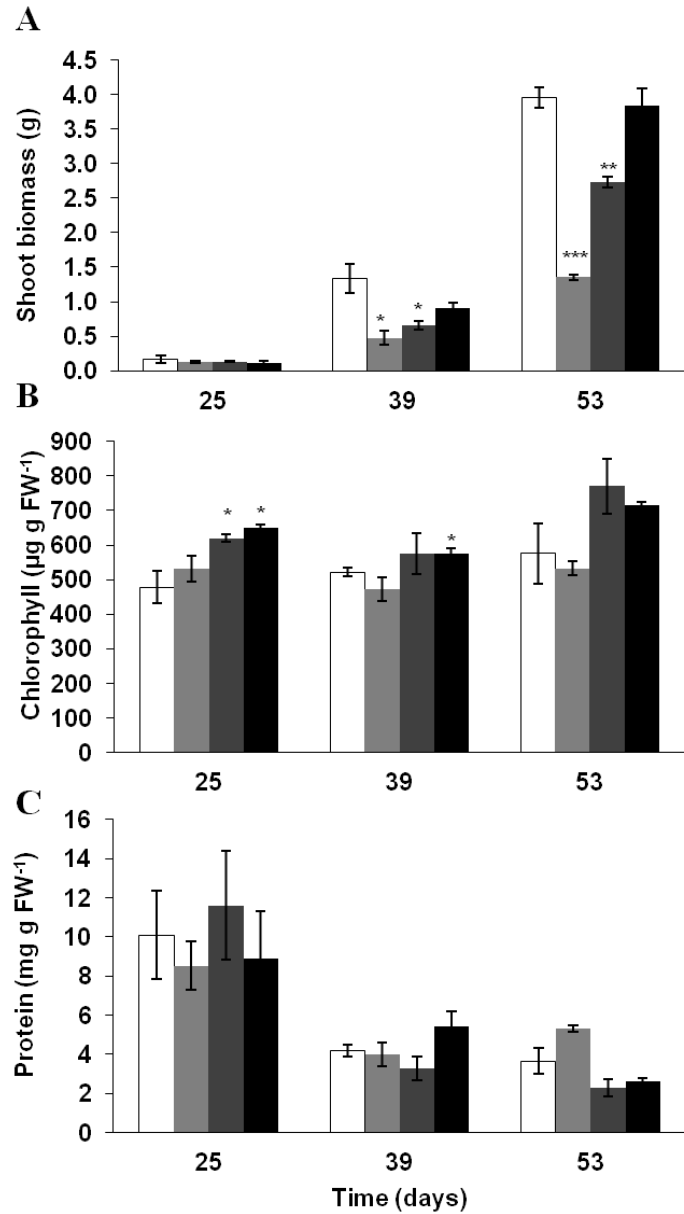


Figure 3.4 A comparison of shoot biomass (A), total chlorophyll (B) and leaf soluble protein contents (C) in the three independent transgenic lines expressing OCI in the cytosol (Cys1, light grey; Cys3, dark grey; and Cys4, black) to the wild type (WT, white). Data are the mean values \pm SE (n = 3). Significant differences between WT and the transgenic lines were calculated with T-test, *p<0.05, **p<0.01, ***p<0.001.

3.2.3 Percentage of flowering in OCI Arabidopsis plants

Flowering was analysed in the wild type Arabidopsis plants and the transgenic OCI lines during plant development at three different time points, 25, 39 and 53 days (Figure 3.5). In most of the plants the first flowers appeared after 25 days. At 39 days, the chloroplast OCI transgenic line PC2 had a higher percentage of flowering plants than the wild type but the remaining transgenic lines PC7 and PC9 had a lower percentage of flowering plants than the wild type (Figure 3.5 A). By day 53, 100% of wild type plants had flowers while the percentages of plants flowering was about 90% in the transgenic line PC2, 80% in the transgenic line PC7 and 55% in the transgenic line PC9 (Figure 3.5 A).

Flowering patterns in the cytosolic OCI transgenic plants were different to those of the OCI chloroplast ones (Figure 3.5 B). Flowers in Cys1 plants developed latest and at 53 days the percentage of plants with flowers was only about 30% (Figure 3.5 B). In contrast, Cys3 and Cys4 had higher percentages of flowering plants than the wild type plants at 39 days (Figure 3.5 B). At 53 days 100% of wild type, Cys3 and Cys4 transgenic lines had developed flowers (Figure 3.5 B).

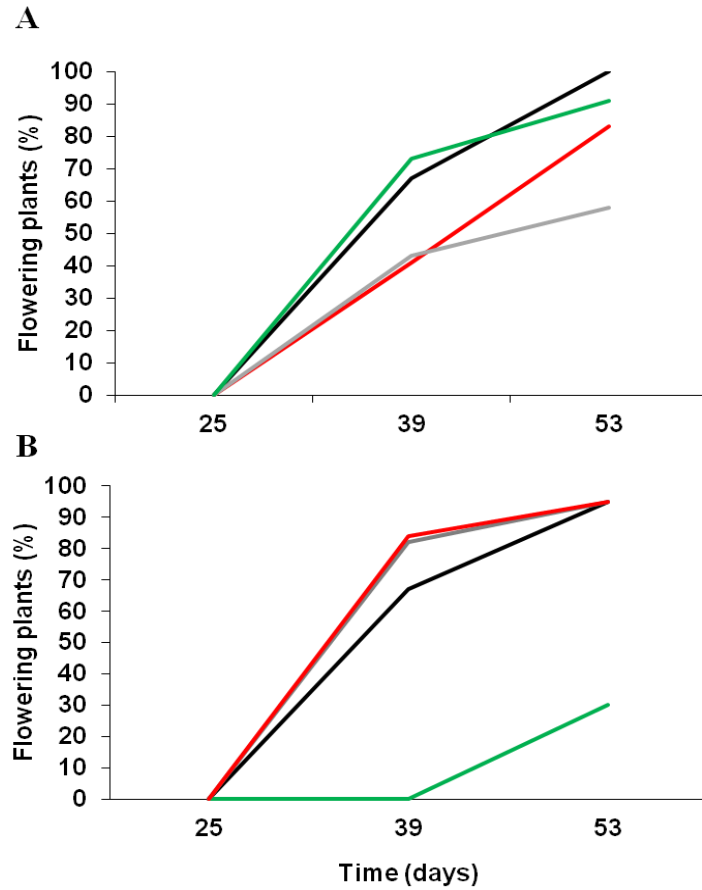


Figure 3.5 A comparison of the percentage of flowering plants in the three independent transgenic lines with ectopic expression of OCI in the chloroplast (PC2, green; PC7, red and PC9, grey; A) and the three independent transgenic lines with ectopic expression of OCI in the cytosol (Cys1, green; Cys3, grey; and Cys4, red; B) to the wild type (WT, black).

3.2.4 Root morphology of the OCI Arabidopsis seedlings

3.2.4.1 Root morphology of the Arabidopsis lines with ectopic expression of OCI in the chloroplast

The root length and number of lateral roots were analyzed in 11-day old transgenic plants expressing OCI in the chloroplast (Figure 3.6). Photos were taken at this point where the seedling root systems were sufficiently developed for analysis (Figure 3.6 A). The primary root length of the transgenic PC7 and PC9 seedlings was similar to the wild type (Figure 3.6 B). However, the OCI transgenic line PC9 had significantly longer primary roots than the wild type with an average of about 35 mm (Figure 3.6 B). Seedlings of the three chloroplast OCI transgenic lines had further significantly higher number of lateral roots than the wild type, with the number of lateral roots of PC9 almost double in comparison to the wild type (Figure 3.6 C). Furthermore, lateral root density was also higher for the three transgenic lines than the wild type (Figure 3.6 D).

3.2.4.2 Root morphology of the Arabidopsis lines with ectopic expression of OCI in the cytosol

Transgenic lines Cys1 and Cys4 with ectopic expression of OCI in the cytosol had significantly longer primary roots than wild-type seedlings, whereas transgenic line Cys3 had a similar primary root length than the wild type (Figure 3.7 B). Further, Cys1 and Cys4 had significantly higher number of lateral roots than the wild type and had also significantly higher lateral root density than the wild type (Figure 3.7 C and D). Whereas the wild type had on average 4 lateral roots, seedlings of the Cys4 transgenic line had, for example, on average 12 lateral roots per seedling (Figure 3.7 C).

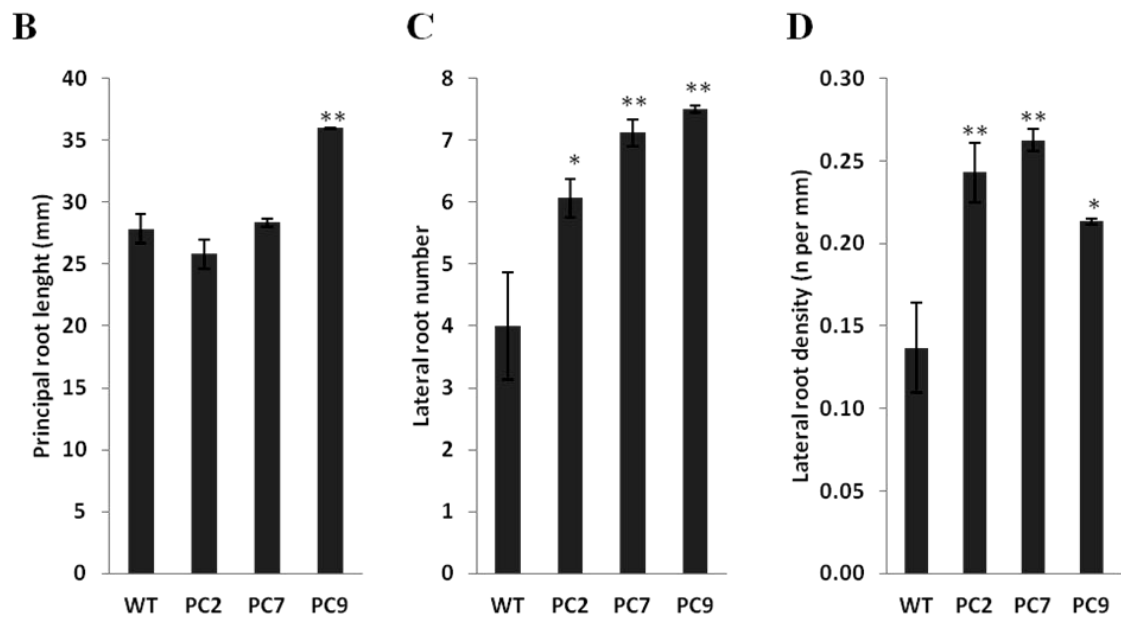
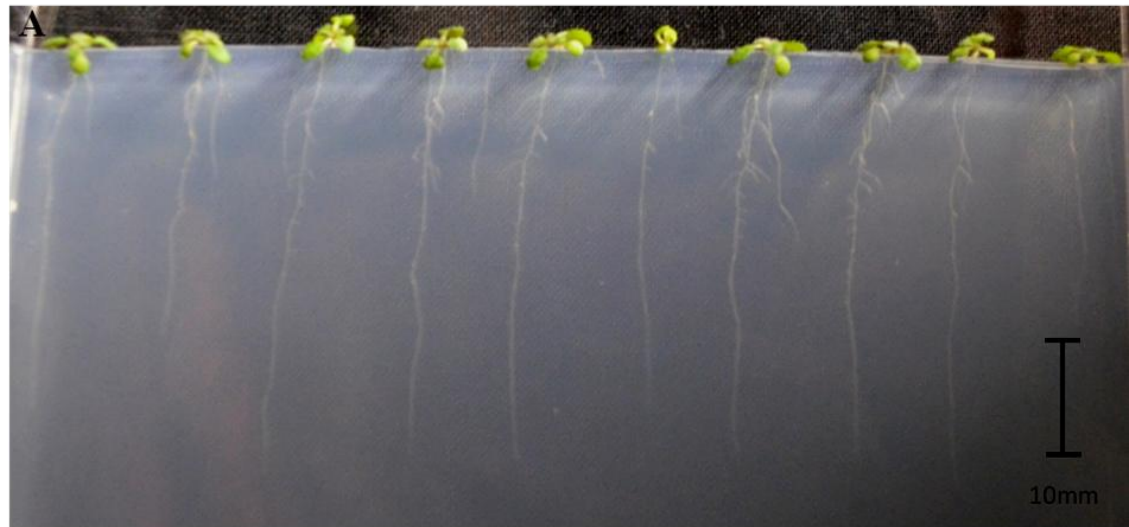


Figure 3.6 A comparison of primary root length (B), number of lateral roots (C) and lateral root density (D) in 11-day old plants of the transgenic lines with chloroplast targeted OCI (PC2, PC7 and PC9) to the wild type (WT). Lateral root density was calculated as lateral root number/primary root length. Data are the mean values \pm SE (n = 16). Significant differences between WT and the transgenic lines were calculated with T-test, * $p < 0.05$, ** $p < 0.01$.

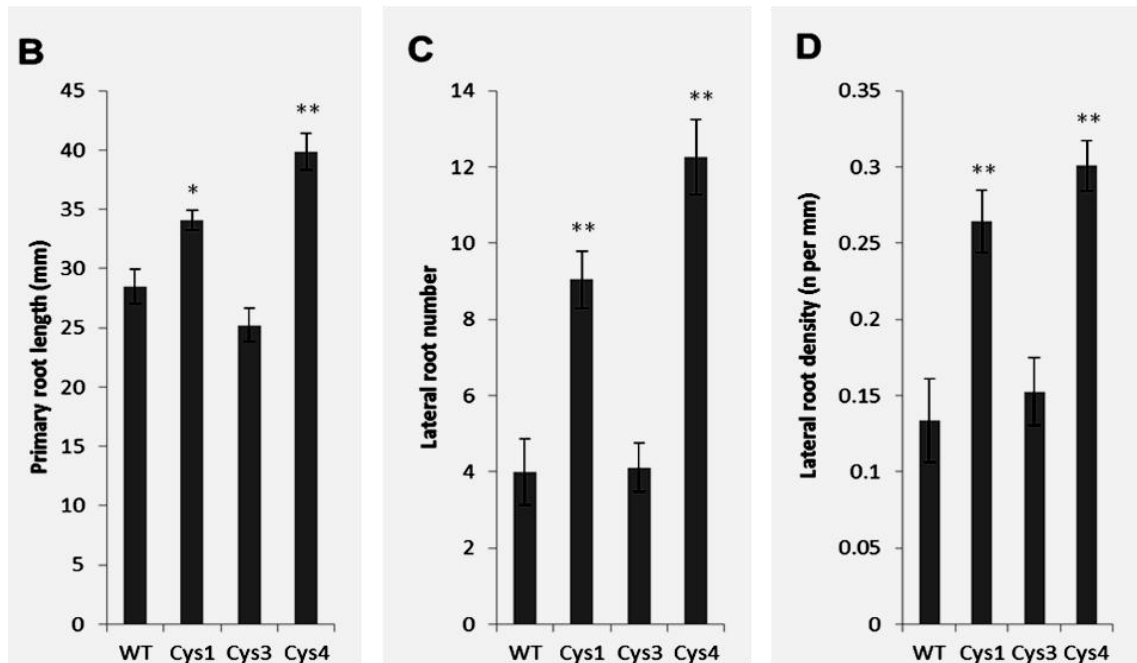


Figure 3.7 A comparison of primary root length (B), number of lateral roots (C) and lateral root density (D) in 11-day old plants of the transgenic lines expressing OCI in the cytosol (Cys1, Cys3 and Cys4) to the wild type (WT). Lateral root density was calculated as lateral root number/primary root length. Data are the mean values \pm SE (n = 30). Significant differences between WT and the transgenic lines were calculated with T-test, * $p < 0.05$. ** $p < 0.01$.

3.2.5 Number of leaves and leaf area of the Arabidopsis lines expressing OCI in the cytosol

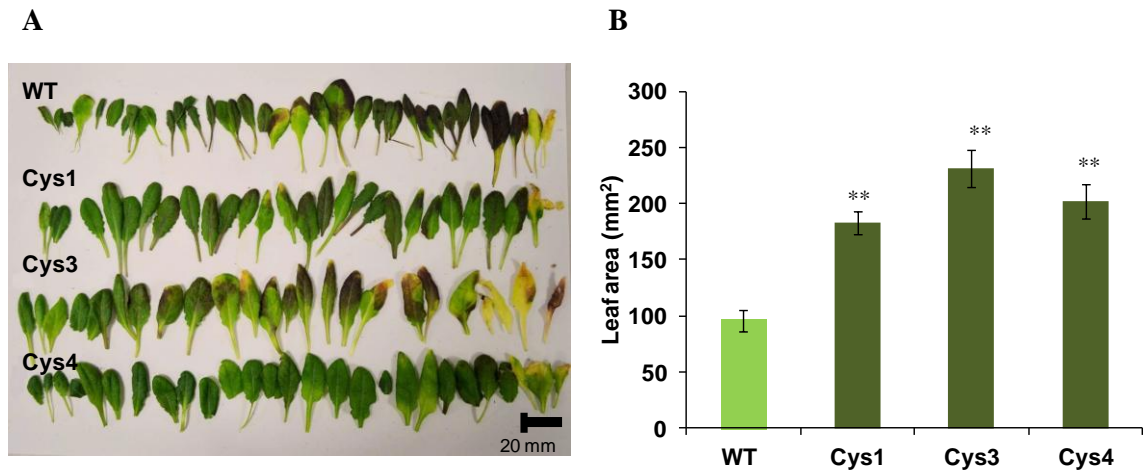


Figure 3.8 A comparison of the number of leaves (A) and leaf area (B) in the in 63-day old plants of the cytosol OCI transgenic lines (Cys1, Cys3 and Cys4) to the wild type (WT). Leaf area data (B) are mean of the surface area of all the leaves of one of each of the plant genotypes. Significant differences between WT and the transgenic lines were calculated with T-test, ** $p < 0.01$.

Leaf phenotype and leaf number was compared in plants at 63 days (Figure 3.8 A). Wild type plants had 37 leaves with most of which had purple or yellow patches (Figure 3.8 A). The OCI transgenic lines Cys1, Cys3 and Cys4 plants had less leaves but they were bigger. Cys1 had 26 leaves, Cys3 had 24 leaves and Cys4 ad 27 leaves (Figure 3.8 A). Transgenic leaves were in general greener than the wild type leaves. Among the lines, the Cys3 plant had a leaf with more purple patches as well as three completely yellow leaves (Figure 3.8 A). The leaf area of the three transgenic lines was further greater when compared to the wild type, on average the leaf area of transgenic plants was double than that of the wild type (Figure 3.8 B).

3.3 Discussion

The studies described in this chapter were performed to analyze the phenotype of Arabidopsis plants with an ectopic expression of the OCI protein either in the cytosol or targeted to the chloroplast. Measurements were taken at three different time points at the approximate ages of 3, 5 and 7 weeks, in order to provide information about the morphology and physiology of the OCI expressing plants. The data obtained showed clear differences in the growth and development of the two set of transgenic plants which are discussed in detail below.

3.3.1 Arabidopsis plants expressing OCI in the cytosol

In this study, the expression of the OCI protein in the cytosol of Arabidopsis plants leads to smaller plants than the controls. Plants of transgenic lines had a significantly decreased rosette diameter and reduced shoot biomass during the first month, plus the plants were considerably shorter at 10 weeks. This confirms previous tobacco results, where OCI expressing tobacco plants had a slower growth in the first weeks despite being taller than wild-type controls at the final stage of development (Prins et al., 2008). OCI transgenic Arabidopsis lines also presented a delayed flowering in comparison to the wild type, with one of the lines only reaching 30% of plants with flowers. The leaf area of the three transgenic lines expressing OCI in the cytosol was significantly increased in comparison with the wild type plants, which is very similar to the data described for OCI tobacco lines (Van der Vyver et al., 2003; Prins et al., 2008). Like the OCI expressing soybean plants (Quain et al., 2014), the cytosolic OCI Arabidopsis plants showed higher amounts of chlorophyll in their leaves along their development and more branching in the final stages of their lives.

3.3.2 Arabidopsis plants expressing OCI in the chloroplast

Arabidopsis plants with an ectopic expression of OCI in the chloroplast looked much smaller than the controls at first stages and two of the lines had also smaller rosettes in the first month. However, they showed similar heights than the wild type at 10 weeks. Unlike the cytosolic OCI lines, chlorophyll and protein contents of the chloroplast OCI leaves were not different to those of the wild type. As it was shown for the OCE tobacco plants (Van der Vyver et al., 2003), two of the transgenic lines showed a delayed flowering in comparison to the wild type. Besides, the three lines presented lower flowering percentage at the end of the experiment.

3.3.3 Ectopic expression of OCI in Arabidopsis plants

Ectopic OCI expression in cytosol as well as in chloroplast had a marked effect on primary roots and lateral root density in Arabidopsis seedlings, suggesting a function of OCI in the control of growth. The OCI protein has been previously linked to strigolactone production, hormones with roles in shoot and root branching (Quain et al., 2014). Altered root branching were also observed in strigolactone synthesis (*max3*) and signalling (*max2*) mutants (Gomez-Roldan et al., 2008; Beveridge et al., 2009). Therefore, these changes in root density could be a result of an altered strigolactone signalling pathway.

Although there are some differences between the two types of transgenic OCI lines, both share similarities such as the smaller size of the rosette and shoots during the first weeks of development. In these experiments, the effect of the over expression of OCI on cytosol and plastids proteases was tested. Targeting OCI to the chloroplast had an effect on the plant development, supporting the idea that degradation is also happening inside of the chloroplast. When the OCI chloroplast plants started to senesce there were not big differences in the phenotypes compared to the controls, so maybe this protein turnover takes place in the first stages of development and during senescence only cytosolic

proteases are active. The ATG-OCI crossed lines will allow the visualization of OCI within the cell under control conditions and when the main degradation pathway, autophagy, is blocked. This will hopefully clarify some of the hypothesis about how the chloroplast proteins are degraded.

3.3.4 Experimental plan for the ATG-OCI Arabidopsis plants

In order to understand the role of OCI in protein turnover, two characterized lines homozygous for the transgene, one with OCI expression in the cytosol and one with OCI targeted to the chloroplasts, were crossed with components involved in the autophagy pathway in the laboratory of Dr Masclaux-Daubresse at INRA Versailles. The two OCI expressing lines were crossed with *atg5* mutant (Guiboileau et al., 2012), and they will be crossed with tagged lines (GFP-ATG8, RFP-ATG8 and Cherry-ATG8) in which intrinsic ATG8 protein of the autophagosome membrane is linked to fluorescent markers to enable visualization of the autophagosomes using confocal microscopy. Once obtained the T3 generation of the described series of plants the following experiments will be performed:

- The effect of OCI ectopic expression on autophagy will be first evaluated using QRT-PCR on several ATG genes.
- Leaves of fluorescent-ATG8 tagged lines will be used to visualise autophagosomes using confocal microscopy.
- The structure of autophagosomes will be checked in OCI expressing using electron microscopy.
- The phenotype of the *atg5* plants with ectopic expression of OCI will be studied under low or high nitrogen nutrition, as both autophagy and cysteine proteases may be required for nitrogen remobilization. Following this idea, the lines will be labelled using ^{15}N in order to monitor nitrogen remobilization efficiency from leaf to leaf and from the rosettes to the seeds.

Chapter 4. Production of transgenic barley and wheat plants expressing the *SAG21* and *OCI* genes

4.1 Introduction

The production of transgenic barley plants was undertaken as part of the research within the EU CropLife program. The aim was to produce transgenic barley plants overexpressing either the rice cystatin, oryzacystatin I (OCI), or the SENESCENCE-ASSOCIATED GENE 21 (*SAG21*/AtLEA 5; At4g02380) from *Arabidopsis*. The transgenic plants would be useful tools for the study of the regulation of developmental senescence, which was a major goal of CropLife research.

OCI was chosen for this research because it is the best characterised plant cystatin. Phytocystatins are competitive inhibitors of papain-like cysteine proteases in plants (Benchabane et al., 2010). Previous studies on ectopic OCI in tobacco has implicated papain-like cysteine proteases in the control of plant development and stress tolerance (Van der Vyver et al., 2003). Similar studies in transgenic soybeans with constitutive OCI expression supported this conclusion (Quain et al., 2014). Taken together, these reports demonstrated that OCI over expression delayed leaf senescence, particularly by causing a greater stability of chloroplast proteins such as Rubisco (Prins et al., 2008). The production of OCI-expressing barley lines would allow an analysis of the functions of papain-like cysteine proteases in the senescence of barley leaves.

SAG21 is a senescence-associated gene and a late embryogenesis abundant (LEA) protein at the same time. It is located in mitochondria and expressed early in leaf senescence and in darkness (Weaver et al., 1998; Salleh et al., 2012). Biotic stress and some types of ROS such as H₂O₂ and superoxide (O²⁻)

can up regulate *SAG21* (Mowla et al., 2006). Previous work with *Arabidopsis* showed a role of *SAG21* in root development (Salleh et al., 2012). Additionally, over-expression of *SAG21* in *Arabidopsis* results in plants with greater biomass and more tolerant to H₂O₂ stress (Salleh et al., 2012). This relation with oxidative stress suggests that *SAG21* is involved in ROS mediated signalling. Due to its localization, it might be possible that *SAG21* influences mitochondrial proteins implicated in ROS production or signalling.

To investigate the roles of these two proteins in relation with natural and stress induced senescence, they were cloned into several constructs to be expressed in barley and wheat. In this chapter the cloning steps for the production of the different expression vectors and the barley transformation process will be described. Detailed components of the reactions are described in the Chapter 2.

4.2 Results

Gateway cloning (Invitrogen) was chosen for the production of expression vectors carrying either *OCI* or *SAG21* genes. In the next sections the steps for the production of the three constructs will be explained. First, the cloning of *SAG21*-YFP into a pBRACT214 vector for barley transformation. Then, the cloning of *OCI* into a pENTR1A vector and into a pDONR201 vector for wheat and barley transformation, respectively.

4.2.1 Gateway cloning overview

The Gateway Technology is an alternative to cut-and-paste cloning methods. It follows the principle of the bacteriophage λ , site-specific recombination reactions to insert and excise its genome in *E. coli*. The basis of the Gateway method is the recombination between sequences flanked by specific sites (*att* sites). For that purpose two different vectors and two main steps are needed:

4.2.1.1 Create an entry clone

The first step is to design *attB* PCR primers for the insert of interest. These must contain the following: a specific structure composed of four guanine (G) residues at the 5' end followed by the 25 bp *attB1* site, followed by at least 18-25 bp of gene-specific sequence. By amplifying the gene of interest with the *attB* primers *attB*-PCR products will be produced (Figure 4.1 A).

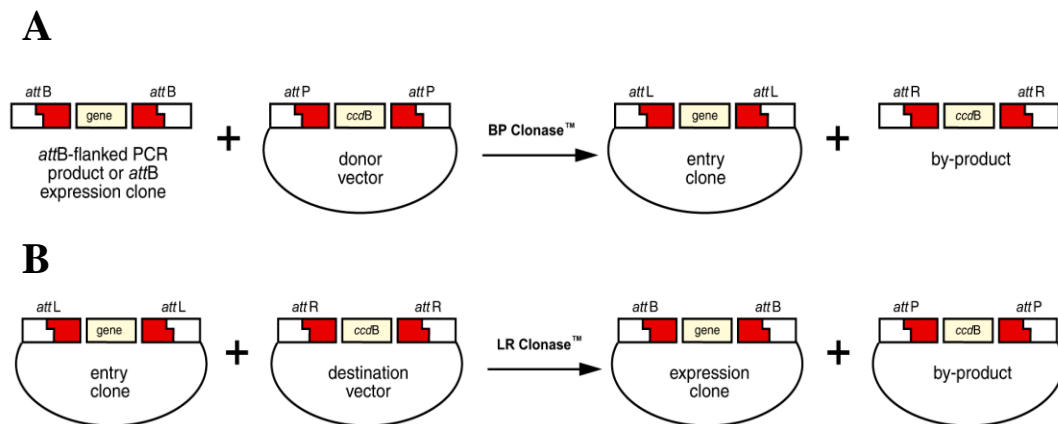


Figure 4.1 Gateway recombination steps. Entry clone (A) and expression clone (B) production. Figure taken from Gateway® Technology, Version E13, May 2010, 25-0522.

The next step is to create entry clones using the BP recombination reaction. The *attB*-PCR product will be inserted into a pDONR-type vector (Figure 4.2) using BP Clonase enzyme mix. During the recombination process the *ccdB* gene is replaced by the gene of interest so only bacteria containing successful entry clones will grow. The bacteria carrying empty pDONR vectors will not be able to grow in most *E. coli* strains (e.g. DH5α™, TOP10), because the *ccdB* protein interferes with *E. coli* DNA gyrase (Bernard and Couturier, 1992).

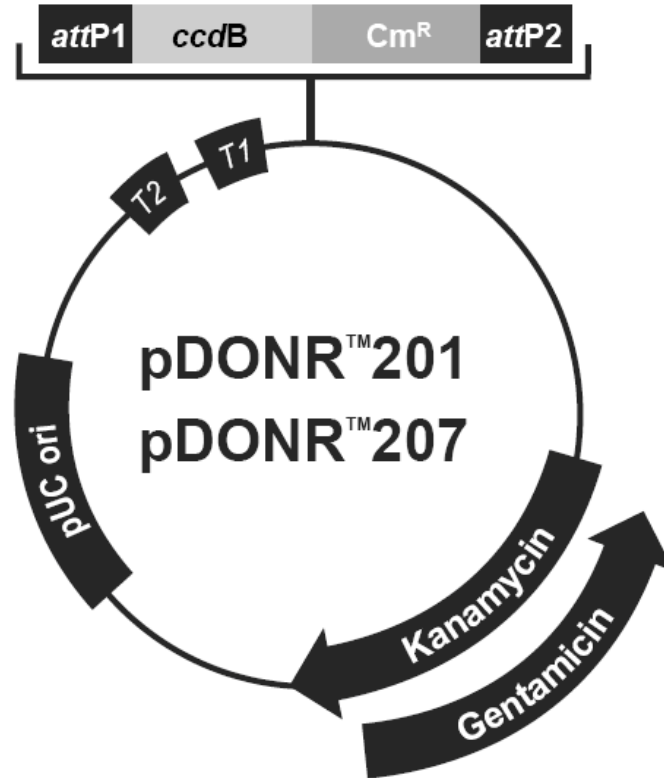


Figure 4.2 pDONR207 vector used to generate entry vector. It contains the *ccdB* gene for negative selection and Gentamicin for positive selection.

4.2.1.2 Create an expression clone

To create an expression clone the entry clone is recombined with a destination vector using the LR Clonase enzyme mix (Figure 4.1 B). The destination vector also has the *ccdB* gene for selection. The positive clones can then be selected for further transformations.

4.2.2 Production of barley transgenic plants expressing SAG21-YFP

4.2.2.1 Create a SAG21-YFP entry clone

4.2.2.1.1 Obtain *attB*-SAG21-YFP PCR products

pGREEN_35S-SAG21ORF-YFP vector was kindly provided from Dr Hilary J Rogers (School of Biosciences, Cardiff University). *attB* PCR primers were designed as described in the Gateway manual (Table 2.2). The manufacturer's instructions for the *Pfu* DNA polymerase were followed to obtain PCR products (#EP0501, Fermentas; Table 2.3). 20 ng of DNA were used in each case. The annealing temperature used was 50°C (Table 2.).

The PCR product was run on a 1% agarose electrophoresis gel. Bands of 1000 bp were obtained corresponding to the size of the SAG21-YFP gene (Figure 4.3). The bands were cut from the gel with a clean blade. The *attB*-PCR products were purified with GeneJET Gel Extraction Kit (#K0691, Fermentas).

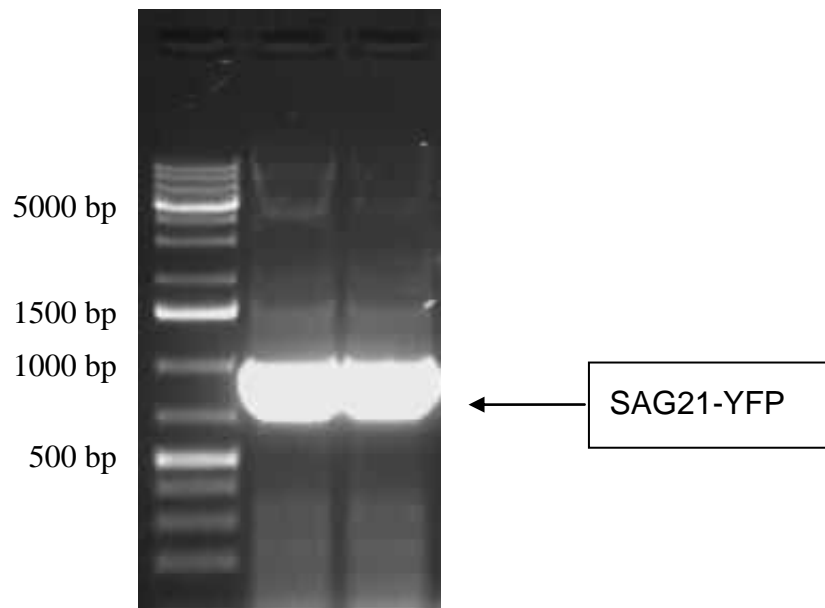


Figure 4.3 SAG21-YFP gene amplification with *attB* PCR primers.

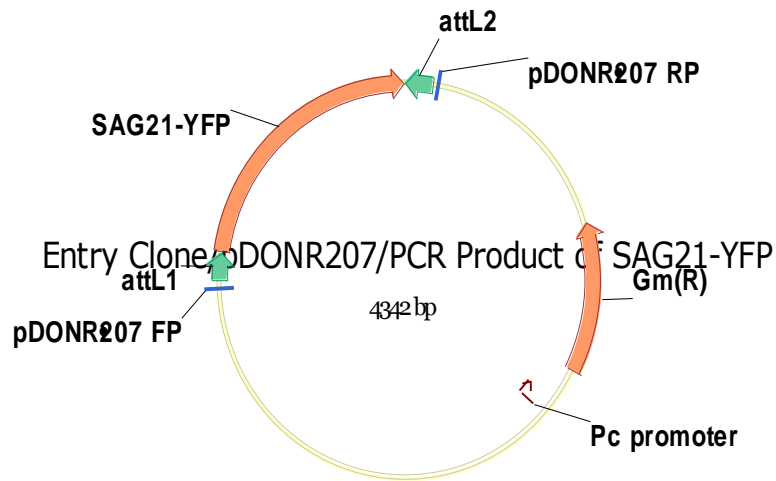


Figure 4.4 Map of the pDONR207 vector containing the SAG21-YFP gene. It consists in a vector with gentamycin gene resistance (Gm(R)), primers were designed in the area flanking the attL sites and SAG-YFP gene (pDONR207 FP and RP).

4.2.2.2 Create a SAG21-YFP expression clone

Using an LR recombination reaction, the SAG21-YFP insert was placed into an expression vector which to be used for plant transformation. For barley transformation pBRACT214 vector was chosen (Figure 4.5). It contains an ubiquitin promoter for high-level constitutive expression of the gene in monocotyledonous plants. It has a kanamycin resistance gene (*npt1*) for bacteria selection and hygromycin resistance gene for transformed plants selection. The components of the LR recombination reaction are shown in Table 2.6 of the material and methods chapter.

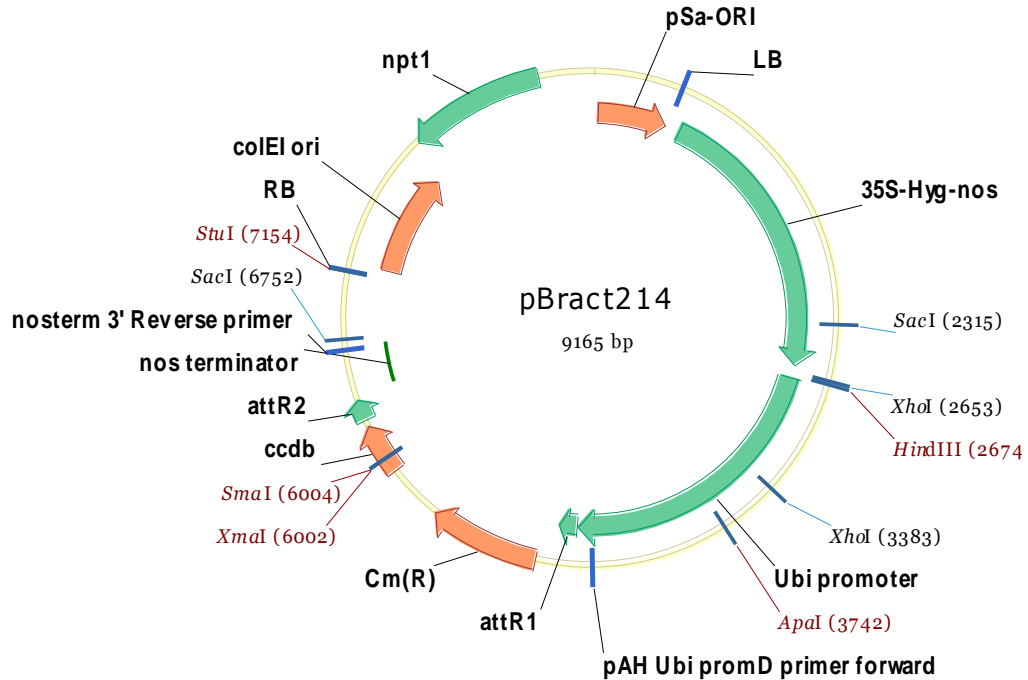


Figure 4.5 pBRACT-type vector used to generate expression vector. It contains ubiquitin promoter (Ubi promoter) for expression in monocotyledonous plants, kanamycin resistance gene (npt1) for bacteria selection and hygromycin resistance gene (Hyg) for positive selection in transformed plants. The components between the LB and RB are transferred to the plant during *Agrobacterium* transformation.

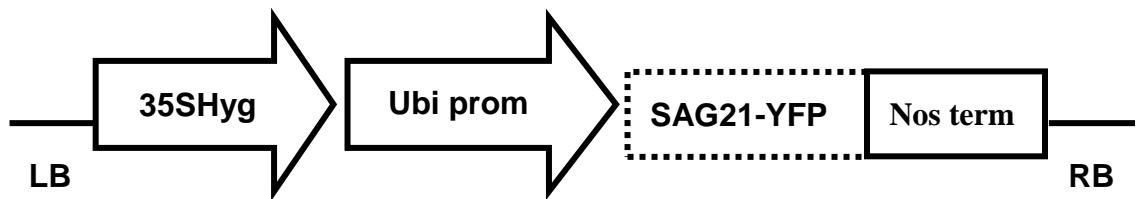


Figure 4.6 Map of the sequence which is located between left border (LB) and right border (RB) in the expression clone pBRACT214_SAG21-YFP. This sequence was integrated in the barley genome as a result of the transformation process.

4.2.2.3 *Agrobacterium* transformation with SAG21-YFP expression clone

Competent dH5 α bacteria were transformed with the product obtained from the LR reaction and DNA was extracted from the successful clones. The barley transformation is mediated by *Agrobacterium* bacteria, the strain selected was AGL1 which is most efficient in barley. The protocols followed for competent AGL1 production and transformation are described in the material and methods chapter (2.11.1.3 and 2.11.1.4).

4.2.2.4 Barley plants transformation

Barley transformation was performed by Diane Davidson at The James Hutton Institute, Dundee. Positive *Agrobacterium* aliquots containing the right vector BRACT214_SAG21-YFP were selected for the transformation. Barley cultivar 'Golden Promise' plants were used. Tillers were harvested at 16 weeks old and embryos were collected (Figure 4.7 pictures 1 and 2). The axis were removed from embryos to stop development of root and shoot apices (Figure 4.7 picture 2) and a drop of *Agrobacterium* culture was inoculated on each of the barley embryos, up to 100 embryos were inoculated (Figure 4.7 picture 3).

The embryos were co-cultivated with *Agrobacterium* cells containing the transformation vector for 3 days in the dark (week 1). Embryos were then transferred to fresh media containing timentin to kill the *Agrobacterium* and hygromycin to select for transformants. The embryos were transferred to fresh media every 2 weeks to induce the development of callus, this process takes 4-6 weeks (Figure 4.7 picture 4). After that embryos were moved on to regeneration media to produce shoots (Figure 4.7 picture 5). Finally transformed barley plants were grown in the glasshouse (Figure 4.7 picture 6). PCR from plants was performed using hygromycin primers to confirm the successful clones (Figures 4.5 and 4.6) and the result was positive for 36 lines (Figure 4.7 picture 7). The selection of firstly single insert seedlings and, secondly, homozygous seedlings will be done in plates with hygromycin (Figure 4.8).

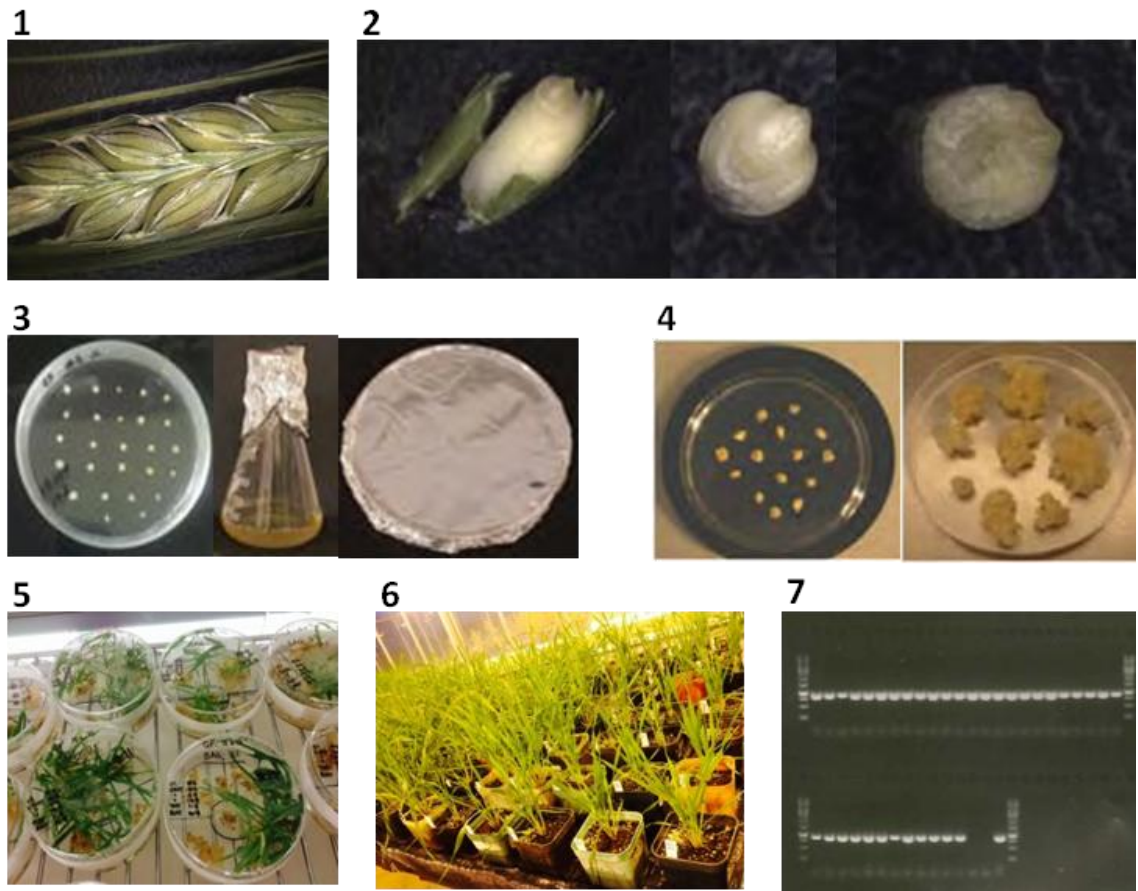


Figure 4.7 Barley transformation process. 16 weeks old barley tiller (1), barley embryo isolation (2), embryos co-cultivated with *Agrobacterium* cells (week 1) (3), embryos are then transferred to fresh media (week 2-6) (4), embryos moved on to regeneration media (5) (week 8-15), plants grown in the glasshouse (6) (week 16-40) and genotyping (7).

Following simple Mendelian inheritance 75% of the seedlings should inherit the resistance. The other 25% will be sensitive to the antibiotic and they will not grow. Deviations from this ratio can indicate multiple inserts. Since we are only using a sample size of 20 seeds this is a rough guide, although it has been routinely used and proves to be quite accurate. The seedlings which are resistant to hygromycin are likely to have a single copy so they are grown to full plant to obtain the next generation. The new generation seeds are grown again on agar with hygromycin media where the lines showing 100% resistant ones are probably homozygous (Figure 4.8).

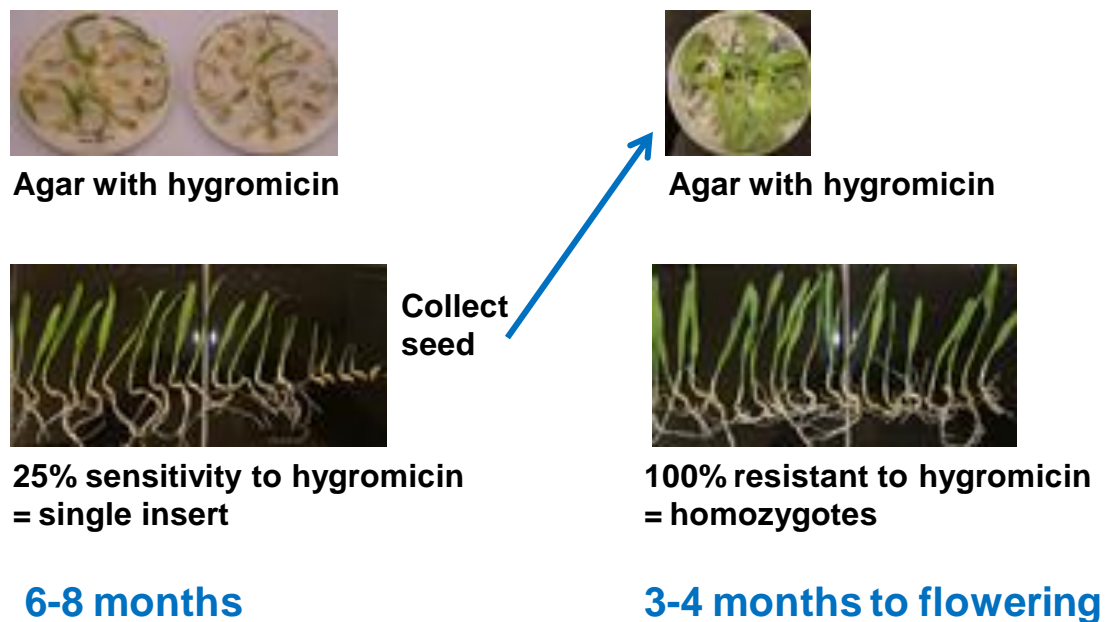


Figure 4.8 Method to obtain homozygous plants with a single insert. First single insert is checked by looking at the plant segregation, 25% of the seedlings are sensitive to hygromycin (no gene integrated) and 75% are resistant to hygromycin (both heterozygous and homozygous). These plants are grown to full plant to obtain next generation seeds which are grown again on hygromycin agar plates, if they are all resistant means that they are all homozygous.

4.2.2.5 State of the work with the SAG21-YFP transgenic barley plants

Barley transformation is a relatively quick procedure producing rooted plantlets within 3 months. However growing to seed and waiting for it to dry takes a long time which varies depending on the season. The transformation was started in February 2013 and we got T2 seeds ready to use by December 2014 (that is the standard time to grow 2 generations). The delay was mostly caused by small problems such as contamination during the first steps, in the co-cultivated embryos as well as in the embryos grown in fresh media. The SAG21 transgenic plants were selected by PCR using hygromycin primers and $T_m = 64^\circ\text{C}$ (Table 2.7). The 36 lines screened gave positive results, a band of 917 bp was obtained in each lane corresponding to the hygromycin gene size (Figure 4.9). For controls, barley plants were transformed in parallel with pBRACT214 vector containing the GUS fragment. They were checked by PCR following the indications described for the transformed SAG21 plants (Table 2.7). Finally, 18 lines of pBRACT214GUS were positive for the hygromycin gene. All the positive lines are currently being selected using the method to obtain homozygous plants with a single insert (Figure 4.8).

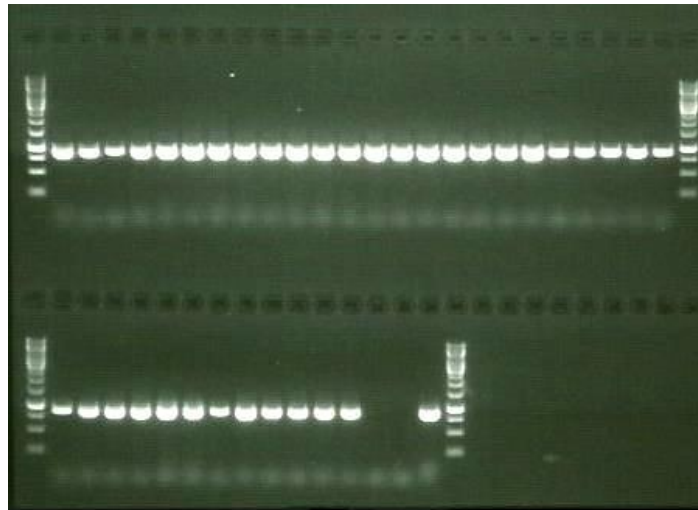


Figure 4.9 PCR results of the SAG21-YFP barley lines. 36 lines were checked together with two negative controls and one positive control (last three lanes).

4.2.3 Cloning of OCI gene into pDONR and pENTR-type vectors

4.2.3.1 pENTR1A-OCI construction

4.2.3.1.1 OCI amplification with *Bam*HI and *Xho*I restriction sites

Cut and paste cloning was performed in order to insert the OCI gene into the pENTR1 vector. The OCI gene was taken from a pLBR19-OCI construct produced before in our lab. A first attempt was done using *Dra*I and *Eco*RV restriction enzymes but no colonies were obtained after transforming bacteria with the ligation product. Both primers began immediately with the restriction sites, so it may be possible that the product did not digest sufficiently for cloning. Therefore a new cloning strategy was designed using *Bam*HI and *Xho*I restriction enzymes (Figure 4.10). The first step was to amplify OCI to attach these new restriction sites to its sequence. Primers containing *Bam*HI and *Xho*I restriction sites were then designed (Table 2.8), this time they had some extra nucleotides before the restriction site (GAAA) to facilitate restriction enzyme binding and efficient digestion. OCI plasmid was diluted 1:30 and 1 µl of it was used in 50 µl PCR reaction using Phusion II polymerase, 2 reactions were performed in a final volume of 50 µl using PCR conditions showed in Table 2.9. The two PCR reactions were then pooled and run on a gel, the OCI amplification was successful (Figure 4.11).

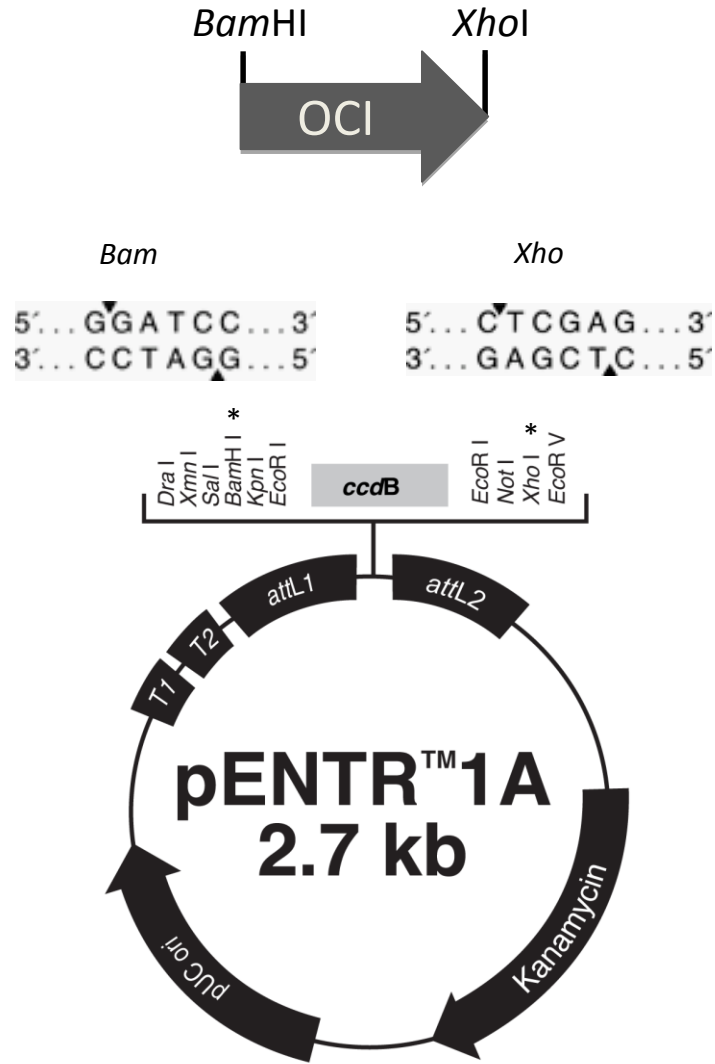


Figure 4.10 Experimental design of the OCI cloning into pENTR1A vector using *Bam*HI and *Xho*I restriction enzymes.

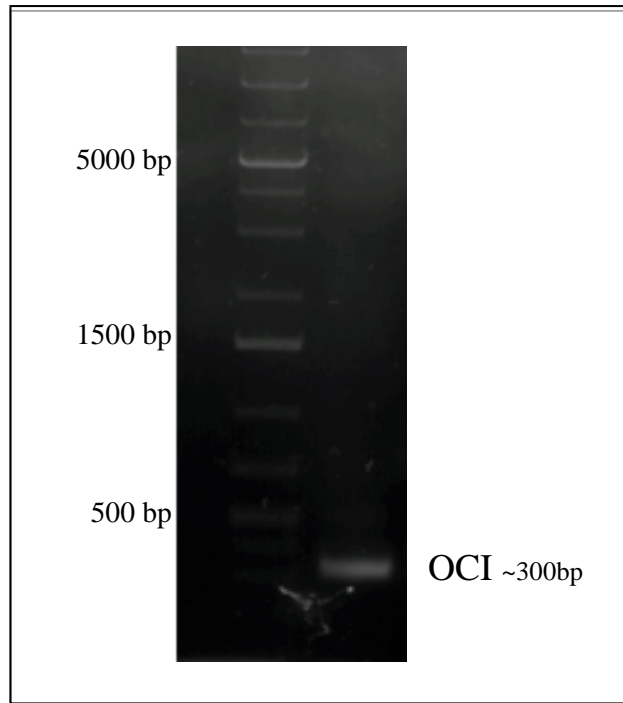


Figure 4.11 OCI PCR product containing *Bam*HI and *Xho*I sites.

4.2.3.1.2 OCI and pENTR1A plasmid digestions and ligation

The amplified OCI insert was purified and digested together with the pENTR1A plasmid at 37°C for 30 min (Table 2.10). After that pENTR1A plasmid was dephosphorylated using FastAP Alkaline Phosphatase (Thermofisher), following their instructions. Ligations were performed using Rapid DNA ligation kit (Thermofisher). 1 µl plasmid and 4 µl insert (or SDW for control) were used in 10 µl reaction, they were kept for 5 min according to manufacturer instructions. DH5α cells were transformed with 3 µl ligation product, 100 µl of the total 500 µl culture were plated onto LB Kanamycin plates.

4.2.3.1.3 pENTR1A-OCI clones verification

pENTR1A-OCI ligation products were extracted from bacteria and digested again with *Bam*HI + *Xho*I restriction enzymes (Figure 4.12). The sized of the bands obtained were 300 bp for OCI and 2.2 Kb for the vector as expected. They were then sent for sequencing for final confirmation.

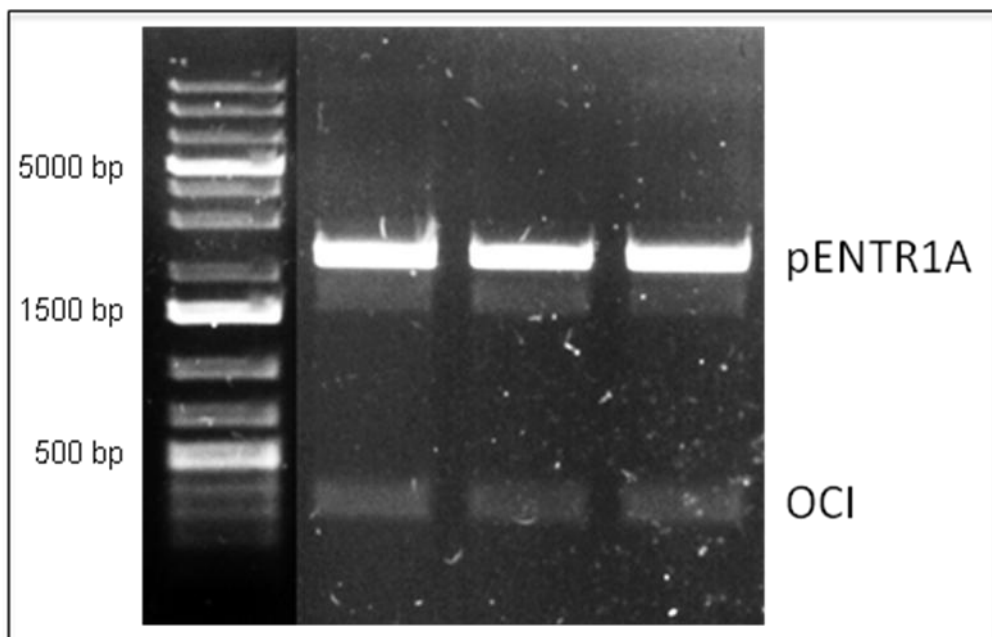


Figure 4.12 *Bam*HI + *Xho*I digests of mini-preps. Bands of 300 bp and 2.2 Kb were obtained which corresponds with the size of OCI insert and pENTR1A vector, respectively.

4.2.3.2 pDONR-OCI construction

4.2.3.2.1 Obtain *attB*_OCI PCR products

The OCI gene was inserted into DONR201 vector (Figure 4.14) using Gateway technology. The first step was to design primers containing *attB* site (Table 2.11). The PCR reaction was performed following Gateway instructions and the *attB* OCI amplification was successful (Figure 4.13).

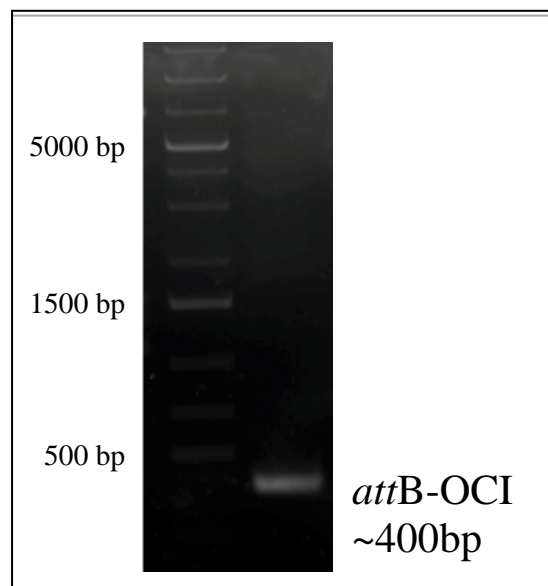


Figure 4.13 OCI PCR product containing *attB* sites.

4.2.3.2.2 Create OCI entry clones using the BP recombination reaction

BP reaction was performed following Gateway instructions and was left to incubate over night, similarly to the reaction performed for SAG21-YFP (Table 2.5). BP reactions were then transformed into DH5 α cells and plated onto LB Kanamycin plates. The positive ones were digested with *Hind*III and *Pvu*I (Figure 4.15) and sent for sequencing for confirmation.

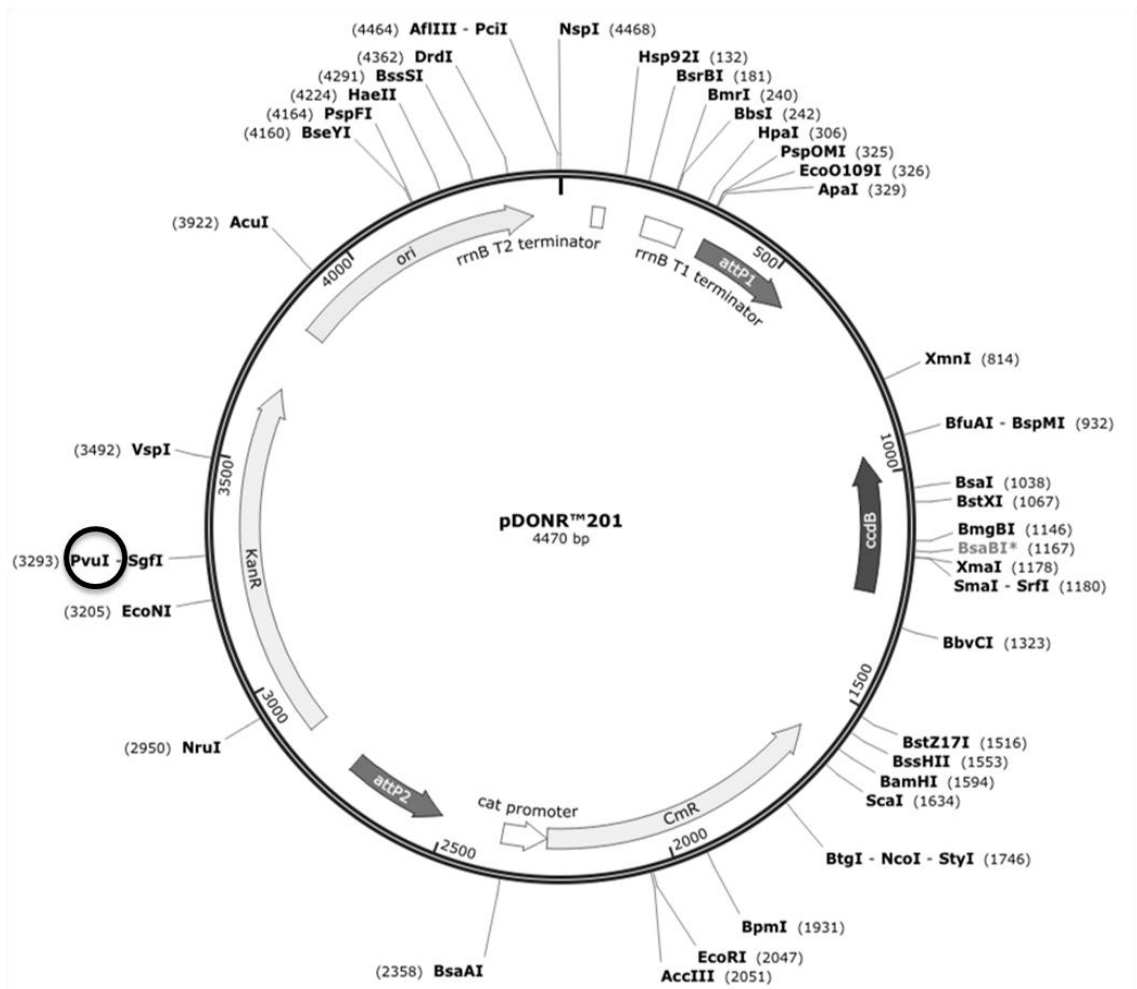


Figure 4.14 Map of pDONR201 vector with restriction sites.

4.2.3.3 Positive OCI clone selection

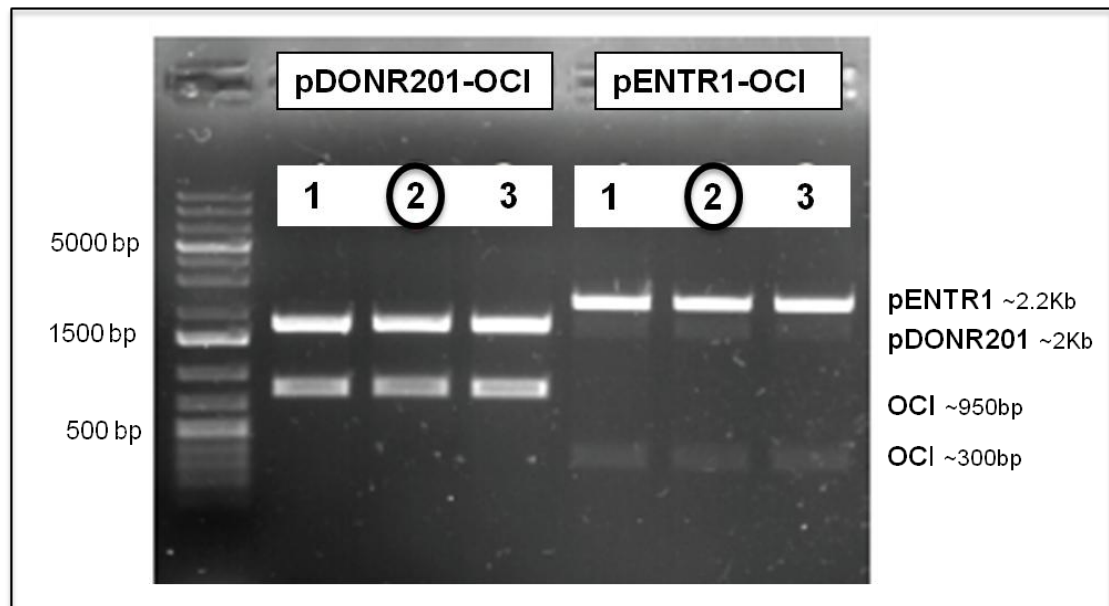


Figure 4.15 Digestions of the two OCI constructs produced. pDONR201-OCI digested with *Hind*III and *Pvu*I and pENTR1-OCI digested with *Bam*HI and *Xho*I.

pDONR201-OCI was digested with *Hind*III and *Pvu*I restriction enzymes (Figure 4.15). *Hind*III is located in the OCI gene insert and *Pvu*I in the pDONR201 vector (3293 bp position, Figure vector 4.14). The expected size of the vector is around 2 Kb and the OCI insert with part of the vector would be around 950 bp, these numbers matched with the sizes of the band obtained so the three clones could be right. pENTR1-OCI was digested with *Bam*HI and *Xho*I (Figure 4.15). Bands of 2.2 Kb and bands of 300 bp were obtained in the three clones checked, these results corresponded with the expected sizes of pENTR1 vector and OCI insert. Clones 1 and 2 were sequencing in each cases and both clones 2s had no errors (Figure 4.15, circles).

4.3 Discussion: future uses of the transformed barley and wheat plants

The SAG21 expression vector for barley transformation was easily produced in a short time and barley plants were successfully transformed, in total 36 transgenic lines were finally generated. However, OCI cloning using the same method was complicated and, after various failed attempts, it was postponed. Later on it was resumed following a request from a research group in the National Institute of Agricultural Botany (NIAB) which was interested in expressing OCI in wheat plants. The modified objective for wheat was to clone the OCI gene first into a pENTR-type vector that could then be used to generate the plant expression clone using Gateway. With the help of Dr Barry Causier, the OCI gene could be finally inserted into a pENTR1A vector and also into a pDONR201 vector. Transgenic wheat plants with an ectopic expression of OCI have been already produced and the pDONR201-OCI vector is available for future uses.

4.3.1 Analysis of the barley transgenic plants expressing SAG21-YFP

The effects of constitutive expression the SAG21 protein on chloroplast protein turnover and leaf senescence will be studied under optimal and stress conditions. Firstly, differences between the transgenic lines and the wild type will be explored under optimal conditions. Parameters related to growth and development such as shoot and root biomass, root architecture, time to flowering and number of tillers will be measured. Since SAG21 is up-regulated by different oxidants and it is thought to be implicated in ROS signalling, cellular redox state of these transgenic plants will be also investigated (Mowla et al., 2006; Salleh et al., 2012). The YFP tag will also allow further microscopy experiments. Similar analyses will be performed under a range of abiotic and biotic stresses; a starting point could be checking the tolerance to H₂O₂ since

the expression of SAG21 in Arabidopsis led more resistant plants (Salleh et al., 2012). Pathogen resistance and aphid fecundity assays might be also run on the SAG21 barley plants.

4.3.2 Analysis of the wheat transgenic plants expressing OCI

The first objective is to determine if the ectopic expression of OCI protein in wheat leads to a delayed leaf senescence and enhanced tolerance to abiotic stress such as drought, as it has been proved for other plant species (Quain et al., 2014). Secondly, protein accumulation in the seeds will be tested. The final aim is to improve performance and quality traits in wheat.

Chapter 5. Characterization of WHIRLY1 RNAi barley lines under optimal and stress conditions

5.1 Introduction

The WHIRLY family of proteins are found in chloroplasts, mitochondria and the nuclei, where they are considered to fulfil important but as yet largely uncharacterised functions. While most plant species including barley have two *WHIRLY* genes (Desveaux et al., 2005), *Arabidopsis* has three genes, the *AtWHIRLY1* and *AtWHIRLY3* being targeted to plastids while *AtWHIRLY2* is targeted to mitochondria (Krause et al., 2005; Krause et al., 2009). The functions of the different WHIRLY proteins has been investigated in knockout mutants that are deficient in one or more of the *WHIRLY* genes or in transgenic plants that has been transformed with RNAi constructs to decrease the expression and hence abundance of the different WHIRLY proteins (Melonek et al., 2010). However, the characterisation of these mutants has not been particularly helpful because relatively few common traits of plants lacking WHIRLY proteins have been revealed to date. For example, the maize *zmwhy1-1* mutants show a severe phenotype and do not survive beyond the 4-leaf stage. The lethal phenotype has been linked to the lack of plastid ribosomes and impaired chloroplast development (Prikryl et al., 2008). In contrast, the *Arabidopsis why1* mutants have no apparent phenotype (Yoo et al., 2007). However, a small percentage of the *Arabidopsis why1why3* mutants have a variegated green/white/yellow leaf phenotype (Marechal et al., 2009; Cappadocia et al., 2010). The functions of WHIRLY1 have also been characterised in transgenic barley (*Hordeum vulgare* cv. "Golden Promise") lines with RNAi-mediated knock-down of the *HvWHIRLY1* gene (Melonek et al., 2010; Krupinska et al., 2014). Like the *Arabidopsis why1* mutants, the WHIRLY1 -deficient (W1) barley lines did not show a marked phenotype when grown under optimal conditions (Melonek et al., 2010; Krupinska et al., 2014).

However, analysis of the homozygous W1-7 line, which has no detectable WHIRLY1 protein, revealed that leaves have up to three times as much plastid (pt) DNA as the wild type, together with a modified nucleoid structure (Krupinska et al., 2014). However, these lines have not yet been extensively characterised, particularly in terms of growth under different conditions. The following studies were therefore undertaken firstly to characterise the growth and development of three independent RNAi knockdown lines (W1-1, W1-7 and W1-9) comparing phenotypic characteristics of plants grown in soil or in vermiculite with nutrient solution. The second objective of these studies was to compare the phenotypes of the W1-1, W1-7 and W1-9 lines grown in vermiculite with complete nutrient solution (nitrogen-replete) with that of plants grown with only low (0.1 mM NO₃⁻) levels of nitrogen (nitrogen-deficient). The third objective was to develop a system for stress-induced senescence based on growth under low nitrogen availability that could be used thereafter to further analyse the phenotype of the RNAi knockdown lines with low WHIRLY1 protein. Low-nitrogen induced senescence was chosen for these studies because the effects of nitrogen limitation on plant growth are well characterised, particularly in terms of photosynthesis, gene expression and premature senescence (Lian et al., 2006; Jukanti et al., 2008). Nevertheless, while many studies on the effects of nitrogen limitation have been conducted on model plants such as *Arabidopsis*, the effects of nitrogen deficiency are less well characterised in crop plants such as barley. In addition, some preliminary experiments were performed to characterise the phenotypes of the WHIRLY1-deficient lines to drought stress.

5.2.1 Shoot phenotypes of plants grown in soil

The shoots of 14 day old W1-1 seedlings were not visibly different from those of the wild type (Figure 5.1 A) but they tended to have fewer leaves (Figure 5.1 B). However, in comparison to the endogenous control line i.e. that has been through the transformation process but did not express the transgene (C W1-7), the shoot phenotype of the 14 day old W1-7 seedlings was visibly smaller (Figure 5.1 C) with fewer leaves (Figure 5.1 D).

The shoots of 14 day old W1-1 seedlings had a similar number of leaves (Figure 5.2 A) and biomass (Figure 5.2 B) to the wild type. However, in comparison to the C W1-7 control, the shoots of the 14 day old W1-7 seedlings had significantly fewer leaves (Figure 5.2 C) with a smaller total shoot biomass (Figure 5.2 D).

The shoots of 14 day old W1-1 seedlings had similar amounts of soluble protein (Figure 5.3 A) and chlorophyll (Figure 5.3 B) to the wild type. Similarly, the shoots of the 14 day old W1-7 seedlings had similar protein (Figure 5.3 C) and chlorophyll (Figure 5.3 D) contents to the C W1-7 controls.

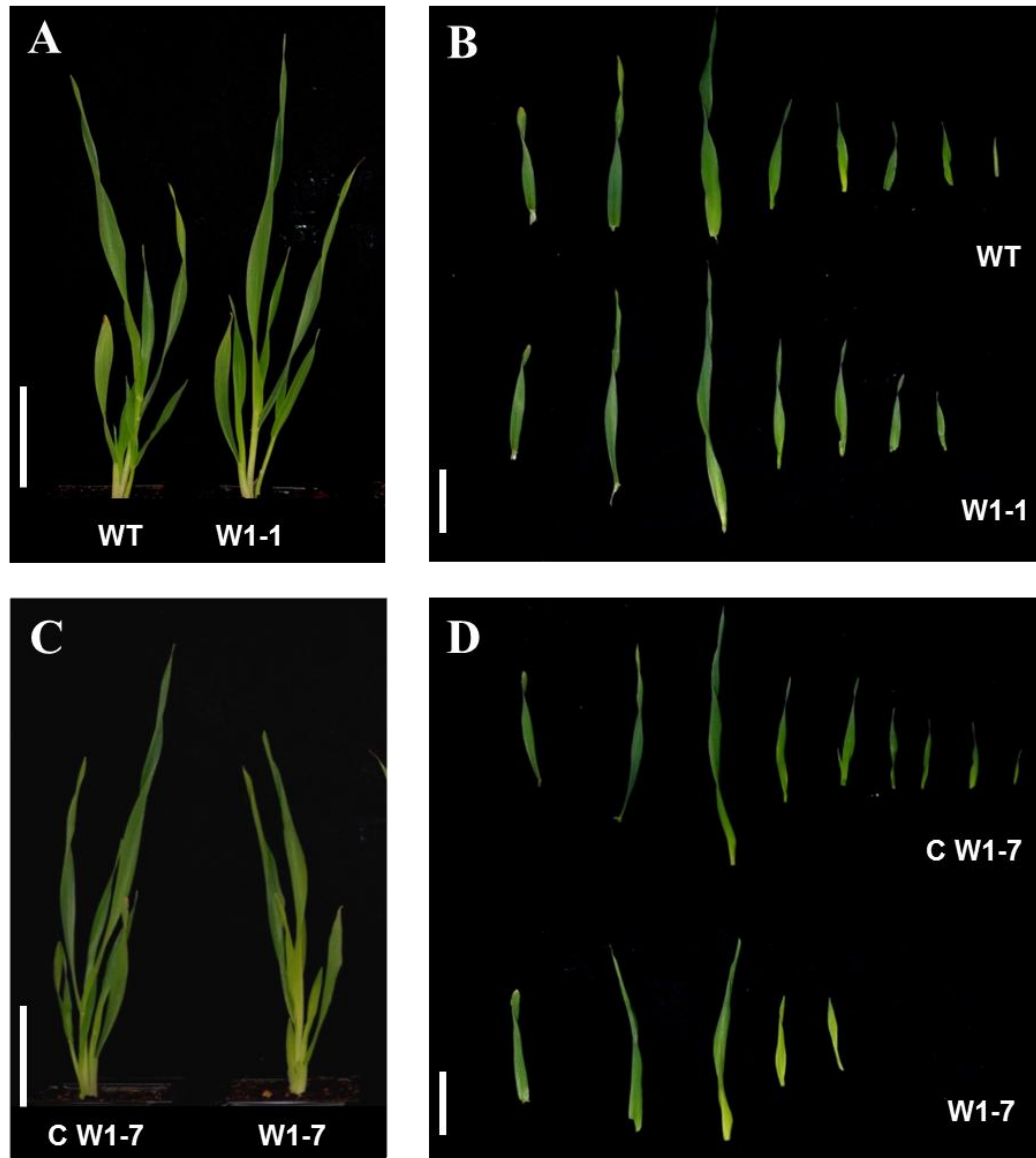


Figure 5.1 A comparison of shoot phenotypes of 14-day old seedlings of the transgenic W1-1 and W1-7 lines to the wild type (WT) and a transgenic control line (C W1-7) lacking the transgene. (Scale bar = 5 cm). Seeds were germinated and grown in soil in controlled environment chambers with a 16h light/ 8h dark photoperiod (irradiance $450 \mu\text{mol m}^{-2}\text{s}^{-1}$), $21^{\circ}\text{C}/16^{\circ}\text{C}$ day/night temperature regime and 60% relative humidity.

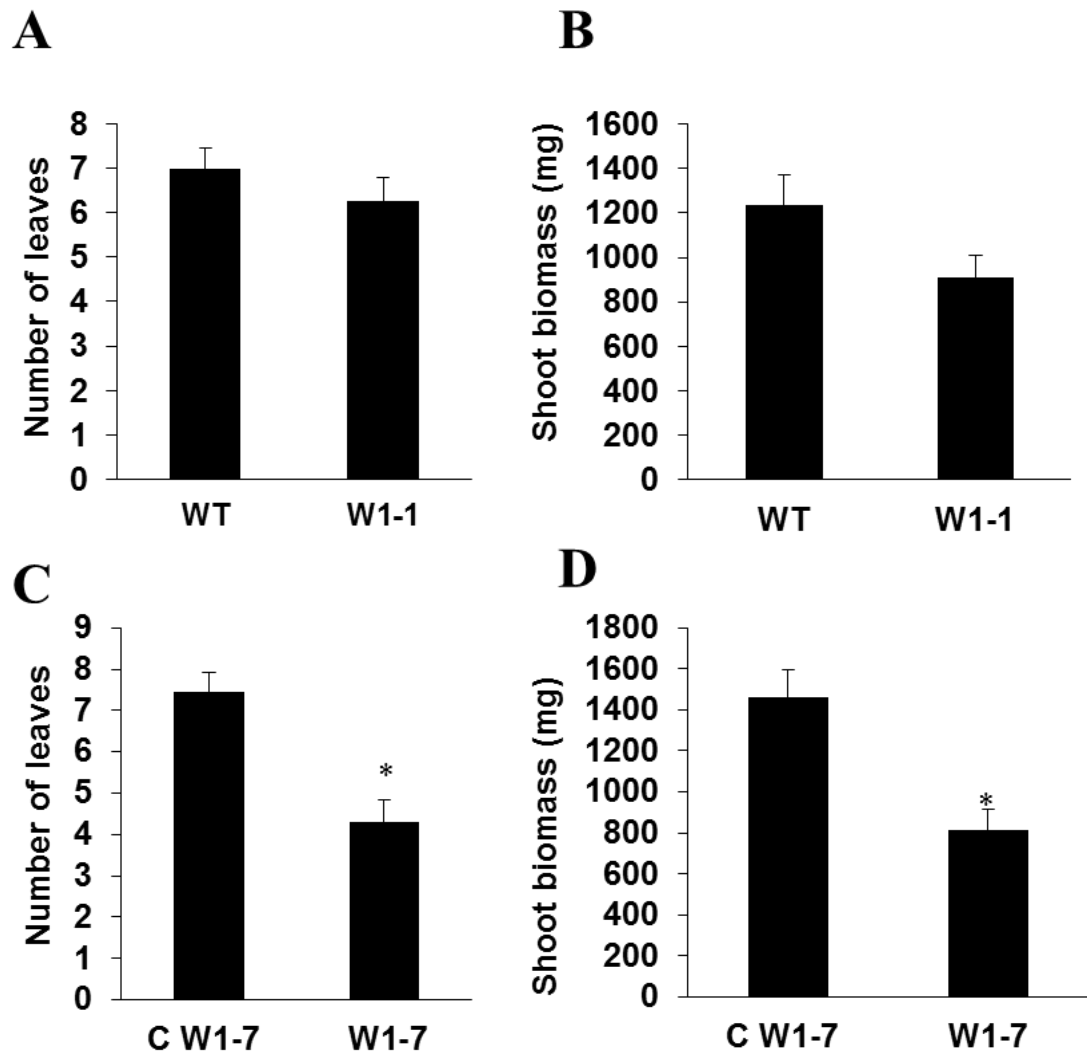


Figure 5.2 A comparison of leaf numbers (A, C) and shoot biomass (B, D; expressed on a fresh weight basis) in 14-day old seedlings of the transgenic W1-1 and W1-7 lines to the wild type (WT) and a transgenic control line (C W1-7) lacking the transgene. Data are the mean values \pm SE (n = 10 A, C) (n = 6 B, D). Values that were significantly different between wild type and W1-7 plants determined using the students T-test are indicated by asterisks ($P < 0.05$).

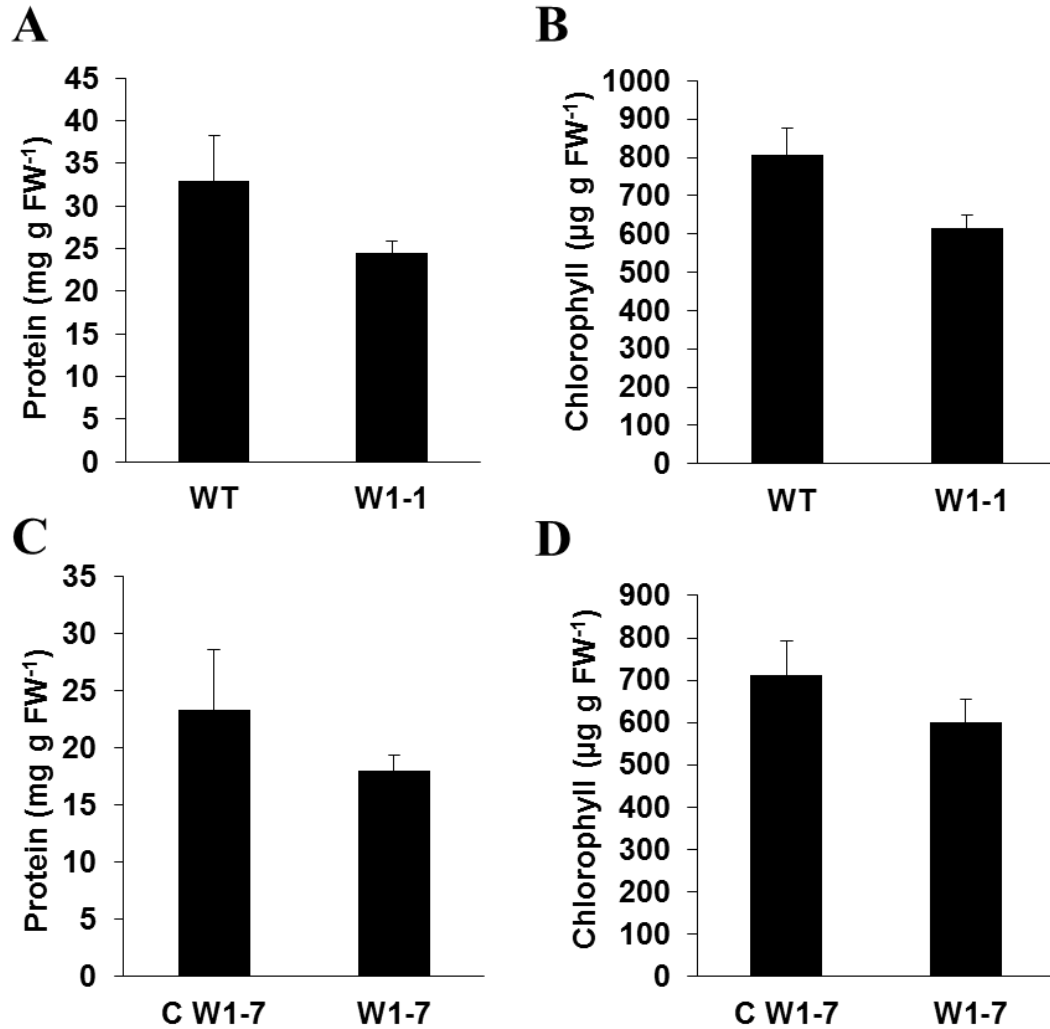


Figure 5.3 A comparison of leaf soluble protein (A, C) and chlorophyll (B, D) contents and shoot biomass in 14-day old seedlings of the transgenic W1-1 and W1-7 lines to the wild type (WT) and a transgenic control line (C W1-7) lacking the transgene. Data are the mean values \pm SE ($n = 5$). Values that were significantly different between wild type and W1-7 plants determined using the students T-test are indicated by asterisks ($P < 0.05$).

Table 5.1 Seed yield in W1-7 and wild type barley plants. The numbers of fertile tillers were counted and total seed yield quantified in plants grown to maturity in soil under in controlled environment glasshouses. Data are the mean values \pm SE (n = 5). Values that were significantly different between wild type and W1-7 plants determined using the students T-test are indicated by asterisks (P<0.05).

	Wild type	W1-7
Number of fertile tillers	10.80 \pm 1.02*	4.80 \pm 1.15*
Total seed yield (g)	13.96 \pm 1.68*	5.86 \pm 1.36*
Seed yield per fertile tiller (g)	1.28 \pm 0.05	0.97 \pm 0.24

The W1-7 plants had significantly lower numbers of fertile tillers than the wild type (Table 5.1). At harvest, the W1-7 plants had on average 5 fertile tillers per plant while the wild type had about 11. As a result of the lower number of tillers per plant, the total seed yield was reduced by half in the transgenic plants relative to the wild type (Table 5.1). However, the seed yield per tiller was not significantly different between the genotypes (Table 5.1).

5.2.1.1 Volatile emission from leaves

The volatile compounds emitted by wild type barley and W1-7 seedlings were analysed by gas chromatography. The wild type barley leaves measured at 16 and 18 days after sowing, showed a pattern of emissions that were similar to those of the W1-7 seedlings (Figure 5.4).

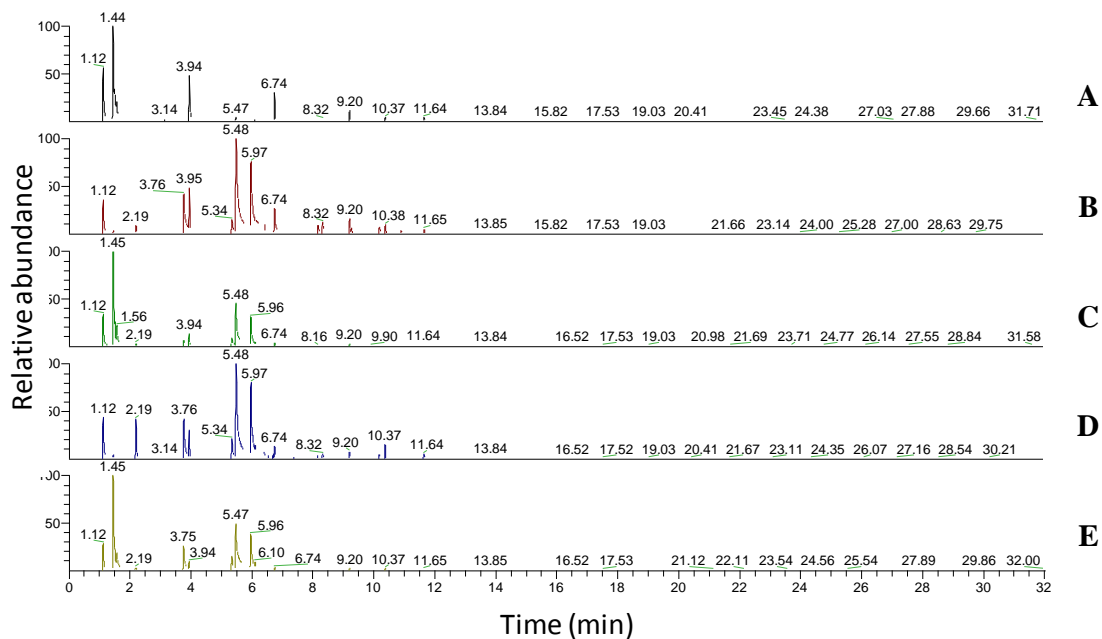


Figure 5.4 A comparison of the volatile compounds emitted by wild type barley and W1-7 seedlings. Volatile compounds were analysed in control (A; soil), two technical replicates (B, C) of wild type barley and two technical replicates of W1-7 seedlings (D, E) 16 and 18 days after sowing.

A closer examination of the profile of the volatile compounds emitted by wild type barley and W1-7 seedlings revealed that a compound with a mass spectrum consistent with that of toluene was a major volatile emitted from barley leaves (Figure 5.5).

Similarly, wild type barley and W1-7 seedlings emitted other aromatic hydrocarbons with spectra consistent with ethylbenzene, p-xylene, o-xylene (Figure 5.6) and 4-hexen-1-ol acetate (Figure 5.7).

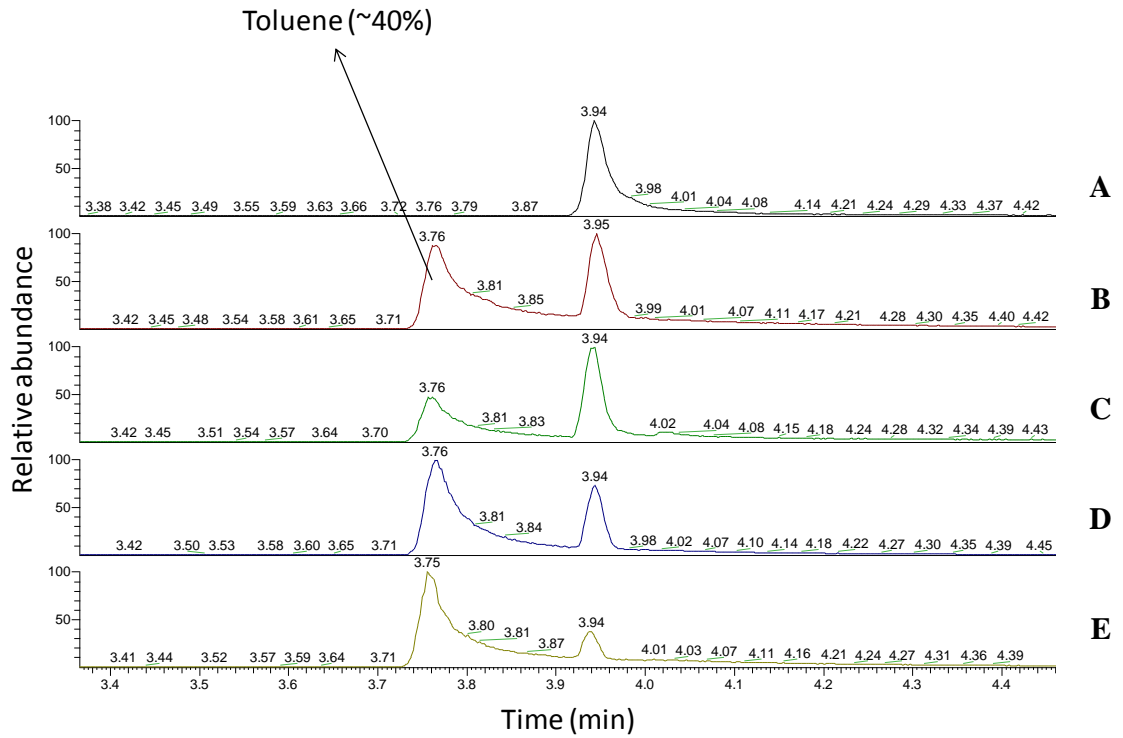


Figure 5.5 Identification of volatile compound emitted by wild type barley and W1-7 seedlings. Volatile compounds were analysed in control (A; soil), two technical replicates (B, C) of wild type barley and two technical replicates of W1-7 seedlings (D, E) 16 and 18 days after sowing.

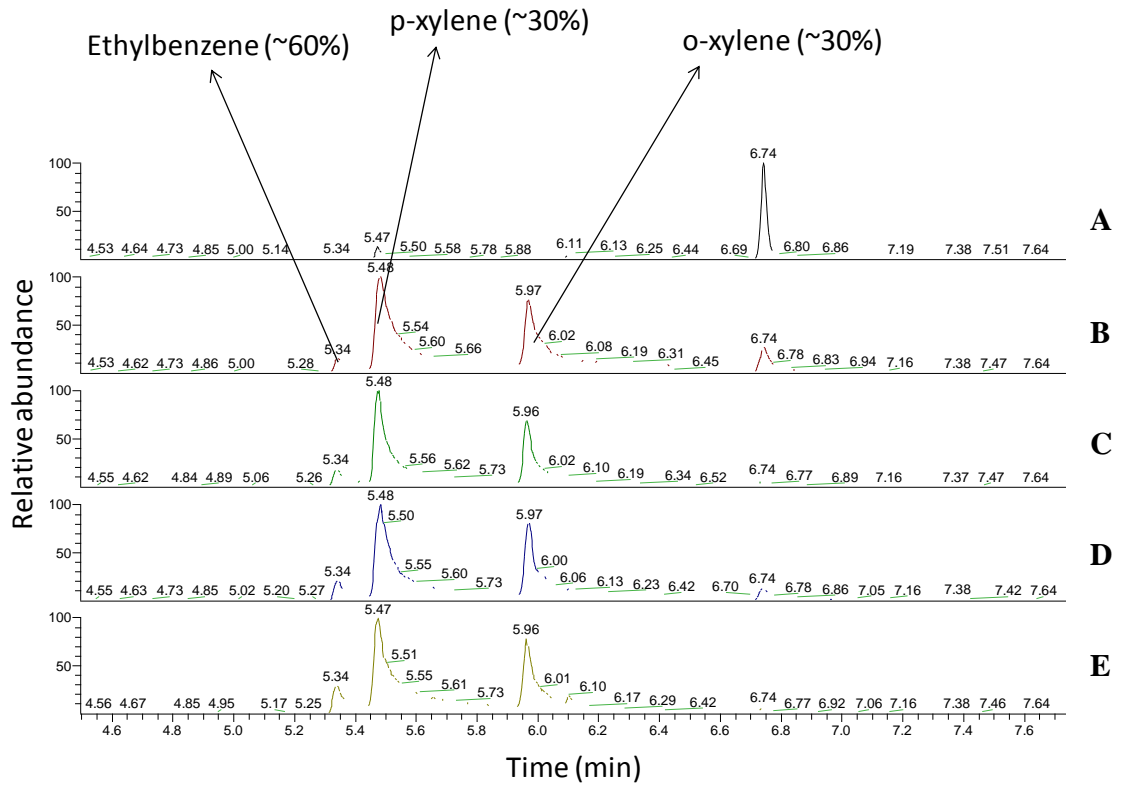


Figure 5.6 Identification of volatile compound emitted by wild type barley and W1-7 seedlings. Volatile compounds were analysed in control (A; soil), two technical replicates (B, C) of wild type barley and two technical replicates of W1-7 seedlings (D, E) 16 and 18 days after sowing.

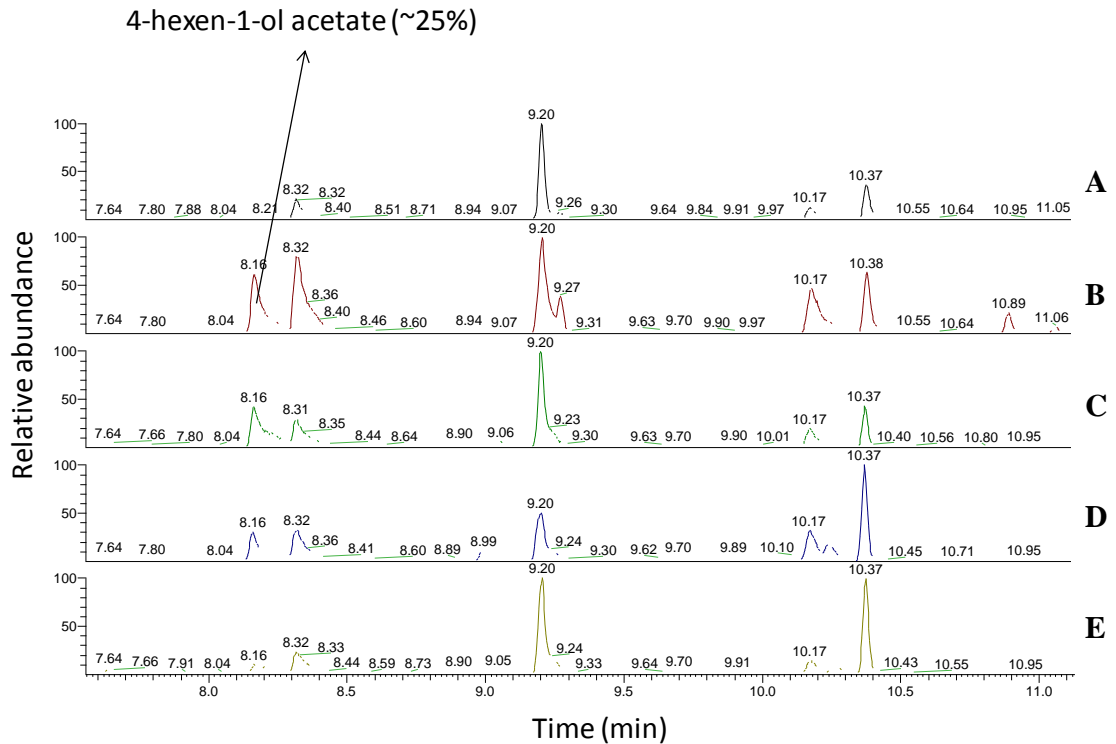


Figure 5.7 Identification of volatile compound emitted by wild type barley and W1-7 seedlings. Volatile compounds were analysed in control (A; soil), two technical replicates (B, C) of wild type barley and two technical replicates of W1-7 seedlings (D, E) 16 and 18 days after sowing.

5.2.2 Shoot phenotypes of plants grown in vermiculite with complete nutrient solution

The shoots of 14 day old W1-1 seedlings were not visibly different from those of the wild type (Figure 5.8 A) but they had the same number of leaves (Figure 5.8 B). Similarly, the shoot phenotype of the W1-7 seedlings was not different to its control C W1-7 (Figure 5.8 C) and they both had 3 leaves (Figure 5.8 D).

The shoots of 14 day old W1-1 seedlings grown in vermiculite had a similar number of leaves (Figure 5.9 A), however their biomass was significantly higher (Figure 5.9 B) than that of the wild type. There were no differences in the number of leaves of the 14 day old W1-7 seedlings in comparison to the C W1-7 control leaves (Figure 5.9 C) with similar total shoot biomass (Figure 5.9 D).

The shoots of 14 day old W1-1 seedlings had similar amounts of soluble protein (Figure 5.10 A) and chlorophyll (Figure 5.10 B) to the wild type. Similarly, the shoots of the 14 day old W1-7 seedlings had similar protein (Figure 5.10 C) and chlorophyll (Figure 5.10 D) contents to the C W1-7 controls.

The shoots of 14 day old W1-1, W1-7 and W1-9 seedlings were similar to those of the wild type (Figure 5.11 A) as well as the shoot and root biomass (Figure 5.11 B). There were no significant differences in the shoot/ root ratios of any of the three transgenic lines compared to the wild type (Figure 5.11 C). The leaves of the transgenic lines showed significantly higher amounts of chlorophyll than the wild type (Figure 5.11 D). Similarly, the carotene content was significantly higher in the lines W1-1 and W1-7 (Figure 5.11 E). Leaf soluble protein content was significantly higher in the W1-1 compared to the wild type (Figure 5.11 F).

Photosynthetic rates, stomatal conductance and transpiration were daily measured on the first leaf of the wild type and W1-7 seedlings for 7 days until the age of 14 days (Figure 5.12). W1-7 showed significantly higher stomatal conductance (Figure 5.12 B) and transpiration rates (Figure 5.12 C) than the wild type despite showing comparable CO₂ assimilation rates along the week (Figure 5.12 A).

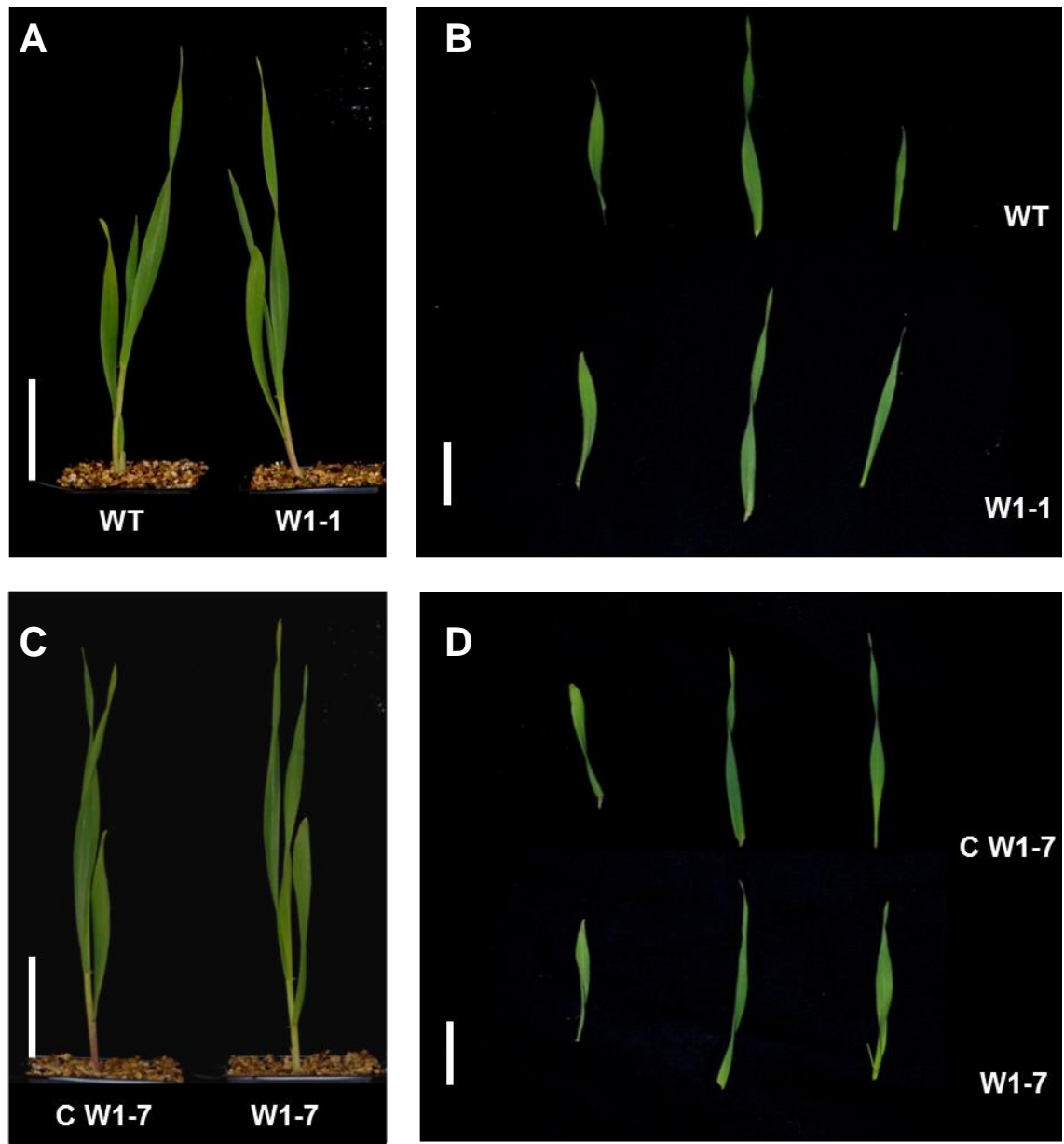


Figure 5.8 A comparison of shoot phenotypes of 14-day old seedlings of the transgenic W1-1 and W1-7 lines to the wild type (WT) and a transgenic control line (C W1-7) lacking the transgene. (Scale bar = 5 cm).

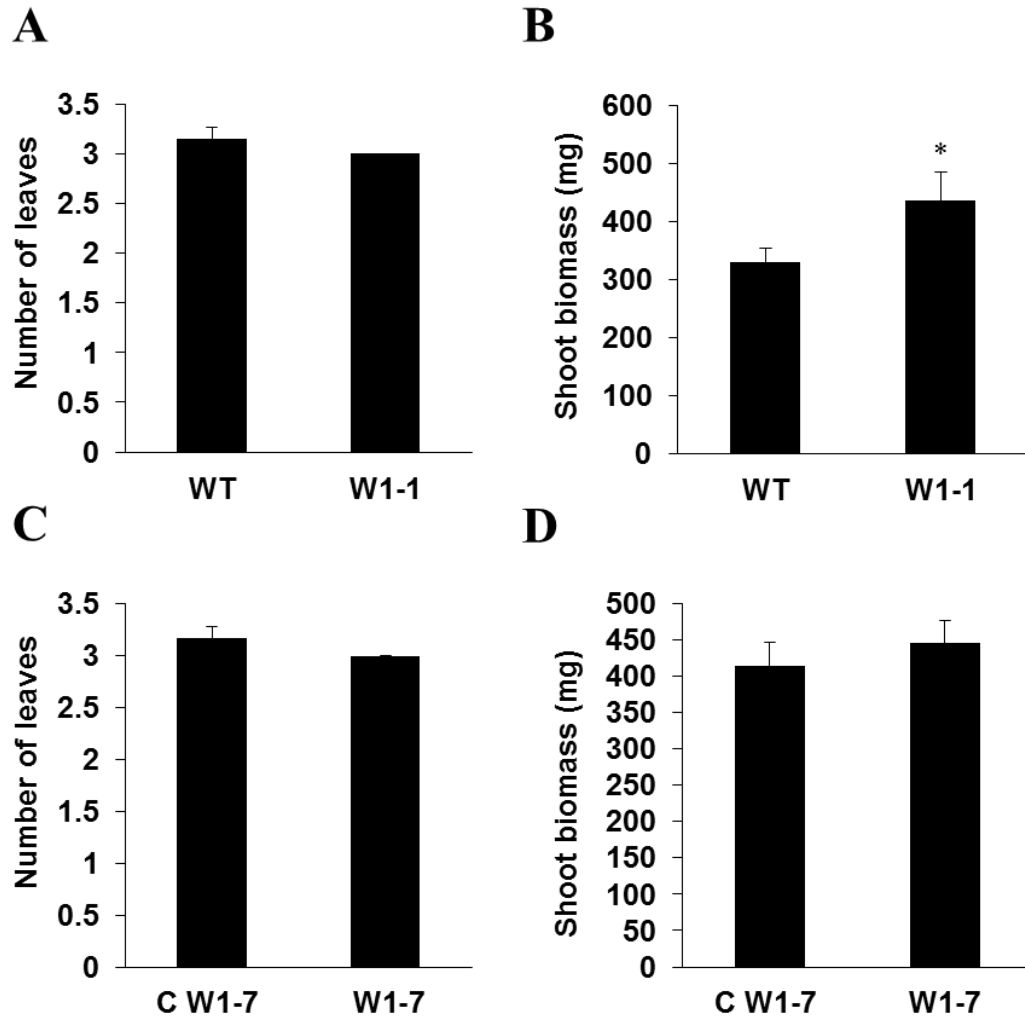


Figure 5.9 A comparison of leaf number (A, C) and shoot biomass (B, D; expressed on a fresh weight basis) in 14-day old seedlings of the transgenic W1-1 and W1-7 lines to the wild type (WT) and a transgenic control line (C W1-7) lacking the transgene. Data are the mean values \pm SE (n = 10 A, C) (n = 6 B, D). Values that were significantly different between wild type and W1-7 plants determined using the students T-test are indicated by asterisks ($P < 0.05$).

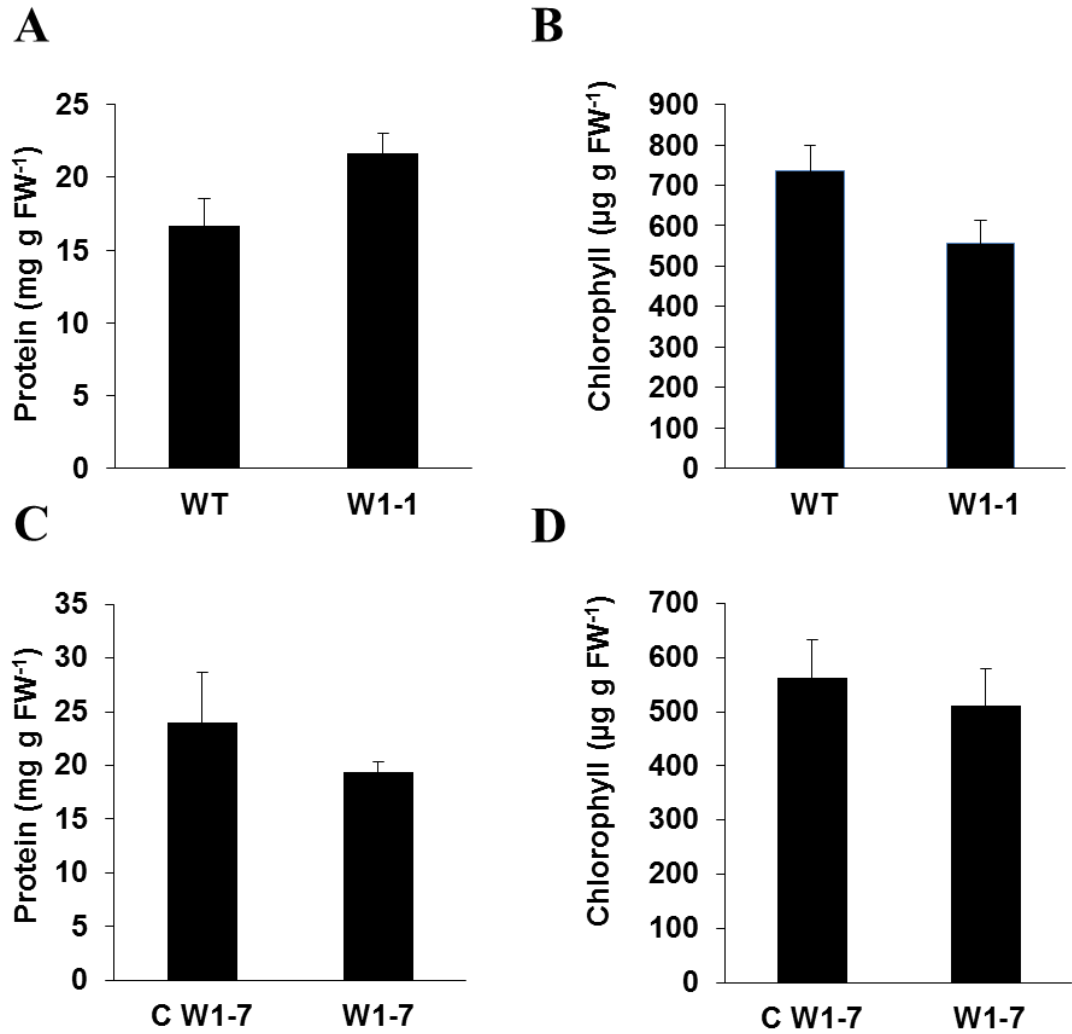


Figure 5.10 A comparison of leaf soluble protein (A, C) and chlorophyll (B, D) contents and shoot biomass in 14-day old seedlings of the transgenic W1-1 and W1-7 lines to the wild type (WT) and a transgenic control line (C W1-7) lacking the transgene. Data are the mean values \pm SE ($n = 5$). Values that were significantly different between wild type and W1-7 plants determined using the students T-test are indicated by asterisks ($P < 0.05$).

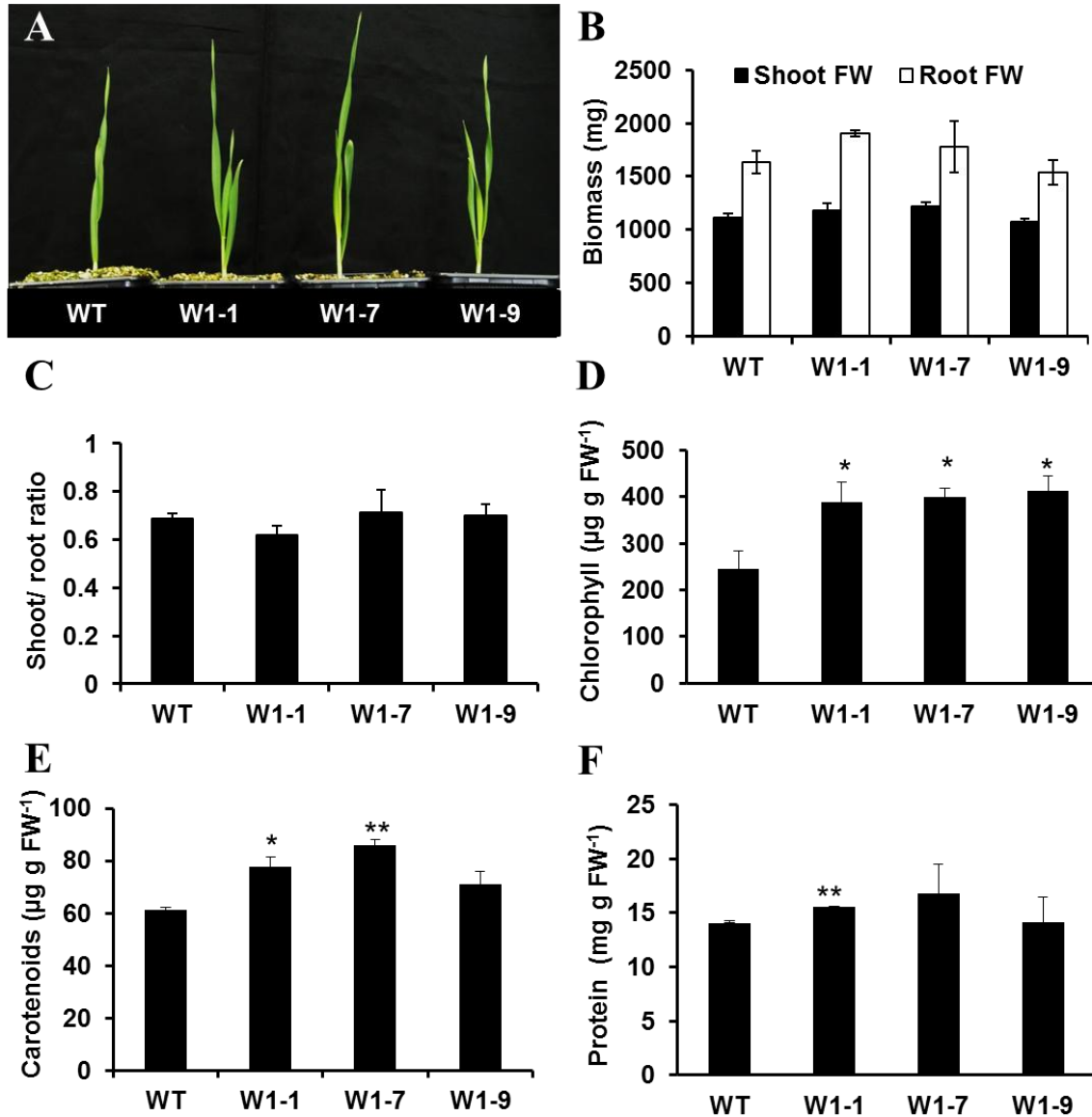


Figure 5.11 A comparison of shoot phenotypes (A), shoot and root biomass (B), shoot/ root ratio (C), chlorophyll (D), carotenoid (E) and leaf soluble protein contents (F) of 14-day old seedlings of the transgenic W1-1, W1-7 and W1-9 lines to the wild type (WT) grown on vermiculite. Data are the mean values \pm SE (n = 5). Values that were significantly different between wild type and W1-7 plants determined using the students T-test are indicated by asterisks ($P < 0.05$ *, $P < 0.01$ **).

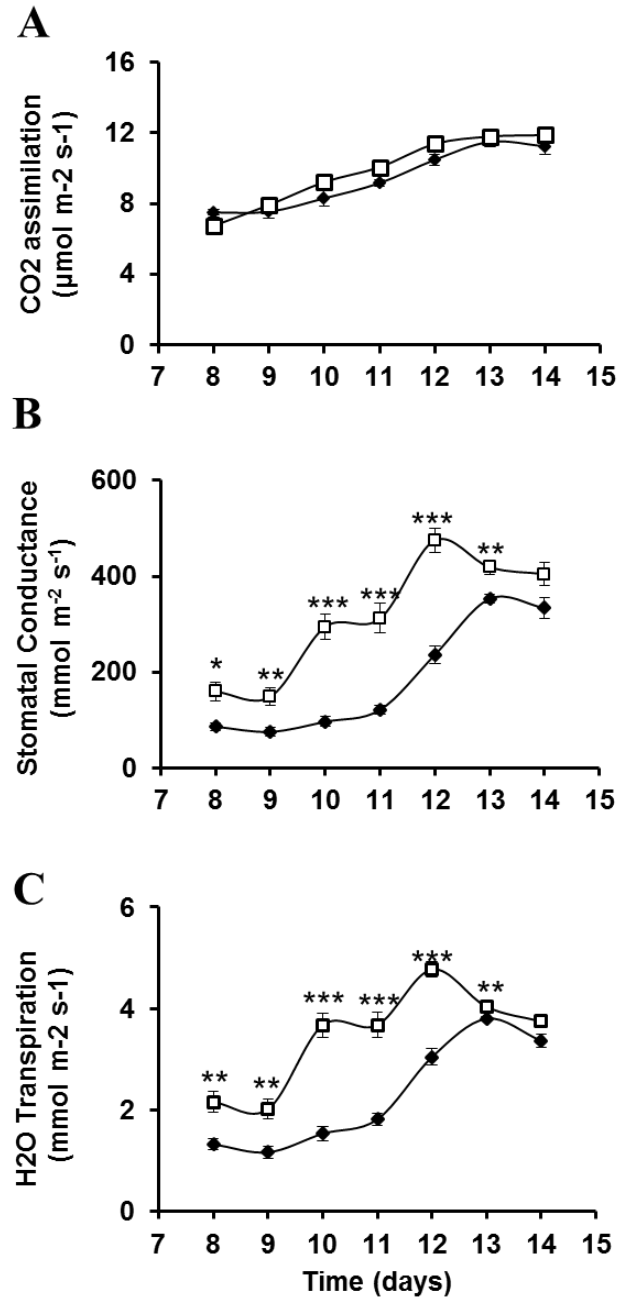


Figure 5.12 A comparison of CO₂ assimilation (A), stomata conductance (B) and transpiration in 14-day old seedlings of the transgenic W1-7 line (white squares) to the wild type (WT, black diamonds). Data are the mean values \pm SE (n = 5). Values that were significantly different between wild type and W1-7 plants determined using the students T-test are indicated by asterisks (P<0.05*, P<0.01**, P<0.001***).

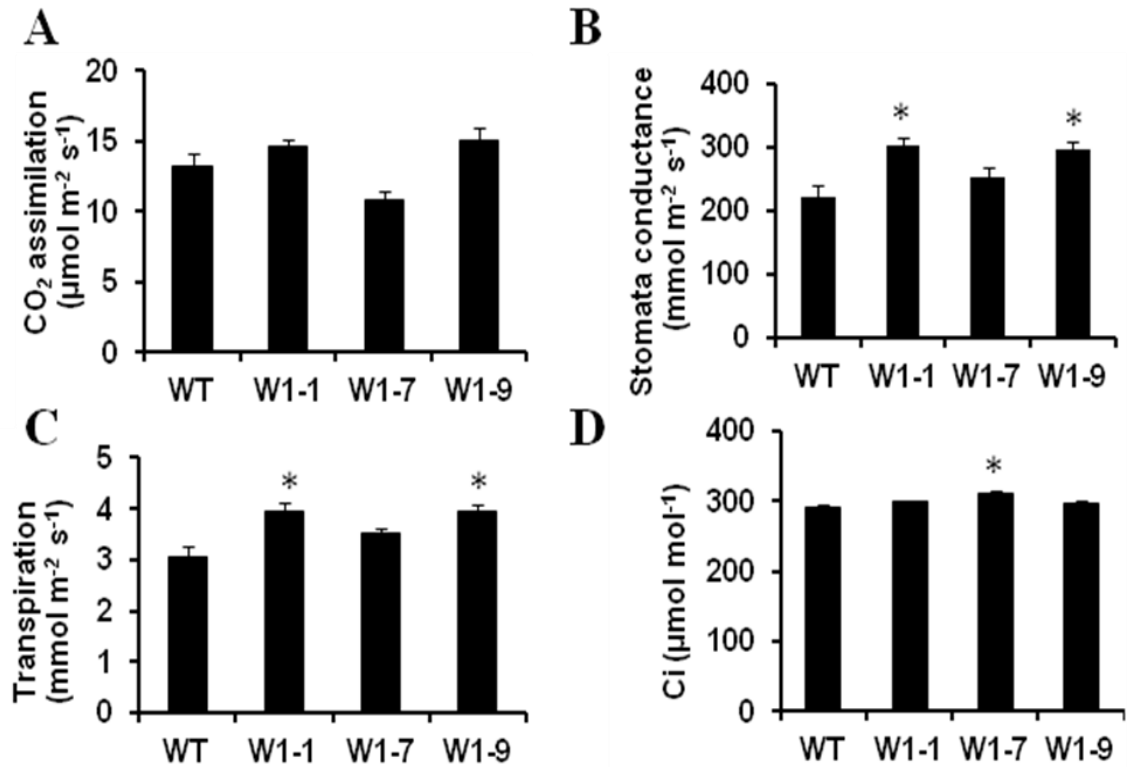


Figure 5.13 A comparison of CO₂ assimilation (A), stomata conductance (B), transpiration and internal CO₂ concentration (Ci, D) in 23-day old seedlings of the transgenic W1-1, W1-7 and W1-9 lines to the wild type (WT). Data are the mean values ± SE (n = 5). Values that were significantly different between wild type and W1-7 plants determined using the students T-test are indicated by asterisks (P<0.05).

23-day old WHIRLY1 deficient lines showed similar CO₂ assimilation rates to the wild type (Figure 5.13 A). However, stomata conductance and transpiration rates of W1-1 and W1-9 were significantly higher (Figure 5.13 B, C). W1-7 contained more internal CO₂ in its leaves (Figure 5.13 D).

CO₂ assimilation increased at the same rate in both genotypes as a result of the increment in the CO₂ concentration (Figure 5.14 A). The measurements were taken at a light intensity of 450 μmol m⁻² s⁻¹. Stomata conductance increased until 400 μmol CO₂, then slowly decreased for higher CO₂ concentrations (Figure 5.14 B). Despite following the same trend than the wild type, stomata conductance of W1-7 was significantly higher (Figure 5.14 B).

W1-7 showed similar carbon and nitrogen contents in shoots and roots to the wild type (Figure 5.15 A, B). Similarly, C/N ratios were not different between the genotypes (Figure 5.15 C).

The leaves of the wild type and W1-7 seedlings had similar amounts of ascorbate (Figure 5.16 A) and glutathione (Figure 5.16 B). Similarly, the levels of pyridine nucleotides did not differ between the genotypes (Figure 5.16 C, D). Moreover, the NADH/NAD ratios (Figure 5.16 C) and the NADPH/NADP ratios (5.16 D) of W1-7 leaves were comparable to those of the wild type (5.16 D).

The number of tillers of the transgenic plants was similar to the wild type except in W1-9 which had significantly more tillers (Figure 5.18 A). The W1-9 line had significantly lower protein content than the wild type (Figure 5.18 B); however the other lines showed a similar content to the wild type. There were no differences between the lines and the wild type in the chlorophyll content in any of the points (Figure 5.18 C).

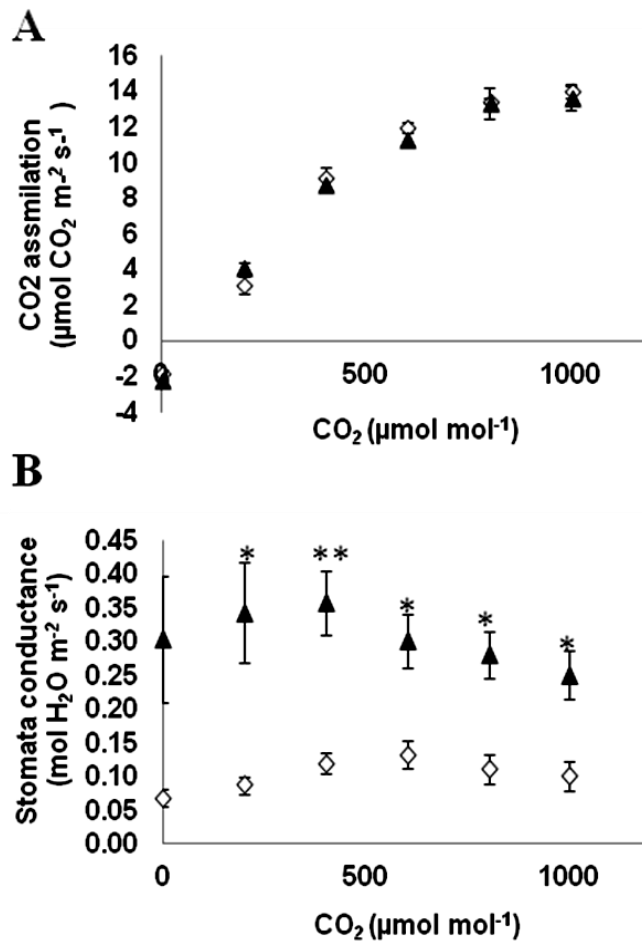


Figure 5.14 A comparison of CO₂ assimilation (A) and stomatal conductance (B) responses to different CO₂ concentrations in 14-day old seedlings of the transgenic W1-7 line to the wild type (WT). White diamonds represent wild type seedlings, while black triangles represent W1-7 seedlings. Data are the mean values \pm SE (n = 3). Values that were significantly different between wild type and W1-7 plants determined using the students T-test are indicated by asterisks (P<0.05*, P<0.01**).

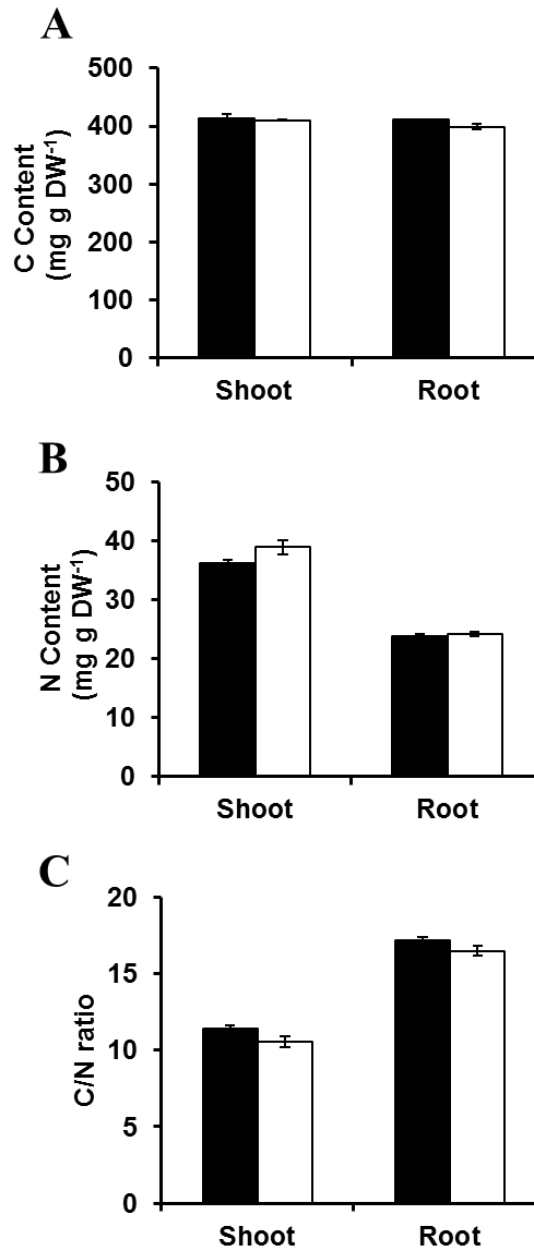


Figure 5.15 A comparison of the total nitrogen and total carbon contents in leaves (A), and roots (B), and the C/N ratios (C) of leaves and roots in 24-day old seedlings of the transgenic W1-7 line to the wild type (WT). The black columns represent wild type seedlings, while open columns represent W1-7 seedlings. Data are the mean values \pm SE ($n = 3$).

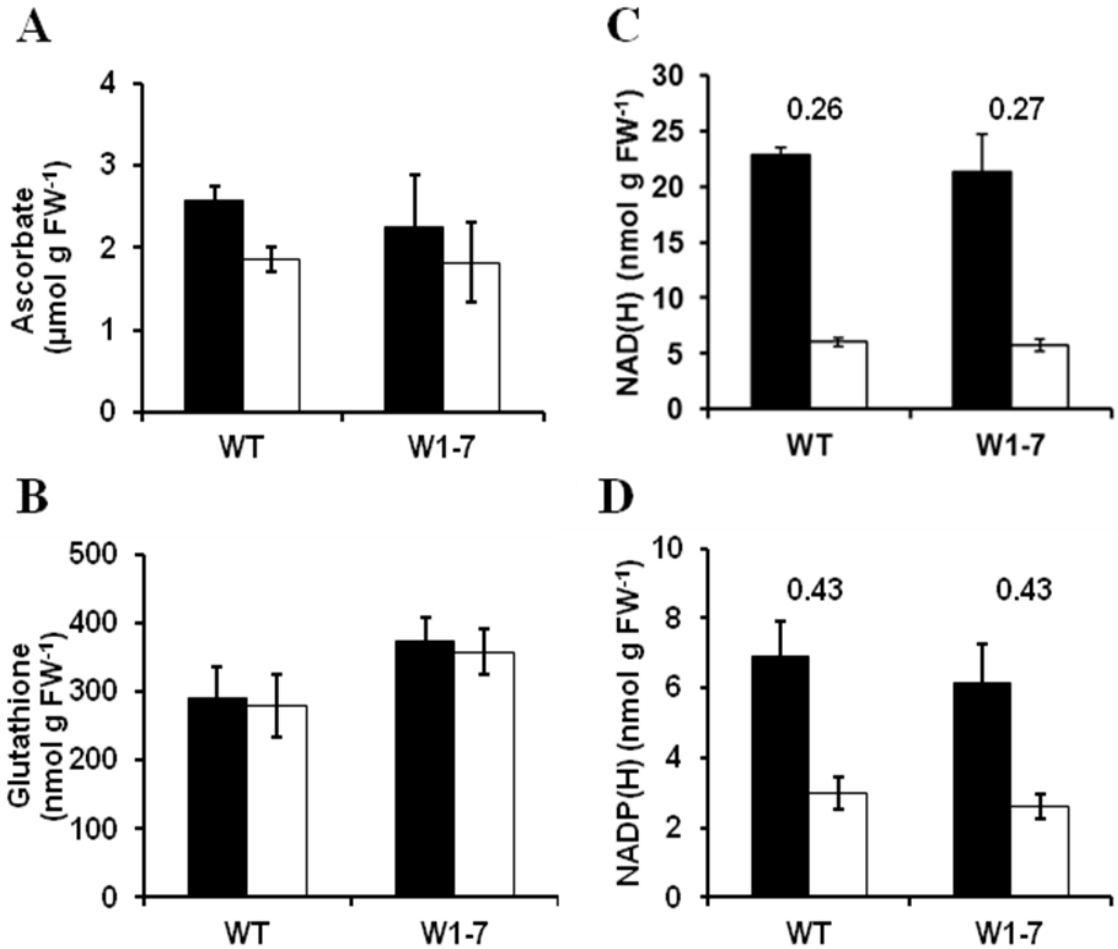


Figure 5.16 A comparison of leaf ascorbate (A), glutathione (B), NAD and NADH (C) and NADP and NADPH (D) in leaves of the 14-day old seedlings of the transgenic W1-7 line to the wild type (WT). In A and B the black columns represent the total pools of ascorbate or glutathione while the open columns represent the amount present in the reduced form. In C and D the black columns represent the oxidised forms (NAD or NADP) while the open columns represent the reduced forms (NADH or NADPH). The numbers above the columns in (C) and (D) are the average NADH/NAD and NADPH/NADP ratios respectively. Data are the mean values \pm SE (n = 4).

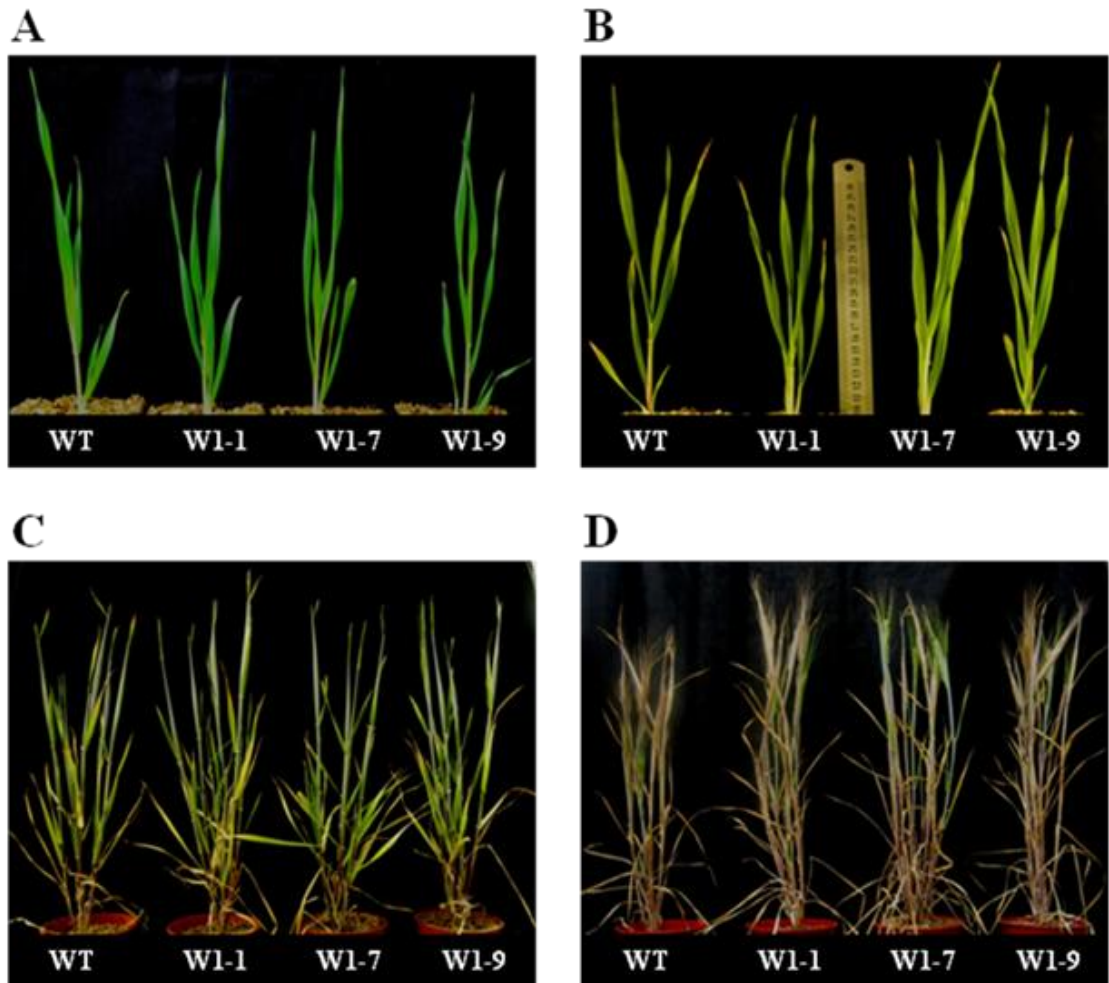


Figure 5.17 A comparison of shoot phenotypes of wild type barley and lines deficient in the WHIRLY1 protein (W1-1, W1-7 and W1-9) at 18 (A), 27 (B), 81 (C) and 130 days (D) after sowing.

The W1-1, W1-7 and W1-9 shoots had a similar visible phenotype to the wild type controls at different stages of development. Unlike the plants grown on soil (Figure 5.1 and Table 5.1) no differences could be detected between the lines when plants were grown on vermiculite with complete nutrient solution for up to 130 days after sowing (Figure 5.17).

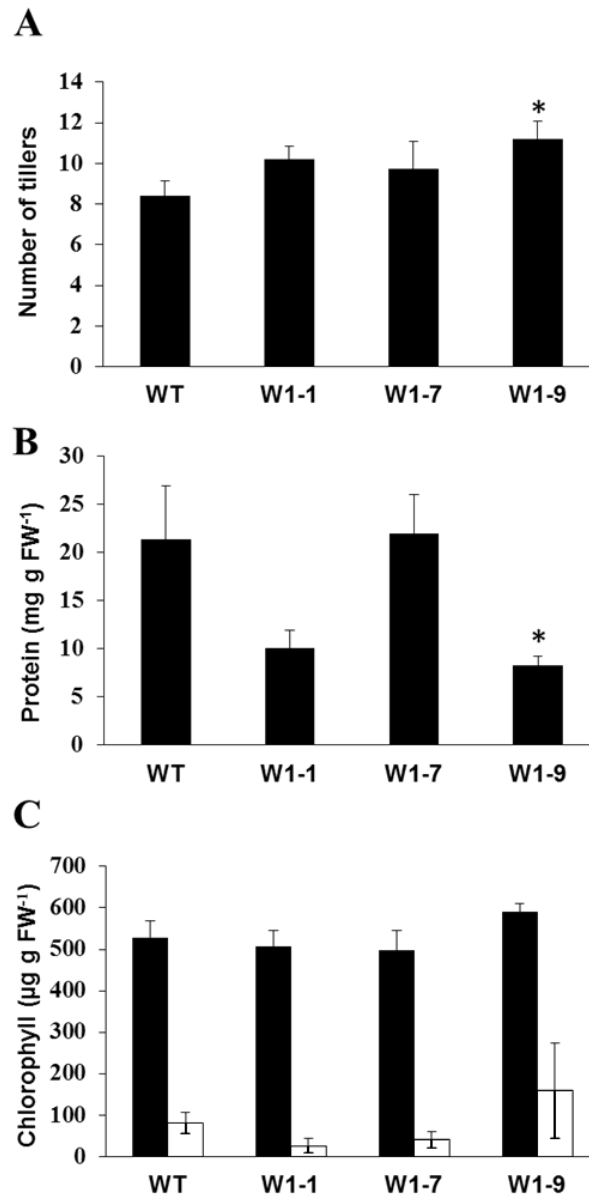


Figure 5.18 A comparison of number of tillers (A), leaf total protein (B), and chlorophyll contents (C) of seedlings of the transgenic W1-1, W1-7 and W1-9 lines to the wild type (WT). Measurements were taken at 130 (A) and 34 (B) days In C the black columns represent 34-day old seedlings, while open columns represent 130-day old seedlings. Data are the mean values \pm SE (n = 4). Values that were significantly different between wild type and W1-7 plants determined using the students T-test are indicated by asterisks ($P < 0.05$).

5.2.3 The effect of nitrogen limitation on the growth and physiology of wild type barley

In these studies, wild type barley seedlings were grown for 7 days in nitrogen-free nutrient solution. The seedlings were then transferred to either nitrogen-replete media containing 5 mM KNO₃ or to media with limiting nitrogen i.e. 0.1 mM KNO₃, in order to induce nitrogen deficiency. Photosynthetic gas exchange measurements were performed and shoot and roots were harvested at the various time-points after transfer to the different growth media, as indicated in the figure legends.

The shoots of the 14 day old wild type barley seedlings that had been grown for 7 days in N-deficient conditions were visibly smaller than the nitrogen-replete controls (Figure 5.19 A). While the chlorophyll contents of the leaves gradually increased in the N-replete controls from 7 to 14 days after sowing, the chlorophyll content of N-deficient seedlings decreased over the same time period, such that the N-deficient leaves have 60% less chlorophyll than the controls after 7 days of nitrogen deficiency (Figure 5.19 B). Photosynthesis gradually increased in the N-replete controls between 7 and 14 days after sowing but it declined slowly in the N-deficient leaves (Figure 5.19 C). At the 14 day time point therefore, the rates of photosynthesis in the N-deficient leaves were only about half the values measured in the nitrogen-replete seedlings (Figure 5.19 C). Leaf protein contents significantly increased in the N-replete controls between 7 and 14 days after sowing (Figure 5.19 D). In contrast, the protein levels of the N-deficient leaves were fairly constant over this time-period. Therefore, at 14 days after sowing the protein levels in the leaves of the nitrogen-replete controls were approximately 75% greater than those of the N-deficient plants (Figure 5.19 D).

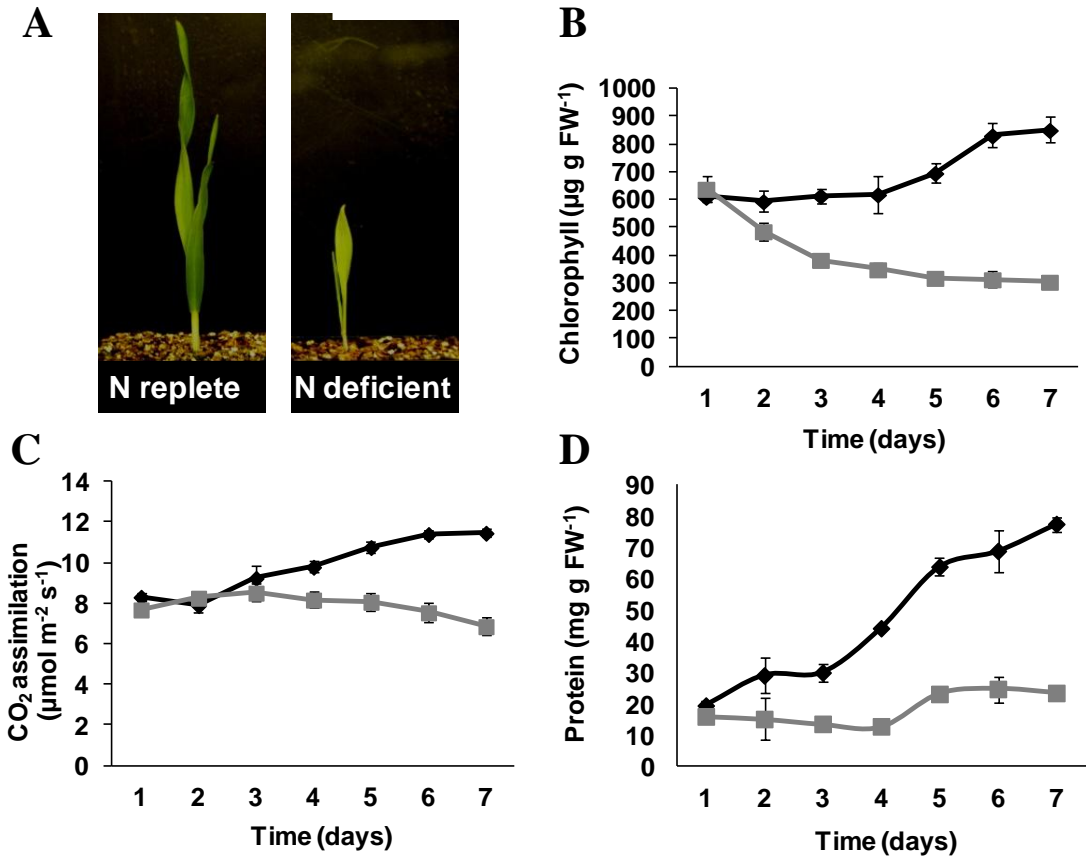


Figure 5.19 A comparison of the phenotypes (A), leaf chlorophyll contents (B), photosynthesis (C) and leaf protein contents (D) in 14 day old seedlings that had been grown for 7 days in the absence of nitrogen and grown with solutions containing either 5 mM KNO_3 (N-replete, black lines) or 0.1 mM KNO_3 (N-deficient, grey lines). Data are mean \pm SE (n = 5).

The shoots of the wild type barley seedlings that had been grown for 23 days in N-deficient conditions were visibly smaller than the seedlings grown under nitrogen-replete conditions and they were yellow in colour (Figure 5.20 A). Shoot biomass was significantly lower in the N-deficient seedlings than the N-replete controls (Figure 5.20 B). Shoot/root ratios were significantly lower (Figure 5.20 C) in the N-deficient seedlings and they had a lower root biomass (Figure 5.20 D) than the N-replete controls.

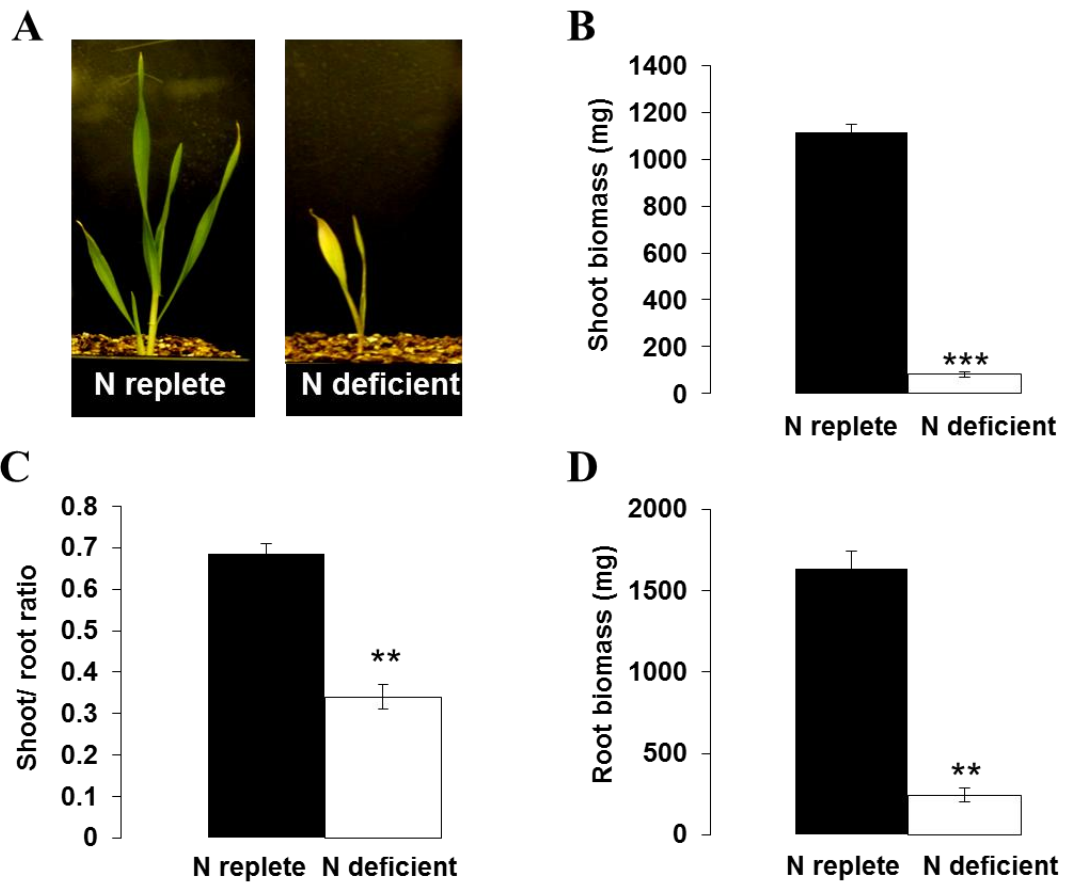


Figure 5.20 A comparison of the phenotypes (A), shoot biomass expressed as fresh weight (B), shoot/root ratios (C) and root biomass expressed as fresh weight (D) of 23-day old seedlings that had been grown for 7 days in the absence of nitrogen and grown with solutions containing either 5 mM KNO_3 (N-replete) or 0.1 mM KNO_3 (N-deficient). Data are the mean values \pm SE ($n = 3$). Values that were significantly different between wild type and W1-7 plants determined using the students T-test are indicated by asterisks ($P < 0.01^{**}$, $P < 0.001^{***}$).

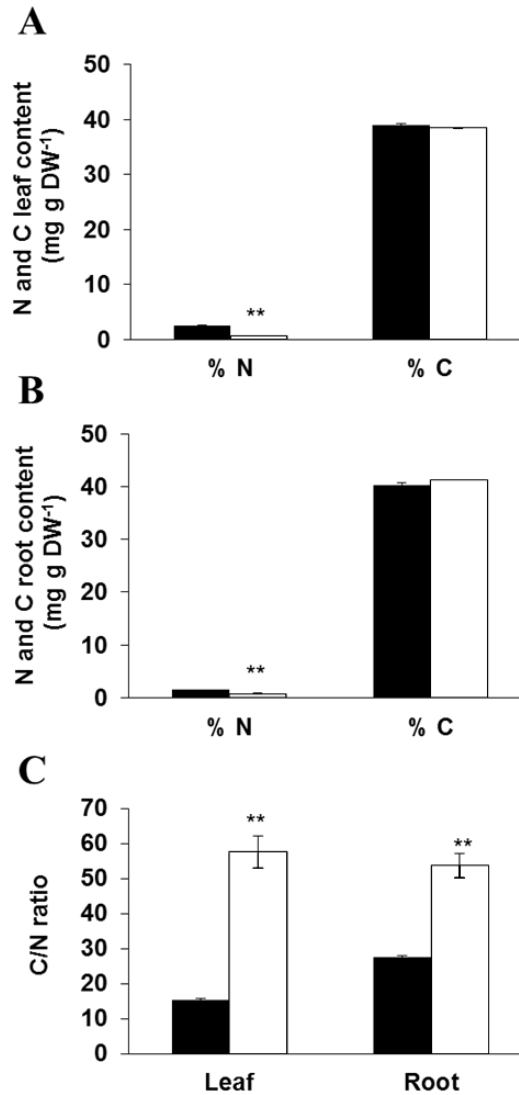


Figure 5.21 A comparison of the total nitrogen and total carbon contents in leaves (A), and roots (B), and the C/N ratios (C) of leaves and roots of 24-day old seedlings grown with either 5 mM (N-replete) or 0.1 mM (N-deficient) KNO_3 for 17 days. The black columns represent seedlings grown under N-replete conditions, while open columns represent N-deficient seedlings. Data are the mean values \pm SE (n = 3). Values that were significantly different between wild type and W1-7 plants determined using the students T-test are indicated by asterisks (P<0.01).

The leaves (Figure 5.21 A) and roots (Figure 5.21 B) of the N-deficient seedlings had significantly lower levels of total nitrogen than the N-replete controls. In contrast, the levels of total carbon were similar in the leaves (Figure 5.21 A) and roots (Figure 5.21 B) of the N-deficient seedlings than the N-replete controls. The N-deficient seedlings hence had significantly higher C/N ratios in both roots and leaves (Figure 5.21 C).

The leaves of the N-deficient and N-replete seedlings had similar amounts of ascorbate (Figure 5.22 A) and glutathione (Figure 5.22 B). However, the leaves of the N-deficient seedlings had significantly lower levels of pyridine nucleotides (Figure 5.22 C, D). Moreover, while the NADH/NAD ratios were similar N-deficient and N-replete seedlings (Figure 5.22 C), the NADPH/NADP ratios were significantly higher in the N-deficient tissues than the N-replete controls (Figure 5.22 D).

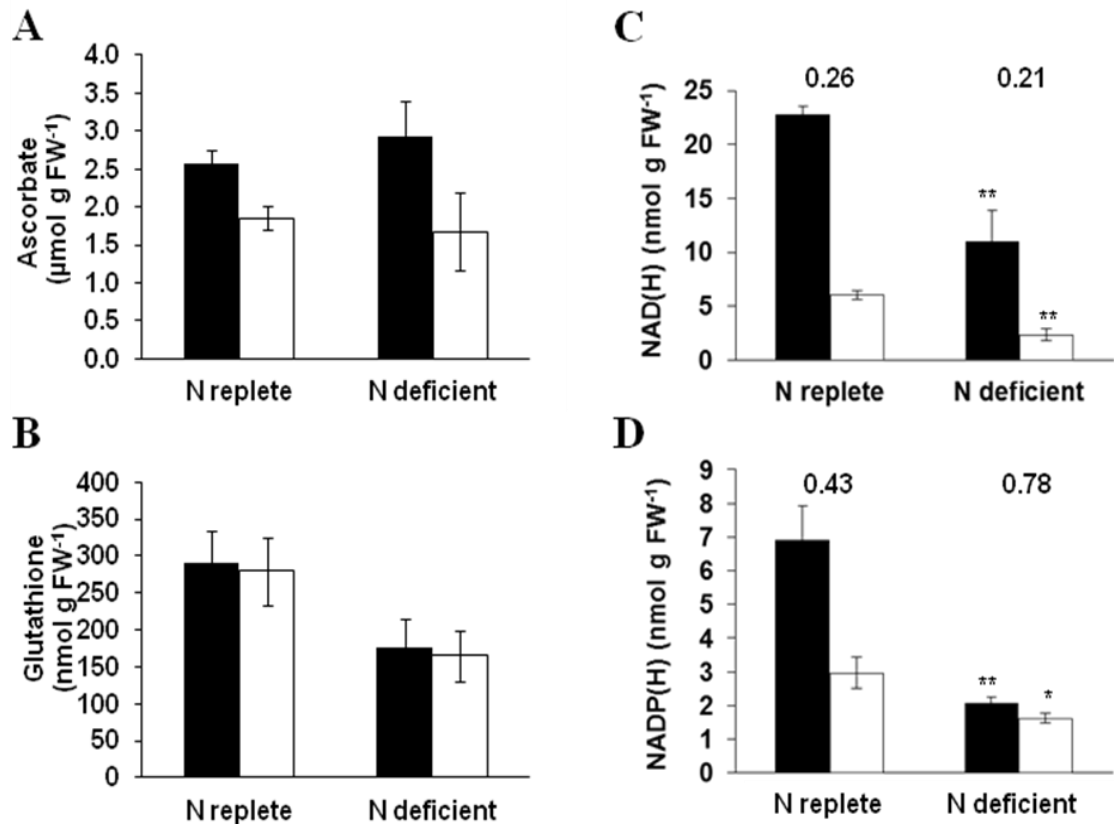


Figure 5.22 A comparison of leaf ascorbate (A), glutathione (B), NAD and NADH (C) and NADP and NADPH (D) in 14 day-old seedlings grown with either 5 mM (N-replete) or 0.1 mM (N-deficient) KNO_3 for 7 days. In A and B the black columns represent the total pools of ascorbate or glutathione while the open columns represent the amount present in the reduced form. In C and D the black columns represent the oxidised forms (NAD or NADP) while the open columns represent the reduced forms (NADH or NADPH). The numbers above the columns in (C) and (D) are the average NADH/NAD and NADPH/NADP ratios respectively. Data are the mean values \pm SE ($n = 4$). Values that were significantly different between wild type and W1-7 plants determined using the students T-test are indicated by asterisks ($P < 0.05^*$, $P < 0.01^{**}$).

5.2.4 The effect of nitrogen limitation on the growth and physiology of W1-7 seedlings

The shoots of 14 day old transgenic W1-1, W1-7 and W1-9 seedlings grown under nitrogen deficiency were visibly bigger than those of the wild type (Figure 5.23 A). Thus, shoot and root biomass were higher in the transgenic lines (Figure 5.23 B, C), although these differences were not significant. Similarly, shoot/root ratios showed a trend to be higher for the transgenic barley lines (Figure 5.23 D).

The transgenic W1-1, W1-7 and W1-9 seedlings subjected to 16 days of N-deficiency showed significantly higher photosynthetic rates than the wild type, which showed negative values (Figure 5.24 A). At this point transpiration (Figure 5.24 B) and stomata conductance (Figure 5.24 C) were also higher. Similarly, internal CO₂ concentration (C_i) was significantly increased in the three transgenic lines compared to the wild type (Figure 5.24 D)

The transgenic W1-1, W1-7 and W1-9 seedlings subjected to 9 days of N-deficiency had higher chlorophyll a and b content in their leaves than the wild type (Figure 5.25 A) Consequently, the total chlorophyll content was significantly increased (Figure 5.25 A). The carotene content was significantly higher in the W1-1 and W1-9 transgenic lines (Figure 5.25 A). In contrast, leaf protein content was in general reduced in the transgenic lines, but this difference was only significant in the transgenic W1-1 line (Figure 5.25 B).

Under N-limitation the leaves of the transgenic W1-1 and W1-7 lines had significantly higher carbon content than the wild type, while the levels of carbon were similar in the roots (Figure 5.26 A). The transgenic W1-7 and W1-9 seedlings had significantly higher levels of total nitrogen in their leaves than wild

type (Figure 5.26 B), although in the roots the nitrogen content was similar to the wild type. The transgenic seedlings showed a trend to reduce the leaf C/N ratios (Figure 5.26 C), they were significantly decreased in the leaves of the W1-9 line. The roots of the transgenic seedlings presented similar C/N ratios to those of the wild type (Figure 5.26 C).

The leaves of the wild type and W1-7 seedlings grown under N-deficiency had similar amounts of ascorbate (Figure 5.27 A). However, glutathione content tended to be higher in the W1-7 line (Figure 5.27 B). The levels of pyridine nucleotides did not differ between the genotypes (Figure 5.27 C, D). The NADH/NAD ratios of W1-7 leaves were comparable to those of the wild type (5.27 C), but the NADPH/NADP ratios were lower in the W1-7 leaves (5.27 D).

Before imposing N-deficiency (Figure 5.28 A) the 7 day old W1-7 seedlings had lower photosynthesis in response to different light intensities. In contrast, the stomata conductance was higher than the wild type (Figure 5.28 B). In 14 day old N-replete seedlings the same result was observed (Figure 5.28 C, D), while the wild type and W1-7 grown under N-deficiency showed a decrease in their photosynthetic capacity (Figure 5.28 C) and stomata conductance (Figure 5.28 D).

The W1-7 seedlings had significantly lower photosynthesis before N-deficiency at 400 μmol of light intensity (Figure 5.29 A). The stomata conductance was similar to the wild type (Figure 5.29 B). There were not significant differences between the 14 day old wild type and W1-7 seedlings grown either under N-replete or N-deficient conditions (Figure 5.29 C, D); their photosynthetic capacity was comparable (Figure 5.29 C) and, although the W1-7 seedlings tended to have a higher stomata conductance, this difference was not significant (Figure 5.29 D).

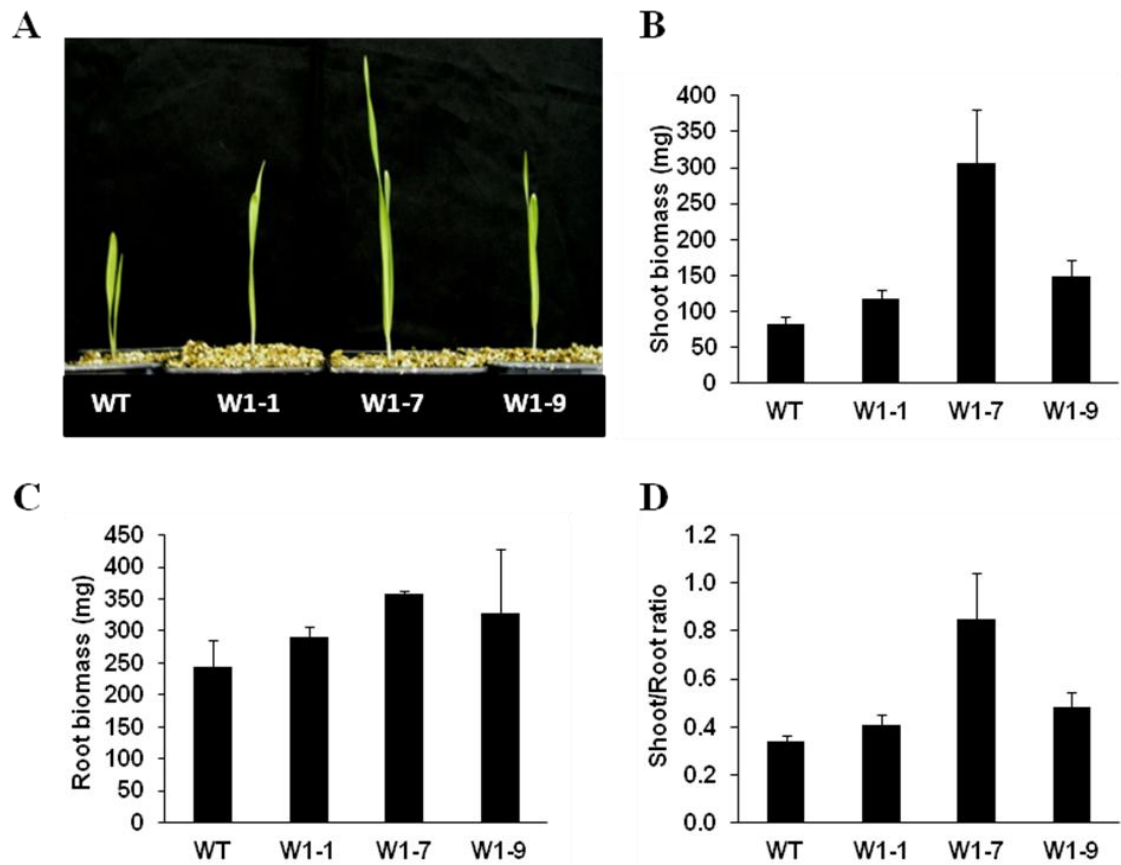


Figure 5.23 A comparison of the effects of nitrogen limitation in the phenotype (A), shoot biomass (B), root biomass (C) and shoot/ root ratio (D) in 23-day old seedlings of the transgenic W1-1, W1-7 and W1-9 lines to the wild type (WT). The picture (A) shows 14 day-old seedlings which have been grown under nitrogen limitation for 7 days. Data are the mean values \pm SE (n = 3).

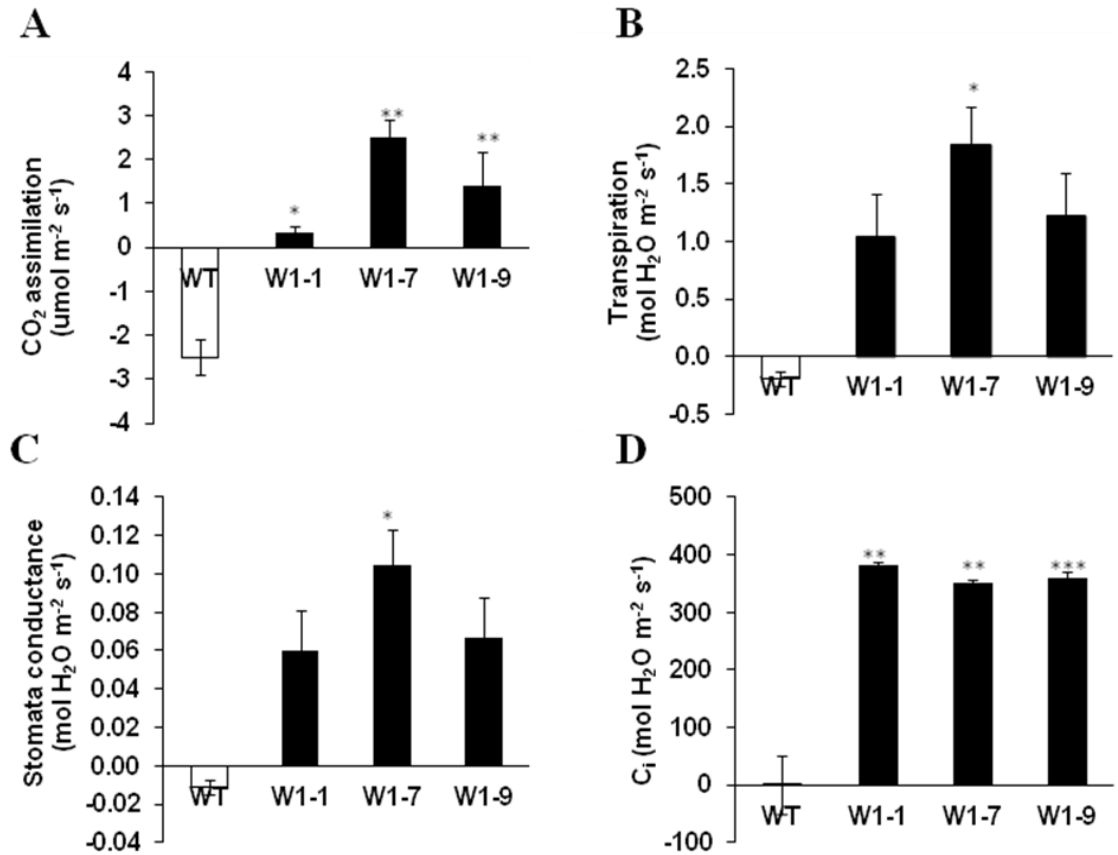


Figure 5.24 A comparison of the effects of nitrogen limitation in CO₂ assimilation (A), stomata conductance (B), transpiration (C) and internal CO₂ concentration (C_i, D) in 23-day old seedlings of the transgenic W1-1, W1-7 and W1-9 lines to the wild type (WT). Data are mean +/- SE (n = 3) p<0.05*, p<0.01**, p<0.001***.

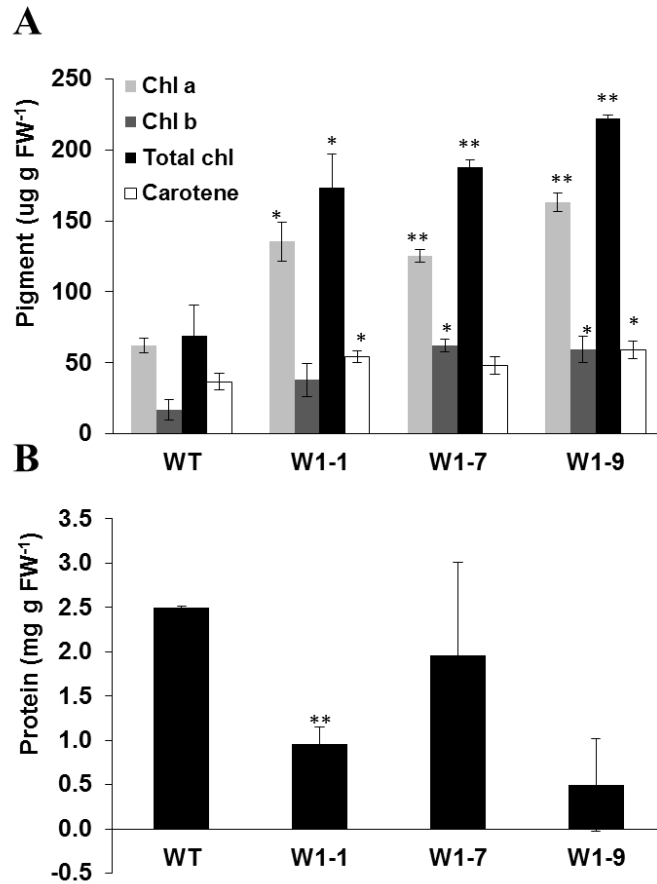


Figure 5.25 A comparison of the effects of nitrogen limitation in leaf pigment (A) and total protein content (B) in 16-day old seedlings of the transgenic W1-1, W1-7 and W1-9 lines to the wild type (WT). Data are mean \pm SE (n = 3) P<0.05*, P<0.01**.

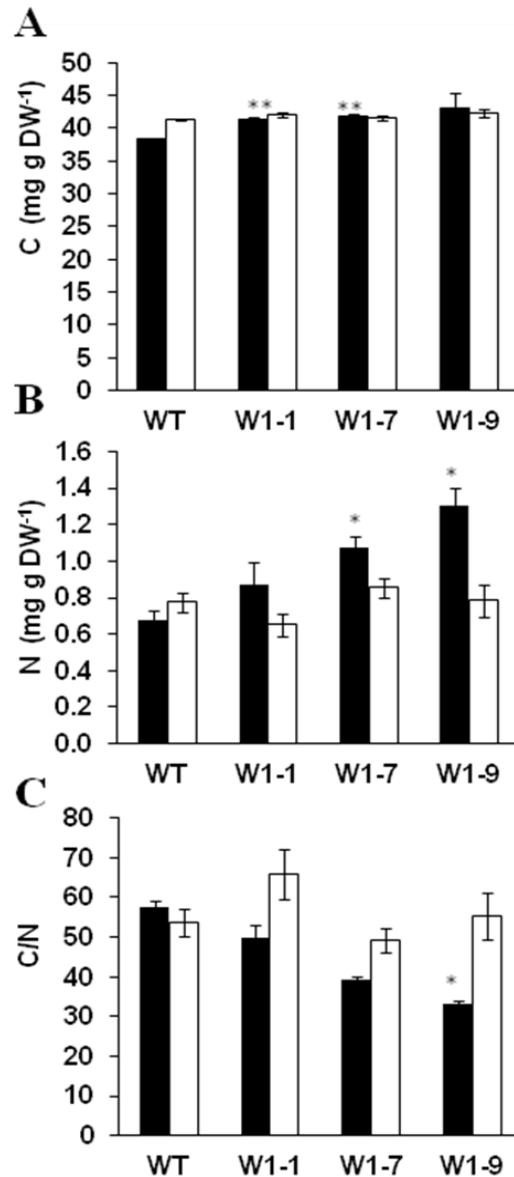


Figure 5.26 A comparison of the effects of nitrogen limitation in total carbon (A) and total nitrogen contents, and in C/N ratios (C) of 24-day old seedlings of the transgenic W1-1, W1-7 and W1-9 lines to the wild type (WT). The black columns represent leaves, while open columns represent roots. Data are the mean values \pm SE (n = 3). Values that were significantly different between wild type and the transgenic lines determined using the students T-test are indicated by asterisks (*P<0.05, **P<0.01).

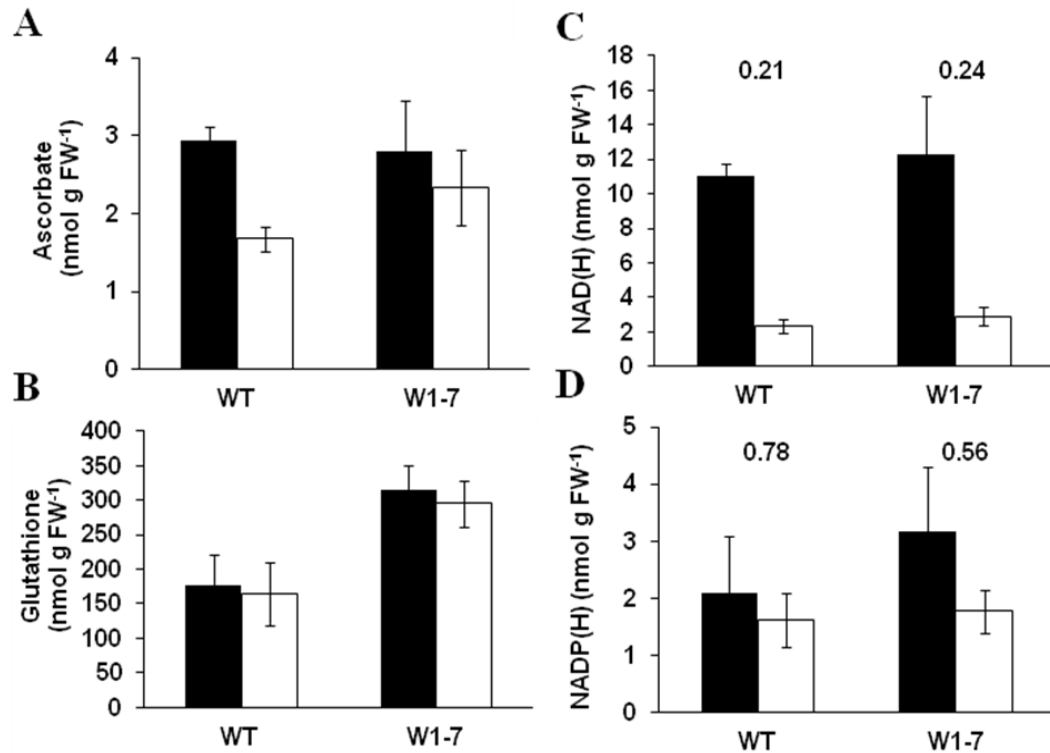


Figure 5.27 A comparison of the effects of nitrogen limitation on leaf ascorbate (A), glutathione (B), NAD and NADH (C) and NADP and NADPH (D) in 14 day-old seedlings that been grown with either 5 mM (N-replete) or 0.1 mM (N-deficient) KNO₃ for 7 days. In A and B the black columns represent the total pools of ascorbate or glutathione while the open columns represent the amount present in the reduced form. In C and D the black columns represent the oxidised forms (NAD or NADP) while the open columns represent the reduced forms (NADH or NADPH). The numbers above the columns in (C) and (D) are the average NADH/NAD and NADPH/NADP ratios respectively. Data are the mean values \pm SE (n = 4).

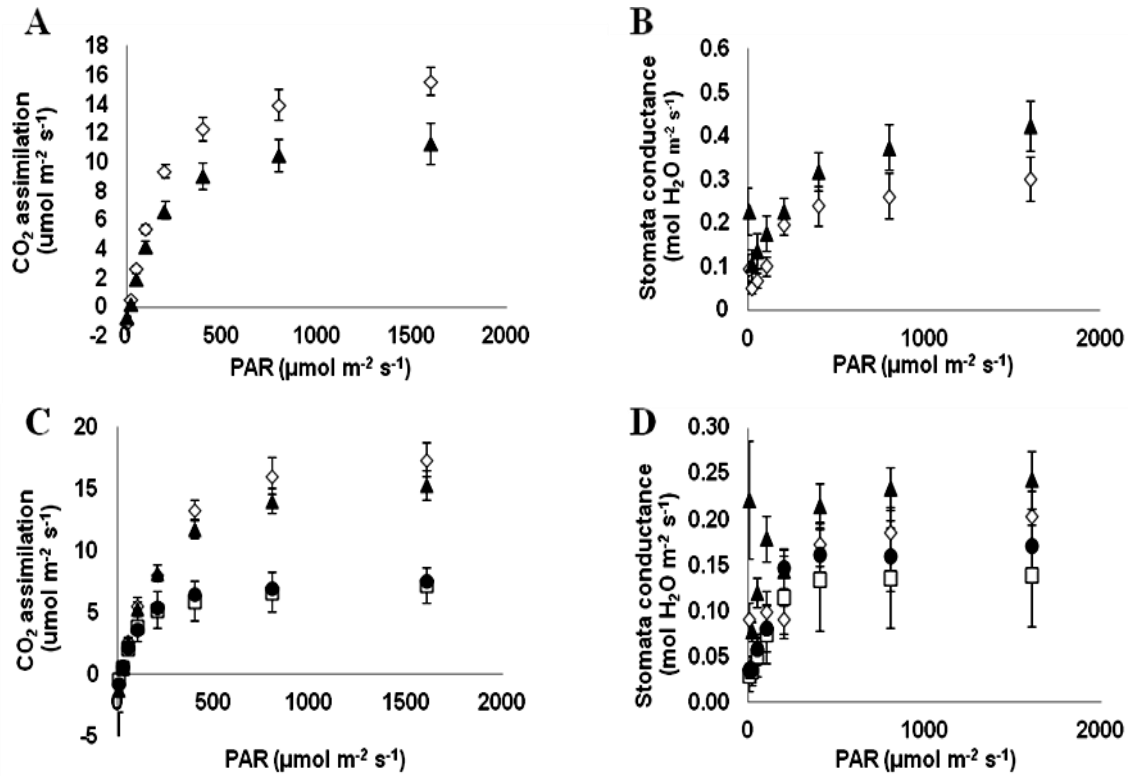


Figure 5.28 A comparison of the effects of nitrogen limitation on light response curves of 7-day old and 14-day old seedlings of the transgenic W1-7 line to the wild type (WT). CO₂ assimilation was measured before (A) and after 7 days of nitrogen deficiency (C). Stomata conductance was measured before (B) and after 7 days of nitrogen deficiency (D). White diamonds represent WT N-replete, black triangles represent W1-7 N-replete, white squares represent WT N-deficient and black circles represent W1-7 N-deficient. Data are the mean values \pm SE (n = 3).

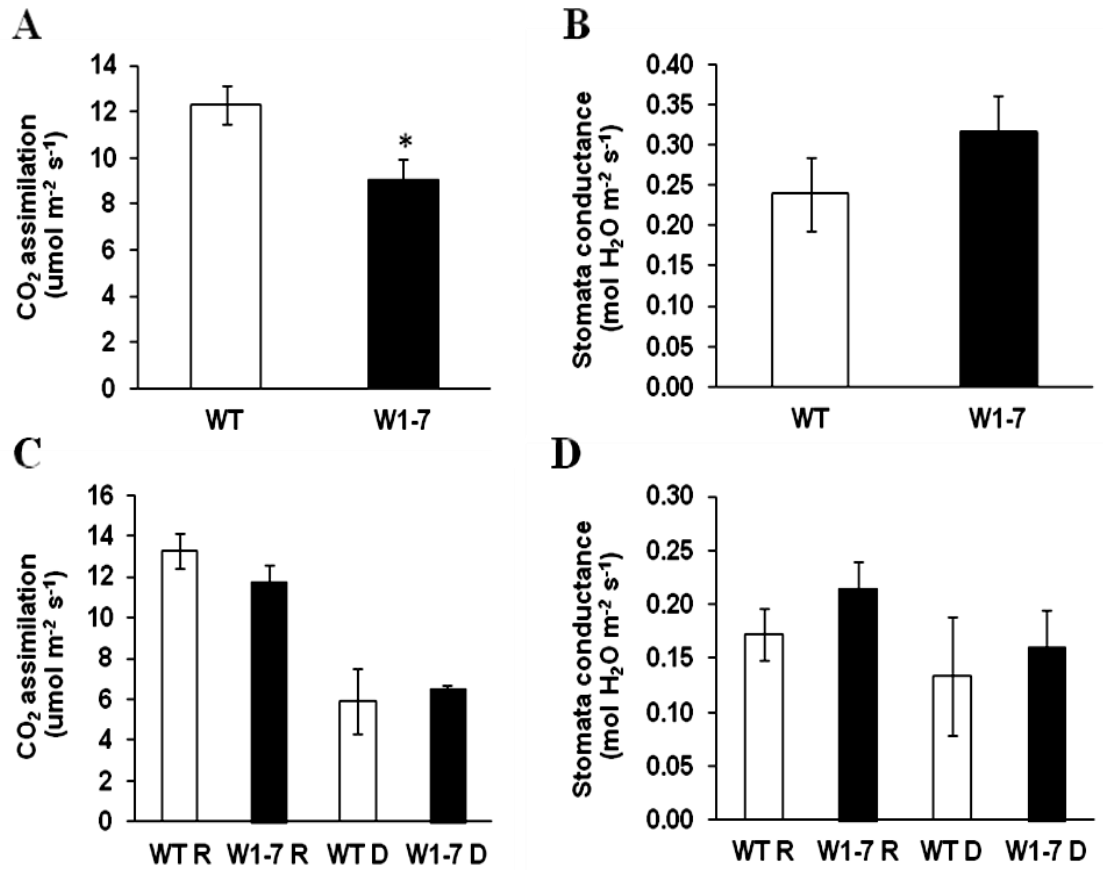


Figure 5.29 A comparison of the effects of nitrogen limitation in CO₂ assimilation and stomata conductance at 400 μmol of light intensity of 7-day old and 14-day old seedlings of the transgenic W1-7 line to the wild type (WT). CO₂ assimilation was measured before (A) and after 7 days of nitrogen deficiency (C). Stomata conductance was measured before (B) and after 7 days of nitrogen deficiency (D). N-replete is indicated by letter R, while N-deficiency is indicated by letter D. Data are the mean values ± SE (n = 3). Values that were significantly different between wild type and W1-7 plants determined using the students T-test are indicated by asterisks (P<0.05).

5.2.5 The effect of drought on the growth and physiology of wild type and W1-7 seedlings.

The 18-day old W1-7 seedlings grown on soil in optimal conditions showed visibly smaller shoots than the wild type, at this point they had 4 leaves while the wild type had 6 leaves (Figure 5.30 A). The seedlings grown under drought stress showed a smaller shoot phenotype (Figure 5.30 B). The leaves of the wild type barley faded while the leaves of the W1-7 seedlings kept the turgidity (Figure 5.30 B).

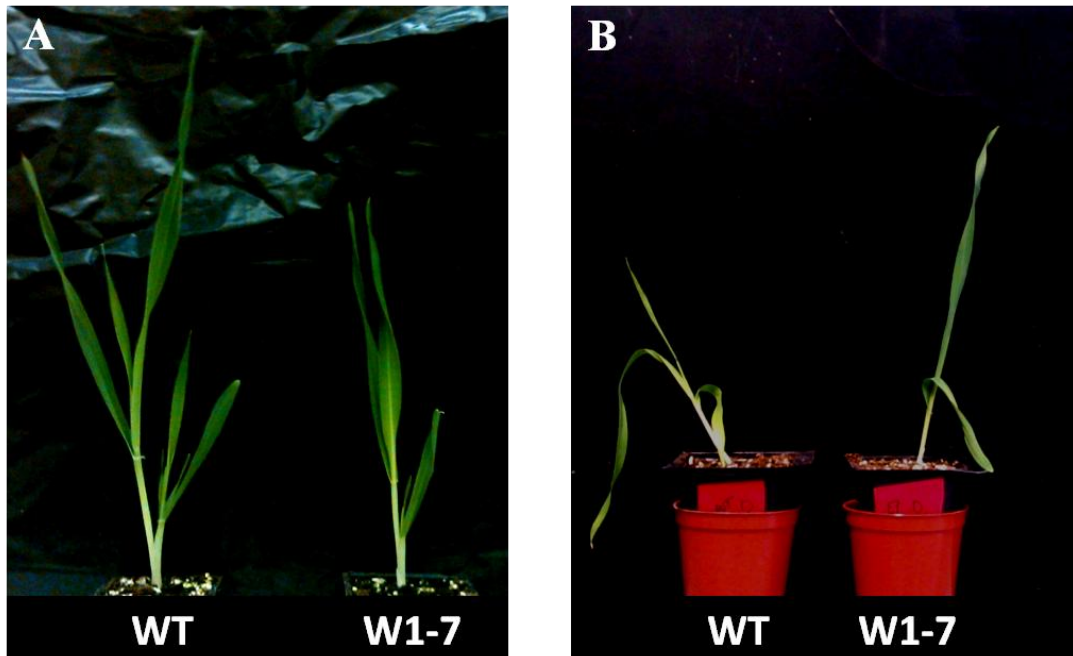


Figure 5.30 A comparison of shoot phenotypes of 18-day old seedlings of the transgenic W1-7 line to the wild type (WT) grown under control conditions (A) and subjected to 10 days of drought stress (B).

The W1-7 seedlings showed the same percentage of soil water content during the first days of drought (Figure 5.31 A), from the day 5 the soil water content of the W1-7 seedlings was significantly higher than that of the wild type. The leaves of the W1-7 seedlings presented a significantly higher water content from the beginning (Figure 5.31 B). However, later on the water content was similar between both genotypes despite being always slightly higher for the W1-7 leaves(Figure 5.31 B).

Drought caused a dramatic decrease in photosynthetic rates, stomata conductance and transpiration in all the plants (Figure 5.32). In optimal conditions the W1-7 seedlings tended to have lower photosynthesis than the wild type (Figure 5.32 A). However, the W1-7 plants grown under drought stress showed similar photosynthetic rates to the wild type (Figure 5.32 A). Stomata conductance and transpiration showed similar patterns in both genotypes (Figure 5.32 B, C). The W1-7 line had higher stomata conductance and transpiration in both conditions; under drought stress these differences were highly significant, specially from third to fifth day of drought (Figure 5.32 B, C).

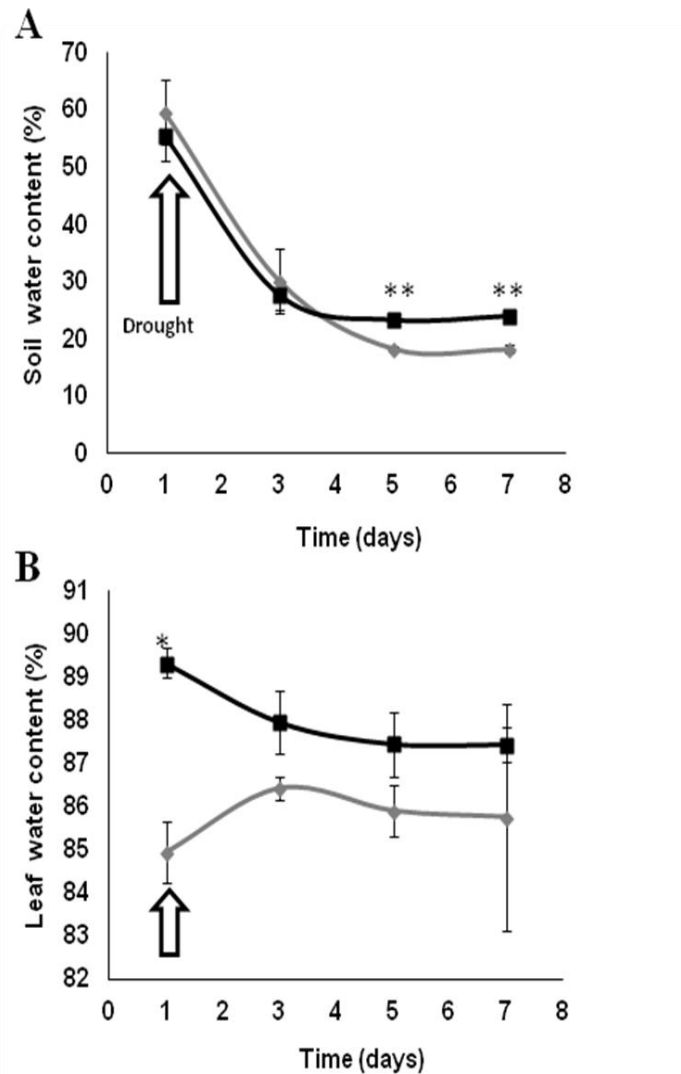


Figure 5.31 A comparison of soil (A) and leaf (B) water content of 7-day old to 14-day old seedlings of the transgenic W1-7 line to the wild type (WT) under drought stress. The grey lines represent wild type seedlings, while the black lines represent W1-7 seedlings. The arrows indicate the starting point of the drought. Data are the mean values \pm SE ($n = 3$). Values that were significantly different between wild type and W1-7 plants determined using the students T-test are indicated by asterisks (* $P < 0.05$, ** $P < 0.01$).

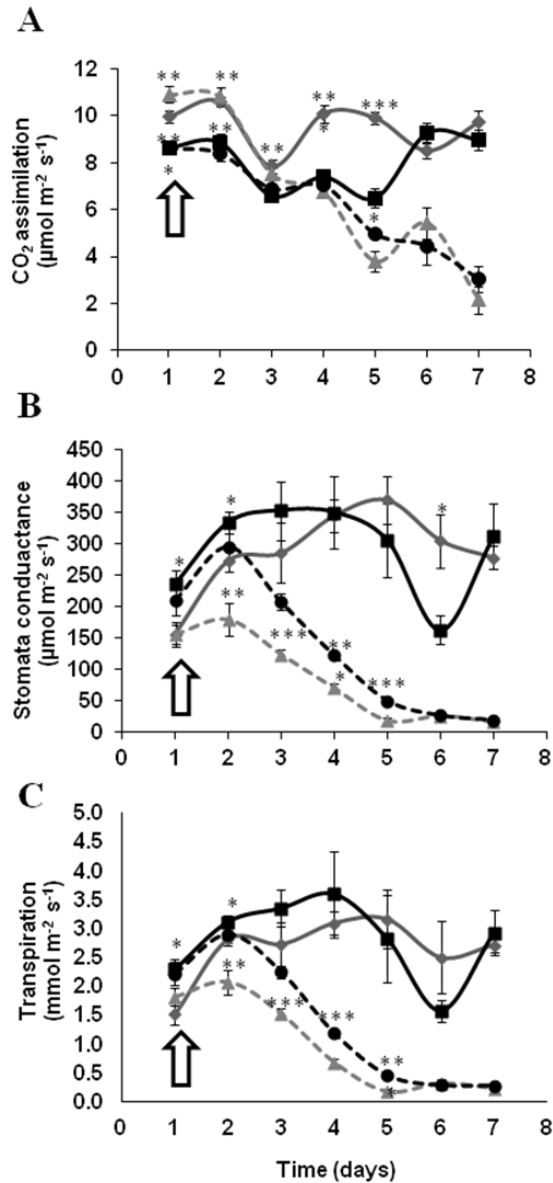


Figure 5.32 A comparison of the effects of 7 days of drought stress in CO₂ assimilation (A), stomata conductance (B), and transpiration rates (C) of 14-day old seedlings of the transgenic W1-7 line to the wild type (WT). Grey colour represents wild type seedlings and black colour represents W1-7 seedlings; full lines indicate optimal conditions while discontinuous lines indicate drought. The arrows indicate the starting point of the drought. Data are mean values \pm SE (n = 5). Values that were significantly different between wild type and W1-7 plants determined using the students T-test are indicated by asterisks (*P<0.05, **P<0.01, ***P<0.001).

5.3 Discussion

The studies that are described in this chapter were undertaken to provide a better understanding of the phenotype of barley seedlings lacking the WHIRLY1 protein. The phenotype of the WHIRLY1-deficient lines was compared in plants grown under a range of conditions, on soil in the absence and presence of drought, and on vermiculite under either a high or low growth nitrogen regime. Taken together the data presented here allows us to draw a number of conclusions.

5.3.1 The phenotype of the WHIRLY1-deficient lines is similar to the wild type in the absence of stress

There are relatively few studies in the literature characterising plants that are deficient in WHIRLY proteins (Yoo et al., 2007; Marechal et al., 2009; Cappadocia et al., 2010). Moreover, a comparison of these studies shows that plants lacking the WHIRLY1 protein have different phenotypes in different species and some of these differences are marked. For example, mutation of the maize *ZMWHY1-1* gene is lethal, such that the *zmwhy1-1* mutants do not survive beyond the seedling stage (Prikryl et al., 2008). In contrast, the *Arabidopsis why1* mutants have no apparent phenotype (Yoo et al., 2007). The data presented here on barley lines with RNAi-mediated knock-down of the *HvWHIRLY1* gene, shows that lack of WHIRLY1 in barley produces a similar lack of phenotype to that observed in *Arabidopsis*. However, when W1-1 and W1-7 plants were grown in soil they had significantly fewer tillers and hence produced fewer seed than the wild type. Moreover, when the WHIRLY1-deficient plants were grown in vermiculite with complete nutrient solution they tended to have more leaf chlorophyll. Similarly, the very young WHIRLY1-deficient leaves had a slower rate of photosynthesis with higher stomatal conductance values

that the wild type. However, these differences disappeared as the leaves developed, and the WHIRLY1-deficient plants appeared to develop and senesce in a similar manner to wild type.

5.3.2 The WHIRLY1-deficient lines are more resistant to nitrogen deficiency than the wild type

At the outset, nitrogen deficiency was chosen as a stress for comparison of the phenotypes of wild type and WHIRLY1-deficient plants because low nitrogen is known to induce rapid leaf senescence. While plant responses to nitrogen deficiency are well characterised, it was important to establish the responses of the wild type barley seedlings to growth of the low nitrogen growth conditions used in these experiments. The data presented here show that after 7 days of nitrogen deficiency the seedlings were smaller with lower shoot/root ratio ratios and significantly less nitrogen in their leaves and roots than the nitrogen-replete controls. Moreover, the leaves of the nitrogen-deficient seedlings had less chlorophyll and protein, with lower rates of photosynthesis than the leaves of the nitrogen-replete plants. The WHIRLY1-deficient seedlings generally showed similar trends in these responses to nitrogen deficiency, except that the WHIRLY1-deficient leaves retained higher levels of chlorophyll than the wild type (Figure 5.25 A). Moreover, at later stages of nitrogen deficiency, when the wild type leaves had lost the capacity for photosynthesis, the WHIRLY1-deficient lines still maintained relatively high rates of photosynthesis (Figure 5.24 A).

5.3.3 The WHIRLY1-deficient lines show lower drought sensitivity in terms of leaf water content than the wild type

The analyses of the WHIRLY1-deficient lines in the absence of stress showed that the young leaves (before 14 days after sowing) had significantly higher rates of stomatal conductance and transpiration than the wild type suggesting that they may be more susceptible to drought than the wild type. The effects of withholding water for 7 days were therefore tested in wild type and W1-7 plants grown in soil. While photosynthesis rates decreased in a similar manner in the wild type and W1-7 plants in response to decreasing soil water, the W1-7 leaves retained more water than the wild type over the whole period of the experiment. Therefore, they were visibly more turgid after an extended period of drought stress than the wild type (Figure 5.30). The higher rates of stomatal conductance and transpiration observed in the W1-7 seedlings do not therefore appear to make them more susceptible to drought. Further analysis of the water relations in the W1-7 plants is required to determine the mechanisms that allow better drought resistance. However, it is worth noting that the Arabidopsis *why1* mutants have an altered sensitivity to ABA and other stress hormones (Isemer et al., 2012).

Chapter 6. Transcript profile of the WHIRLY1 transgenic leaves under optimal and nitrogen deficient conditions

6.1 Introduction

The analysis of the phenotype of the shoots of WHIRLY1 seedlings grown in soil described in chapter 5 revealed that WHIRLY1-deficient plants had fewer leaves with a smaller total shoot biomass than the wild type (Figure 5.1 D and Figure 5.2 D). However, when WHIRLY1 deficient plants were grown in vermiculite with complete nutrient solution they had a phenotype that was similar to the wild type (Figure 5.8). While nitrogen deficiency caused a limitation of the growth of both the wild type and WHIRLY1-deficient seedlings, the plants lacking WHIRLY1 were more resistant to the stress.

Nitrogen is one of the most important macronutrients for plant growth. It is remobilised from source leaves during times of deficiency or at seed production leading to senescence (Egli et al., 1978; Gregersen et al., 2013). Transcriptome profiling approaches have been extensively used over the last 15 years to identify nitrogen-responsive genes, mostly using plant models such as *Arabidopsis* (Wang et al., 2000; Wang et al., 2003; Scheible et al., 2004; Wang et al., 2004; Hermans et al., 2006). These studies have shown that nitrate deficiency stimulates the expression of genes involved in amino acid catabolism, protein degradation, autophagy and ubiquitin-proteasome pathways as well as genes encoding phenylpropanoid metabolism, while genes encoding photosynthetic proteins and biosynthetic pathways that require nitrogen-containing metabolites tend to be down-regulated.

Crop models such as rice have been also employed to investigate rapid responses to low nitrogen stress (Lian et al., 2006). These experiments

revealed a higher number of down-regulated genes, the majority of them related to photosynthesis and energy metabolism. Biotic and abiotic stress genes were found to be both up-regulated and down-regulated as response to nitrogen limitation. More recent studies demonstrated how low nitrogen induced senescence can be reversed by nitrogen resupply (Balazadeh et al., 2014). Only one transcriptomic study has been performed on barley suffering nitrogen limitation (Jukanti et al., 2008). In these experiments near-isogenic lines were grown under low nitrogen in order to understand the regulation of nitrogen recycling; it was demonstrated that genes like leucine-rich repeat transmembrane protein kinases and a glycine-rich RNA-binding protein are involved in plant nitrogen reallocation.

The following experiments were performed to characterise the leaf transcriptome profiles of the 14-day old W1-7 line and the wild type barley seedlings under optimal nitrogen nutrition and under nitrogen deficiency. This analysis should identify:

1. Transcripts whose abundance was changed in the W1-7 line relative to wild type under optimal growth conditions.
2. Transcripts whose abundance was changed in the W1-7 line relative to wild type under nitrogen deficiency conditions.
3. Transcripts that are changed in wild type barley in response to nitrogen deficiency.

6.2 Results

6.2.1 An overview of the number of transcripts changed in expression between WT and W1-7 under the two nitrogen conditions

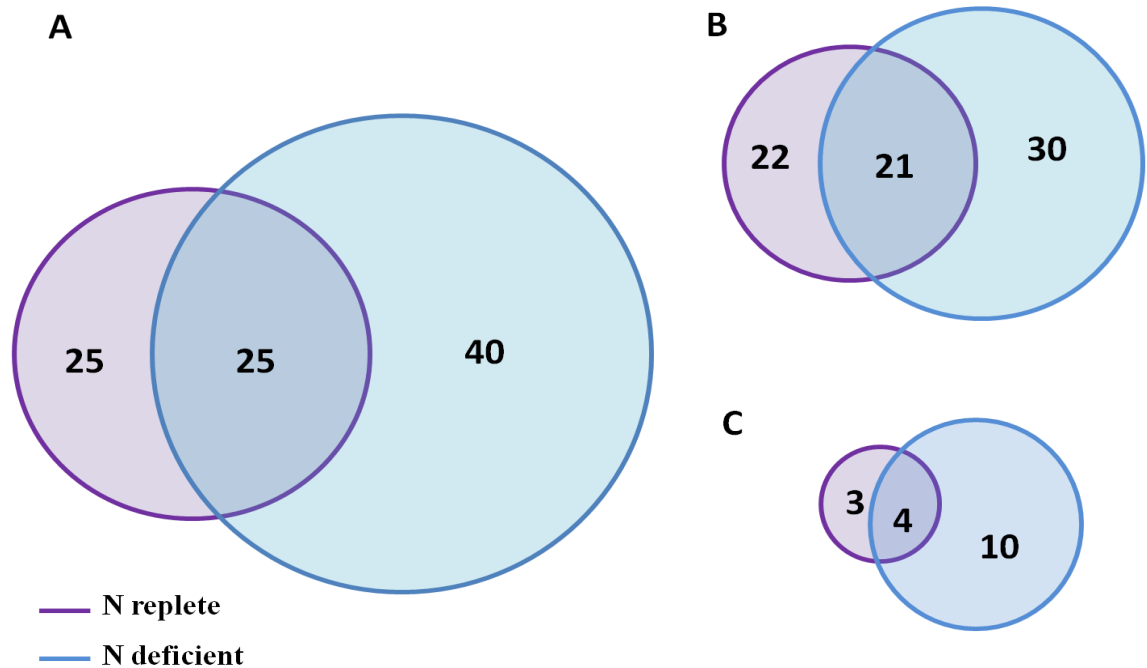


Figure 6.1 Transcript profile comparison of 14 day old wild type barley and the WHIRLY1 deficient barley line 7 (W1-7) grown for 7 days under either nitrogen replete (N replete) or nitrogen deficient (N deficient) conditions. Venn diagram illustrating the total number of differentially abundant transcripts under each condition (A), transcripts that were up regulated (B) and down regulated (C) in the transgenic line 7 (W1-7) respect the wild type. Significant differences between genotypes were determined using a moderated T-test with Benjamini-Hochberg multiple testing correction ($p < 0.05$, $FC > 2$). (Genespring 12, Agilent Technologies).

The total number of transcripts altered in their expression in the W1-7 leaves relative to the wild type was 50 in N replete and 65 in N deficient conditions, from which 25 were commonly changed in both nitrogen regimes (Figure 6.1 A). 25 transcripts were only changed in N replete and 40 transcripts were only changed in N deficient conditions, these exclusive transcripts and the common ones will be presented in the next figures (Figure 6.1 A). In both conditions the abundance of up regulated transcripts was higher (Figure 6.1 B), there were 43 transcripts which were up regulated in N replete and 51 transcripts up regulated in N deficiency. On the other side, only 13 transcripts were down regulated, 7 transcripts in N replete and 14 transcripts in N deficient conditions (Figure 6.1 C).

6.2.2 Transcript changes in the W1-7 line relative to the wild type under nitrogen replete conditions

25 transcripts were changed in abundance in the W1-7 seedlings in comparison to the wild type only under N replete conditions (Figure 6.2 B). The transcript profile of the W1-7 leaves was characterized by increases in the abundance of large numbers of transcripts encoding proteins involved in protein metabolism (Figure 6.2 A, B). Other transcripts that were differentially expressed were classified in transport, photosynthesis, DNA, stress and signalling categories (Figure 6.2 A, B). In general these transcripts were much more abundant in the W1-7 leaves; however there were a few transcripts which were down regulated belonging to protein, stress and transport groups (Figure 6.2 C).

Transcripts related to DNA that were more abundant in W1-7 leaves include B3 domain-containing protein, C2H2 and C2HC zinc fingers superfamily protein and DNA gyrase (Table 6.1). The first two transcripts encode proteins that are part of large transcription factor families with diverse and important roles in plants (Trappe et al., 2002; Waltner et al., 2005). In *Arabidopsis thaliana* DNA gyrases localize in chloroplasts and mitochondria and they have been shown to be important for DNA replication and transcription in organelles (Wall et al., 2004).

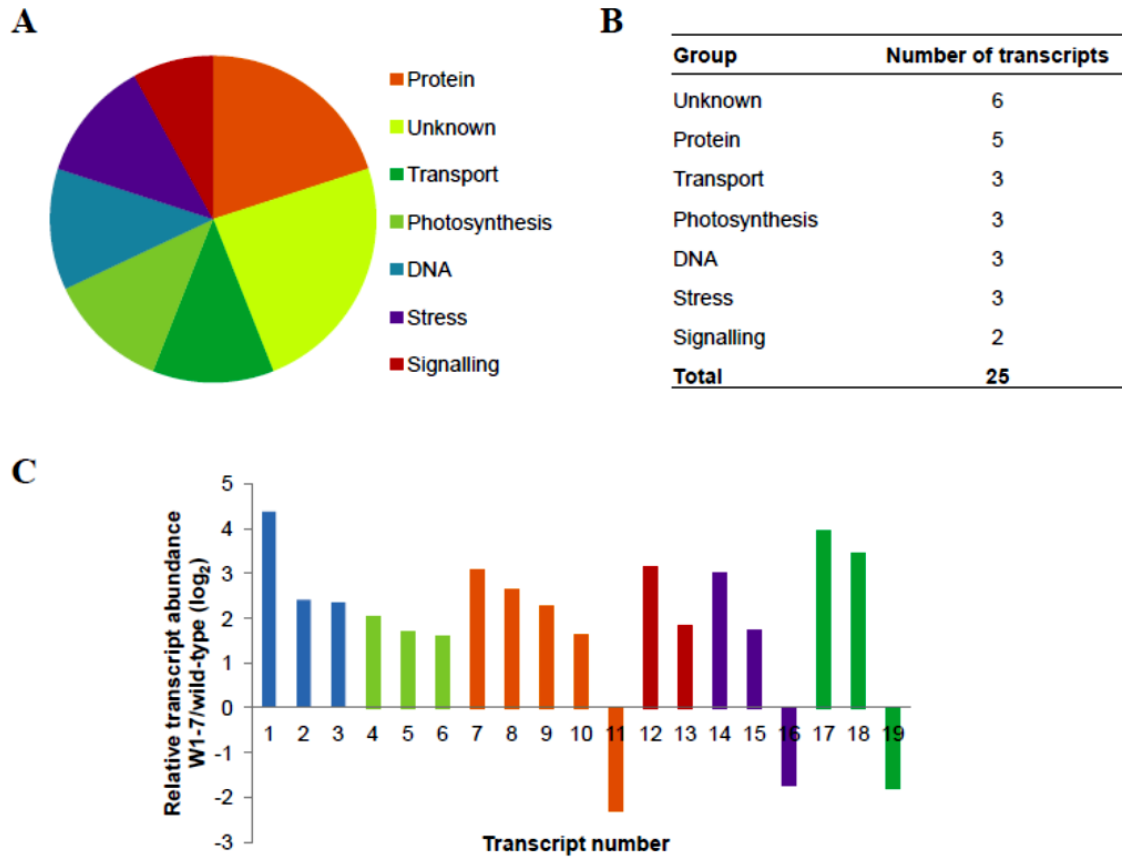


Figure 6.2 Transcript profile of the 14 day-old W1-7 leaves relative to the wild type grown in N replete conditions. Pie chart showing the different groups of transcripts that were differentially expressed only under N replete conditions in the wild type and W1-7 (A). Number of transcripts in each functional group (B). Relative transcript abundance W1-7/WT; colours indicate functional classification as described in (A) and numbers represent individual transcripts (C). The differentially expressed genes were identified using a moderated T-test with Benjamini-Hochberg multiple testing correction ($p < 0.05$, $FC > 2$) (Genespring 12, Aligent Technologies).

Table 6.1 Transcripts with significantly different abundance in the W1-7 and wild type leaves under N replete conditions.

Number ^a	Accession ^b	Description ^c	Abundance ^d
1	AK251585	B3 domain-containing protein	4.38
2	MLOC 11871	C2H2 and C2HC zinc fingers superfamily protein	2.42
3	MLOC 17276	DNA gyrase	2.36
4	MLOC 24776	Cytochrome C assembly protein	2.04
5	MLOC 9149	NADH-Ubiquinone oxidoreductase (complex I), chain 5 protein	1.70
6	MLOC 61567	NADH-Ubiquinone oxidoreductase (complex I), chain 5 protein	1.62
7	MLOC 60252	SET domain group 4	3.10
8	AK366252	O-methyltransferase	2.63
9	MLOC 68719	RNA polymerase associated factor	2.27
10	MLOC 32552	50S ribosomal protein L23, chloroplastic	1.64
11	MLOC 37150	F-box protein	-2.30
12	AK359751	Phytochelatin synthase	3.15
13	MLOC 16007	Jasmonate sulphotransferase	1.83
14	AK248474	Cu/Zn SOD	3.03
15	MLOC 70674	Zinc knuckle (CCHC-type) family protein	1.74
16	MLOC 39273	Glutathione S-transferase	-1.74
17	MLOC 7242	Major facilitator superfamily protein	3.96
18	AK357471	Major facilitator superfamily protein	3.45
19	MLOC 2306	YELLOW STRIPE like 3	-1.81
-	MLOC 13735	MADS-box family gene MIKC type-box	4.68

^a Transcript number given in the Figure 6.2

^b Barley gene model primary accession number (The International Barley Genome Sequencing Consortium, 2012).

^c Description of protein product.

^d Transcript abundance in W1-7 seedlings relative to transcript abundance in WT seedlings (\log_2).

Photosynthesis-related transcripts were also increased in abundance in the W1-7 leaves, within this group there was one transcript encoding a cytochrome C assembly protein and two transcripts encoding NADH-Ubiquinone oxidoreductase (complex I), chain 5 protein. The NADH complex is located in the chloroplast and formed by nuclear and chloroplast encoded subunits and it is likely to participate in electron flow around PSI (Peng et al., 2009; Peng and Shikanai, 2011) (Table 6.1).

Transcripts numbered from 7 to 11 were clustered in protein metabolism group. There were two transcripts encoding proteins with methyltransferase functions, SET domain group 4 and O-methyltransferase, which showed an increased expression. These proteins are of great importance as they can regulate chromatin and gene expression (Dillon et al., 2005). Other up regulated transcripts in the W1-7 seedlings encoded a RNA polymerase associated factor and the chloroplastic 50S ribosomal protein L23. There was a transcript related to protein degradation encoding an F-box protein that was less abundant in the absence of WHIRLY1 protein (Table 6.1).

Many transcripts related to stress and signalling were altered in expression in the W1-7 leaves. There was a transcript encoding a phytochelatin synthase, these proteins are induced in response to heavy metal stress (Cobbett, 2000). There was another up regulated transcript related to jasmonate, this hormone is involved in plant defence responses and senescence (Shan et al., 2011) (Table 6.1).

In the stress group there were two up regulated transcripts and one down regulated transcript. The one encoding the Cu/Zn SOD was the most up

regulated transcript, this enzyme has a role in defence against ROS (Alscher et al., 2002). The second transcript in this group encoded a zinc knuckle (CCHC-type) family protein, which is thought to be involved in RNA binding and splicing (Lopato et al., 1999). One transcript encoding a glutathione S-transferase was down regulated in the W1-7 leaves; glutathione S-transferases (GSTs) are involved in numerous stress responses from pathogen attack to oxidative stress (Marrs, 1996) (Table 6.1).

In the W1-7 seedlings there were two transcripts encoding major facilitator superfamily proteins which suffered a large increase, this is an important family with roles in transmembrane transport of different solutes (Saier Jr et al., 1999). In absence of the WHIRLY1 protein one transcript encoding a YELLOW STRIPE like 3 protein was down regulated; besides its functions in metal translocation, the YELLOW STRIPE like 3 protein is involved in pathogen resistance and it is positively regulated by SA signalling through NPR1 (Chen et al., 2014) (Chen et al., 2014). A transcript with increased abundance in W1-7 leaves was later identified (MLOC 13735); interestingly it shows homology to an *Oryza sativa* plant specific type II MIKC MADS box gene.

6.2.3 Transcript changes in the W1-7 relative to the wild type in response to nitrogen deficiency

The transcript profile of the W1-7 leaves exhibit a distinct response to low nitrogen. In total 40 transcripts were changed in abundance in the W1-7 seedlings in comparison with the wild type only under N deficient conditions (Figure 6.3 B). The transcript profile of the W1-7 leaves was characterized by increases in the abundance of large numbers of transcripts encoding proteins involved in signalling (Figure 6.3 A, B). Other transcripts that were differentially expressed were classified in DNA, RNA, protein, lipid and transport categories (Figure 6.3 A, B). In general these transcripts were much more abundant in the W1-7 leaves, however there were a few transcripts which were down regulated belonging to DNA, protein, signalling and transport groups (Figure 6.3 C).

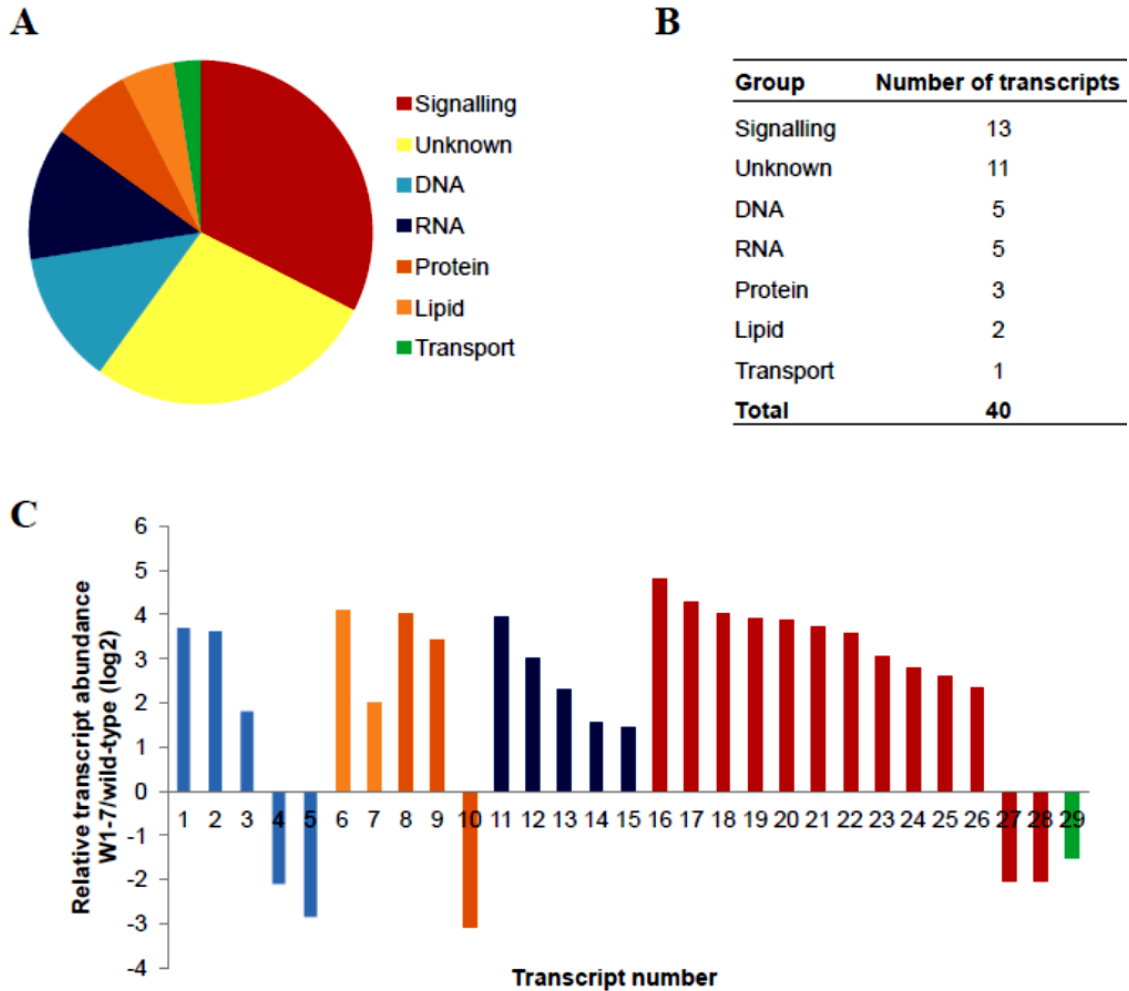


Figure 6.3 Transcript profile of the 14 day-old W1-7 leaves relative to the wild type grown in N deficiency. Pie chart showing the different groups of transcripts that were differentially expressed only under N deficient conditions in the wild type and W1-7 (A). Number of transcripts in each functional group (B). Relative transcript abundance W1-7/ wild type; colours indicate functional classification as described in (A) and numbers represent individual transcripts (C). The differentially expressed genes were identified using a moderated T-test with Benjamini-Hochberg multiple testing correction ($p < 0.05$, $FC > 2$) (Genespring 12, Aligent Technologies).

Table 6.2 Transcripts with significantly different abundance in the W1-7 and wild type leaves under N deficient conditions.

Number ^a	Accession ^b	Description ^c	Abundance ^d
1	MLOC 43326	AAA-type ATPase family protein	3.70
2	MLOC 80344	Zinc knuckle (CCHC-type) family protein	3.62
3	MLOC 45258	F-box/RNI-like superfamily protein	1.80
4	AK377144	F-box and associated interaction domains-containing protein	-2.10
5	AK374335	XH/XS domain-containing protein	-2.85
6	AK358685	GDSL esterase/lipase	4.10
7	AK374428	3-beta-hydroxysteroid-dehydrogenase/decarboxylase	1.99
8	MLOC 49988	hAT dimerisation domain-containing protein-like	4.00
9	MLOC 53891	Kinesin like protein for actin based chloroplast movement 2	3.43
10	MLOC 61005	Eukaryotic initiation factor 4A (ATP-dependent RNA helicase eIF4A)	-3.07
11	MLOC 3220	Ribonuclease H-like superfamily protein	3.94
12	MLOC 47282	2-oxoglutarate-dependent oxygenase superfamily protein	3.00
13	MLOC 47783	MuDR family transposase	2.30
14	MLOC 24779	DNA-directed RNA polymerase subunit beta	1.56
15	MLOC 60339	DNA-directed RNA polymerase subunit beta	1.45
16	MLOC 26819	FAR1-related sequence	4.79

17	MLOC 42641	Histidine kinase	4.26
18	MLOC 42368	Histidine kinase	4.03
19	MLOC 77822	Histidine kinase	3.92
20	MLOC 42987	Histidine kinase	3.85
21	MLOC 32009	Histidine kinase	3.72
22	MLOC 46366	Protein kinase superfamily protein	3.59
23	MLOC 65973	Lectin-like receptor kinase	3.03
24	MLOC 38819	STRUBBELIG-receptor family	2.78
25	AK250032	Wall associated kinase	2.58
26	MLOC 80386	Histidine kinase	2.35
27	MLOC 78892	Histidine kinase	-2.02
28	AK372631	Protein kinase superfamily protein	-2.05
29	MLOC 61723	Amino acid transporter	-1.50

^a Transcript number given in the Figure 6.3

^b Barley gene model primary accession number (The International Barley Genome Sequencing Consortium, 2012).

^c Description of protein product.

^d Transcript abundance in W1-7 seedlings relative to transcript abundance in WT seedlings (\log_2).

The first five transcripts were classified in DNA related group (Table 6.2). Some of them like the AAA-type ATPase family protein and F box proteins are involved in protein degradation processes. Other transcripts like the one encoding a zinc knuckle (CCHC-type) family protein are thought to be splicing factors (Lopato et al., 1999).

A couple of transcripts encoding a GDSL esterase/lipase and a 3-beta-hydroxysteroid-dehydrogenase/decarboxylase form the lipid group (Table 6.2). GDSL esterases/lipases have functions in the hydrolysis and synthesis of esters (Chepyshko et al., 2012) and 3-beta-hydroxysteroid-dehydrogenase/decarboxylase is involved in sterol biosynthesis (Kim et al., 2012).

A transcript encoding a component of the Eukaryotic Initiation Factor 4F (eIF4F) complex was largely decreased (Table 6.2), this protein recognizes the 7-methylguanosine cap of messenger RNA and is involved in the initiation phase of eukaryotic translation by assembling the 80S ribosome (Mayberry et al., 2011).

Among the signalling transcripts with an increased abundance in the W1-7 under nitrogen deficiency conditions several transcripts encoding histidine kinases were found (Table 6.2). In addition, the levels of one transcript encoding a FAR-RED IMPAIRED RESPONSE1 (FAR1) like protein were greatly increased in the W1-7. FAR1 is a component of the phytochrome A pathway that positively regulates ABA signalling in *Arabidopsis*, which confers adaptation to abiotic stresses. Besides, FAR1 is also involved in the regulation of stomatal opening (Tang et al., 2013).

Another transcript with considerably higher expression in the W1-7 plants under N deficiency encoded a STRUBBELIG-receptor family protein (Table 6.2). STRUBBELIG is a receptor-like kinase that allows signal transfer across membranes and communication between different cell layers influencing cell morphogenesis, the orientation of the division plane, and cell proliferation (Eyuboglu et al., 2007).

6.2.4 Transcript changes in the W1-7 relative to the wild type in both nitrogen conditions

Plastid DNA contains 11 *ndh* genes whose expression is linked to protection against stress (Casano et al., 2001). The chloroplast NADH complex, which is composed of chloroplast- and nuclear-encoded subunits, is suggested to function in cyclic electron flow around PSI (Peng et al., 2009; Peng and Shikanai, 2011). A large number of transcripts encoding chloroplast-associated proteins were significantly increased in abundance in W1-7 leaves relative to the wild type (Table 6.3). These include a number of components associated with the thylakoid NADH dehydrogenase complex (NDHA, NDHC, NDHD, NDHF, NDHB.2, NDHH, NDHJ, NDHI and NDHG), the chloroplast RNA polymerase (RPOC2, RPOB and RPOC1), the cytochrome b/f complex (PETA, PETD and YCF5), chloroplast ribosomes (RPL20, RPL23.2, RPL33 and RPS2) and minor components associated with the PSII (PSBF, PSBB and PSBJ) and PSI (PSAC, PSAJ) reaction centres (Table 6.3). A more detailed table containing primary accession numbers and relative abundance of the transcripts can be found in Appendix II.

Table 6.3 Barley transcripts homologous to plastid encoded genes in Arabidopsis that exhibit significant differences in abundance in WT and W1-7 seedlings.

NADH complex	NDHA, NDHC, NDHD, NDHF, NDHB.2, NDHH, NDHJ, NDHI and NDHG
Chloroplast RNA polymerase	RPOC2, RPOB and RPOC1
Cytochrome b/f complex	PETA, PETD and YCF5
Chloroplast ribosomes	RPL20, RPL23.2, RPL33 and RPS2
PSII reaction centre	PSBF, PSBB and PSBJ
PSI reaction centre	PSAC, PSAJ and YCF5

Table 6.4 Transcripts with significantly different abundance in W1-7 and wild type barley leaves under differing nitrogen availability.

Accession ^a	Description ^b	N replete ^c	N deficient ^d
MLOC 52339	Microtubule end binding protein	4.92	5.39
MLOC 53680	HAT dimerisation domain-containing protein-like	3.51	3.80
MLOC 26181	Microtubule end binding protein	3.00	3.41
MLOC 44822	Beta-lactamase-like protein	2.32	2.04
MLOC 514	30S ribosomal protein S18, chloroplastic	2.13	2.27
MLOC 61005	Eukaryotic initiation factor 4A (ATP-dependent RNA helicase eIF4A)	-3.01	-3.07
MLOC 24854	NAD(P)H-quinone oxidoreductase chain 4, chloroplastic	2.89	2.70
MLOC 25280	NAD(P)H-quinone oxidoreductase subunit 5, chloroplastic	1.67	1.88
MLOC 54735	Polymerase gamma	4.71	4.51
MLOC 31928	C2H2 and C2HC zinc fingers superfamily protein	1.94	3.22
AK365452	DNA-binding protein p24, whirly1	-4.36	-3.07
MLOC 25313	tRNA modification GTPase	1.82	3.38
MLOC 1704	DNA-directed RNA polymerase subunit beta	2.48	1.56
MLOC 24746	DNA-directed RNA polymerase subunit beta	2.29	1.42

^a Barley gene model primary accession number (The International Barley Genome Sequencing Consortium, 2012).

^b Description of protein product.

^c Transcript abundance in W1-7 seedlings relative to transcript abundance in WT seedlings in N replete conditions (\log_2).

^d Transcript abundance in W1-7 seedlings relative to transcript abundance in WT seedlings in N deficient conditions (\log_2)

In total 25 transcripts were changed between W1-7 and the wild type under both conditions and all of them followed the same pattern of enhanced or decreased expression (Table 6.4). 11 of the transcripts could not be classified due to their unknown function. Under both nitrogen regimes, the majority of the transcripts were more abundant in the W1-7 leaves. The first 6 transcripts of the table, with the exception of beta-lactamase-like protein which has protease activity (Liobikas et al., 2006), are implicated in protein synthesis.

There were also 2 transcripts encoding chains 4 and 5 of the chloroplast NAD(P)H-quinone oxidoreductase which were up regulated in the W1-7 seedlings (Table 6.4).

The transcript encoding the polymerase gamma was one of the most up regulated under both conditions (Table 6.4). The polymerase gamma is homologous to the barley organelle DNA polymerase; it is thought to be regulated by WHIRLY1 protein, thus being both implicated in DNA repair (Parent et al., 2011; Krupinska et al., 2014).

The expression of the transcript encoding the DNA-binding protein p24, which is the WHIRLY1 protein (Krause et al., 2005), was highly decreased specially in nitrogen replete conditions (Table 6.4).

There was only one transport related transcript encoding a tRNA modification GTPase and it was up regulated in the W1-7 line, specially under nitrogen deficiency. DNA-directed RNA polymerase subunit beta was up regulated in the W1-7 leaves, in a higher level under optimal conditions (Table 6.4).

6.2.5 Transcript changes in the wild type barley seedlings in response to nitrogen deficiency

The transcriptomic profile of the 14-day old wild type leaves was analyzed individually to know how transcripts were changed in response to low nitrogen. A first classification of transcripts showing a different abundance between nitrogen conditions was done based in their functions (Figure 6.4). The table lists the MapMan bins containing differentially abundant transcripts and provides the number of transcripts in each bin. Most of the differentially expressed transcripts under nitrogen deficiency were up regulated (Figure 6.4). Among these transcripts, protein-related transcripts (MapMan bin 29) and signalling-related transcripts were the most abundant (MapMan bin 30), followed by transport (MapMan bin 34) and stress (MapMan bin 20) associated transcripts. Less number of transcripts were found to be down regulated under nitrogen limitation; RNA, transport, protein and stress were some of the functional groups with a higher number of down regulated transcripts. Photosynthesis (MapMan bin 1) was the only group having more transcripts which are down regulated than up regulated under nitrogen deficiency.

The number of transcripts was reduced calculating nitrogen deficient/ nitrogen replete ratio and selecting the ones with a fold change of at least 2 ($FC > 2$, \log_2). The most important groups were then represented (Figure 6.5).

Under nitrogen deficiency signalling was the group with the higher number of transcripts up regulated (108), followed by protein (76) and RNA (71) (Figure 6.5 A). In contrast, only 1 photosynthesis-related transcript was up regulated. There were also a number of transcripts related to transport (37), stress (23) and hormones (10) which were found to be up regulated in the barley seedlings suffering 7 days of low nitrogen. There were considerably less transcripts down regulated in nitrogen deficient conditions (Figure 6.5 B), the group with more down regulated transcripts was RNA which had 12 transcripts.

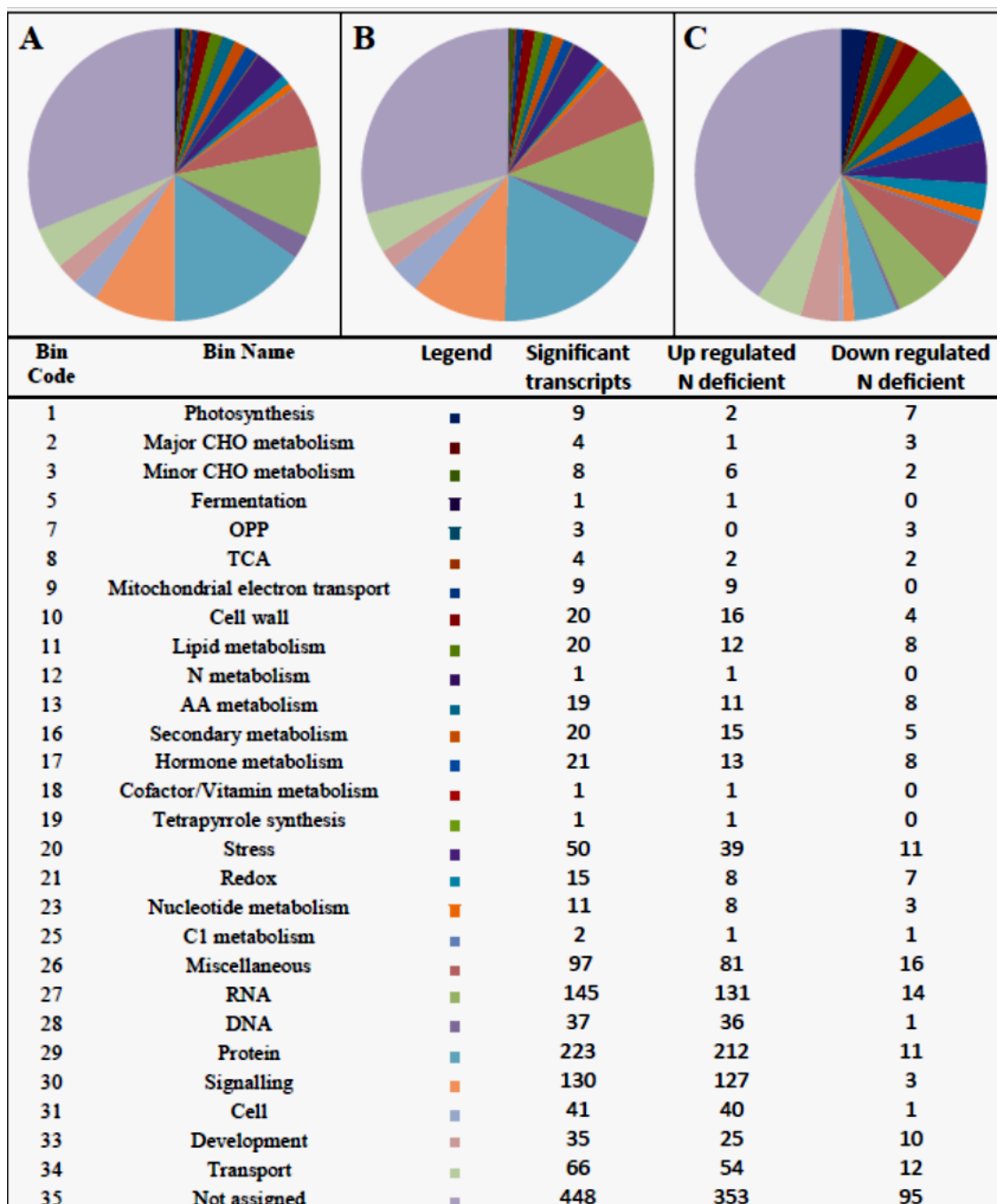


Figure 6.4 Functional classification of the total number of transcripts exhibiting significantly different abundance under N replete or N deficient conditions. Pie charts illustrate the relative numbers of transcripts that were significantly differentially abundant (A) or those more (B) or less (C) abundant under nitrogen deficiency.

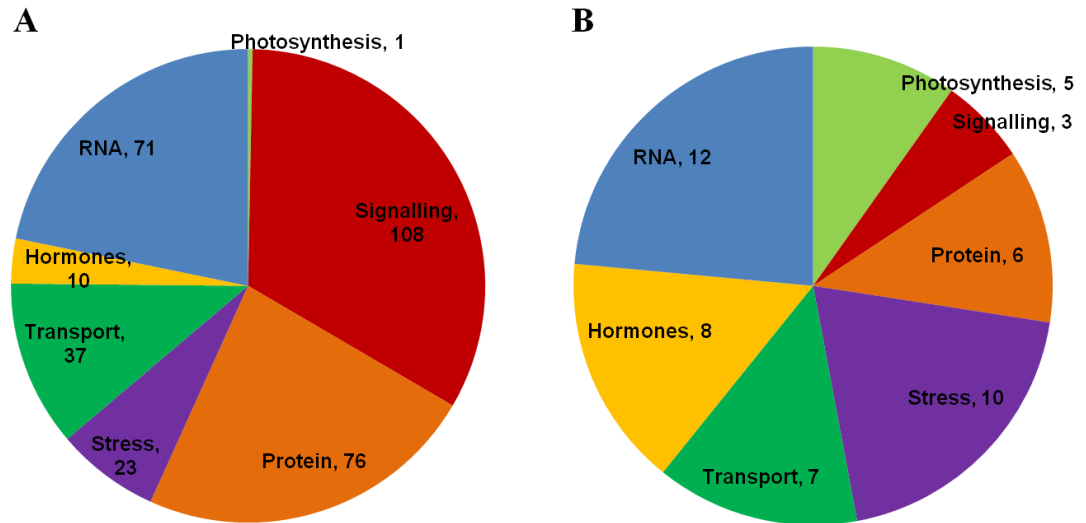


Figure 6.5 Number of transcripts that were up regulated (A) or down regulated (B) in the wild type barley leaves grown under nitrogen deficiency relative to the nitrogen replete conditions classified into functional categories. The differentially expressed genes were identified using a moderated T-test with Benjamini-Hochberg multiple testing correction ($p < 0.05$, $FC > 2$) (Genespring 12, Aligent Technologies).

The following tables show a classification of the main functional groups of transcripts which were changed in expression under nitrogen limitation. A more complete and detailed transcript description can be found in the Appendix III.

6.2.5.1 Most of the signalling transcripts changed in expression under nitrogen deficiency were receptor kinases

Table 6.5 Classification of the signalling related transcripts changed in expression in the wild type barley seedlings grown under nitrogen deficiency relative to the nitrogen replete conditions. The total number of transcripts is represented in the first column, the number of up regulated transcripts is represented in the second column and the number of down regulated transcripts is represented in the third column. The differentially expressed genes were identified using a moderated T-test with Benjamini-Hochberg multiple testing correction ($p < 0.05$, $FC > 2$). (Genespring 12, Agilent Technologies). Groups are given by MapMan.

Signalling	Total	Up	Down
Receptor kinases. DUF 26	43	43	-
Receptor kinases. Wall associated kinase	16	15	1
Receptor kinases. Leucine rich repeat III	13	13	-
Calcium	14	12	2
Receptor kinases. Miscellaneous	8	8	-
Receptor kinases. S-locus glycoprotein like	7	7	-
G protein	5	5	-
Sugar and nutrient physiology	4	4	-
Phosphoinositides	1	1	-

Under nitrogen deficiency signalling related transcripts were the most abundant in the wild type leaves (Table 6.5). The highest number of up regulated transcripts encoded different receptor kinases, mainly DUF 26 (43 transcripts) but also leucine rich repeat III, wall associated kinases and S-locus glycoprotein like. DUF 26 (Domain of Unknown Function 26) belong to the receptor like

kinase (RLK) family in barley, they may act as abiotic stress mediators, thus they could be involved in the regulation of pathogen defence and programmed cell death (Wrzaczek et al., 2010) and they are induced by oxidative stress (Bechtold et al., 2008). The most abundant transcript in this group encodes a wall associate kinase protein (WAK2) and its expression was over 6 times enhanced relative to nitrogen replete condition (Appendix III). Some receptor kinases were senescence-induced receptor-like serine/threonine-protein kinase precursors which expression was enhanced more than 6 times under nitrogen deficiency. In this group there were also few transcripts encoding proteins involved in sugar signalling such as glutamate receptors which were highly up regulated. The *Arabidopsis* phospholipase C2 was the only member of phosphoinositides subgroup which was found to be up regulated more than two times with respect to the control conditions.

6.2.5.2 Many transcription factors were changed in expression under nitrogen deficiency

In the RNA group most of the transcripts were up regulated (Table 6.6). There were a high number of transcripts with functions in regulation processes, examples of that were transcripts encoding a SET domain containing protein, a transcription factor jumonji family protein and two zinc finger family proteins (Appendix III). Regulation of transcription includes transcripts that were highly up regulated such as RAV2, which is a regulator of the ATPase of the vacuolar membrane, an AP2 domain-containing transcription factor family protein and a MADS-box transcription factor 29. The WRKY family has many members related to senescence and 10 of them appeared to be up regulated under low nitrogen stress. Some of the transcripts encoding WRKY transcription factors showed a really increased expression, WRKY67 was up to 60 fold more expressed under this condition. Within the RNA processing subgroup helicases and ribonucleases were found to be up regulated. Transcripts encoding different subunits of the RNA polymerase were classified in the transcription group and all had their expression enhanced. MYB transcription factors were in general up regulated.

Table 6.6 Classification of the RNA related transcripts changed in expression in the wild type barley seedlings grown under nitrogen deficiency relative to the nitrogen replete conditions. The total number of transcripts is represented in the first column, the number of up regulated transcripts is represented in the second column and the number of down regulated transcripts is represented in the third column. The differentially expressed genes were identified using a moderated T-test with Benjamini-Hochberg multiple testing correction ($p < 0.05$, $FC > 2$). (Genespring 12, Agilent Technologies). Groups are given by MapMan.

RNA	Total	Up	Down
Regulation others	26	25	1
Regulation of transcription	22	15	7
WRKY	10	10	-
Processing	10	8	2
Transcription	7	7	-
MYB	8	6	2

6.2.5.3 The majority of the up regulated transcripts in the protein group had functions in protein degradation

Transcripts related to different protein processes were mostly up regulated in the wild type seedlings suffering low nitrogen stress (Table 6.7). The groups linked to protein degradation had the highest number of transcripts.

Table 6.7 Classification of the protein related transcripts changed in expression in the wild type barley seedlings grown under nitrogen deficiency relative to the nitrogen replete conditions. The total number of transcripts is represented in the first column, the number of up regulated transcripts is represented in the second column and the number of down regulated transcripts is represented in the third column. The differentially expressed genes were identified using a moderated T-test with Benjamini-Hochberg multiple testing correction ($p < 0.05$, $FC > 2$). (Genespring 12, Agilent Technologies). Groups are given by MapMan.

Protein	Total	Up	Down
Degradation.ubiquitin.E1, E2, E3	25	24	1
Postranslational modification	14	10	4
Synthesis. Ribosomal protein. Eukaryotic	8	8	-
Synthesis. Ribosomal protein. Prokaryotic	5	5	-
Degradation. AAA type	5	5	-
Proteases	4	4	-
Amino acid activation	3	3	-
Synthesis. Ribosome biogenesis	3	3	-
Targeting. Secretory pathway.	3	3	-
Targeting. Nucleus	2	2	-
Targeting. Chloroplast	2	2	-
Protein folding	2	2	-
Glycosilation	1	1	-
Synthesis. Initiation and elongation	1	1	-
Targeting. Mitochondria	2	1	1
Assembly and cofactor ligation	2	2	-

The second most numerous group was the one with roles in protein post-translational modification, with up regulated transcripts encoding several kinases and protein phosphatases 2C and a few down regulated transcripts encoding serine/threonine-proteins and other kind of kinases (Appendix III).

Among the proteases group, serine proteases were the only type which was significantly up regulated (Appendix III). Amino acid activation, ribosome biogenesis and secretory pathway had three up regulated transcripts each. Nucleus and chloroplast protein targeting, protein folding and glycosylation presented two up regulated transcripts per group. A transcript encoding a E3 ubiquitin-protein ligase EL5 was the most up regulated with 5 fold higher expression under nitrogen deficiency.

6.2.6 Microarray validation and sample variation

Microarray analysis was performed using RNA extracted from leaves of the 14-day old W1-7 seedlings and the wild type grown under both nitrogen conditions. In order to confirm the microarray results eight transcripts which showed different expression between wild type and the W1-7 line were chosen for qRT-PCR analysis (Figure 6.6 A). The data obtained by the two different techniques is highly similar as the values were consistent with a Pearson correlation coefficient $r = 0.9679$ (Figure 6.1 B).

Sample variation was estimated using principal components analysis. The scores plot showed a good separation of the samples since the 3 replicates used in the analysis remained together (Figure 6.7 A). The abundance of many more transcripts was changed in response to nitrogen availability (blue) than genotypic differences (red) (Figure 6.7 B). The highest number of transcripts localised in the nitrogen deficient area (right), while the lowest number of transcripts corresponded with changes due to the wild type genotype (down).

A

Primary accession	Description
AK364080	Cysteine proteinase
MLOC 74270	Heat shock transcription factor
AK369769	Amino acid permease
AK365405	Alternative oxidase
MLOC 5569	Poly [ADP-ribose] polymerase, putative
MLOC 65259	Glutaredoxin family protein
MLOC 24854	NAD(P)H-quinone oxidoreductase chain 4, chloroplastic
AK252569	Ammonium transporter, putative

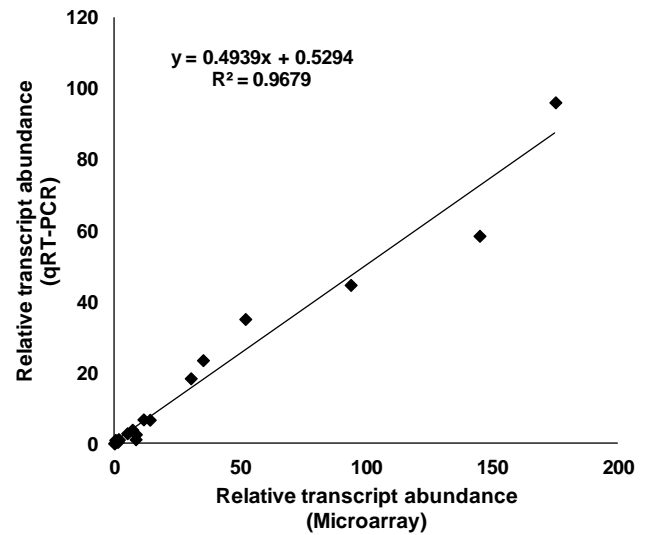
B

Figure 6.6 Validation of microarray data by qRT-PCR. Eight transcripts were selected based on their differences in expression between wild type and W1-7 (A). Correlation of data obtained by the micro array and by the qR-PCR for the eight transcripts. The data is presented relative to the wild type in nitrogen replete conditions so 3 groups of transcripts or points in the graph are shown: wild type nitrogen deficient, W1-7 nitrogen replete and W1-7 nitrogen deficient (B).

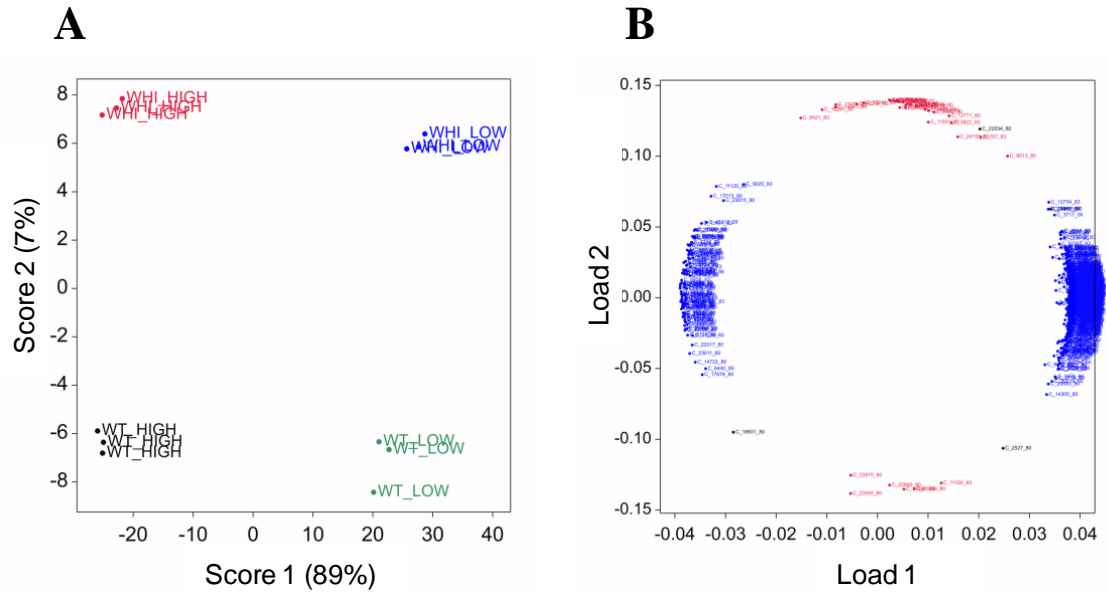


Figure 6.7 Principal components analysis (PCA) of the transcript profile of the W1-7 line and wild type seedlings subjected to 7 days of nitrogen deprivation. The analysis shows genotypic and nitrogen-induced changes in the transcript profile. The score 1 (x-axis) explains 89% of the variation in the samples and it is given by the nitrogen treatment, samples with a positive score are N-deficient and negative score are N-replete. The score 2 (y-axis) explains 7% of the variation determined by the genotypes, W1-7 has positive scores and wild type has negative scores (A). Transcript distribution based on the factor which affects their different expression (B).

6.3 Discussion

The studies reported in this chapter were undertaken to investigate the differences in the leaf transcript profile between the W1-7 transgenic line that is deficient in the WHIRLY1 protein and the wild type in seedlings grown under optimal or nitrogen-deficient conditions. This analysis revealed that only a small number (up to 65 transcripts) were significantly changed in the W1-7 line compared to the wild type under both growth conditions. Moreover, the

transcripts that were differentially expressed between the transgenic and wild type lines were clustered into a small number of functional categories that are discussed in detail below.

6.3.1 Transcripts whose abundance was changed in the W1-7 line relative to wild type under optimal growth conditions

When plants were grown under the optimal nitrogen regime only 25 transcripts were changed in abundance in the W1-7 seedlings compared to the wild type (Figure 6.2 B). Most of the differentially expressed transcripts were more abundant in the W1-7 leaves, with only transcripts encoding an F box protein (MLOC 37150), a glutathione S-transferase (MLOC 39273) and YELLOW STRIPE like 3 (YSL3; MLOC 2306) being less abundant than in the wild type.

ATWHY1 is required for both salicylic acid (SA)-dependent full basal and specific disease resistance responses (Desveaux et al., 2004). It is therefore possible that the W1-7 plants cannot activate a full SA-dependent defence response even though there are relatively few transcript changes that would support this conclusion, except for YSL3. YSL3 has been suggested to function in pathogen resistance in a manner that is dependent on NONEXPRESSOR OF PATHOGEN RESISTANCE 1 (NPR1) (Chen et al., 2014). WHIRLY1 and NPR1 are both required for the activation of SA-induced genes, but they participate in independent pathways (Desveaux et al., 2004); the decrease in YSL3 transcripts may reflect the absence of the NPR1-independent pathway that is mediated by the WHIRLY1 protein. Moreover, YSL3 is negatively regulated by JA signalling (Chen et al., 2014). It might be that JA signalling pathways are also activated in the absence of a functional WHIRLY1. Of the transcripts that were increased in abundance in W1-7 leaves relative to the wild type, only one encodes a protein involved in jasmonate metabolism and signalling. This transcript encodes jasmonate sulphotransferase (MLOC 16007), which metabolises jasmonic acid (JA) to hydroxyjasmonate. The enzyme is thought to decrease the endogenous levels of a hydroxylated product of jasmonic (JA) acid, 12-hydroxyjasmonate (12-OHJA) and to be important in the regulation of

the relative levels of JA and/or 12-OHJA in plants (Shan et al., 2011). The increase in jasmonate sulphotransferase transcripts may therefore suggest an activation of jasmonic acid (JA) and related oxylipin pathways in the absence of a functional WHIRLY1. Antagonism between the JA and SA signalling pathways has been observed in some circumstances (Kunkel and Brooks, 2002). The data presented here suggests that WHIRLY1 might participate in such an interaction, at least in the regulation of YSL3 and jasmonate sulphotransferase. The increased abundance of transcripts encoding O-methyltransferase (AK366252) may also reflect the increase in JA signalling.

A key signature in the W1-7 profile is the increased levels of transcripts encoding chloroplast proteins, which is discussed in detail below.

6.3.2 Transcripts whose abundance was changed in the W1-7 line relative to wild type under nitrogen deficiency conditions

As discussed below, half of the transcripts that were more abundant in W1-7 leaves than the wild type under optimal nitrogen were also more abundant in conditions of nitrogen deficiency. Low nitrogen induced the differential expression of a further 40 transcripts. In general, the transcripts that were differentially expressed under low nitrogen were significantly more abundant in the W1-7 leaves than the wild type. However, there were 6 transcripts which were lower under nitrogen deficiency. These encoded an F-box- and associated interaction domains-containing protein (AK377144), a XH/XS domain-containing protein (AK374335), an eukaryotic initiation factor 4A (MLOC 61005), a histidine kinase (MLOC 78892), a protein kinase superfamily protein (AK372631) and an amino acid transporter (MLOC 61723).

The transcript profile of the WHIRLY1-deficient barley seedlings was scrutinised to determine whether the observed transcript changes might provide insights into the mechanism that allow the W1-7 plants to be resistant to nitrogen deficiency. A sub-set of transcripts encoding signalling proteins were found to

be much more abundant in the W1-7 plants than in the wild type. At least some of the enhanced resistance to low nitrogen might be explained by the large increase in transcripts encoding a FAR1-like protein. FAR1 is a component of the phytochrome A pathway that acts as a positive regulator of ABA signalling in *Arabidopsis*, enabling plants to adapt better to environmental stresses (Tang et al., 2013). FAR1 binds directly to the promoter of ABA-Insensitive5 and decreases the expression of this important ABA-signalling component. While these studies provide no additional evidence of altered ABA signalling in the W1-7 plants relative to the wild type, the altered levels of FAR1-like transcripts may provide a basis for the enhanced stress resistance observed in WHIRLY1-deficient lines. Alterations in ABA-mediated regulation of seed germination have already been reported in *why1* *Arabidopsis* mutants, together with evidence for a role for the intracellular localization of WHIRLY1 on ABA sensitivity (Isemer et al., 2012).

Other transcripts that might provide clues regarding the high resistance to low nitrogen observed in the W1-7 plants encode signalling proteins. Such transcripts that are differentially increased in WHIRLY1-deficient leaves encode histidine kinases and *STRUBBELIG* (*SUB*). *STRUBBELIG* is a receptor-like kinase that allows signal transfer across membranes and communication between different cell layers influencing cell morphogenesis, the orientation of the division plane and cell proliferation (Eyuboglu et al., 2007).

6.3.3 Transcripts whose abundance was changed in the W1-7 line relative to wild type under both growth conditions

A large number of transcripts encoding chloroplast-associated proteins were significantly increased in abundance in W1-7 leaves under both growth conditions. Transcripts encoding a number of proteins associated with the thylakoid NADH dehydrogenase and cytochrome b/f complexes, and also transcripts encoding proteins involved in the expression of plastid genes such as RNA polymerase and ribosomes. These observations suggest that WHIRLY1 might participate in the co-ordination of expression of genes encoded

by the plastid and nuclear genomes that encode proteins involved in thylakoid complexes. For example, the expression of plastid-encoded and nuclear-encoded *ndh* genes appears to change in the absence of WHIRLY1. It is possible to speculate that an impaired ability to bind and/or stabilize the ssDNA conformation in the absence of WHIRLY1 leads to specific changes in the expression of chloroplast and nuclear genes involved in photosynthetic electron transport, particularly cyclic electron flow (Miyake, 2010; Foyer et al., 2012). Transcripts encoding core PSI and PSII reaction centre or light harvesting components were not changed in leaves lacking WHIRLY1. This finding is surprising given the sensitivity of PSI and PSII gene expression to light and metabolic controls (Foyer et al., 2012).

The altered levels of transcripts encoding the gamma polymerase in the WHIRLY knockdown lines are consistent with an earlier observation that transcripts encoding a polymerase that is homologous to the barley organelle DNA polymerase were higher in WHIRLY1-deficient leaves than the wild type (Krupinska et al., 2014). The Arabidopsis double mutants that lack WHIRLY1 and an organelle DNA polymerase showed enhanced DNA instability suggesting that these proteins function together in DNA repair (Parent et al., 2011). Moreover, it has been suggested that the WHIRLY1 protein regulates the organelle DNA polymerase (Krupinska et al., 2014). The data here are consistent with a link between WHIRLY1 and the level of gamma polymerase transcripts that is independent of the environment conditions used in these experiments.

6.3.4 Transcripts that are changed in wild type barley in response to nitrogen deficiency.

The above discussion has considered only changes in transcripts associated with the loss of WHIRLY1 function. However, these datasets reveal more general information concerning the effects of low nitrogen on the barley leaf transcript profile. In total, 1441 transcripts were changed in expression in barley leaves as a result of nitrogen deficiency. Most of these transcripts were more

abundant under low nitrogen stress than under the optimal nitrogen regime. The most important functional groups of proteins encoded by these transcripts were involved in cell signalling, RNA, protein metabolism, transport and stress. The overall response of transcript profile to low nitrogen is consistent with previous observations in other species (Lian et al., 2006; Peng et al., 2007). For example, nitrogen limitation increased the abundance of transcripts associated with protein metabolism such as proteases and proteins associated with ubiquitin-mediated proteasome. Large numbers of transcripts encoding proteins associated with the post-translational modification of proteins were also altered in abundance in leaves suffering nitrogen limitation particularly protein kinases and protein phosphatases. Moreover, transcripts encoding receptor-like kinases were more abundant in leaves under low nitrogen conditions. The data presented here suggest that protein phosphorylation and dephosphorylation might play a role in the re-direction of metabolism that occurs following imposition of low nitrogen stress, as discussed in Chapter 7.

Chapter 7. Metabolic profile of the WHIRLY1 transgenic leaves under optimal and nitrogen deficient conditions

7.1 Introduction

Growth under nitrogen limiting conditions triggers premature leaf senescence, with the recycling and remobilisation of nitrogen and other nutrients to support the growth of developing leaves, flowers and grain (Himmelblau and Amasino, 2001; Kichey et al., 2007; Diaz et al., 2008; Distelfeld et al., 2014). Leaf senescence is thought to depend on the abundance of certain types of metabolites (Wingler et al., 2006), such as a lack of sugars (van Doorn, 2008). Progressive changes in the levels of amino acids, sugars and secondary metabolites were observed in the senescence of Arabidopsis leaves (Watanabe et al., 2013). Although the metabolite profiles of leaves undergoing senescence is well characterised (Wingler et al., 2006), the changes in metabolites observed in nitrogen-deficient leaves relative to leaves of plants grown with adequate nitrogen nutrition depends on the leaf ranks analysed and the time of harvest. For example, amino acids were increased in Arabidopsis plants exposed to low nitrogen stress together with a decreased abundance of the organic acids (Tschoep et al., 2009). In contrast, nitrogen deficiency in tomato caused a decrease in many amino acids, while carbohydrates and a number of secondary metabolites increased (Urbanczyk-Wochniak and Fernie, 2005).

Comparisons of the metabolite profiles in maize subjected to long-term low nitrogen deficiency revealed that the levels of over 70 metabolites were significantly changed as a result of nitrogen deficiency with major effects on most of the amino acid pools (18), as well as a number of N-containing molecules derived from glutamine and glutamate, such as γ -aminobutyric acid (GABA) together with decreases in a number of organic acids, particularly those involved in the tricarboxylic acid (TCA) cycle, as well as changes in soluble

carbohydrates such as glucose and fructose (Amiour et al., 2012). Moreover, nitrogen deficiency triggers more general biotic and abiotic stress responses in transcripts and metabolites. Like other abiotic stresses, nitrogen deficiency causes changes in the metabolic network which allows adaptation to the stress conditions (Obata and Fernie, 2012).

In barley there is no published literature available regarding the metabolic changes that occur in response to nitrogen deficiency.

The following experiments were therefore performed to characterise the leaf metabolic profiles of barley seedlings to nitrogen deficiency. In these studies wild type and W1-7 seedlings were grown for 7 days under conditions of low or optimal nitrogen in order to identify:

1. Metabolites that are changed in wild type barley in response to nitrogen deficiency.
2. Metabolites whose abundance was changed in the W1-7 line relative to wild type under optimal growth conditions.
3. Metabolites whose abundance was changed in the W1-7 line relative to wild type under nitrogen deficiency conditions.

7.2 Results

In total 86 metabolites were identified in this analysis. Of these, about a quarter were significantly changed in the leaves as a result of nitrogen deficiency. For simplicity these metabolites have been grouped in the following categories, amino acids, TCA cycle intermediates, sugars, carboxylic acids and phytol metabolites.

7.2.1 Metabolites that are changed in wild type barley in response to nitrogen deficiency

7.2.1.1 Amino acids

The ratio of some amino acids such as Gly/Ser, Gln/Glu and Asn/Asp was changed in plants suffering nitrogen limitation (Figure 7.1). For example, the Gly/Ser ratio was about 5 times higher under N-limited conditions than under optimal nitrogen. Moreover, the Gln/Glu ratio under N limited conditions was double that measured under N-replete conditions. Similarly, the Asn/Asp ratio was 3 times higher than under N replete conditions

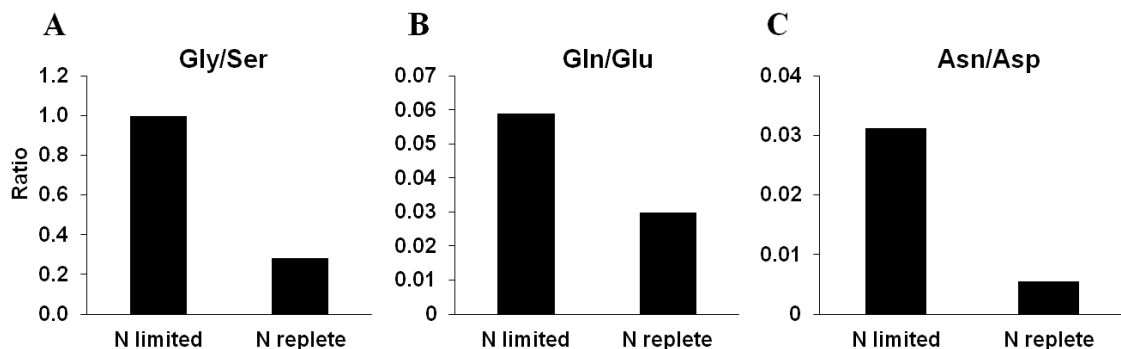


Figure 7.1 Glycine to serine (A), glutamine to glutamate (B) and asparagine to aspartate (C) ratios in wild type barley leaves in N limited and N replete conditions.

Table 7.1 Influence of N availability on amino acid content in barley leaves.

Amino Acid ^a	Relative concentration ^b		Ratio limited: N replete	N Significance ^c
	N limited	N replete		
Lys	31.65 +/- 9.89	0.32 +/- 0.18	99.84	0.087
Tyr	24.16 +/- 6.29	0.50 +/- 0.25	48.61	0.064
Met	6.47 +/- 1.14	0.15 +/- 0.06	44.28	0.031
Ile	12.80 +/- 2.62	0.42 +/- 0.19	30.34	0.041
Pro	11.02 +/- 2.92	0.42 +/- 0.20	26.24	0.068
GABA	109.22 +/- 24.13	8.02 +/- 4.50	13.61	0.048
Gly	19.47 +/- 2.78	1.84 +/- 0.80	10.59	0.001
Phe	22.00 +/- 2.21	2.85 +/- 0.87	7.71	0.001
Asn	0.55 +/- 0.06	0.07 +/- 0.03	7.57	0.001
Leu	28.24 +/- 9.492	4.48 +/- 3.84	6.30	0.049
Thr	4.22 +/- 0.66	0.98 +/- 0.36	4.33	0.006
Gln	2.72 +/- 0.46	0.86 +/- 0.23	3.16	0.011
Ser	19.56 +/- 2.57	6.57 +/- 2.48	2.97	0.016
Glu	46.03 +/- 25.51	29.94 +/- 6.80	1.59	0.488
Oxo-pro	17.21 +/- 2.85	10.91 +/- 5.28	1.58	0.389
Ala	0.06 +/- 0.02	0.05 +/- 0.01	1.4	0.492
Asp	17.47 +/- 5.27	12.93 +/- 4.53	1.35	0.543

^a Amino acids are indicated using the standard three letter code.

GABA, γ -Amino butyric acid.

^b Mean amino acid content (n = 4) is reported as peak area relative to the internal standard.

^c Significance level estimated using the Students t-test.

Nitrogen deficiency caused a large change in the amino acid profile of the leaves (Table 7.1). All amino acids that were identified in this study were significantly increased in abundance except for Asp, Ala, Oxo-pro, Glu, Pro, Try and Lys (Table 7.1). In particular, large increases in Met, Ile and GABA were observed in the nitrogen-deficient leaves relative to the controls.

7.2.1.2 Sugars and carboxylic acids

The levels of a large number of TCA cycle intermediates and sugars were increased in response to nitrogen limitation in barley leaves (Table 7.2). The TCA cycle intermediates, succinic acid and malic acid were significantly higher in leaves suffering N limitation compared to plants with adequate nitrogen nutrition. Similarly, while the levels of sucrose were not highly different between the conditions, the levels of fructose and glucose were much higher in plants suffering nitrogen limitation as were galactose and maltose (Table 7.2).

Table 7.2 Influence of N availability on content of metabolites associated with sugar and carboxylic acid metabolism in barley leaves.

Metabolite	Relative concentration ^a		Ratio limited: replete	N N Significance ^b
	N limited	N replete		
TCA Intermediates				
Succinic acid	4.03 +/- 0.80	0.16 +/- 0.06	25.18	0.039
Malic acid	454.88 +/- 29.35	30.27 +/- 6.67	15.03	0.001
Citric acid	552.45 +/- 164.01	60.51 +/- 12.24	9.13	0.095
Fumaric acid	1.08 +/- 0.24	0.43 +/- 0.17	2.53	0.071

Sugars and related metabolites

Galactose	64.08 +/- 14.99	0.54 +/- 0.26	119.11	0.051
		27.46 +/-	32.80	0.005
Fructose	900.92 +/- 63.13	8.52		
		0.17 +/-	22.95	0.092
Threonic acid	3.90 +/- 1.22	0.051		
Inositol	56.24 +/- 11.54	2.96 +/- 0.41	18.99	0.044
	1091.92 +/-	57.86 +/-	18.87	0.004
Glucose	78.36	14.83		
Maltose	3.84 +/- 0.62	0.22 +/- 0.10	17.38	0.025
Glyceric acid	48.72 +/- 22.11	4.84 +/- 1.61	10.05	0.185
	1183.64 +/-	449.51 +/-	2.63	0.27
Sucrose	486.62	53.41		

^a Mean amino acid content (n = 4) is reported as peak area relative to the internal standard.

^b Significance level estimated using the Students t-test.

7.2.1.3 Phytols

In contrast to the general increases in metabolite abundance observed under N deficiency presented in Tables 7.1 and 7.2, the phytol contents of the leaves was decreased under low nitrogen (Table 7.3). Significant changes in the levels of phytol B and phytol C were observed. The levels of these metabolites were decreased by about half relative to the concentration in the N replete plants (Table 7.3).

Table 7.3 Influence of N availability on phytol content in barley leaves.

Phytol	Relative concentration ^a		Ratio N limited: N replete	Significance ^b
	N limited	N replete		
Phytol A	1.04 +/- 0.25	1.81 +/- 0.58	0.6	0.301
Phytol B	1.83 +/- 0.55	4.19 +/- 0.65	0.4	0.037
Phytol C	0.60 +/- 0.21	1.72 +/- 0.37	0.4	0.051
Phytol methyl ether	85.97 +/- 39.47	206.41 +/- 43.01	0.4	0.100
Phytol methyl ether 2	86.30 +/- 39.73	202.83 +/- 41.50	0.4	0.095

^a Mean phytol content (n = 4) is reported as peak area relative to the internal standard.

^b Significance level estimated using the Students t-test.

7.2.2 Metabolite changes in the W1-7 line relative to the wild type under nitrogen replete conditions

The levels of most leaf metabolites were similar in the W1-7 and wild type leaves when plants were grown under optimal nitrogen nutrition (Figure 7.2). However, the levels of sucrose were significantly lower in the W1-7 leaves than the wild type (Figure 7.3). In contrast, octadecanol levels were significantly higher in the W1-7 leaves than the wild type (Figure 7.3).

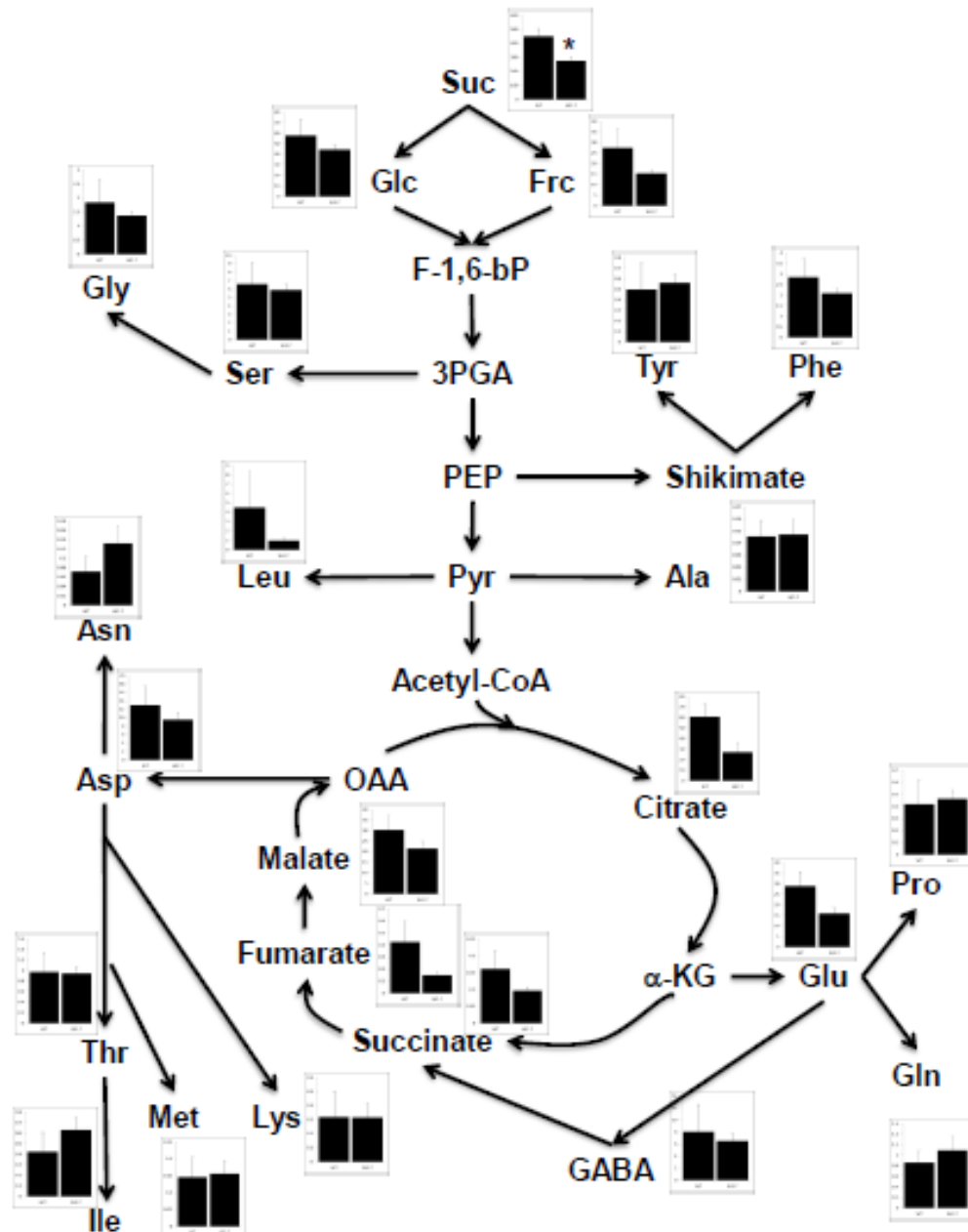


Figure 7.2 A comparison of the leaf metabolite profiles of 17 day old wild type seedlings and WHIRLY-1 deficient barley line W1-7, shown as schematic of key metabolic pathways. The bar charts represent the relative concentrations of each metabolite in the wild-type (left hand bar) and W1-7 (right hand bar) leaves. Data are mean \pm SE values (n = 4). Asterisks indicate significant differences between lines, estimated using the students T-test (P<0.05).

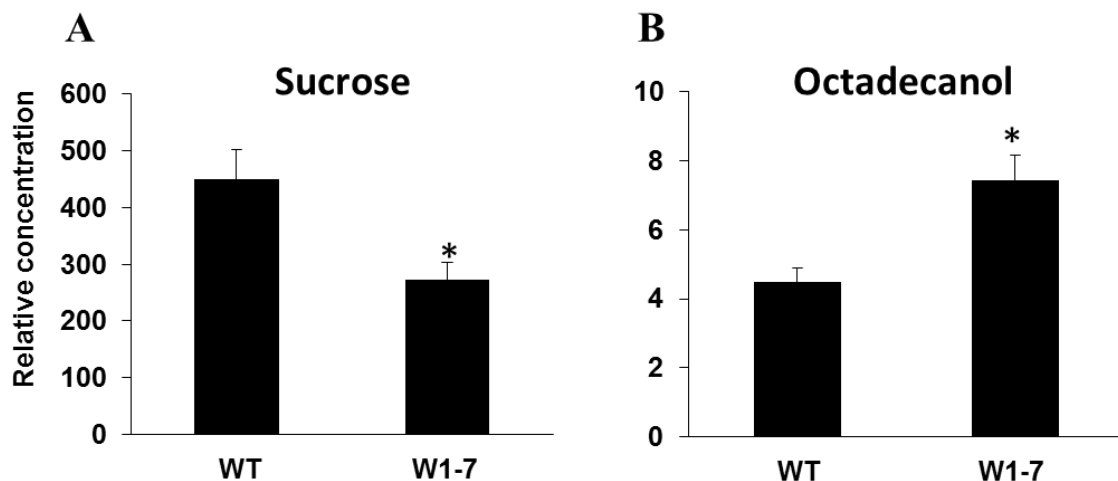


Figure 7.3 Sucrose and octadecanol relative concentrations in N replete conditions in the wild type and W1-7 leaves. Mean compound content \pm SE normalised to the appropriate internal standard (n = 4). Asterisks indicate significant differences between lines, estimated using the students T-test ($P < 0.05$).

7.2.3 Metabolite changes in the W1-7 relative to the wild type in response to nitrogen deficiency

The levels of most leaf metabolites were similar in the W1-7 and wild type leaves when plants were grown under deficient nitrogen nutrition. However, the abundance of two sugars and two organic acids were changed between the wild type and the W1-7 leaves grown under nitrogen limitation (Figure 7.4). The levels of glucose, fructose and malic acid were significantly lower in the W1-7 leaves than the wild type (Figure 7.4 A, B and C). In contrast, pentadecanoic acid levels were significantly higher in the W1-7 leaves than the wild type (Figure 7.4 D).

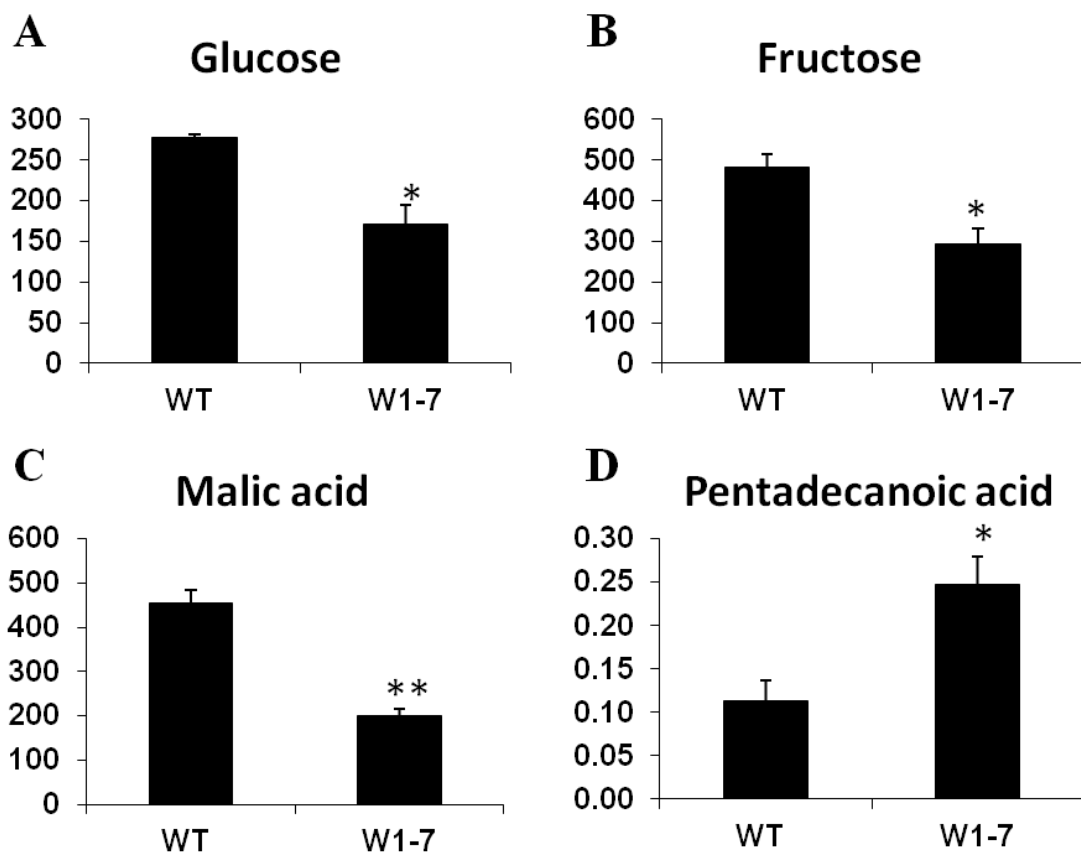


Figure 7.4 Glucose (A), fructose (B), malic acid (C) and pentadecanoic acid (D) relative concentrations in N deficient conditions in the wild type and W1-7 leaves. Mean compound content +/- SE normalised to the appropriate internal standard (n = 4).

7.2.4 Sample variation

Principal components analysis (PCA) of the metabolic profiles of the W1-7 and wild type leaves subjected to 7 days of nitrogen deprivation revealed a little variation between the different biological replicates (Figure 7.5). The score 1, which separates all the replicates from the N replete and N deficient treatments shows that there was a clear separation between samples harvested under the two different treatments. However, the score 2 which separates the wild type from the W1-7 replicates does not show as clear separation (Figure 7.5).

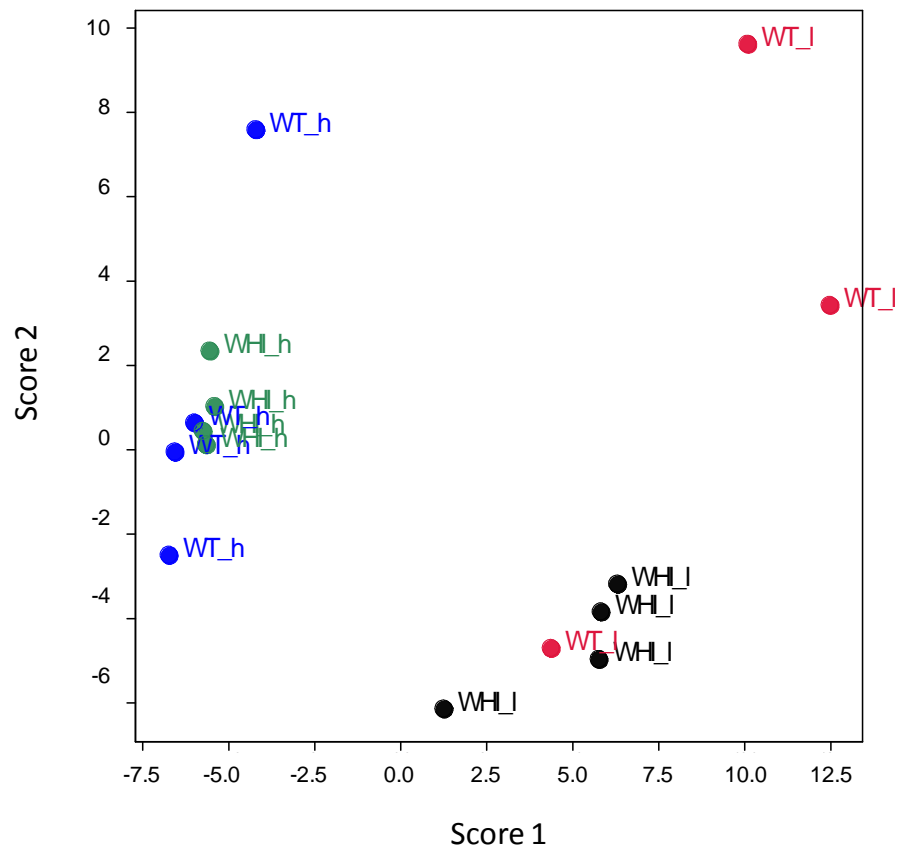


Figure 7.5 Principal components analysis (PCA) of the metabolic profiles of the W1-7 (WH) and wild type (WT) leaves under optimal nitrogen (WT h, WH h) and after 7 days of nitrogen deprivation (WT l, WH l).

7.3 Discussion

The effects of low nitrogen on leaf metabolite profiles are well characterized. All literature studies report large changes in the levels of leaf amino acids. The data presented here shows that the levels of most of the leaf amino acids were increased as a result of nitrogen deficiency, in agreement with previous findings in *Arabidopsis* (Diaz et al., 2005). Moreover, N-containing molecules derived from glutamine and glutamate, such as γ -aminobutyric acid (GABA) were also increased, in line with previous observations.

The ratios of some amino acids such as Gly/Ser, Gln/Glu and Asn/Asp can be useful indicators of metabolic status, particularly carbon and nitrogen status in relation to photosynthesis and photorespiration (Novitskaya et al., 2002). Ratios of different amino acids have also been discussed in relation to senescence (Diaz et al., 2005; Watanabe et al., 2013). The Gln/Glu and Asn/Asp ratio were greatly increased under N limitation, suggesting that under nitrogen limitation the leaves accumulate nitrogen-rich amino acids. This finding is perhaps surprising given that decreases in these ratios are often taken to be markers of N limitation (Foyer et al., 2003; Fritz et al., 2006; Watanabe et al., 2013). However, increases in the Gln/Glu and Asn/Asp ratios are also indicative of the remobilisation of resources during leaf senescence (Watanabe et al., 2013). The increases in the ratios of these amino acids are therefore indicative of the onset of leaf senescence. Unlike Gln and Glu, the leaf Gly, Ser, Asp and Ala pools respond rapidly to changes in photorespiration (Wingler et al., 1999; Wingler et al., 2000; Novitskaya et al., 2002). Given that the Gly/Ser ratio has been shown to be a marker of the rate of photorespiration (Novitskaya et al., 2002) the data presented here showing that the Gly/Ser ratio was about 5 times higher under N-limited conditions than under optimal nitrogen suggests that photorespiration was favoured in the N-limited barley leaves. This finding is consistent with increased stomatal closure in the plants suffering from nitrogen deficiency. Moreover, the lower levels of phytol pools observed under N deficiency would suggested that there is less investment in metabolites associated with light harvesting pigments in these conditions.

Low nitrogen stress often leads to increased amounts of organic acids in leaves (Watanabe et al., 2013), particularly those involved in the tricarboxylic acid (TCA) cycle. The data presented here are consistent with these observations, suggesting that TCA cycle activity is increased in barley leaves as a result of nitrogen limitation. Soluble carbohydrates such as glucose and fructose also increase in leaves under nitrogen deficiency (Amiour et al., 2012). The data presented here suggest that sucrose levels were unchanged by the growth nitrogen regime but the levels of glucose and fructose and some other sugars increased. This finding may suggest that sucrose breakdown as a result of the action of invertase was increased in the barley leaves as a result of nitrogen limitation consistent with low nitrogen-dependent re-organization of metabolic network that allows adaptation to stress (Obata and Fernie, 2012).

The absence of a functional WHIRLY1 protein had not a marked effect on the leaf metabolite pools under nitrogen replete conditions. Most leaf metabolites have similar levels in the W1-7 and wild type leaves under optimal nitrogen nutrition (Figure 7.2). However, the significantly lower levels of sucrose observed in the W1-7 leaves may suggest that the rate of photosynthetic carbon assimilation and hence sucrose production is slower in leaves lacking a functional WHIRLY1 protein than in the wild type (Figure 7.3). Conversely, the higher octadecanol levels observed in the W1-7 leaves under this condition may suggest that rates of some pathways related to fatty acids are higher than in the wild type (Figure 7.3).

The responses of the leaf metabolic profiles to nitrogen deficiency were different in the W1-7 and wild type leaves. Glucose, fructose and malic acid were decreased in W1-7 leaves respect the wild type under nitrogen limitation (Figure 7.4). These three metabolites were significantly increased in the wild type grown under low nitrogen conditions (Table 7.2), the fact that this increase was not as marked in the W1-7 plants might help to explain the ability of these plants to grow better in such conditions.

The PCA analysis of the metabolic profiles of the W1-7 and wild type leaves (Figure 7.5) is consistent with the conclusion that while metabolism was greatly changed as a result of the difference in nitrogen status used in these studies, there was much less separation of the metabolite profiles of the wild type from the W1-7 replicates.

Chapter 8. General discussion

8.1 OCI and Rubisco degradation during senescence

Leaf senescence is a complex and dynamic process that remains poorly understood. In particular, it is uncertain how the regulation of stress-induced senescence differs from the developmental senescence program. In both cases, leaf senescence is characterised by a decrease in chlorophyll and protein, together with progressive loss of photosynthetic functions and associated gene expression. At the same time, SAGs are expressed and leaf protease activities are increased so that amino acids and other nutrients are recycled to other organs (Lin and Wu, 2004; Breeze et al., 2011; Guo, 2013). Cysteine proteases are considered to fulfil important functions in leaf senescence, as well as in other processes such as programmed cell death (Corr-Menguy et al., 2002; Belenghi et al., 2003; Kiyosaki et al., 2007; Weeda et al., 2009). An excellent example is the sweet potato papain-like cysteine protease (SPCP2). This vacuolar cysteine protease is expressed during developmental senescence but it is also expressed in response to plant hormones such as ethylene, ABA and JA. Intriguingly, constitutive expression of SPCP2 in *Arabidopsis* resulted in enhanced stress tolerance as well as a slightly earlier transition from vegetative to reproductive growth (Chen et al., 2010).

Many papain-like cysteine proteases are regulated *in vivo* by tight binding inhibitors called cystatins. Of these, the rice cystatin, OCI is perhaps the best characterised in terms of effects on plant growth and development as well as stress tolerance (Van der Vyver et al., 2003; Prins et al., 2008; Quain et al., 2014). In this study, OCI was either expressed in the cytosol or targeted to the chloroplast of transgenic *Arabidopsis* lines. Interestingly, constitutive OCI expression decreased the growth of the rosettes in terms of rosette diameter

and biomass accumulation relative to controls (Figure 8.1) independent of the promoter used to drive gene expression. This suggests that inhibition of leaf cysteine proteases decrease leaf growth regardless of the intracellular localisation of OCI, i.e. in the cytosol or chloroplasts. This finding is surprising because there has been little evidence to support the concept that chloroplasts contain cysteine proteases. To date, only metallo- and aspartic proteases have been found to contribute to Rubisco degradation in chloroplasts (Kato et al., 2004; Roberts et al., 2012). Recent immuno-detection studies, however, suggest that the barley cysteine protease PAP14 (*HvPAP14*) is localised in the chloroplasts (Hollmann et al., 2014, abstract T4.5 of the 7th European Workshop on Plant Senescence). It is possible therefore that plastid localised cysteine proteases contribute to the regulation of leaf growth. Furthermore, chloroplast proteome analysis has previously shown that an OTU-like cysteine protease family protein is present in the chloroplast fraction (Bayer et al., 2011). Expression of OCI in the cytosol of tobacco leaves demonstrated that inhibition of leaf cysteine proteases protects photosynthesis and delays degradation of Rubisco during developmental and stress-induced senescence (Van der Vyver et al., 2003; Prins et al., 2008). Further analysis of photosynthesis and Rubisco functions are required to determine whether inhibition of leaf cysteine proteases in the cytosol or chloroplasts have differential effects on these processes.

In addition to effects of shoot growth, constitutive OCI expression altered root growth and architecture. The primary roots of the transgenic lines were longer with a higher lateral root density than the wild type *Arabidopsis* plants, whether OCI was expressed in the cytosol or chloroplasts. These changes in root morphology are similar to those observed in strigolactone synthesis (*max3*) and signalling (*max2*) (Gomez-Roldan et al., 2008; Beveridge et al., 2009). Moreover, addition of the cysteine protease inhibitor E64 also caused similar changes in root morphology suggesting that cysteine proteases might have a role in the regulation of strigolactone synthesis or signalling (Quain et al., 2014).

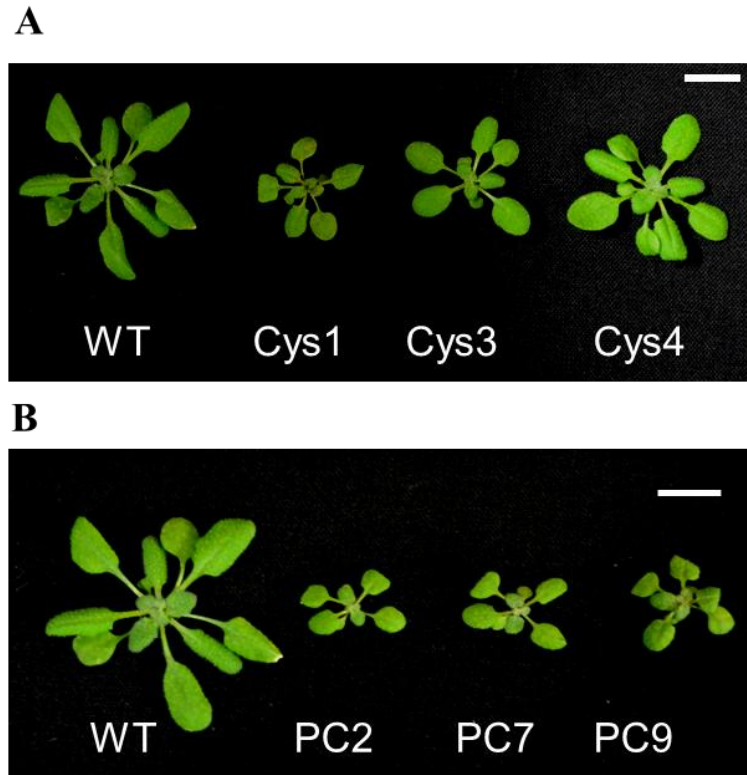


Figure 8.1 A comparison of the rosette phenotypes at 30 days of the three independent transgenic lines with ectopic expression of OCI in the cytosol (A) and OCI targeted to the chloroplast (B) to the wild type (WT). (Scale bar = 1 cm) Taken from Figures 3.1 and 3.2.

The data presented here suggest that OCI has the potential to regulate root and shoot growth, in a manner that might be economically important for agriculture. The experiments undertaken here have produced transgenic wheat plants expressing the OCI coding sequence in the cytosol. Future analysis of the growth and development of the transgenic OCI wheat plant in relation to yield will be required to determine whether ectopic OCI expression has benefits that are agronomically important in plants, as has been shown in model species such as tobacco (Van der Vyver et al., 2003). In addition, OCI-expressing wheat lines should have better resistance to coleopteran insects as demonstrated previously in other species (Zhao et al., 1996; Delledonne et al., 2001; Christou et al., 2006; Kiggundu et al., 2010).

A more-in-depth characterisation of the transformed *A thaliana* lines with constitutive OCI expression either in the cytosol or targeted to the chloroplasts is required to characterise the functions of cysteine proteases in the degradation of chloroplast proteins including Rubisco. Furthermore, it should be possible to determine the action of OCI with respect to the autophagy pathway and the CVV pathway (Figure 8.2). One set of experiments that has already been initiated involves crossing the OCI lines with mutants in the autophagy pathway such as the *atg5*. The plan is also to make crosses with tagged lines (GFP-ATG8, RFP-ATG8 and Cherry-ATG8) in which intrinsic ATG8 protein of the autophagosome membrane is linked to fluorescent markers to enable visualization of the autophagosomes using confocal microscopy. This will allow visualization of autophagosomes and senescence associated vacuoles in leaves of Arabidopsis lines with ectopic OCI expression compared to wild type. Similarly, the OCI lines can be crossed with mutants in the CVV pathway to determine the possible role of cysteine proteases in this type of stress-induced chloroplast protein turnover.

While the transformation of barley with the OCI construct was unsuccessful, OCI has successfully been expressed in transgenic wheat lines, which will be used to investigate the functions of OCI-targeted cysteine proteases in natural and stress-induced senescence in this major cereal crop, with a specific focus on flag leaf lifespan and grain yield. Similarly, transgenic barley lines overexpressing SAG21 have already been produced and the first homozygous lines are now been characterised in terms of the relationship between photosynthesis, leaf lifespan and stress-induced senescence. While the results of these studies are beyond the scope of this thesis, the production of these transgenic lines as part of my thesis studies has laid the foundation for future work in these key areas.

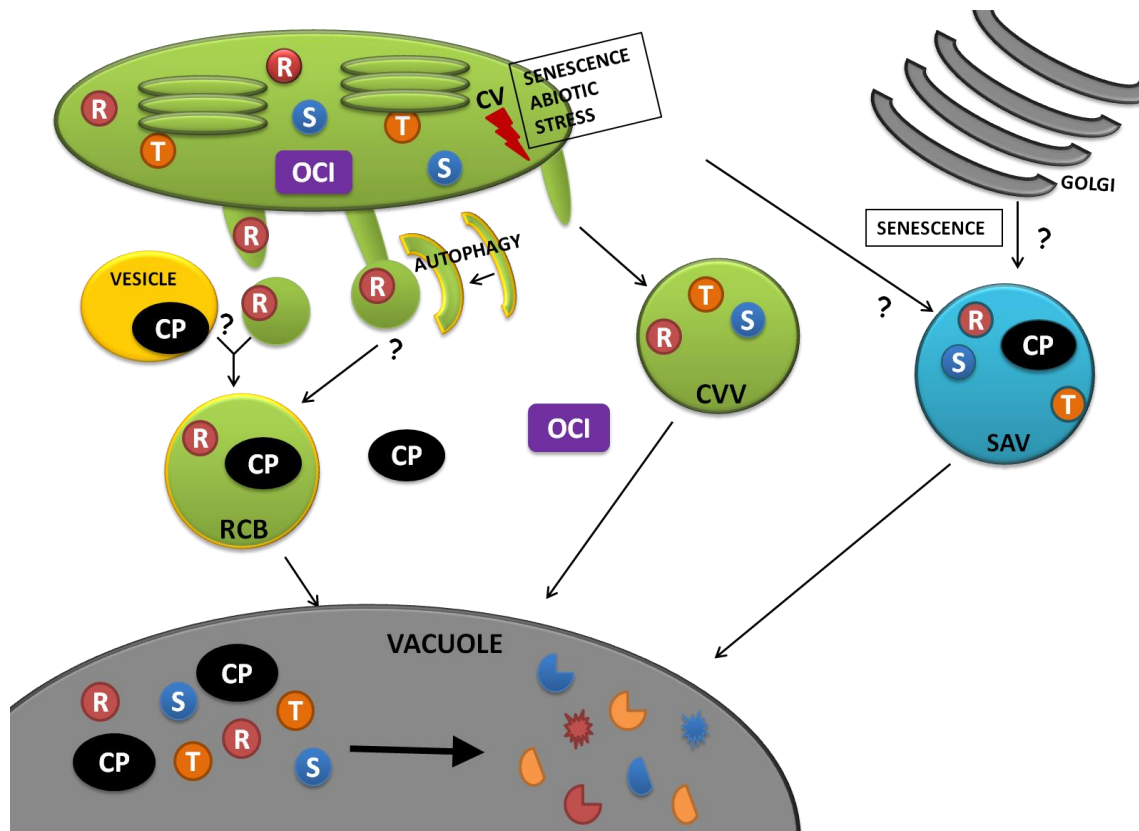


Figure 8.2 Scheme of potential pathways of chloroplast protein degradation during leaf senescence with OCI located to cytosol and chloroplast. CP, Cysteine protease (black); OCI, Oryzacystatin I (purple); R, Rubisco (red); T, thylakoid protein (orange); S, stroma protein (blue); RCB, Rubisco-containing body; SAV, senescence-associated vacuole; CVV, CV-containing vesicles. Modified from Diaz-Mendoza et al. (2014).

8.2 WHIRLY1 in barley

A key feature of the studies described in this thesis concerns the characterisation of transgenic RNAi barley lines that have greatly reduced expression of WHIRLY1. Moreover, the effects of nitrate deficiency on the leaf transcript and metabolite profiles of barley seedlings were characterised. Nitrogen deficiency was chosen as a main focus of the present analysis of

WHIRLY1 functions in abiotic stress tolerance because a strong relationship has been demonstrated between the period of flag leaf photosynthesis and increased yield in plants grown under conditions of nitrogen deficiency (Derkx et al., 2012; Gaju et al., 2014). The data presented here show that WHIRLY1 has an impact on the photosynthetic machinery under optimal and stress conditions. In particular, leaf chlorophyll was higher in the WHIRLY1-deficient lines than the type in all the growth conditions used in these studies.

Wild type barley seedlings grown for 7 days under low nitrogen were smaller than those grown on optimal nitrogen and the leaves had only about 40% of the chlorophyll with respect to the nitrogen-replete controls. The leaf carbon/nitrogen ratio was significantly increased under low nitrogen consistent with data in other species such as in maize (Amiour et al., 2012; Schluter et al., 2013). Photosynthetic rates, leaf phytol contents and the abundance of transcripts encoding photosynthetic proteins were significantly decreased as a result of nitrogen deficiency. However, transcripts encoding ACCLIMATION OF PHOTOSYNTHESIS TO ENVIRONMENT (APE1) were significantly increased under low nitrogen. APE1 is required for the acclimation of photosynthetic apparatus to high light stress (Walters et al., 2003). In addition, ATP-dependent metalloproteases (AAA proteases), which are involved in the turnover of PSII were also increased under nitrogen limitation (Chi et al., 2012). Interestingly, the expression of the *WHIRLY1* gene was increased in barley plants grown under low nitrogen (Appendix IV). However, the role of WHIRLY1 in plant responses to low nitrogen had not been studied previously. Additionally, although the functions of WHIRLY1 have been studied in Arabidopsis mutants and transgenic maize lines that lack a functional WHIRLY1, little is known about the role of WHIRLY1 in barley. Moreover, the W1-1, W1-7 and W1-9 barley lines that are deficient in the WHIRLY1 protein have not been previously characterised in detail. The data presented here suggest that low levels of the WHIRLY1 protein increase the resistance of barley seedlings to low nitrogen stress.

8.2.1 Effect of WHIRLY1 on photosynthesis under optimal nitrogen

Photosynthetic CO₂ assimilation rates were similar in the wild type and WHIRLY1-deficient barley lines grown under optimal nitrogen. However, the data in Figure 5.29 suggest that photosynthesis is lower at the earliest stages of leaf development, i.e. before 7 days. It would be interesting to study the effects of WHIRLY1 on chloroplast and leaf development. While this analysis could not be performed during the present study, seeds of the different lines were sent for RNAseq analysis to provide base-line information on the transcript changes in seeds, with a view to following transcript changes from germination through the early stages of leaf development.

Regardless of the absence of effects on photosynthetic CO₂ assimilation rates in leaves after 14 days of development, the leaf chlorophyll and sucrose contents were higher in WHIRLY1-deficient leaves than the wild type suggesting that WHIRLY1 has a strong influence on the photosynthetic machinery and related processes. The transcript and metabolite profiling analysis performed here does not allow further insights into the mechanisms involved but this would be an interesting topic for further study. Perhaps a starting point in this respect might be an analysis of chlorophyll fluorescence parameters in wild type and WHIRLY1-deficient leaves.

8.2.2 Effect of WHIRLY1 on photosynthesis under low nitrogen

The WHIRLY1-deficient plants maintained leaf chlorophyll and photosynthetic competence for a longer period than the wild type under nitrogen deficiency. The resistance of the WHIRLY1-deficient plants to nitrogen limitation might be explained at least in part by the up regulation of the transcript encoding FAR1, which confers adaptation to abiotic stress via ABA regulation (Tang et al., 2013). Besides, the higher activity of FAR1 may explain the higher chlorophyll content of the transgenic plants, as this protein has the ability to regulate chlorophyll biosynthesis (Tang et al., 2013). Furthermore, FAR1 has been

shown to alter stomatal morphology and functioning leading to the *far1* mutants being more sensitive to drought (Tang et al., 2013). The higher stomatal conductance observed in the WHIRLY1-deficient lines under abiotic stresses could be related to FAR1 up regulation, plus the phenotype and response of these plants to drought stress also indicate an improved resistance relative to the wild type. A number of altered transcripts involved in signalling could further contribute to the enhanced resistance. Several transcripts encoding histidine kinases and STRUBBELIG, a receptor-like kinase with cell signal transduction functions, were up regulated in W1-7 leaves (Eyuboglu et al., 2007). At the same time, the metabolic response to low nitrogen of the W1-7 leaves differed from the one of the wild type. The levels of glucose, fructose and malic acid in the transgenic plants were not as decreased as in the wild type, which could be an adaptation strategy to the adverse conditions.

8.2.3 The WHIRLY1 protein has important functions within the chloroplasts

WHIRLY1-deficient leaves exhibited marked changes in the abundance of transcripts encoding photosynthetic proteins relative to the wild type. Transcripts encoding proteins associated with the thylakoid NADH dehydrogenase, cytochrome b/f complexes, RNA polymerase and ribosomes were more abundant under both growth conditions. These data support the studies regarding plastid DNA copy number regulation by WHIRLY1 (Krupinska et al., 2014). The chloroplast NADH complex functions in cyclic electron flow around PSI, this pathway produces ATP but not excessive amounts of NADPH which could damage the stroma (Peng et al., 2009; Peng and Shikanai, 2011). The NADH complex also protects against stress in barley (Casano et al., 2001). In the transcriptomic analysis 9 of the total 11 *ndh* genes which are part of the plastid DNA showed an altered expression. These findings indicate that the presence of WHIRLY1 inhibits the expression of the cited genes which are important in the cyclic electron flow (Miyake, 2010; Foyer et al., 2012). In contrast, transcripts encoding PSI and PSII reaction centre complexes and light harvesting components were unaffected by WHIRLY1, which could explain the similar photosynthetic rates observed between both genotypes. Although the

differences were not significant, the transgenic lines tended to have slightly lower photosynthesis. This fact could lead to the lower sucrose content of the W1-7 leaves, plus suggesting that the influence of WHIRLY1 extends to carbon metabolism.

8.2.4 Other potential roles of WHIRLY1 in barley

The altered expression of a MADS box transcription factor might be responsible for the reduction in the number of fertile tillers and seed yield in the W1-7 line. A transcript that shows homology to an *Oryza sativa* plant specific type II MIKC MADS box gene was increased in abundance in W1-7 leaves relative to the wild type (Table 6.1). A transcription factor of this type, the *Triticum aestivum* AGAMOUS-like 33 (TaAGL33), has been shown to be involved in developmental processes such as flowering time and seed development (Winfield et al., 2009). Moreover, the expression of TaAGL33 represses flowering by down-regulation of a group of genes related to the Arabidopsis FLOWERING PROMOTING FACTOR 1 (Greenup et al., 2010). Therefore, the reduction in the number of fertile tillers and seed yield in W1-7 plants compared to the wild type could be explained by the enhanced abundance of the type II MIKC MADS box transcripts in W1-7 plants.

WHIRLY1 participates in DNA repair and interacts with the organelle DNA polymerase. Arabidopsis DNA polymerases have important functions in DNA replication. Besides, and similarly to WHIRLY proteins, the organelle DNA polymerase IB (*pollB*) has been proposed to have a further role in DNA repair (Marechal et al., 2009; Cappadocia et al., 2010; Parent et al., 2011). Experiments with triple mutants *pollb-1/why1why3* indicate that these proteins repair DNA independently. Accordingly, a barley plastid DNA polymerase has been recently characterized and resulting to be more abundant in WHIRLY1 deficient plants (Krupinska et al., 2014). In agreement with those findings, a transcript homologous to Arabidopsis gamma polymerase, identified as the barley organelle DNA polymerase, had higher levels of expression in WHIRLY1-deficient leaves independently of the nitrogen treatment. Hence, it is

possible that WHIRLY1 and the plastid DNA polymerase have complementary effects. Another explanation would be that the increased level of this transcript in the WHIRLY1 knock down leaves is a consequence of the higher plastid DNA amount present in these plants (Krupinska et al., 2014).

The WHIRLY1 protein has been implicated in plant innate immune resistance pathways and so it might be that deficiency in WHIRLY1 could decrease protection against biotic stress. The role of WHIRLY1 in stress has been shown before in potato where it participates in disease resistance response (Desveaux et al., 2004). However, there were no differences in classic patterns of hormone-related defence transcripts except for those encoding YELLOW STRIPE like 3 and jasmonate sulphotransferase, whose possible interactions were discussed in chapter 6 (Shan et al., 2011; Chen et al., 2014). Moreover, in a separate study, no differences in the susceptibility of the barley lines to aphid infestation were observed. Nevertheless, more experiments are needed to exclude that WHIRLY1 confers pathogen resistance in barley plants.

The levels of several stress related transcripts were changed in the W1-7 leaves, including FAR1, YELLOW STRIPE like 3, jasmonate sulphotransferase and various chains of the NDH complex. Furthermore, the transcript encoding WHIRLY1 was much more abundant in the wild type plants suffering nitrogen deprivation (Appendix IV). These findings maintain previous hypothesis concerning WHIRLY1 activity in response to abiotic stress (Foyer et al., 2014). It is thought that destabilization of the electron transport chain release WHIRLY1 from the thylakoid membrane as monomers, and that such breakdown might be triggered by thioredoxins and kinases. The analysis of the W1-7 leaves under nitrogen deficiency revealed a further increase in the abundance of eight transcripts encoding kinases, which have been demonstrated to have important roles in chloroplast-to nucleus signalling. This fact is in agreement with a possible influence of kinases in WHIRLY1 activity under stress conditions.

The findings obtained in this thesis support previous literature on the roles of the WHIRLY1 protein in the chloroplasts, linked with stress and senescence. Moreover, they establish a possible connection of this protein with nitrogen metabolism, hence proposing a potential new target for better nitrogen use efficiency in crop plants. However, further experiments will be required to explore WHIRLY1 functions in more detail.

Bibliography

Abe K, Emori Y, Kondo H, Suzuki K, Arai S (1987) Molecular cloning of a cysteine proteinase inhibitor of rice (oryzacystatin). Homology with animal cystatins and transient expression in the ripening process of rice seeds. *J Biol Chem* **262**: 16793-16797

Alscher RG, Erturk N, Heath LS (2002) Role of superoxide dismutases (SODs) in controlling oxidative stress in plants. *J Exp Bot* **53**: 1331-1341

Amiour N, Imbaud S, Clement G, Agier N, Zivy M, Valot B, Balliau T, Armengaud P, Quillere I, Canas R, Tercet-Laforgue T, Hirel B (2012) The use of metabolomics integrated with transcriptomic and proteomic studies for identifying key steps involved in the control of nitrogen metabolism in crops such as maize. *J Exp Bot* **63**: 5017-5033

Arai S, Matsumoto I, Emori Y, Abe K (2002) Plant seed cystatins and their target enzymes of endogenous and exogenous origin. *J Agric Food Chem* **50**: 6612-6617

Araus JL, Slafer GA, Royo C, Serret MD (2008) Breeding for Yield Potential and Stress Adaptation in Cereals. *Critical Reviews in Plant Sci* **27**: 377-412

Balazadeh S, Schildhauer J, Araújo WL, Munné-Bosch S, Fernie AR, Proost S, Humbeck K, Mueller-Roeber B (2014) Reversal of senescence by N resupply to N-starved *Arabidopsis thaliana*: transcriptomic and metabolomic consequences. *J Exp Bot* **65**: 3975-3992

Bayer RG, Stael S, Csaszar E, Teige M (2011) Mining the soluble chloroplast proteome by affinity chromatography. *Proteomics* **11**: 1287-1299

Bechtold U, Richard O, Zamboni A, Gapper C, Geisler M, Pogson B, Karpinski S, Mullineaux PM (2008) Impact of chloroplastic- and extracellular-

sourced ROS on high light-responsive gene expression in Arabidopsis. *J Exp Bot* **59**: 121-133

Beed F, Paveley N, Sylvester-Bradley R (2007) Predictability of wheat growth and yield in light-limited conditions. *J Agric Sci* **145**: 63-79

Belenghi B, Acconcia F, Trovato M, Perazzolli M, Bocedi A, Polticelli F, Ascenzi P, Delledonne M (2003) AtCYS1, a cystatin from Arabidopsis thaliana, suppresses hypersensitive cell death. *Eur J Biochem* **270**: 2593-2604

Benchabane M, Schluter U, Vorster J, Goulet MC, Michaud D (2010) Plant cystatins. *Biochimie* **92**: 1657-1666

Bernard P, Couturier M (1992) Cell killing by the F plasmid CcdB protein involves poisoning of DNA-topoisomerase II complexes. *J Mol Biol* **226**: 735-745

Besagni C, Kessler F (2013) A mechanism implicating plastoglobules in thylakoid disassembly during senescence and nitrogen starvation. *Planta* **237**: 463-470

Beveridge CA, Dun EA, Rameau C (2009) Pea has its tendrils in branching discoveries spanning a century from auxin to strigolactones. *Plant Physiol* **151**: 985-990

Bhalerao R, Keskitalo J, Sterky F, Erlandsson R, Bjorkbacka H, Birve SJ, Karlsson J, Gardestrom P, Gustafsson P, Lundeberg J, Jansson S (2003) Gene expression in autumn leaves. *Plant Physiol* **131**: 430-442

Bradford MM (1976) A rapid and sensitive method for the quantitation of microgram quantities of protein utilizing the principle of protein-dye binding. *Anal Biochem* **72**: 248-254

Breeze E, Harrison E, McHattie S, Hughes L, Hickman R, Hill C, Kiddle S, Kim YS, Penfold CA, Jenkins D, Zhang C, Morris K, Jenner C, Jackson S, Thomas B, Tabrett A, Legaie R, Moore JD, Wild DL, Ott S, Rand D, Beynon J, Denby K, Mead A, Buchanan-Wollaston V (2011) High-resolution temporal

profiling of transcripts during Arabidopsis leaf senescence reveals a distinct chronology of processes and regulation. *Plant Cell* **23**: 873-894

Burrows PA, Sazanov LA, Svab Z, Maliga P, Nixon PJ (1998) Identification of a functional respiratory complex in chloroplasts through analysis of tobacco mutants containing disrupted plastid *ndh* genes. *EMBO J* **17**: 868–876

Cappadocia L, Marechal A, Parent JS, Lepage E, Sygusch J, Brisson N (2010) Crystal structures of DNA-Whirly complexes and their role in Arabidopsis organelle genome repair. *Plant Cell* **22**: 1849-1867

Cappadocia L, Parent JS, Zampini E, Lepage E, Sygusch J, Brisson N (2012) A conserved lysine residue of plant Whirly proteins is necessary for higher order protein assembly and protection against DNA damage. *Nucleic Acids Res* **40**: 258-269

Carrion CA, Costa ML, Martinez DE, Mohr C, Humbeck K, Guiamet JJ (2013) In vivo inhibition of cysteine proteases provides evidence for the involvement of 'senescence-associated vacuoles' in chloroplast protein degradation during dark-induced senescence of tobacco leaves. *J Exp Bot* **64**: 4967-4980

Casano LM, Lascano HR, Martin M, Sabater B (2004) Topology of the plastid Ndh complex and its NDH-F subunit in thylakoid membranes. *Biochem J* **382**: 145-155

Casano LM, Martin M, Sabater B (2001) Hydrogen peroxide mediates the induction of chloroplastic Ndh complex under photooxidative stress in barley. *Plant Physiol* **125**: 1450-1458

Casano LM, Zapata JM, Martin M, Sabater B (2000) Chlororespiration and poisoning of cyclic electron transport. Plastoquinone as electron transporter between thylakoid NADH dehydrogenase and peroxidase. *J Biol Chem* **275**: 942-948

Chen CC, Chien WF, Lin NC, Yeh KC (2014) Alternative functions of Arabidopsis Yellow Stripe-Like3: from metal translocation to pathogen defense. PLoS One **9**: e98008

Chen HJ, Su CT, Lin CH, Huang GJ, Lin YH (2010) Expression of sweet potato cysteine protease SPCP2 altered developmental characteristics and stress responses in transgenic Arabidopsis plants. J Plant Physiol **167**: 838-847

Chepyshko H, Lai C-P, Huang L-M, Liu J-H, Shaw J-F (2012) Multifunctionality and diversity of GDSL esterase/lipase gene family in rice (*Oryza sativa* L. japonica) genome: new insights from bioinformatics analysis. BMC genomics **13**: 309

Chi W, Sun X, Zhang L (2012) The roles of chloroplast proteases in the biogenesis and maintenance of photosystem II. Bioenergetics **1817**: 239-246

Chiba A, Ishida H, Nishizawa NK, Makino A, Mae T (2003) Exclusion of ribulose-1,5-bisphosphate carboxylase/oxygenase from chloroplasts by specific bodies in naturally senescing leaves of wheat. Plant Cell Physiol **44**: 914-921

Christou P, Capell T, Kohli A, Gatehouse JA, Gatehouse AM (2006) Recent developments and future prospects in insect pest control in transgenic crops. Trends Plant Sci **11**: 302-308

Christou P, Capell T, Kohli A, Gatehouse JA, Gatehouse AMR (2006) Recent developments and future prospects in insect pest control in transgenic crops. Trends in Plant Sci **11**: 302-308

Christova P, Christov N, Imai R (2006) A cold inducible multidomain cystatin from winter wheat inhibits growth of the snow mold fungus, *Microdochium nivale*. Planta **223**: 1207-1218

Clough SJ, Bent AF (1998) Floral dip: a simplified method for *Agrobacterium*-mediated transformation of *Arabidopsis thaliana*. Plant J **16**: 735-743

Cobbett CS (2000) Phytochelatin biosynthesis and function in heavy-metal detoxification. *Curr Opin Plant Biol* **3**: 211-216

Corr-Menguy F, Cejudo FJ, Mazubert C, Vidal J, Lelandais-Briere C, Torres G, Rode A, Hartmann C (2002) Characterization of the expression of a wheat cystatin gene during caryopsis development. *Plant Mol Biol* **50**: 687-698

Cruz de Carvalho MH, d'Arcy-Lameta A, Roy-Macauley H, Gareil M, El Maarouf H, Pham-Thi A-T, Zuily-Fodil Y (2001) Aspartic protease in leaves of common bean (*Phaseolus vulgaris* L.) and cowpea (*Vigna unguiculata* L. Walp): enzymatic activity, gene expression and relation to drought susceptibility. *FEBS Lett* **492**: 242-246

Delledonne M, Allegro G, Belenghi B, Balestrazzi A, Picco F, Levine A, Zelasco S, Calligari P, Confalonieri M (2001) Transformation of white poplar (*Populus alba* L.) with a novel *Arabidopsis thaliana* cysteine proteinase inhibitor and analysis of insect pest resistance. *Mol Breed* **7**: 35-42

Derkx AP, Orford S, Griffiths S, Foulkes MJ, Hawkesford MJ (2012) Identification of differentially senescing mutants of wheat and impacts on yield, biomass and nitrogen partitioning. *J Integr Plant Biol* **54**: 555-566

Despres C, Subramaniam R, Matton DP, Brisson N (1995) The Activation of the Potato PR-10a Gene Requires the Phosphorylation of the Nuclear Factor PBF-1. *Plant Cell* **7**: 589-598

Desveaux D, Allard J, Brisson N, Sygusch J (2002) A new family of plant transcription factors displays a novel ssDNA-binding surface. *Nat Struct Biol* **9**: 512-517

Desveaux D, Despres C, Joyeux A, Subramaniam R, Brisson N (2000) PBF-2 is a novel single-stranded DNA binding factor implicated in PR-10a gene activation in potato. *Plant Cell* **12**: 1477-1489

Desveaux D, Marechal A, Brisson N (2005) Whirly transcription factors: defense gene regulation and beyond. *Trends Plant Sci* **10**: 95-102

- Desveaux D, Subramaniam R, Despres C, Mess JN, Levesque C, Fobert PR, Dangl JL, Brisson N** (2004) A "Whirly" transcription factor is required for salicylic acid-dependent disease resistance in Arabidopsis. *Dev Cell* **6**: 229-240
- Diaz-Mendoza M, Velasco-Arroyo B, Gonzalez-Melendi P, Martinez M, Diaz I** (2014) C1A cysteine protease-cystatin interactions in leaf senescence. *J Exp Bot* **65**: 3825-3833
- Diaz C, Lemaitre T, Christ A, Azzopardi M, Kato Y, Sato F, Morot-Gaudry JF, Le Dily F, Masclaux-Daubresse C** (2008) Nitrogen recycling and remobilization are differentially controlled by leaf senescence and development stage in Arabidopsis under low nitrogen nutrition. *Plant Physiol* **147**: 1437-1449
- Diaz C, Purdy S, Christ A, Morot-Gaudry JF, Wingler A, Masclaux-Daubresse C** (2005) Characterization of markers to determine the extent and variability of leaf senescence in Arabidopsis. A metabolic profiling approach. *Plant Physiol* **138**: 898-908
- Dillon SC, Zhang X, Trievel RC, Cheng X** (2005) The SET-domain protein superfamily: protein lysine methyltransferases. *Genome Biol* **6**: 227
- Distelfeld A, Avni R, Fischer AM** (2014) Senescence, nutrient remobilization, and yield in wheat and barley. *J Exp Bot* **65**: 3783-3798
- Driever SM, Lawson T, Andralojc PJ, Raines CA, Parry MA** (2014) Natural variation in photosynthetic capacity, growth, and yield in 64 field-grown wheat genotypes. *J Exp Bot* **65**: 4959-4973
- Egli D, Leggett J, Duncan W** (1978) Influence of N stress on leaf senescence and N redistribution in soybeans. *Agron J* **70**: 43-47
- Estavillo GM, Chan KX, Phua SY, Pogson BJ** (2012) Reconsidering the nature and mode of action of metabolite retrograde signals from the chloroplast. *Front Plant Sci* **3**: 300
- Eyuboglu B, Pfister K, Haberer G, Chevalier D, Fuchs A, Mayer KF, Schneitz K** (2007) Molecular characterisation of the STRUBBELIG-

RECEPTOR FAMILY of genes encoding putative leucine-rich repeat receptor-like kinases in *Arabidopsis thaliana*. *BMC Plant Biol* **7**: 16

Feller U, Anders I, Demirevska K (2008) Degradation of Rubisco and other chloroplast proteins under abiotic stress. *Genet Plant Phys* **34 (1-2)**: 5-18

Foyer CH, Karpinska B, Krupinska K (2014) The functions of WHIRLY1 and REDOX-RESPONSIVE TRANSCRIPTION FACTOR 1 in cross tolerance responses in plants: a hypothesis. *Philos Trans R Soc Lond B Biol Sci* **369**: 20130226

Foyer CH, Neukermans J, Queval G, Noctor G, Harbinson J (2012) Photosynthetic control of electron transport and the regulation of gene expression. *J Exp Bot* **63**: 1637-1661

Foyer CH, Parry M, Noctor G (2003) Markers and signals associated with nitrogen assimilation in higher plants. *J Exp Bot* **54**: 585-593

Fritz C, Mueller C, Matt P, Feil R, Stitt M (2006) Impact of the C–N status on the amino acid profile in tobacco source leaves. *Plant Cell Environ* **29**: 2055-2076

Gaju O, Reynolds MP, Sparkes DL, Mayes S, Ribas-Vargas G, Crossa J, Foulkes MJ (2014) Relationships between physiological traits, grain number and yield potential in a wheat DH population of large spike phenotype. *Field Crop Res* **164**: 126-135

Gaude N, Brehelin C, Tischendorf G, Kessler F, Dormann P (2007) Nitrogen deficiency in *Arabidopsis* affects galactolipid composition and gene expression and results in accumulation of fatty acid phytyl esters. *Plant J* **49**: 729-739

Gomez-Roldan V, Fermas S, Brewer PB, Puech-Pages V, Dun EA, Pillot J-P, Letisse F, Matusova R, Danoun S, Portais J-C, Bouwmeester H, Becard G, Beveridge CA, Rameau C, Rochange SF (2008) Strigolactone inhibition of shoot branching. *Nature* **455**: 189-194

- Grabowski E, Miao Y, Mulisch M, Krupinska K** (2008) Single-Stranded DNA-Binding Protein Whirly1 in Barley Leaves Is Located in Plastids and the Nucleus of the Same Cell. *Plant Physiol* **147**: 1800-1804
- Greenup AG, Sasani S, Oliver SN, Talbot MJ, Dennis ES, Hemming MN, Trevaskis B** (2010) ODDSOC2 is a MADS box floral repressor that is down-regulated by vernalization in temperate cereals. *Plant Physiol* **153**: 1062-1073
- Gregersen PL, Culetic A, Boschian L, Krupinska K** (2013) Plant senescence and crop productivity. *Plant Mol Biol* **82**: 603-622
- Guera A, Calatayud A, Sabater B, Barreno E** (2005) Involvement of the thylakoidal NADH-plastoquinone-oxidoreductase complex in the early responses to ozone exposure of barley (*Hordeum vulgare* L.) seedlings. *J Exp Bot* **56**: 205-218
- Guiboileau A, Yoshimoto K, Soulay F, Bataillé M-P, Avice J-C, Masclaux-Daubresse C** (2012) Autophagy machinery controls nitrogen remobilization at the whole-plant level under both limiting and ample nitrate conditions in *Arabidopsis*. *New Phytol* **194**: 732-740
- Guo Y** (2013) Towards systems biological understanding of leaf senescence. *Plant Mol Biol* **82**: 519-528
- Guo Y, Cai Z, Gan S** (2004) Transcriptome of *Arabidopsis* leaf senescence. *Plant Cell Environ* **27**: 521-549
- Gutiérrez-Campos R, Torres-Acosta JA, de Jesús Pérez-Martínez J, Gómez-Lim MA** (2001) Pleiotropic effects in transgenic tobacco plants expressing the oryzacystatin I gene. *HortScience* **36**: 118-119
- Harris JB, Arnott HJ** (1973) Effects of senescence on chloroplasts of the tobacco leaf. *Tissue Cell* **5**: 527-544
- Hawkesford MJ, Araus J-L, Park R, Calderini D, Miralles D, Shen T, Zhang J, Parry MAJ** (2013) Prospects of doubling global wheat yields. *Food Energy Sec* **2**: 34-48

- Hermans C, Hammond JP, White PJ, Verbruggen N** (2006) How do plants respond to nutrient shortage by biomass allocation? *Trends Plant Sci* **11**: 610-617
- Himelblau E, Amasino RM** (2001) Nutrients mobilized from leaves of *Arabidopsis thaliana* during leaf senescence. *Plant Physiol* **158**: 1317-1323
- Hortensteiner S** (2006) Chlorophyll degradation during senescence. *Annu Rev Plant Biol* **57**: 55-77
- Hortensteiner S, Feller U** (2002) Nitrogen metabolism and remobilization during senescence. *J Exp Bot* **53**: 927-937
- Hwang JE, Hong JK, Lim CJ, Chen H, Je J, Yang KA, Kim DY, Choi YJ, Lee SY, Lim CO** (2010) Distinct expression patterns of two *Arabidopsis* phytocystatin genes, AtCYS1 and AtCYS2, during development and abiotic stresses. *Plant Cell Rep* **29**: 905-915
- Irving LJ, Robinson D** (2006) A dynamic model of Rubisco turnover in cereal leaves. *New Phytol* **169**: 493-504
- Ischebeck T, Zbierzak AM, Kanwischer M, Dormann P** (2006) A salvage pathway for phytol metabolism in *Arabidopsis*. *J Biol Chem* **281**: 2470-2477
- Isemer R, Mulisch M, Schafer A, Kirchner S, Koop HU, Krupinska K** (2012) Recombinant Whirly1 translocates from transplastomic chloroplasts to the nucleus. *FEBS Lett* **586**: 85-88
- Ishida H, Yoshimoto K, Izumi M, Reisen D, Yano Y, Makino A, Ohsumi Y, Hanson MR, Mae T** (2008) Mobilization of rubisco and stroma-localized fluorescent proteins of chloroplasts to the vacuole by an ATG gene-dependent autophagic process. *Plant Physiol* **148**: 142-155
- Je J, Song C, Hwang J, Chung W, Lim C** (2014) DREB2C acts as a transcriptional activator of the thermo tolerance-related phytocystatin 4 (AtCYS4) gene. *Transgenic Res* **23**: 109-123

Jeong H-J, Shin JS, Ok SH (2011) Barley DNA-binding methionine aminopeptidase, which changes the localization from the nucleus to the cytoplasm by low temperature, is involved in freezing tolerance. *Plant Sci* **180**: 53-60

Jukanti AK, Heidlebaugh NM, Parrott DL, Fischer IA, McInnerney K, Fischer AM (2008) Comparative transcriptome profiling of near-isogenic barley (*Hordeum vulgare*) lines differing in the allelic state of a major grain protein content locus identifies genes with possible roles in leaf senescence and nitrogen reallocation. *New Phytol* **177**: 333-349

Kato Y, Murakami S, Yamamoto Y, Chatani H, Kondo Y, Nakano T, Yokota A, Sato F (2004) The DNA-binding protease, CND41, and the degradation of ribulose-1,5-bisphosphate carboxylase/oxygenase in senescent leaves of tobacco. *Planta* **220**: 97-104

Kato Y, Yamamoto Y, Murakami S, Sato F (2005) Post-translational regulation of CND41 protease activity in senescent tobacco leaves. *Planta* **222**: 643-651

Kaup MT, Froese CD, Thompson JE (2002) A role for diacylglycerol acyltransferase during leaf senescence. *Plant Physiol* **129**: 1616-1626

Ke D, Yahia E, Hess B, Zhou L, Kader AA (1995) Regulation of fermentative metabolism in avocado fruit under oxygen and carbon dioxide stresses. *J Am Soc Hortic Sci* **120**: 481-490

Khanna-Chopra R, Srivalli B, Ahlawat YS (1999) Drought induces many forms of cysteine proteases not observed during natural senescence. *Biochem Biophys Res Commun* **255**: 324-327

Kichey T, Hirel B, Heumez E, Dubois F, Le Gouis J (2007) In winter wheat (*Triticum aestivum* L.), post-anthesis nitrogen uptake and remobilisation to the grain correlates with agronomic traits and nitrogen physiological markers. *Field Crops Res* **102**: 22-32

Kiggundu A, Muchwezi J, Van der Vyver C, Viljoen A, Vorster J, Schluter U, Kunert K, Michaud D (2010) Deleterious effects of plant cystatins against the banana weevil *Cosmopolites sordidus*. *Arch Insect Biochem Physiol* **73**: 87-105

Kim B, Kim G, Fujioka S, Takatsuto S, Choe S (2012) Overexpression of 3beta-hydroxysteroid dehydrogenases/C-4 decarboxylases causes growth defects possibly due to abnormal auxin transport in *Arabidopsis*. *Mol Cells* **34**: 77-84

Kiyosaki T, Matsumoto I, Asakura T, Funaki J, Kuroda M, Misaka T, Arai S, Abe K (2007) Gliadain, a gibberellin-inducible cysteine proteinase occurring in germinating seeds of wheat, *Triticum aestivum* L., specifically digests gliadin and is regulated by intrinsic cystatins. *FEBS Journal* **274**: 1908-1917

Kondo H, Abe K, Nishimura I, Watanabe H, Emori Y, Arai S (1990) Two distinct cystatin species in rice seeds with different specificities against cysteine proteinases. Molecular cloning, expression, and biochemical studies on oryzacystatin-II. *J Biol Chem* **265**: 15832-15837

Krause K, Herrmann U, Fuss J, Miao Y, Krupinska K (2009) Whirly proteins as communicators between plant organelles and the nucleus? *Endocytobiosis Cell Res* **19**: 51-62

Krause K, Kilbienski I, Mulisch M, Rodiger A, Schafer A, Krupinska K (2005) DNA-binding proteins of the Whirly family in *Arabidopsis thaliana* are targeted to the organelles. *FEBS Lett* **579**: 3707-3712

Krupinska K, Dähnhardt D, Fischer-Kilbienski I, Kucharewicz W, Scharrenberg C, Trösch M, Buck F (2014) Identification of WHIRLY1 as a Factor Binding to the Promoter of the Stress- and Senescence-Associated Gene HvS40. *J Plant Growth Regul* **33**: 91-105

Krupinska K, Oetke S, Desel C, Mulisch M, Schafer A, Hollmann J, Kumlehn J, Hensel G (2014) WHIRLY1 is a major organizer of chloroplast nucleoids. *Front Plant Sci* **5**: 432

- Kunert KJ, van Wyk SG, Cullis CA, Vorster BJ, Foyer CH** (2015) Potential use of phytocystatins in crop improvement, with a particular focus on legumes. *J Exp Bot* **66**: 3559-3570
- Kunkel BN, Brooks DM** (2002) Cross talk between signaling pathways in pathogen defense. *Curr Opin Plant Biol* **5**: 325-331
- Lascano HR, Casano LM, Martin M, Sabater B** (2003) The activity of the chloroplastic Ndh complex is regulated by phosphorylation of the NDH-F subunit. *Plant Physiol* **132**: 256-262
- Lawlor DW** (2013) Genetic engineering to improve plant performance under drought: physiological evaluation of achievements, limitations, and possibilities. *J Exp Bot* **64**: 83-108
- Leister D** (2012) Retrograde signaling in plants: from simple to complex scenarios. *Front Plant Sci* **3**: 135
- Leister D, Wang X, Haberer G, Mayer KFX, Kleine T** (2011) Intracompartamental and Intercompartmental Transcriptional Networks Coordinate the Expression of Genes for Organellar Functions. *Plant Physiol* **157**: 386-404
- Lepage E, Zampini E, Brisson N** (2013) Plastid genome instability leads to reactive oxygen species production and plastid-to-nucleus retrograde signaling in Arabidopsis. *Plant Physiol* **163**: 867-881
- Li J, Xu Y, Chong K** (2012) The novel functions of kinesin motor proteins in plants. *Protoplasma* **249 Suppl 2**: S95-100
- Lian X, Wang S, Zhang J, Feng Q, Zhang L, Fan D, Li X, Yuan D, Han B, Zhang Q** (2006) Expression profiles of 10,422 genes at early stage of low nitrogen stress in rice assayed using a cDNA microarray. *Plant Mol Biol* **60**: 617-631
- Lichtenthaler HK** (1987) Chlorophylls and carotenoids: Pigments of photosynthetic biomembranes. *Method Enzymol* **148**: 350-382

Lin JF, Wu SH (2004) Molecular events in senescing Arabidopsis leaves. *Plant J* **39**: 612-628

Liobikas J, Baniulis D, Stanys V, Toleikis A, Eriksson O (2006) Identification and analysis of a novel serine β -lactamase-like plant protein by a bioinformatic approach. *Biologija* **3**: 126–129

Lohman KN, Gan S, John MC, Amasino RM (1994) Molecular analysis of natural leaf senescence in Arabidopsis thaliana. *Physiol Plantarum* **92**: 322-328

Lopato S, Gattoni R, Fabini G, Stevenin J, Barta A (1999) A novel family of plant splicing factors with a Zn knuckle motif: examination of RNA binding and splicing activities. *Plant Mol Biol* **39**: 761-773

Lopes MS, Reynolds MP (2012) Stay-green in spring wheat can be determined by spectral reflectance measurements (normalized difference vegetation index) independently from phenology. *J Exp Bot* **63**: 3789-3798

Majeran W, Friso G, Asakura Y, Qu X, Huang M, Ponnala L, Watkins KP, Barkan A, van Wijk KJ (2012) Nucleoid-enriched proteomes in developing plastids and chloroplasts from maize leaves: a new conceptual framework for nucleoid functions. *Plant Physiol* **158**: 156-189

Makino A (2011) Photosynthesis, grain yield, and nitrogen utilization in rice and wheat. *Plant Physiol* **155**: 125-129

Marechal A, Parent JS, Veronneau-Lafortune F, Joyeux A, Lang BF, Brisson N (2009) Whirly proteins maintain plastid genome stability in Arabidopsis. *Proc Natl Acad Sci U S A* **106**: 14693-14698

Marrs KA (1996) The functions and regulation of glutathione s-transferases in plants. *Annu Rev Plant Physiol Plant Mol Biol* **47**: 127-158

Marschner H, Kirkby EA, Cakmak I (1996) Effect of mineral nutritional status on shoot-root partitioning of photoassimilates and cycling of mineral nutrients. *J Exp Bot* **47**: 1255-1263

- Martinez DE, Costa ML, Gomez FM, Otegui MS, Guiamet JJ** (2008) 'Senescence-associated vacuoles' are involved in the degradation of chloroplast proteins in tobacco leaves. *Plant J* **56**: 196-206
- Martinez M, Cambra I, Gonzalez-Melendi P, Santamaria ME, Diaz I** (2012) C1A cysteine-proteases and their inhibitors in plants. *Physiol Plant* **145**: 85-94
- Martínez M, Cambra I, González-Melendi P, Santamaría ME, Díaz I** (2012) C1A cysteine-proteases and their inhibitors in plants. *Physiol Plantarum* **145**: 85-94
- Masclaux-Daubresse C, Daniel-Vedele F, Dechorgnat J, Chardon F, Gaufichon L, Suzuki A** (2010) Nitrogen uptake, assimilation and remobilization in plants: challenges for sustainable and productive agriculture. *Ann Bot* **105**: 1141-1157
- Masclaux-Daubresse C, Reisdorf-Cren M, Orsel M** (2008) Leaf nitrogen remobilisation for plant development and grain filling. *Plant Biology* **10**: 23-36
- Matton D, Prescott G, Bertrand C, Camirand A, Brisson N** (1993) Identification of cis-acting elements involved in the regulation of the pathogenesis-related gene *STH-2* in potato. *Plant Mol Biol* **22**: 279-291
- Mayberry LK, Allen ML, Nitka KR, Campbell L, Murphy PA, Browning KS** (2011) Plant cap-binding complexes eukaryotic initiation factors eIF4F and eIFISO4F: molecular specificity of subunit binding. *J Biol Chem* **286**: 42566-42574
- Melonek J, Mulisch M, Schmitz-Linneweber C, Grabowski E, Hensel G, Krupinska K** (2010) Whirly1 in chloroplasts associates with intron containing RNAs and rarely co-localizes with nucleoids. *Planta* **232**: 471-481
- Miao Y, Jiang J, Ren Y, Zhao Z** (2013) The single-stranded DNA-binding protein WHIRLY1 represses WRKY53 expression and delays leaf senescence in a developmental stage-dependent manner in *Arabidopsis*. *Plant Physiol* **163**: 746-756

Miyake C (2010) Alternative Electron Flows (Water–Water Cycle and Cyclic Electron Flow Around PSI) in Photosynthesis: Molecular Mechanisms and Physiological Functions. *Plant Cell Physiol* **51**: 1951-1963

Mowla SB, Cuypers A, Driscoll SP, Kiddle G, Thomson J, Foyer CH, Theodoulou FL (2006) Yeast complementation reveals a role for an *Arabidopsis thaliana* late embryogenesis abundant (LEA)-like protein in oxidative stress tolerance. *Plant J* **48**: 743-756

Novitskaya L, Trevanion SJ, Driscoll S, Foyer CH, Noctor G (2002) How does photorespiration modulate leaf amino acid contents? A dual approach through modelling and metabolite analysis. *Plant Cell Environ* **25**: 821-835

Obata T, Fernie A (2012) The use of metabolomics to dissect plant responses to abiotic stresses. *Cell Mol Life Sci* **69**: 3225-3243

Olinares PD, Kim J, van Wijk KJ (2011) The Clp protease system; a central component of the chloroplast protease network. *Biochim Biophys Acta* **1807**: 999-1011

Otegui MS, Noh YS, Martinez DE, Vila Petroff MG, Staehelin LA, Amasino RM, Guiamet JJ (2005) Senescence-associated vacuoles with intense proteolytic activity develop in leaves of *Arabidopsis* and soybean. *Plant J* **41**: 831-844

Parent JS, Lepage E, Brisson N (2011) Divergent roles for the two Poll-like organelle DNA polymerases of *Arabidopsis*. *Plant Physiol* **156**: 254-262

Peng L, Fukao Y, Fujiwara M, Takami T, Shikanai T (2009) Efficient operation of NAD(P)H dehydrogenase requires supercomplex formation with photosystem I via minor LHCl in *Arabidopsis*. *Plant Cell* **21**: 3623-3640

Peng L, Shikanai T (2011) Supercomplex formation with photosystem I is required for the stabilization of the chloroplast NADH dehydrogenase-like complex in *Arabidopsis*. *Plant Physiol* **155**: 1629-1639

Peng M, Bi YM, Zhu T, Rothstein SJ (2007) Genome-wide analysis of Arabidopsis responsive transcriptome to nitrogen limitation and its regulation by the ubiquitin ligase gene NLA. *Plant Mol Biol* **65**: 775-797

Powikrowska M, Oetke S, Jensen PE, Krupinska K (2014) Dynamic composition, shaping and organization of plastid nucleoids. *Front Plant Sci* **5**: 424

Prikryl J, Watkins KP, Friso G, van Wijk KJ, Barkan A (2008) A member of the Whirly family is a multifunctional RNA- and DNA-binding protein that is essential for chloroplast biogenesis. *Nucleic Acids Res* **36**: 5152-5165

Prins A, van Heerden PD, Olmos E, Kunert KJ, Foyer CH (2008) Cysteine proteinases regulate chloroplast protein content and composition in tobacco leaves: a model for dynamic interactions with ribulose-1,5-bisphosphate carboxylase/oxygenase (Rubisco) vesicular bodies. *J Exp Bot* **59**: 1935-1950

Purwar S, Sundaram S, Verma P, Srivastava S, Kumar A (2012) A Physiologically Regulated Multidomain Cystatin of Wheat Shows Stage-Dependent Immunity Against Karnal Bunt (*Tilletia indica*). *Appl Biochem Biotechnol* **168**: 2344-2357

Quain MD, Makgopa ME, Marquez-Garcia B, Comadira G, Fernandez-Garcia N, Olmos E, Schnaubelt D, Kunert KJ, Foyer CH (2014) Ectopic phytocystatin expression leads to enhanced drought stress tolerance in soybean (*Glycine max*) and *Arabidopsis thaliana* through effects on strigolactone pathways and can also result in improved seed traits. *Plant Biotechnol J* **12**: 903-913

Queval G, Noctor G (2007) A plate reader method for the measurement of NAD, NADP, glutathione, and ascorbate in tissue extracts: Application to redox profiling during *Arabidopsis* rosette development. *Anal Biochem* **363**: 58-69

Rajjou L, Belghazi M, Huguet R, Robin C, Moreau A, Job C, Job D (2006) Proteomic Investigation of the Effect of Salicylic Acid on *Arabidopsis* Seed

Germination and Establishment of Early Defense Mechanisms. *Plant Physiol* **141**: 910-923

Reynolds MP, Pellegrineschi A, Skovmand B (2005) Sink-limitation to yield and biomass: a summary of some investigations in spring wheat. *Ann Appl Biol* **146**: 39-49

Roberts IN, Caputo C, Criado MV, Funk C (2012) Senescence-associated proteases in plants. *Physiol Plant* **145**: 130-139

Saier Jr MH, Beatty JT, Goffeau A, Harley KT, Heijne W, Huang S-C, Jack DL, Jahn P, Lew K, Liu J (1999) The major facilitator superfamily. *J Mol Microbiol Biotechnol* **1**: 257-279

Sakai A, Takano H, Kuroiwa T (2004) Organelle nuclei in higher plants: structure, composition, function, and evolution. *Int Rev Cytol* **238**: 59-118

Salleh FM, Evans K, Goodall B, Machin H, Mowla SB, Mur LA, Runions J, Theodoulou FL, Foyer CH, Rogers HJ (2012) A novel function for a redox-related LEA protein (SAG21/AtLEA5) in root development and biotic stress responses. *Plant Cell Environ* **35**: 418-429

Sandaña PA, Harcha CI, Calderini DF (2009) Sensitivity of yield and grain nitrogen concentration of wheat, lupin and pea to source reduction during grain filling. A comparative survey under high yielding conditions. *Field Crop Res* **114**: 233-243

Scheible WR, Morcuende R, Czechowski T, Fritz C, Osuna D, Palacios-Rojas N, Schindelasch D, Thimm O, Udvardi MK, Stitt M (2004) Genome-wide reprogramming of primary and secondary metabolism, protein synthesis, cellular growth processes, and the regulatory infrastructure of Arabidopsis in response to nitrogen. *Plant Physiol* **136**: 2483-2499

Schluter U, Colmsee C, Scholz U, Brautigam A, Weber AP, Zellerhoff N, Bucher M, Fahnenstich H, Sonnewald U (2013) Adaptation of maize source

leaf metabolism to stress related disturbances in carbon, nitrogen and phosphorus balance. *BMC Genomics* **14**: 442

Seki M, Narusaka M, Abe H, Kasuga M, Yamaguchi-Shinozaki K, Carninci P, Hayashizaki Y, Shinozaki K (2001) Monitoring the Expression Pattern of 1300 Arabidopsis Genes under Drought and Cold Stresses by Using a Full-Length cDNA Microarray. *Plant Cell* **13**: 61-72

Serrago RA, Miralles DJ (2014) Source limitations due to leaf rust (caused by *Puccinia triticina*) during grain filling in wheat. *Crop Pasture Sci* **65**: 185-193

Shakirova FM, Sakhabutdinova AR, Bezrukova MV, Fatkhutdinova RA, Fatkhutdinova DR (2003) Changes in the hormonal status of wheat seedlings induced by salicylic acid and salinity. *Plant Sci* **164**: 317-322

Shan X, Li C, Peng W, Gao B (2011) New perspective of jasmonate function in leaf senescence. *Plant Signal Behav* **6**: 575-577

Shinozaki K, Yamaguchi-Shinozaki K, Seki M (2003) Regulatory network of gene expression in the drought and cold stress responses. *Curr Opin Plant Biol* **6**: 410-417

Simova-Stoilova L, Demirevska K, Petrova T, Tsenov N, Feller U (2009) Antioxidative protection and proteolytic activity in tolerant and sensitive wheat (*Triticum aestivum* L.) varieties subjected to long-term field drought. *J Plant Growth Regul* **58**: 107-117

Stieger P, Feller U (1994) Nutrient accumulation and translocation in maturing wheat plants grown on waterlogged soil. *Plant Soil* **160**: 87-95

Subramaniam R, Despres C, Brisson N (1997) A functional homolog of mammalian protein kinase C participates in the elicitor-induced defense response in potato. *Plant Cell* **9**: 653-664

Tang W, Ji Q, Huang Y, Jiang Z, Bao M, Wang H, Lin R (2013) FAR-RED ELONGATED HYPOCOTYL3 and FAR-RED IMPAIRED RESPONSE1

transcription factors integrate light and abscisic acid signaling in Arabidopsis. *Plant Physiol* **163**: 857-866

Thoenen M, Herrmann B, Feller U (2007) Senescence in wheat leaves: is a cysteine endopeptidase involved in the degradation of the large subunit of Rubisco? *Acta Physiol Plant* **29**: 339-350

Thomas H, Howarth CJ (2000) Five ways to stay green. *J Exp Bot* **51 Spec No**: 329-337

Thomas H, Ougham H (2014) The stay-green trait. *J Exp Bot* **65**: 3889-3900

Trappe R, Buddenberg P, Uedelhoven J, Gläser B, Buck A, Engel W, Burfeind P (2002) The murine BTB/POZ zinc finger gene Znf131: predominant expression in the developing central nervous system, in adult brain, testis, and thymus. *Biochem bioph res co* **296**: 319-327

Tschoep H, Gibon Y, Carillo P, Armengaud P, Szecowka M, NUNES-NESI A, Fernie AR, Koehl K, Stitt M (2009) Adjustment of growth and central metabolism to a mild but sustained nitrogen-limitation in Arabidopsis. *Plant Cell environ* **32**: 300-318

Urbanczyk-Wochniak E, Fernie AR (2005) Metabolic profiling reveals altered nitrogen nutrient regimes have diverse effects on the metabolism of hydroponically-grown tomato (*Solanum lycopersicum*) plants. *J Exp Bot* **56**: 309-321

Van der Vyver C, Schneiderei J, Driscoll S, Turner J, Kunert K, Foyer CH (2003) Oryzacystatin I expression in transformed tobacco produces a conditional growth phenotype and enhances chilling tolerance. *Plant Biotechnol J* **1**: 101-112

van Doorn WG (2008) Is the onset of senescence in leaf cells of intact plants due to low or high sugar levels? *J Exp Bot* **59**: 1963-1972

van Doorn WG, Beers EP, Dangl JL, Franklin-Tong VE, Gallois P, Hara-Nishimura I, Jones AM, Kawai-Yamada M, Lam E, Mundy J, Mur LA,

- Petersen M, Smertenko A, Taliansky M, Van Breusegem F, Wolpert T, Woltering E, Zhivotovsky B, Bozhkov PV** (2011) Morphological classification of plant cell deaths. *Cell Death Differ* **18**: 1241-1246
- van Loon LC, Pierpoint WS, Boller T, Conejero V** (1994) Recommendations for naming plant pathogenesis-related proteins. *Plant Mol Biol Rep* **12**: 245-264
- Vidi PA, Kanwischer M, Baginsky S, Austin JR, Csucs G, Dormann P, Kessler F, Brehelin C** (2006) Tocopherol cyclase (VTE1) localization and vitamin E accumulation in chloroplast plastoglobule lipoprotein particles. *J Biol Chem* **281**: 11225-11234
- Wall MK, Mitchenall LA, Maxwell A** (2004) Arabidopsis thaliana DNA gyrase is targeted to chloroplasts and mitochondria. *Proc Natl Acad Sci U S A* **101**: 7821-7826
- Walters RG, Shephard F, Rogers JJ, Rolfe SA, Horton P** (2003) Identification of mutants of Arabidopsis defective in acclimation of photosynthesis to the light environment. *Plant Physiol* **131**: 472-481
- Waltner JK, Peterson FC, Lytle BL, Volkman BF** (2005) Structure of the B3 domain from Arabidopsis thaliana protein At1g16640. *Protein Sci* **14**: 2478-2483
- Wang R, Guegler K, LaBrie ST, Crawford NM** (2000) Genomic analysis of a nutrient response in Arabidopsis reveals diverse expression patterns and novel metabolic and potential regulatory genes induced by nitrate. *Plant Cell* **12**: 1491-1509
- Wang R, Okamoto M, Xing X, Crawford NM** (2003) Microarray analysis of the nitrate response in Arabidopsis roots and shoots reveals over 1,000 rapidly responding genes and new linkages to glucose, trehalose-6-phosphate, iron, and sulfate metabolism. *Plant Physiol* **132**: 556-567

Wang R, Tischner R, Gutierrez RA, Hoffman M, Xing X, Chen M, Coruzzi G, Crawford NM (2004) Genomic analysis of the nitrate response using a nitrate reductase-null mutant of Arabidopsis. *Plant Physiol* **136**: 2512-2522

Wang S, Blumwald E (2014) Stress-induced chloroplast degradation in Arabidopsis is regulated via a process independent of autophagy and senescence-associated vacuoles. *Plant Cell* **26**: 4875-4888

Watanabe M, Balazadeh S, Tohge T, Erban A, Giavalisco P, Kopka J, Mueller-Roeber B, Fernie AR, Hoefgen R (2013) Comprehensive dissection of spatiotemporal metabolic shifts in primary, secondary, and lipid metabolism during developmental senescence in Arabidopsis. *Plant Physiol* **162**: 1290-1310

Weaver LM, Gan S, Quirino B, Amasino RM (1998) A comparison of the expression patterns of several senescence-associated genes in response to stress and hormone treatment. *Plant Mol Biol* **37**: 455-469

Weeda SM, Mohan Kumar GN, Richard Knowles N (2009) Developmentally linked changes in proteases and protease inhibitors suggest a role for potato multicystatin in regulating protein content of potato tubers. *Planta* **230**: 73-84

Winfield MO, Lu C, Wilson ID, Coghill JA, Edwards KJ (2009) Cold- and light-induced changes in the transcriptome of wheat leading to phase transition from vegetative to reproductive growth. *BMC Plant Biol* **9**: 55-55

Wingler A, Lea PJ, Quick WP, Leegood RC (2000) Photorespiration: metabolic pathways and their role in stress protection. *Philos Trans R Soc Lond B Biol Sci* **355**: 1517-1529

Wingler A, Purdy S, MacLean JA, Pourtau N (2006) The role of sugars in integrating environmental signals during the regulation of leaf senescence. *J Exp Bot* **57**: 391-399

Wingler A, Quick WP, Bungard RA, Bailey KJ, Lea PJ, Leegood RC (1999) The role of photorespiration during drought stress: an analysis utilizing barley

mutants with reduced activities of photorespiratory enzymes. *Plant Cell Environ* **22**: 361-373

Witcombe JR, Hollington PA, Howarth CJ, Reader S, Steele KA (2008) Breeding for abiotic stresses for sustainable agriculture. *Philos Trans R Soc Lond B Biol Sci* **363**: 703-716

Wrzaczek M, Brosche M, Salojarvi J, Kangasjarvi S, Idanheimo N, Mersmann S, Robatzek S, Karpinski S, Karpinska B, Kangasjarvi J (2010) Transcriptional regulation of the CRK/DUF26 group of receptor-like protein kinases by ozone and plant hormones in *Arabidopsis*. *BMC Plant Biol* **10**: 95

Xiao Y, Savchenko T, Baidoo EE, Chehab WE, Hayden DM, Tolstikov V, Corwin JA, Kliebenstein DJ, Keasling JD, Dehesh K (2012) Retrograde signaling by the plastidial metabolite MEcPP regulates expression of nuclear stress-response genes. *Cell* **149**: 1525-1535

Xiong JY, Lai CX, Qu Z, Yang XY, Qin XH, Liu GQ (2009) Recruitment of AtWHY1 and AtWHY3 by a distal element upstream of the kinesin gene AtKP1 to mediate transcriptional repression. *Plant Mol Biol* **71**: 437-449

Yamaguchi-Shinozaki K, Shinozaki K (2005) Organization of cis-acting regulatory elements in osmotic- and cold-stress-responsive promoters. *Trends Plant Sci* **10**: 88-94

Yang XY, Chen ZW, Xu T, Qu Z, Pan XD, Qin XH, Ren DT, Liu GQ (2011) *Arabidopsis* kinesin KP1 specifically interacts with VDACC3, a mitochondrial protein, and regulates respiration during seed germination at low temperature. *Plant Cell* **23**: 1093-1106

Yao X, Xiong W, Ye T, Wu Y (2012) Overexpression of the aspartic protease ASPG1 gene confers drought avoidance in *Arabidopsis*. *J Exp Bot* **63**: 2579-2593

Yoo HH, Kwon C, Lee MM, Chung IK (2007) Single-stranded DNA binding factor AtWHY1 modulates telomere length homeostasis in Arabidopsis. *Plant J* **49**: 442-451

Zampini E, Lepage E, Tremblay-Belzile S, Truche S, Brisson N (2015) Organelle DNA rearrangement mapping reveals U-turn-like inversions as a major source of genomic instability in Arabidopsis and humans. *Genome Res* **25**: 645-654

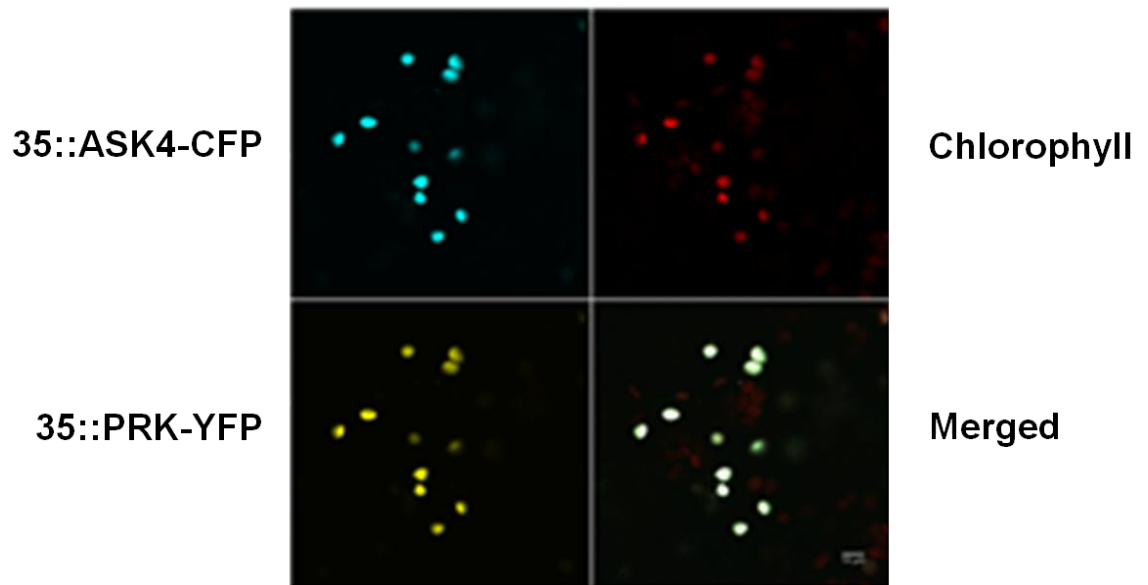
Zapata JM, Guera A, Esteban-Carrasco A, Martin M, Sabater B (2005) Chloroplasts regulate leaf senescence: delayed senescence in transgenic *ndhF*-defective tobacco. *Cell Death Differ* **12**: 1277-1284

Zhang X, Liu S, Takano T (2008) Two cysteine proteinase inhibitors from Arabidopsis thaliana, AtCYSa and AtCYSb, increasing the salt, drought, oxidation and cold tolerance. *Plant Mol Biol* **68**: 131-143

Zhao Y, Botella MA, Subramanian L, Niu X, Nielsen SS, Bressan RA, Hasegawa PM (1996) Two wound-inducible soybean cysteine proteinase inhibitors have greater insect digestive proteinase inhibitory activities than a constitutive homolog. *Plant Physiol* **111**: 1299-1306

Appendix

Appendix I. Chloroplast localization of the 35S::PRK-YFP plasmid in transiently transformed tobacco leaves.



Appendix II. Barley transcripts homologous to plastid encoded genes in Arabidopsis that exhibit significant differences in abundance in WT and W1-7 seedlings

Accession ^a	Transcript abundance RNAi- W1-7/WT ^b	Top Arabidopsis match ^c	Arabidopsis gene description ^d
MLOC 24854.1	8.59	AtCg01050	NDHD, NADH-Ubiquinone/plastoquinone (complex I) protein
MLOC 24746.1	4.76	AtCg00190	RPOB, RNA polymerase subunit β
MLOC 1704.1	4.74	AtCg00190	RPOB, RNA polymerase subunit β
MLOC 54708.1	4.56	AtCg00170	RPOC2, RNA polymerase family protein
MLOC 24776.1	3.96	AtCg01040	YCF5, Cyt C assembly protein
MLOC 9149.1	3.24	AtCg01010	NDHF, NADH-Ubiquinone oxidoreductase (complex I), chain 5 protein
MLOC 9313.1	3.09	AtCg00040	MATK, Maturase K
MLOC 25280.1	3.047	AtCg01010	NDHF, NADH-Ubiquinone oxidoreductase (complex I), chain 5 protein
MLOC 61567.1	2.92	AtCg01010	NDHF, NADH-Ubiquinone oxidoreductase (complex I), chain 5 protein
MLOC 456.1	2.87	AtCg00170	RPOC2, RNA polymerase family protein
MLOC 32552.1	2.87	AtCg01300	RPL23.2, Ribosomal protein L23
MLOC 34251.1	2.81	AtCg01050	NDHD, NADH-Ubiquinone/plastoquinone (complex I) protein
MLOC 24733.1	2.81	AtCg00180	RPOC1, RNA polymerase family protein
MLOC 24753.1	2.78	AtCg01050	NDHD, NADH-Ubiquinone/plastoquinone (complex I) protein
MLOC24802.1	2.63	AtCg00040	MATK, Maturase K

MLOC 36249.1	2.62	AtCg01050	NDHD, NADH-Ubiquinone/plastoquinone (complex I) protein
MLOC 26369.1	2.61	AtCg01250	NDHB.2, NADH-Ubiquinone/plastoquinone (complex I) protein
MLOC 63387.1	2.58	AtCg01110	NDHH, NAD(P)H dehydrogenase subunit H
MLOC 9538.1	2.53	AtCg00180	RPOC1, RNA polymerase family protein
MLOC 34273.1	2.47	AtCg00040	MATK, Maturase K
MLOC 8394.1	2.47	AtCg00360	YCF3, Tetratricopeptide repeat (TPR)-like superfamily protein
MLOC 33340.1	2.40	AtCg01250	NDHB.2, NADH-Ubiquinone/plastoquinone (complex I) protein
MLOC 365.2	2.34	AtCg01250	NDHB.2, NADH-Ubiquinone/plastoquinone (complex I) protein
MLOC 77504.1	2.23	AtCg01250	NDHB.2, NADH-Ubiquinone/plastoquinone (complex I) protein
MLOC 6335.1	2.16	AtCg00590	ORF31, Electron carriers
MLOC 36200.1	2.11	AtCg00730	PETD, Photosynthetic electron transfer D
MLOC 36158.1	2.11	AtCg00590	ORF31, Electron carriers
MLOC 9573.1	2.10	AtCg00170	RPOC2, RNA polymerase family protein
MLOC 2607.1	2.06	AtCg00570	PSBF, Photosystem II reaction centre protein F
MLOC 24780.1	2.03	AtCg00730	PETD, Photosynthetic electron transfer D
MLOC 24745.1	2.02	AtCg00660	RPL20, Ribosomal protein L20
MLOC 9018.1	2.00	AtCg00640	RPL33, Ribosomal protein L33
MLOC 8945.1	1.95	AtCg00420	NDHJ, NADH dehydrogenase subunit J
MLOC 7873.1	1.95	AtCg01090	NDHI, Subunit of the chloroplast NAD(P)H dehydrogenase complex
MLOC 9520.1	1.93	AtCg00470	ATPE, ATP synthase σ chain
MLOC 3829.1	1.93	AtCg00530	YCF10

MLOC 8957.1	1.91	AtCg00420	NDHJ, NADH dehydrogenase subunit J
MLOC 9641.1	1.90	AtCg00530	YCF10
MLOC 36232.1	1.88	AtCg00160	RPS2, Ribosomal protein S2
MLOC 9681.1	1.87	AtCg00530	YCF10
MLOC 61555.1	1.86	AtCg01080	NDHG, NADH-Ubiquinone/plastoquinone oxidoreductase, chain 6
MLOC 8426.1	1.85	AtCg00530	YCF10
MLOC 12189.1	1.82	AtCg00420	NDHJ, NADH dehydrogenase subunit J
MLOC 65510.1	1.82	AtCg01090	NDHI, Subunit of the chloroplast NAD(P)H dehydrogenase complex
MLOC 24811.1	1.78	AtCg00420	NDHJ, NADH dehydrogenase subunit J
MLOC 41067.1	1.77	AtCg00630	PSAJ, PSI subunit J
MLOC 68023.1	1.76	AtCg00530	YCF10
MLOC 34111.1	1.75	AtCg00540	PETA, Photosynthetic electron transfer A
MLOC 9478.1	1.69	AtCg00160	RPS2, Ribosomal protein S2
MLOC 61315	1.68	AtCg00480	ATPB, ATP synthase subunit α
MLOC 9572.1	1.64	AtCg01100	NDHA, NADH dehydrogenase family protein
MLOC 59993.1	1.59	AtCg00440	NDHC, NADH dehydrogenase D3 subunit
MLOC 63096.1	1.31	AtCg00680	PSBB, PSII reaction centre protein B
MLOC 9455.1	1.30	AtCg00680	PSBB, PSII reaction centre protein B
MLOC 9691.1	1.22	AtCg00550	PSBJ, PSII reaction centre protein J
MLOC 24726.1	0.61	AtCg01060	PSAC, PsaC subunit of PSI
MLOC 9445.1	0.45	AtCg01110	NDHH, NAD(P)H dehydrogenase subunit H


a Barley gene model primary accession number (The International Barley Genome Sequencing Consortium, 2012).

b Transcript abundance in RNAi-W1-7 seedlings relative to transcript abundance in WT seedlings.

c TAIR accession of top Arabidopsis match based on BLAST e-value.

d TAIR annotation of Arabidopsis gene.

Appendix III. Transcripts significantly altered in abundance in response to N deficiency in wild type barley leaves.

	FUNCTIONAL CATEGORY	ACCESSION	DESCRIPTION	-5  5	LOG FC	
Photosynthesis	Photosynthesis	ak363486	APE1 (ACCLIMATION OF PHOTOSYNTHESIS TO ENVIRONMENT)		2.97	
		ak354522	PSBR (photosystem II subunit R)		-1.18	
		mloc_945	LHB1B2; chlorophyll binding		-2.99	
		ak370975	LHB1B2; chlorophyll binding		-4.74	
		mloc_58758	LHB1B2; chlorophyll binding		-5.53	
		mloc_78528	LHB1B2; chlorophyll binding		-5.73	
Hormones	ABA	ak360249	Abscisic-aldehyde oxidase		-1.00	
	Auxin	mloc_53867.1	Auxin efflux carrier component 5		-1.38	
		ak363815	Auxin-responsive protein-related		-5.26	
		ak376866	Auxin-responsive SAUR gene family protein		-2.26	
		mloc_21495.1	Auxin-responsive SAUR gene family protein		4.00	
		mloc_38622.3	Unknown protein		1.05	
		mloc_58443.1	Growth regulator protein		1.39	
		mloc_58799.1	Auxin-responsive protein		1.43	
		mloc_65368.1	Auxin-responsive SAUR gene family member		2.07	
		mloc_9883.3	Auxin-independent growth promoter		-3.28	
	Brassinosteroid	mloc_75615.1	SMT2 (STEROL METHYLTRANSFERASE 2)		2.10	
		mloc_79130.1	Cycloartenol synthase		-3.34	
	Ethylene	mloc_1557.1	Gibberellin 2-beta-dioxygenase 7		-3.06	
		mloc_55123.1	flavonol synthase/flavanone 3-hydroxylase		1.36	
	Jasmonate	mloc_59596.1	flavonol synthase/flavanone 3-hydroxylase		2.69	
mloc_61817.2		Lipoxygenase A		2.47		
mloc_21933.2		Cytochrome P450 74A2		-5.31		
	mloc_71784.1	12-oxophytodienoate reductase 2		2.48		
Stress	Biotic	mloc_56904.1	NBS-LRR disease resistance protein		1.84	
		ak252675.1	Leaf-specific thionin DB4 precursor		-5.91	
		ak367511	NBS-LRR disease resistance protein		1.76	
		mloc_20651.1	NBS-LRR disease resistance protein		2.91	
		ak360496	RPM1 (RESISTANCE TO P. SYRINGAE PV MACULICOLA 1)		1.26	
		mloc_12509.1	NBS-LRR disease resistance protein		2.83	
		ak369539	RPM1 (RESISTANCE TO P. SYRINGAE PV MACULICOLA 1)		1.30	
		mloc_76181.1	LCR69 precursor		2.32	
		mloc_10643.2	NBS-LRR disease resistance protein		1.49	
		mloc_12508.2	NBS-LRR disease resistance protein		3.45	
		ak370783	Endochitinase A precursor		-1.03	
		mloc_53432.1	Dirigent-like protein pDIR17		1.72	
		ak360510	NBS-LRR disease resistance protein		5.57	
		ak357884	Thionin precursor		-5.75	
		ak354849	Cleavage and polyadenylation specificity factor 5		1.31	
		ak365151	NBS-LRR disease resistance protein		-1.46	
		mloc_45134.1	Tobamovirus multiplication 3		1.09	
		ak251469.1	Loricrin-related protein		-1.39	
		mloc_30800.1	Adenylate kinase isoenzyme 6		1.03	
		Heat	mloc_11286.1	Heat shock factor		3.66
			ak353723	ARC6 (ACCUMULATION AND REPLICATION OF CHLOROPLASTS 6)		2.33
			ak362103	DNAJ heat shock protein		2.39
			mloc_15242.1	Heat shock 70 kDa protein, mitochondrial precursor		1.56
			ak355146	17.6 KDA CLASS II HEAT SHOCK PROTEIN		-1.61
			mloc_55999.1	Luminal-binding protein 3 precursor		1.08
			ak360584	Endoplasmin homolog precursor		1.73
		Cold	ak361801	CSDP1 (cold shock domain protein 1)		1.04
mloc_65405.2	ERD4 protein			2.56		
Drought	ak355456	Retrotransposon protein		-1.92		
Wound	Other	mloc_7319.1	Ozone-responsive stress-related protein		2.20	
		mloc_50963.2	Pollen Ole e 1 allergen and extensin family protein		-1.55	
		mloc_69539.4	Ethylene-responsive protein		-1.56	
Transport	Sugars	mloc_51073.3	Phospholipid-transporting ATPase 12		1.32	
		mloc_57236.1	STP1; Sugar transport protein 1		2.40	
		ak361677	MSS1; Carbohydrate transmembrane transporter		2.63	
		ak369803	MSS2; Carbohydrate transmembrane transporter		3.54	
		ak354614	Hexose carrier protein HEX6		2.56	
		ak361403	Metabolite transport protein csbC		2.48	
		mloc_51792.3	Transporter-related		1.63	
		mloc_66307.1	Monosaccharide transporter		5.56	
		ak355981	Transporter-related		1.51	

FUNCTIONAL CATEGORY	ACCESSION	DESCRIPTION	-5	5	LOG FC	
Transport	Amino acid	ak359096	STP1; Sugar transport protein 1		1.67	
		mloc_16705.3	LHT1; amino acid transmembrane transporter		1.63	
		ak252705.1	AAP3; amino acid transmembrane transporter		3.84	
		mloc_73950.1	BAT1 (BIDIRECTIONAL AMINO ACID TRANSPORTER 1)		1.12	
		mloc_51108.1	CAT9 (CATIONIC AMINO ACID TRANSPORTER 9)		1.07	
		ak369769	AAP1 (AMINO ACID PERMEASE 1)		7.18	
		mloc_20163.2	Amino acid permease		-1.64	
		mloc_40001.1	Amino acid transporter family protein		-2.22	
	Ammonium	ak248644.1	Ammonium transporter 1		-2.74	
		ak252569.1	Ammonium transporter 2		4.93	
	Phosphate	ak358394	Inorganic phosphate transporter 1-5		2.02	
	Envelope membrane	ak358695	Glucose-6-phosphate/phosphate translocator-related		1.23	
	Mitochondrial membrane	ak357275	SAMC1 (S-ADENOSYLMETHIONINE CARRIER 1)		2.05	
		mloc_53924.1	Mitochondrial phosphate transporter		1.82	
	NDP-sugars at the ER	mloc_72730.1	UDP-galactose transporter-related		3.16	
	Metal	mloc_16333.1	ZIP6; cation transmembrane transporter		1.08	
		mloc_60720.1	ZIP5; cation transmembrane transporter		1.70	
		mloc_71993.1	ZIP11; cation transmembrane transporter		2.26	
	Peptides and oligopeptides	mloc_61170.4	YSL3 (YELLOW STRIPE LIKE 3)		1.22	
		mloc_66939.1	Proton-dependent oligopeptide transport (POT) family protein		-4.87	
		ak359923	PTR3 (PEPTIDE TRANSPORTER 3)		2.75	
	Cations	mloc_10854.2	Bile acid sodium symporter/ transporter protein		1.18	
		mloc_21938.1	Urea active transporter protein		2.51	
		mloc_58742.2	Cation transporter HKT7		3.46	
	ABC	mloc_57925.2	Multidrug resistance protein 4		2.24	
		mloc_75332.6	ATATH6; ATPase		1.52	
		mloc_9877.1	Pleiotropic drug resistance protein 4		1.04	
		ak366518	Carbohydrate transporter		-1.97	
		mloc_73133.1	Pleiotropic drug resistance protein 4		4.80	
		mloc_58493.2	ATATH6; ATPase		1.19	
	ANIONS	ak356986	Chloride channel protein		-3.38	
	Channels	ak366449	Cyclic nucleotide-gated ion channel 1		1.08	
	Miscellaneous	mloc_76072.2	Synaptic vesicle 2-related protein		-2.56	
		ak357414	carbohydrate transporter		1.66	
		mloc_22248.7	secretory carrier membrane protein (SCAMP) family protein		1.18	
	Signalling	Sugars	ak360490	glutamate receptor		4.46
			mloc_39963	glutamate receptor		4.30
			ak369617	glutamate receptor		2.75
			ak367236	glutamate receptor		1.74
		Calcium	mloc_36714.1	calmodulin-binding protein		3.78
			mloc_38109.1	ACA9 (AUTOINHIBITED CA(2+)-ATPASE 9)		3.37
			ak370044	EF hand family protein		3.01
			ak368448	calcium-binding protein		2.82
			mloc_61579.1	calcium-binding EF hand family protein		2.49
			ak367231	CAST calcium-binding protein		1.97
			ak372866	CPK16 (calmodulin-domain protein kinase 16)		1.57
			mloc_66071.3	calmodulin-binding protein		1.53
		ak366527	CPK5 (calmodulin-domain protein kinase 5)		1.36	
		ak376591	polcalcicn		1.31	
		ak360154	CPK7 (calmodulin-domain protein kinase 7)		1.17	
		mloc_15522.2	calcium ion binding protein		1.14	
		ak363848	calcium-binding EF hand family protein		-2.27	
		ak376271	calcium-binding EF hand family protein		-3.00	
Phosphinositides		ak372605	ATPLC2 (PHOSPHOLIPASE C 2)		1.33	
G protein		mloc_64738.1	ERG GTP-binding protein		1.75	
		ak368106	transducin family protein		1.65	
		mloc_61580.2	ROP9 (RHO-RELATED PROTEIN FROM PLANTS 9)		1.64	
		mloc_530.1	ERG GTP-binding protein		1.55	
		ak248783.1	AtRABA4a (Rab GTPase homolog A4a)		1.05	
Leucine kinase		ak354430	RLK902 protein receptor kinase		1.98	
		mloc_12619.1	RPK1_IPONI Receptor-like protein kinase precursor		1.17	
		mloc_56710.3	receptor-like protein kinase 5 precursor		2.64	
		ak370749	RPK1_IPONI Receptor-like protein kinase precursor		2.63	
		mloc_60385.1	RPK1_IPONI Receptor-like protein kinase precursor		1.32	
		ak367109	receptor-like protein kinase 5 precursor		3.44	

FUNCTIONAL CATEGORY	ACCESSION	DESCRIPTION	-5	5	LOG FC
DUF26 kinase	ak248596.1	RPK1_IPONI Receptor-like protein kinase precursor			3.53
	mloc_64475.1	RPK1_IPONI Receptor-like protein kinase precursor			3.99
	ak355931	receptor-like protein kinase precursor			1.71
	mloc_12762.1	RPK1_IPONI Receptor-like protein kinase precursor			1.38
	mloc_19405.1	brassinosteroid insensitive 1-associated receptor kinase 1 precursor			1.22
	mloc_12807.2	RPK1_IPONI Receptor-like protein kinase precursor			1.02
	mloc_70200.1	RPK1_IPONI Receptor-like protein kinase precursor			2.99
	ak374633	S-locus lectin protein kinase family protein			1.01
	mloc_23445.1	NBS-LRR disease resistance protein			1.14
	ak362486	lectin protein kinase			1.16
	mloc_64218.2	protein kinase family protein			1.24
	mloc_56446.6	ATP binding protein			1.24
	ak365850	serine/threonine protein kinase			1.28
	mloc_5745.4	protein kinase family protein			1.29
	ak371972	ARK3 (A. THALIANA RECEPTOR KINASE 3)			1.37
	mloc_5530.2	S-locus lectin protein kinase family protein			1.45
	ak362417	leucine-rich repeat family protein			1.54
	ak364424	leucine-rich repeat family protein			1.55
	mloc_56554.1	protein kinase family protein			1.55
	ak374914	CRK10 (CYSTEINE-RICH RLK10)			1.83
	ak355364	lectin protein kinase			1.84
	mloc_63888.1	receptor-like protein kinase homolog RK20-1			1.91
	mloc_13564.2	S-locus lectin protein kinase family protein			1.93
	ak357681	CRK10 (CYSTEINE-RICH RLK10)			1.98
	ak367087	CRK10 (CYSTEINE-RICH RLK10)			2.06
	mloc_21679.1	S-locus lectin protein kinase family protein			2.23
	mloc_39471.1	B120; ATP binding			2.25
	ak360116	protein kinase family protein			2.25
	mloc_68993.1	S-locus lectin protein kinase family protein			2.26
	mloc_60803.1	B120; ATP binding			2.33
	mloc_14359.1	B120; ATP binding			2.43
	mloc_64164.1	lectin protein kinase			2.48
	ak363955	protein TAK14			2.59
	ak354150	lectin protein kinase family protein			2.60
	mloc_13320.1	S-locus lectin protein kinase family protein			2.63
	mloc_40180.1	serine/threonine protein kinase			2.69
	ak366027	serine/threonine protein kinase			3.05
	mloc_29026.1	S-locus lectin protein kinase family protein			3.33
	mloc_66502.1	lectin protein kinase			3.38
	mloc_15040.1	lectin protein kinase			3.48
	mloc_64775.1	protein kinase family protein			4.11
	ak355239	lectin protein kinase			4.15
	ak361438	lectin protein kinase			4.17
	ak360069	S-locus lectin protein kinase family protein			4.25
	ak252462.1	SD2-5 (S-DOMAIN-2 5); carbohydrate binding			4.44
mloc_22093.1	legume lectin family protein			4.62	
ak369396	ARK3 (A. THALIANA RECEPTOR KINASE 3)			4.69	
mloc_55684.2	protein kinase family protein			5.25	
ak364020	receptor-like protein kinase			5.27	
mloc_58954.2	protein kinase			5.69	
S-locus glycoprotein like kinase	mloc_19071.1	S-locus lectin protein kinase family protein			3.69
	mloc_37963.1	ARK3 (A. THALIANA RECEPTOR KINASE 3)			1.80
	mloc_13320.1	S-locus lectin protein kinase family protein			2.63
	ak371972	ARK3 (A. THALIANA RECEPTOR KINASE 3)			1.37
	ak360069	S-locus lectin protein kinase family protein			4.25
Wall associated kinase	ak369396	ARK3 (A. THALIANA RECEPTOR KINASE 3)			4.69
	ak374633	S-locus lectin protein kinase family protein			1.01
	mloc_59786.2	WAK5 (WALL ASSOCIATED KINASE 5)			1.45
	ak354694	WAK5 (WALL ASSOCIATED KINASE 5)			6.15
	ak364262	WAK2 (WALL ASSOCIATED KINASE 2)			-1.66
	mloc_44440.1	WAK receptor-like protein kinase			2.82
	mloc_488.1	WAK receptor-like protein kinase			4.85
	mloc_63265.1	WAK5 (WALL ASSOCIATED KINASE 5)			2.00
	mloc_45581.1	WAK receptor-like protein kinase			5.19
	ak252312.1	WAK3 (wall associated kinase 3)			5.05

FUNCTIONAL CATEGORY	ACCESSION	DESCRIPTION	-5	5	LOG FC
Signalling	Miscellaneous	mloc_65440.2	WAK2 (WALL ASSOCIATED KINASE 2)		1.53
		ak362513	WAK2 (WALL ASSOCIATED KINASE 2)		6.24
		mloc_55615.4	WAK2 (WALL ASSOCIATED KINASE 2)		1.71
		ak360724	WAK5 (WALL ASSOCIATED KINASE 5)		1.41
		mloc_58234.1	wall-associated kinase		2.65
		mloc_26478.1	WAK receptor-like protein kinase		2.49
		mloc_39549.1	WAK3 (wall associated kinase 3)		5.48
		mloc_73855.1	WAK2 (WALL ASSOCIATED KINASE 2)		5.19
		mloc_40282.1	OsWAK receptor-like protein kinase		5.53
		mloc_22093.1	ATP binding protein		4.62
		ak369666	light repressible receptor protein kinase		3.89
		mloc_44415.3	receptor-like protein kinase		3.02
		mloc_7907.1	senescence-induced receptor-like ser/thr-protein kinase precursor		2.71
		ak368497	senescence-induced receptor-like ser/thr-protein kinase precursor		2.70
		mloc_58234.1	OsWAK receptor-like protein kinase		2.65
		ak369415	senescence-induced receptor-like ser/thr-protein kinase precursor		2.58
RNA	Processing	mloc_79750.1	ribosomal RNA adenine dimethylase family protein		2.59
		ak362230	polyribonucleotide nucleotidyltransferase		2.30
		ak355680	ATP-dependent RNA helicase		1.15
		ak252056.1	DEAD box RNA helicase		1.61
		mloc_33219.1	RNS1 (RIBONUCLEASE 1)		-2.53
		ak355627	exosome complex exonuclease RRP43		1.61
		mloc_79172.1	Pathogenesis-related protein 1 (AOPR1)		-1.25
		mloc_11500.1	rpp14 family protein		1.32
		mloc_6117.2	ribonuclease P family protein		1.00
		mloc_38205.5	CAF1 family ribonuclease		1.38
	Transcription	mloc_44151.2	DNA-directed RNA polymerase		1.75
		ak365017	RNA polymerase III subunit RPC82 family protein		1.18
		mloc_65625.1	RDR1 (RNA-DEPENDENT RNA POLYMERASE 1)		2.33
		mloc_49910.1	DNA-directed RNA polymerase		1.94
		mloc_24746.1	RNA polymerase beta chain		2.03
		mloc_60339.1	RNA polymerase beta chain		1.48
		ak375542	RNA polymerase I polypeptide 2,		1.96
		mloc_38307.2	PTAC6 (PLASTID TRANSCRIPTIONALLY ACTIVE6)		2.05
		mloc_45039.1	RAV2 (regulator of the atpase of the vacuolar membrane)		1.34
		mloc_68143.1	AL4 (ALFIN-LIKE 4)		1.23
	Regulation of transcription	ak371941	RAV2 (regulator of the atpase of the vacuolar membrane)		3.92
		ak364562	AP2 domain-containing transcription factor family protein		2.38
		mloc_45039.1	RAV2 (regulator of the atpase of the vacuolar membrane)		1.34
		mloc_7325.1	AP2 domain transcription factor		-2.24
		mloc_55768.1	beta HLH protein 93		-1.11
		mloc_43080.2	helix-loop-helix DNA-binding domain containing protein		-3.45
		mloc_43888.2	basic helix-loop-helix (bHLH) family protein		-1.09
		mloc_11223.12	transcription factor		1.44
		ak248746.1	helix-loop-helix DNA-binding domain containing protein		-2.55
		mloc_70258.1	basic helix-loop-helix (bHLH) family protein		2.22
		mloc_3763.3	STH2 (SALT TOLERANCE HOMOLOG2)		-2.53
		mloc_54725.2	OBP3 (OBF-BINDING PROTEIN 3)		1.53
		mloc_56963.2	GATA zinc finger family protein		2.45
		mloc_51405.1	AZF2 (ARABIDOPSIS ZINC-FINGER PROTEIN 2)		3.41
		mloc_37929.1	MYB-like DNA-binding domain		2.32
		ak375760	MYB family transcription factor		-3.14
		ak367226	Chitin-inducible gibberellin-responsive protein 2		2.34
		mloc_69561.1	SCARECROW-like protein		1.81
		mloc_11286.1	Heat shock factor		3.66
		mloc_38850.2	MADS-box transcription factor 29		2.38
		mloc_75842.1	Auxin-responsive Aux/IAA gene family member		1.02
		mloc_15957.1	Auxin response factor 23		2.02
		mloc_71395.2	DNA binding		1.65
		ak374788	Transferase, transferring glycosyl groups		-2.28
		mloc_69611.1	Transcription factor jumonji (jmj) family protein		1.74
		ak368188	DNA-binding family protein		1.57
mloc_34067.1	DNA-binding protein		1.09		
ak375301	Pentatricopeptide (PPR) repeat-containing protein		1.63		
mloc_433.1	PCNA1 (PROLIFERATING CELLULAR NUCLEAR ANTIGEN)		1.44		

FUNCTIONAL CATEGORY	ACCESSION	DESCRIPTION	-5	5	LOG FC	
RNA	MYB	mloc_37806.3	SET domain containing protein		2.44	
		ak367793	Multivesicular body protein 5		1.11	
		ak358161	RAX2 (REGULATOR OF AXILLARY MERISTEMS 2)		4.11	
		mloc_52439.6	MYB59 (MYB DOMAIN PROTEIN 59)		-1.17	
		mloc_71418.2	MYB63 (MYB DOMAIN PROTEIN 63)		1.92	
		ak358405	MYB4 (MYB DOMAIN PROTEIN 4)		-1.66	
	WRKY	mloc_55846.2	SANT/MYB protein		1.04	
		mloc_53628.1	SANT/MYB protein		3.31	
		mloc_53626.2	SANT/MYB protein		2.85	
		mloc_74184.1	ATRL1 (ARABIDOPSIS RAD-LIKE 1)		1.06	
		ak361795	WRKY41		2.92	
		ak367621	WRKY45		3.86	
		mloc_70190.1	WRKY18		4.70	
		mloc_81131.1	WRKY51		2.83	
		mloc_60283.1	WRKY72		5.01	
		ak376482	WRKY33		2.58	
		ak369804	WRKY53		3.54	
		ak371133	WRKY67		5.92	
	RNA binding	mloc_67851.2	WRKY33		1.84	
		mloc_60890.1	WRKY40		1.11	
		mloc_74341.1	RNA-binding protein		1.01	
		mloc_54877.1	RNA recognition motif (RRM)-containing protein		1.17	
		ak356508	BTR1L (BINDING TO TOMV RNA 1L (LONG FORM))		1.21	
	Unclassified	ak375398	KH domain-containing protein		1.05	
		mloc_897.1	RBP2 protein		1.02	
		ak354714	ATRBP47C' (RNA-binding protein 47C')		1.05	
		mloc_62671.5	Remorin family protein		1.72	
		mloc_57482.2	Binding		1.28	
		mloc_71411.1	Zinc finger (C2H2 type) family protein		1.01	
		mloc_7288.1	c-myc binding protein		1.12	
		ak250903.1	RNA-binding post-transcriptional regulator csx1		1.12	
mloc_54789.1		Zinc finger (DHHC type) family protein		1.04		
ak249801.1		PDF5 (PREFOLDIN 5); unfolded protein binding		1.38		
ak370203		Aspartyl protease family protein		1.78		
ak250734.1		Single-stranded DNA-binding protein		2.40		
Protein metabolism		Protease	mloc_47161.1	SAG12 (SENESCENCE-ASSOCIATED GENE 12)		-1.42
			ak373733	cysteine protease inhibitor, putative		-2.33
	mloc_1375		LON1; serine protease		1.75	
	mloc_57547		LON1; serine protease		1.92	
	ak354978		ERD1 (EARLY RESPONSIVE TO DEHYDRATION 1)		1.82	
	ak353618		ERD1 (EARLY RESPONSIVE TO DEHYDRATION 1)		1.44	
	Aa activation	ak356015	ARA12; serine-type endopeptidase		-4.47	
		mloc_67682.1	tRNA pseudouridine synthase family protein		1.31	
		mloc_4430.1	Pseudouridine synthase family protein		1.30	
	Prokaryotik ribosomal protein	mloc_4966.5	Isoleucyl-tRNA synthetase		1.19	
		ak251390.1	Ribosomal protein L1 family protein		1.64	
		ak358901	RPL3P (RIBOSOMAL PROTEIN L3 PLASTID)		1.56	
		ak250951.1	Ribosomal protein L25/Gln-tRNA synthetase		1.44	
		mloc_17696.1	Ribosomal protein S11 containing protein		1.21	
		ak369305	Ribosomal protein L4 family protein		1.03	
		Eukaryotik ribosomal protein	mloc_65017.2	RPS11C; 40S ribosomal protein S11		2.80
			mloc_75214.1	RPS23B; 40S ribosomal protein S23		1.46
			mloc_55662.1	40S ribosomal protein SA		1.18
			ak249800.1	PGY2; 60S ribosomal protein L9		1.13
	ak250607.1		40S ribosomal protein S20 (RPS20C)		1.10	
	mloc_38744.1		40S ribosomal protein S24 (RPS24A)		1.07	
	mloc_7955.1		60S ribosomal protein L12 (RPL12C)		1.03	
	Ribosome biogenesis	ak361902	NAP57; h/ACA ribonucleoprotein complex subunit 4,		1.26	
		mloc_679.1	TOZ (TORMOZEMBRYO DEFECTIVE)		1.24	
		mloc_30800.1	Adenylate kinase isoenzyme 6		1.03	
	Protein synthesis	ak370185	Elongation factor Tu		1.12	
	Targeting nucleus	ak369923	Protein transporter		1.84	
	Targeting mitochondria	mloc_4994.1	Importin beta-2 subunit family protein		1.07	
		mloc_61199.2	Tim17/Tim22/Tim23 family protein		1.08	
		mloc_60208.1	OEP16 (OUTER PLASTID ENVELOPE PROTEIN 16-1)		-1.17	

	FUNCTIONAL CATEGORY	ACCESSION	DESCRIPTION	-5	5	LOG FC
Protein metabolism	Targeting chloroplast	ak374606	ATTOC64-V (translocon at the outer membrane of chloroplasts 64-v)			1.22
		ak356088	Tic22; chloroplast inner membrane import protein			1.08
	Secretory pathway	ak365106	SEC14 cytosolic factor			1.69
		mloc_60570.1	Mitochondrial inner membrane protease subunit 2			1.62
		mloc_3582.1	SEC14 cytosolic factor			1.54
	Posttranslational modification	mloc_18690.1	RLK1 (RECEPTOR-LIKE PROTEIN KINASE 1)			5.12
		mloc_5569.6	PARP2 (POLY(ADP-RIBOSE) POLYMERASE 2)			2.84
		mloc_67251.4	Protein phosphatase 2C family protein / PP2C family protein			2.46
		mloc_20513.1	Protein phosphatase 2C, putative / PP2C			2.03
		ak365611	Protein kinase family protein			1.68
		ak372866	CPK16			1.57
		mloc_6120.2	CDC2B (CYCLIN-DEPENDENT KINASE B1;1)			1.54
		mloc_12321.3	DBR1; calcineurin-like phosphoesterase family protein			1.49
		ak372120	MAP kinase 10			1.43
		ak360154	CPK7 (calmodulin-domain protein kinase 7)			1.17
		ak361985	Calcium-dependent protein kinase 2			-1.31
		mloc_63787.3	SAPK4 serine/threonine-protein kinase			-1.49
		mloc_75549.1	Mitogen-activated protein kinase			-1.71
		mloc_52019.1	CIPK2 (CBL-INTERACTING PROTEIN KINASE 2)			-3.68
	AAA protein degradation	ak370706	Cell Division Protein AAA ATPase family			4.86
		ak248264.1	Cell Division Protein AAA ATPase family			3.83
		mloc_40499.1	AATP1 (AAA-ATPase 1)			3.58
		ak358311	AAA-type ATPase family protein			1.38
		ak367055	AAA-type ATPase family protein			1.02
	Ubiquitin degradation	mloc_6744.1	SAE2 (SUMO-ACTIVATING ENZYME 2)			1.52
		ak249816.1	UBC9 (UBIQUITIN CONJUGATING ENZYME 9)			-1.81
		mloc_50479.1	E3 ubiquitin-protein ligase EL5			3.22
		ak353806	E3 ubiquitin-protein ligase EL5			2.07
		ak360626	E3 ubiquitin-protein ligase EL6			1.76
		ak365049	RGLG2 (RING domain Ligase2); ubiquitin-protein ligase			1.44
		mloc_19130.1	Zinc finger family protein			1.89
		mloc_51041.2	RING-H2 finger protein ATL3C			2.10
		mloc_66488.1	Zinc finger family protein			1.07
		mloc_23887.1	E3 ubiquitin-protein ligase EL5			5.21
		ak356262	RING-H2 finger protein ATL3			3.03
		mloc_36739.2	Protein binding / zinc ion binding			1.76
		ak248493.1	Ring finger protein			1.50
		mloc_74646.1	Immediate-early fungal elicitor protein CMPG1			3.45
		mloc_2875.1	Zinc finger family protein			1.44
		mloc_5208.1	PUB23 ubiquitin-protein ligase			1.71
		ak370916	BRH1 (BRASSINOSTEROID-RESPONSIVE RING-H2)			2.01
		ak367107	VFB1 (VIER F-BOX PROTEINE 1); ubiquitin-protein ligase			1.33
		mloc_18585.1	F-box domain containing protein			1.66
		mloc_69879.2	F-box family protein (FBL10)			1.65
		mloc_78189.2	F-box domain containing protein			1.21
		mloc_60706.2	EMB2771 (EMBRYO DEFECTIVE 2771); ubiquitin-protein ligase			1.98
		mloc_38598.1	APC2; ubiquitin protein ligase binding / ubiquitin-protein ligase			1.06
		mloc_36638.1	BPM2 (BTB-POZ AND MATH DOMAIN 2); protein binding			1.10
	Protein folding	ak374404	HSP60 (HEAT SHOCK PROTEIN 60);			2.37
	Glycosylation	mloc_5270.2	Transferase			2.40
	mloc_39786.1	Transferase			3.14	
Assembly and cofactor ligation	ak364131	Cytochrome c biogenesis protein family			1.15	
	ak368377	HCF165; oxidoreductase			1.01	

Appendix IV. A comparison of the WHIRLY1 transcript abundance in the wild type and W1-7 leaves under N replete and N deficient conditions.

